

**THE PI5P 4-KINASE ORTHOLOG PPK-2
OF *CAENORHABDITIS ELEGANS* ACTS IN
SYNAPTIC TRANSMISSION AND NEURONAL MEMBRANE TRAFFICKING**

Dissertation

for the award of the degree

Doctor rerum naturalium

(Dr. rer. nat.)

Division of Mathematics and Natural Sciences
of the Georg-August-Universität Göttingen

submitted by

Wiebke Anna Sassen

from Gifhorn, Germany

Göttingen 2010

Thesis Committee

Dr. Dieter Klopfenstein (1st reviewer and supervisor)
(Department of Biochemistry II, Faculty of Medicine, University of Göttingen, Germany)

Prof. Dr. Ivo Feußner (2nd reviewer)
(Department of Plant Biochemistry, Albrecht-von-Haller-Institute for Plant Sciences, Faculty of
Biology, University of Göttingen, Germany)

Prof. Dr. Nils Brose
(Molecular neurobiology, Max-Planck-Institute of Experimental Medicine, Göttingen, Germany)

Date of oral examination:

Herewith I declare that I prepared the dissertation

“The PI5P 4-kinase ortholog PPK-2 of *Caenorhabditis elegans* acts in synaptic transmission and neuronal membrane trafficking”

on my own and with no other sources and aids than quoted.

Wiebke Anna Sassen

Göttingen, 31.03.2010

There is a theory

which states that if ever anybody discovers exactly what the Universe is for and why it is here, it will instantly disappear and be replaced by something even more bizarre and inexplicable.

There is another theory which states that this has already happened.

Douglas Adams (1952-2001)

Abbreviations

ANF	atrial natriuretic factor	PI3,4P ₂	phosphatidylinositol 3,4-bisphosphate
ATP	adenosine triphosphate	PI3,5P ₂	phosphatidylinositol 3,5-bisphosphate
<i>att</i>	attachment site	PI3P	phosphatidylinositol 3-phosphate
BLAST	Basic Local Alignment Search Tool	PI4,5P ₂	phosphatidylinositol 4,5-bisphosphate
cDNA	complementary DNA	PI4P	phosphatidylinositol 4-phosphate
CFP	cyan fluorescent protein	PI5P	phosphatidylinositol 5-phosphate
CGC	<i>Caenorhabditis</i> Genetics Center	PIP	phosphatidylinosolphosphate
C-terminus	carboxyterminus	PIP ₂	double-phosphorylated PIP
DAG	diacylglycerol	PM	plasma membrane
DCV	dense core vesicle	PTZ	pentylene tetrazole
DNA	deoxyribonucleic acid	RNA	ribonucleic acid
dsRNA	double-stranded RNA	RNAi	RNA interference
ER	endoplasmic reticulum	SV	synaptic vesicle
GABA	gamma-aminobutyric acid	TLC	thin-layer-chromatography
GC	gas chromatography		
gDNA	genomic DNA		
GFP	green fluorescent protein		
mCherry	red fluorescent protein		
NMJ	neuromuscular junction		
N-terminus	aminoterminus		
P	promoter	<i>E. coli</i>	<i>Escherichia coli</i>
PC	phosphatidylcholine	<i>R. norvegicus</i>	<i>Rattus norvegicus</i>
PCR	polymerase chain reaction	<i>C. elegans</i>	<i>Caenorhabditis elegans</i>
PI	phosphatidylinositol	<i>H. sapiens</i>	<i>Homo sapiens</i>
PI3,4,5P ₃	phosphatidylinositol 3,4,5-triphosphate	<i>M. musculus</i>	<i>Mus musculus</i>

Table of Contents

	<i>page</i>
1 Introduction	11
1.1 The endomembrane system and membrane trafficking in eukaryotic cells	11
1.2 Membrane trafficking in neurons	13
1.3 Phosphatidylinositolphosphates are important regulators of membrane trafficking	16
1.3.1 Phosphatidylinositol 4,5-bisphosphate	17
1.3.2 Phosphatidylinositol 4-phosphate	18
1.3.3 Phosphatidylinositol 3-phosphate	18
1.3.4 Phosphatidylinositol 3,5-bisphosphate	18
1.3.5 Phosphatidylinositol 3,4,5-triphosphate and phosphatidylinositol 3,4-bisphosphate	19
1.3.6 Phosphatidylinositol 5-phosphate	19
1.4 PIP-metabolizing enzymes	20
1.4.1 PI and PIP kinases	20
1.4.1.1 PI and PIP 3-kinases	21
1.4.1.2 PI 4-kinases	21
1.4.1.3 PIP 4-kinases and PIP 5-kinases	21
1.4.2 PIP phosphatases	22
1.4.2.1 PIP 3-phosphatases	23
1.4.2.2 PIP 4-phosphatases and PIP 5-phosphatases	23
1.4.2.3 The Sac domain	24
1.5 The soil nematode <i>C. elegans</i> as a model system	25
1.6 Aim of this study	26
2 Material and methods	27
2.1 Chemicals and reagents	27
2.2 Molecular cloning	28
2.2.1 <i>E. coli</i> strains and maintenance	28
2.2.2 Polymerase chain reaction	29
2.2.3 Cloning with Gateway	29
2.2.4 Conventional cloning	30
2.2.5 Transformation of <i>E. coli</i>	30
2.2.5.1 Preparation of chemically competent <i>E. coli</i>	30
2.2.5.2 Transformation of chemically competent <i>E. coli</i>	30
2.2.6 Plasmid DNA purification and DNA sequencing	31
2.2.7 Vectors used in this study	31
2.3 Working with <i>C. elegans</i>	35
2.3.1 <i>E. coli</i> strains for nematode feeding	35
2.3.2 <i>C. elegans</i> maintenance	35

2.3.3	Generation of transgenic nematodes by microinjection	35
2.3.4	Isolation of genomic <i>C. elegans</i> DNA	36
2.3.5	RNA isolation and cDNA synthesis	36
2.3.6	Nematode crossing and genotyping	37
2.3.7	<i>C. elegans</i> strains used in this study	37
2.3.8	RNA interference	37
2.3.8.1	<i>E. coli</i> for RNAi feeding (maintenance, transformation, and induction)	39
2.3.8.2	Preparation of RNAi-hypersensitive nematodes	39
2.3.8.3	Setup of the RNAi screen	40
2.3.8.4	RNAi control constructs	40
2.3.9	Neurotoxin assays	40
2.3.9.1	Aldicarb	40
2.3.9.2	Levamisole	41
2.3.9.3	Pentylentetrazole	41
2.3.10	Motility analysis	41
2.3.10.1	Video tracking	41
2.3.10.2	Trace analysis	41
2.3.11	Quantification of progeny	41
2.3.12	Microscopy	42
2.3.13	Analysis of nervous system development	42
2.3.14	Analysis of coelomocytes and dorsal cords	42
2.3.15	Preparation of large synchronous L1 larvae populations and biochemical analysis of phospholipids	43
2.3.15.1	Preparation of large synchronous L1 larvae populations	43
2.3.15.2	Acidic extraction of phospholipids	43
2.3.15.3	Quantification of phosphoinositides according to gas-chromatographic detection of the associated fatty acids	43
2.4	Working with <i>S. cerevisiae</i>	44
2.4.1	<i>S. cerevisiae</i> strains and maintenance	44
2.4.2	Transformation of <i>S. cerevisiae</i>	45
2.4.3	Isolation of total DNA of <i>S. cerevisiae</i>	45
2.4.4	Protein extraction of <i>S. cerevisiae</i>	46
2.4.5	Protein detection by Western Blotting	46
2.4.6	Analysis of phenotype characteristic of <i>sac1delta</i>	46
2.4.6.1	Cold sensitivity	46
2.4.6.1	Slow growth	47
2.4.6.3	Inositol auxotrophy	47
2.5	Recombinant protein expression in <i>E. coli</i> and <i>in vitro</i> assays	47
2.5.1	Recombinant expression of GST-PPK	47
2.5.2	Phosphoinositide kinase assay	48
2.6	Bioinformatics and image editing	49

3	Results	50
3.1	RNAi screen for PIP-metabolizing enzymes in neuronal membrane trafficking	50
3.2	Analysis of the putative PI5P 4-kinase PPK-2 in the nervous system of <i>C. elegans</i>	54
3.2.1	PPK-2 is homolog to mammalian PI5P 4-kinases	54
3.2.2	RNAi knock down of <i>ppk-2</i> is specific	59
3.2.3	Analysis of two different <i>ppk-2</i> mutants	60
3.2.3.1	Transcript analysis	60
3.2.3.2	Putative structural changes of PPK-2 mutants	62
3.2.3.3	Neurotoxin assays	63
3.2.3.4	Motility analysis	65
3.2.3.5	Development of acetylcholinergic and GABAergic neurons	66
3.2.3.6	Quantification of progeny	68
3.2.3.7	Analysis of SV and DCV markers	68
3.2.3.8	Biochemical analysis of phospholipids	72
3.2.4	Subcellular localizations of PPK-2	73
3.2.4.1	Localization of PPK-2 in neurons	73
3.2.4.2	Localization of PPK-2 mutants in neurons	76
3.2.4.3	Coexpression of PPK-2 and PPK-1 in neurons	76
3.2.4.4	Coexpression of PPK-2 mutants and PPK-1 in neurons	78
3.2.4.5	PPK-2 particles move along neuronal processes	81
3.2.4.6	Particles of PPK mutant fusions move along neuronal processes	84
3.2.4.7	Velocities of PPK-2 particles in neuronal processes	86
3.2.4.8	The localization of PPK-2 depends on kinesin-3	87
3.2.5	<i>In vitro</i> assay of PPK-2 kinase activity	90
3.3	Initial characterizations of two PIP phosphatases	91
3.3.1	Initial characterization of the <i>C. elegans</i> Sac1p homolog	91
3.3.1.1	<i>C. elegans</i> F30A10.6 is homolog to yeast Sac1p and human Sac1	91
3.3.1.2	<i>C. elegans</i> F30A10.6 can replace Sac1p in yeast	92
3.3.1.3	Subcellular localization of F30A10.6 in neurons	94
3.3.2	Initial characterization of the <i>C. elegans</i> PTEN homolog	96
3.3.2.1	<i>daf-18</i> mutants show resistance to aldicarb	97
3.3.2.2	Velocity of <i>daf-18</i> mutants	98
3.2.2.3	Biochemical analysis of phospholipids	99
4	Discussion	100
4.1	New players in neuronal membrane traffic in <i>C. elegans</i>	100
4.2	Characterization of the Type II PIP kinase PPK-2	102
4.2.1	<i>ppk-2</i> regulates neurotransmitter and neuropeptides release	102
4.2.2	PPK-2 interacts with PPK-1	104
4.2.3	PPK-2 localizes to endomembranes	105
4.2.4	PPK-2 is actively transported into neuronal processes	107
4.2.5	Two sites of action for PPK-2	108

4.3	Novel functions in neuronal membrane trafficking for six PIP-metabolizing enzymes in <i>C. elegans</i>	109
4.4	Concluding remarks	111
5	Summary	112
6	References	113
7	Figures and tables	129
8	Acknowledgements	131
9	Appendix	
10	Curriculum vitae	

1 Introduction

1.1 The endomembrane system and membrane trafficking in eukaryotic cells

Biological membranes are the crucial structural elements of cells. They mainly consist of lipids and to varying amounts of proteins. Lipids have an amphiphilic nature, meaning they are composed of a hydrophilic head group and a hydrophobic tail. This molecular structure causes them to form bilayers in aqueous environments whereby the head group is exposed to the hydrophilic environment and the water-fearing tail is directed to the interior. Thus assembled, the lipid bilayer is the basic structure of all cellular membranes. Associated proteins can have structural importance, but also influence all conceivable cellular functions (Edidin, 2003).

Membranes are dynamic, fluid structures, in which most molecules can move laterally. However, the passage of water-soluble molecules across the bilayer is restricted, resulting in their distinctive impermeability for polar molecules (Gouaux and MacKinnon, 2005). The outside boundaries of every cell are defined by the plasma membrane (PM) which separates the cytosol from the cellular environment and controls the selective intake and release of a large variety of molecules, making the cell an autonomously unit separated from the environment (Alberts *et al.*, 2008).

While in prokaryotes the cytoplasm of a cell is only marginally organized, the interior of eukaryotic cells is highly organized as represented by several membrane-enclosed compartments called organelles or – in their entirety – the endomembrane system. Different compartments thereby carry out different functions in the complex eukaryotic cell (Alberts *et al.*, 2008).

The naming compartment of the eukaryotic cell is the nucleus (greek: karyon), comprised of the genomic deoxyribonucleic acid (gDNA) and associated transcription machinery (Alberts *et al.*, 2008). This entity of every eukaryotic cell is surrounded by the membrane system of the nuclear envelope (Hetzer *et al.*, 2005). The nuclear envelope itself is interconnected with the endoplasmic reticulum (ER), an intracellular compartment where most lipid bilayers are assembled and many proteins, lipids, carbohydrates and other molecules are synthesized (Voeltz *et al.*, 2002). The ER output is transported to an organelle called the Golgi apparatus where it is sorted and distributed to different locations within the cell (Glick, 2000; Ellgaard and Helenius, 2003).

Since the ER and the Golgi apparatus are not directly linked with each other, metabolites of all kinds have to be loaded into small, more or less spherical membrane-surrounded compartments. These membrane containers are usually called vesicles and bud constantly from the ER, travel to the Golgi apparatus, fuse with its surrounding membrane and release their content to the Golgi lumen. Golgi apparatus-derived vesicles can also travel back to the ER, what leads to constant and balanced exchange of membrane material and therewith metabolites between these two compartments (Lee *et al.*, 2004). This phenomenon is called membrane trafficking or membrane traffic and is an essential and complex process proceeding between all components of the endomembrane system and the PM (Figure 1; Mellman and Warren, 2000). Membrane traffic occurs along highly organized directional pathways which are dependent on motor proteins like kinesins which bind specifically to their membranous cargo and transport it along cytoskeleton tracks (Hirokawa, 1998).

The membrane traffic between the ER and the Golgi apparatus is the first step of the so-called biosynthetic-secretory pathway:

Proteins and other metabolites from the ER are sorted in Golgi apparatus-derived vesicles, which are directed to the cell periphery. There, these exocytotic (or secretory) vesicles fuse with the PM, resulting in the secretion of their cargo, a process called exocytosis (Traub and Kornfeld, 1997). In contrast to exocytosis, vesicles can also bud from the PM, the initial step of the so-called endocytosis or endocytic pathway (Mellman, 1996). The latter results in an uptake of membrane material from the PM. Beside membrane material, membrane-associated proteins and particles from the environment (e.g. nutrients) are also absorbed by the cell during endocytosis (Maxfield and McGraw, 2004; Alberts *et al.*, 2008).

In the course of endocytosis, the absorbed material is delivered to compartments called endosomes. So-called early endosomes are found next to the PM, while more mature late endosomes are located close to the Golgi apparatus and the nucleus (Alberts *et al.*, 2008). Retrieved endocytosed membrane and membrane proteins can be recycled from both early and late endosomes or - like endocytosed extracellular particles - are further transported to lysosomes where cellular degradation mainly takes place (Bonifacino and Traub, 2003; Gruenberg and Stenmark, 2004; Maxfield and McGraw, 2004).

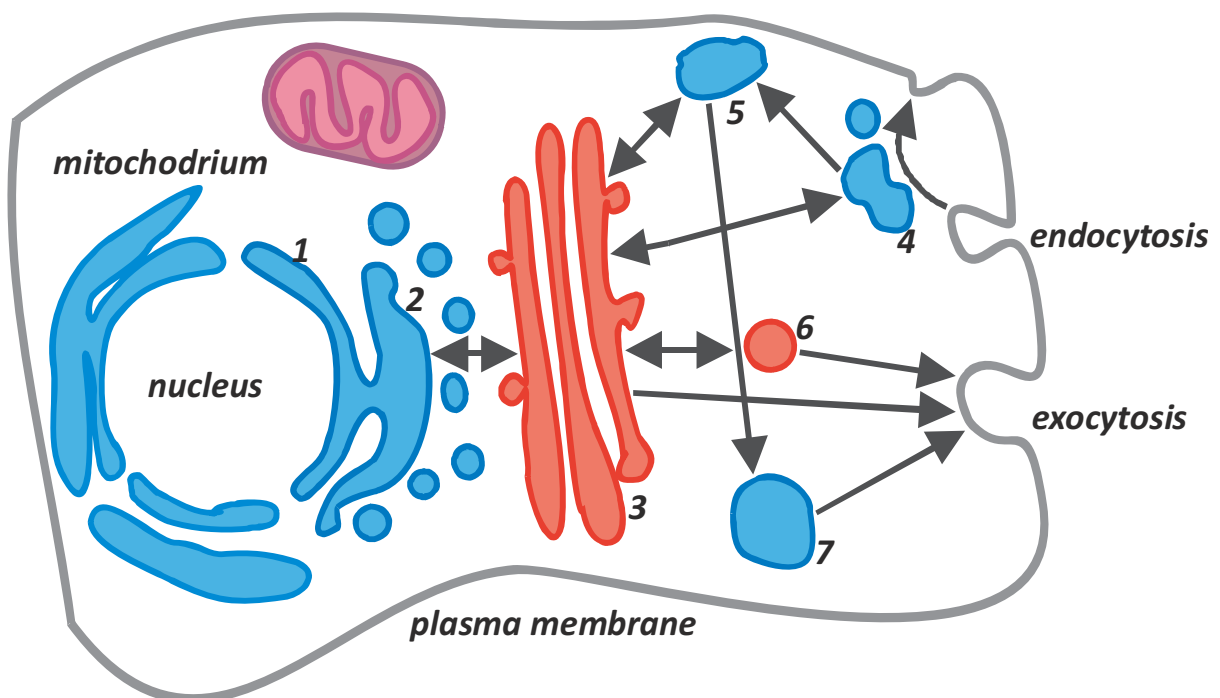


Figure 1 The endomembrane system of an animal cell

Routes of membrane trafficking are indicated with arrows. 1, nuclear envelope; 2, endoplasmic reticulum; 3, Golgi apparatus; 4, early endosome; 5, late endosome; 6, secretory vesicle; 7, lysosome (according to Alberts *et al.*, 2008, modified).

However, endosomes appear to have more functions than to lead endocytosed material to degradation. Many transport vesicles derived from the Golgi apparatus undergo a passage through

the endosomal membrane system. The vesicle contents are again sorted and the transport vesicle emerges as a 'mature' secretory vesicle, which travels further to the PM. Hence, early endosomes are also called sorting endosomes (Seaman, 2008).

Lysosomes contain digestive enzymes that degrade macromolecules as well as whole organelles. They allow the cell to recycle its depleted or excessive constituent parts. Upon digestion in lysosomes, the building blocks of organelles and macromolecules (e.g. lipids, amino acids, sugars, etc.) are again available for diverse cellular pathways. The cells of plants and fungi possess organelles related to animal cell lysosomes, called vacuoles. Vacuoles are very large fluid-filled compartments and are important for the storage of different metabolites (Andrews, 2000; Rouillé *et al.*, 2000; De Duve, 2005).

In eukaryotic cells, the vast majority of energy needed for the diverse and complex mechanisms contributing to life is located in a membrane-enclosed machinery as well: the mitochondrion. Mitochondria are double membrane-enclosed organelles which generate adenosine triphosphate (ATP) using the unique structure of biological membranes. Here, a membrane allows a proton gradient to be generated, powering the enzyme ATPase thus enabling the production of ATP (Saraste, 1999). Beside mitochondria, plant cells harbor another energy producing cellular component: the chloroplast. As well as the mitochondrion, the chloroplast is a double membrane-enclosed organelle and its enveloping membrane allows this organelle to produce ATP (Blankenship, 2006). Both reviewed compartments possess their own genome and biosynthesis machineries, allowing them to reproduce autonomously. These properties make them unique among the other cellular components (Dyall *et al.*, 2004).

Among the organelles of the endomembrane system an exchange of membrane and membrane-associated proteins occurs continuously, a highly regulated process termed constitutive membrane traffic. Transport vesicles bud from the donor compartment and are selectively transported to the acceptor compartment where they fuse specifically with the membrane of the target compartment (Spang, 2008). In parallel, retrieval pathways bring back membrane and associated metabolites to the compartment of origin (Alberts *et al.*, 2008), keeping the membrane flow in a finely tuned balance.

1.2 Membrane trafficking in neurons

Neurons (or nervous cells) are special cell types exclusively found in higher animals. Here, they form a body spanning network – the nervous system. The nervous system links and coordinates the actions of all parts of the organism by processing and transmitting information by electrochemical signaling. Neurons are highly polarized cells and can be subdivided into three major parts: the cell body (soma), several branches called dendrites, and most commonly one elongated process termed axon (Figure 2). In general, dendrites receive chemical signals and process them to electrical impulses which depolarize the PM. These impulses are then integrated via dendrites and the cell body and propagated to the nerve terminal of the axon, where the electrical signals (action potentials) are remodulated to chemical signals (Alberts *et al.*, 2008). An essential prerequisite for this is a specialized transport and trafficking machinery within the neuronal cell. Therefore, beside the constitutive membrane trafficking, neurons own a specifically regulated membrane trafficking route:

the synaptic vesicle cycle which is found at the nerve terminal, the synapse (Südhof, 2004; Rohrbough and Broadie, 2005).

A synapse is an intercellular junction between two neurons, or neurons and muscle cells (neuromuscular junction, NMJ). Different synapse types have been described, whereby the most common one is the chemical synapse which allows the communication between two excitable cells by signaling molecules termed neurotransmitters. The chemical synapse consists of the presynapse, a specialized membrane region at the axon of the first neuron and the postsynaptic membrane region of the second cell, both separated by the synaptic cleft (Figure 2). One of the most important morphological features of the presynapse is a big number of small membranous vesicles located nearby the PM. These synaptic vesicles (SVs) are loaded with neurotransmitters. Upon arrival of an action potential at the presynapse, voltage gated calcium channels are opened what results in a massive but localized influx of calcium ions from the environment. The increase of calcium ion concentration in the cytosol actuates the fusion of SVs with the PM and the subsequent exocytosis of neurotransmitters to the synaptic cleft. Once released, the neurotransmitters bind to their cognate receptors in the PM of the postsynapse. In turn, this leads to the opening of calcium channels and membrane depolarization of the postsynaptic cell (Alberts *et al.*, 2008).

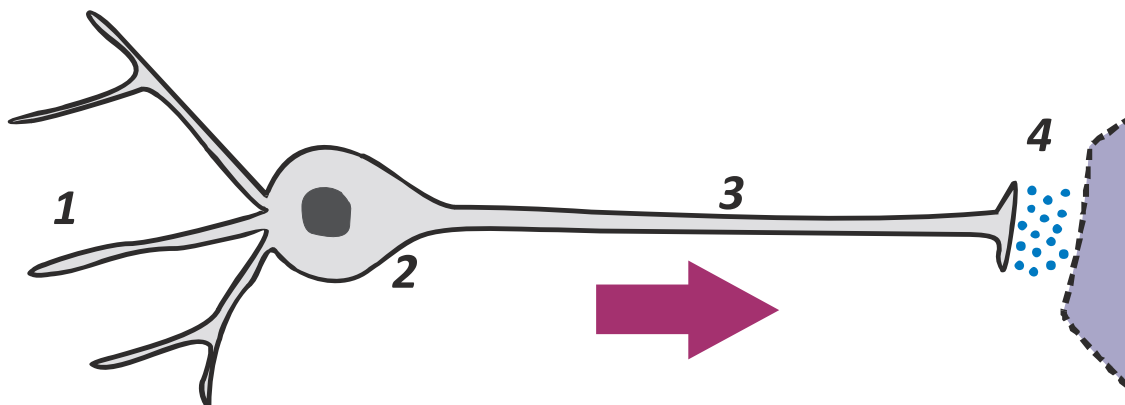


Figure 2 Schematic representation of a neuron

Typical structure of a nervous cell with dendrites (1) branching from the soma (2). The prerequisite for the release of neurotransmitters (blue) in the synaptic cleft (4) between the presynaptic terminal and the postsynaptic cell (dark grey) is the highly organized transport (arrow) of synaptic vesicle precursors and other metabolites along the axon (3).

Neurons fall into different classes, dependent on the released neurotransmitters. One class of nervous cells is termed cholinergic neurons which exocytose acetylcholine to the synaptic cleft of so-called excitatory synapses. Subsequent to exocytosis, acetylcholine binds to acetylcholine receptors at the postsynapse resulting in the aforementioned depolarization, thus propagating the electrochemical signal. Shortly after, the neurotransmitter is degraded by the enzyme acetylcholinesterase, thus preventing a continuous depolarization of the postsynapse. In case of inhibitory synapses, the postsynapse is not depolarized. In fact, it is hyperpolarized, triggered by inhibitory neurotransmitters e.g. gamma-aminobutyric acid (GABA). Once hyperpolarized, the chance

for a depolarization of the postsynaptic cell decreases, accompanied with a decreased feasibility for an action potential to occur (Alberts *et al.*, 2008).

After exocytosis, the membrane material together with specific SV proteins is recovered via endocytosis. At present, different models are discussed aiming to describe this 'SV recycling'. One of the discussed models is the formation of endocytic pits and subsequent budding, mediated by the coat protein clathrin. SV formation can occur directly from the PM or from bigger invaginated membrane tubes. Upon completion of the recycling procedure, the SVs are loaded with neurotransmitters and are rendered fusion-competent again for another round of exo-/endocytosis of the SV cycle (Figure 3; Farsad and De Camilli, 2004).

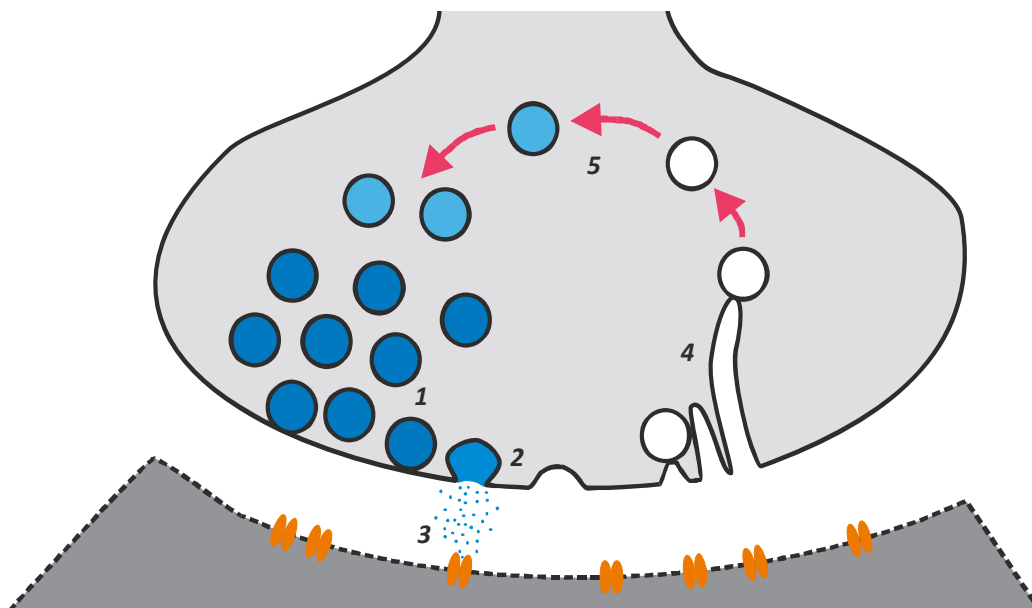


Figure 3 The synaptic vesicle cycle at the synapse

The main morphological feature of synapses is the presence of a big number of small vesicular structures termed synaptic vesicles (1) loaded with neurotransmitters (blue). Once fused with the synaptic plasma membrane (2), the vesicles release the signaling molecules to the synaptic cleft (3), where they can bind to cognate receptors (orange) at the plasma membrane PM of the postsynaptic cell (dark grey). Membrane material and according proteins are recycled by the direct budding of vesicles from the plasma membrane or from invaginated membrane tubes (4). After this, the vesicle is reloaded with neurotransmitters (light blue; 5) and is ready for another round of exo-/endocytosis (according to Farsad and De Camilli, 2004, modified).

'Mature' SVs are only found in proximity to the presynapse. Hence, the material necessary for SV assembly must be transported all the way from the soma to the nerve terminal. Membranes and associated proteins are generated at the ER, sorted to transport vesicles (SV precursors), and transported by a specific subset of motor proteins along the microtubules of the axon to the nerve terminal (Goldstein *et al.*, 2008). Since these transport vesicles do not exhibit the size or shape of SVs, it is widely accepted that SVs are generated directly at the synapse. This notion is supported by the facts, that different SV proteins are transported by different vesicular containers, and that readily assembled SVs are solely loaded with neurotransmitters at the nerve terminal (Hannah *et al.*, 1999).

As a conclusion of these observations, it was hypothesized that pre-SV transport vesicles have to fuse with the synaptic PM to contribute new material to the SV cycle, supported by synaptic endosomal sorting compartments (Bonanomi *et al.*, 2006).

Synaptic transmission is not regulated by SVs alone, but is also significantly regulated by the exocytosis of so-called dense core vesicles (DCVs). These electron-dense spherical structures are secretory vesicles which bud directly from the Golgi apparatus. Unlike SVs which exocytose only directly at the active site of the presynapse, a specialized membrane region, DCVs can in principle fuse at any site of the PM, and release their contents to the cell environment. Another property which sets them apart from SVs is the fact, that they are not recycled. In contrast to neurotransmitters, DCVs transport signaling peptides termed neuropeptides. These neuropeptides do not directly facilitate synaptic transmission but essentially trigger it by regulating neurotransmitter signaling (Sieburth *et al.*, 2007).

1.3 Phosphatidylinositolphosphates are important regulators of membrane trafficking

The glycerophospholipid phosphatidylinositol (PI) has two non-polar fatty acid tails which are embedded in the cytosolic leaflet of membranes. Its hydrophilic head group linked via a phosphate group is an inositol ring, which is pointing towards the cytosol. The inositol ring can be phosphorylated at the 3rd, 4th, and 5th hydroxyl group in seven different combinations (hydroxyl groups D-2 and D-6 are not phosphorylated due to steric hindrance). These PI derivatives are called phosphatidylinositolphosphates (PIPs) (Figure 4). An alternative designation for PIPs is the term phosphoinositides. All PIPs can be reversibly phosphorylated and hence interconverted by a large variety of specific enzymes (section 1.4; Parker, 2004).

Although PI and PIPs are only minor components of eukaryotic membranes, they have essential functions in cell physiology. During the last two decades, it became clear that each of the seven PIP species carries out at least one essential cellular function, however, most of them play crucial roles in membrane trafficking (Roth, 2004).

As an essential prerequisite for targeted membrane traffic, it is necessary that membranes of different compartments can be distinguished and have an own identity. This membrane identity comprises all possible types and amounts of lipids i.e. structural or signaling lipids, and associated proteins such as membrane-embedded proteins but also interacting cytosolic proteins which are often found only at one special sort of organelle (Munro, 2004; Itoh and De Camilli, 2004). The seven differently phosphorylated PIP species are heterogeneously distributed among organelles, so that - simply said - every organelle has its own specific phosphoinositide (Roth, 2004). Therefore, they are key components of membrane identity and membrane traffic. Based on the PI backbone, the synthesis of distinct PIPs is locally restricted and maintained by a network of kinases and phosphatases (section 1.4). Phosphoinositides act as 'membrane ligands' for all kind of proteins with diverse physiological functions. These protein-lipid interactions are enabled by a set of protein domains which can bind specifically to different PIP species (Lemmon, 2003; Stahelin, 2009).

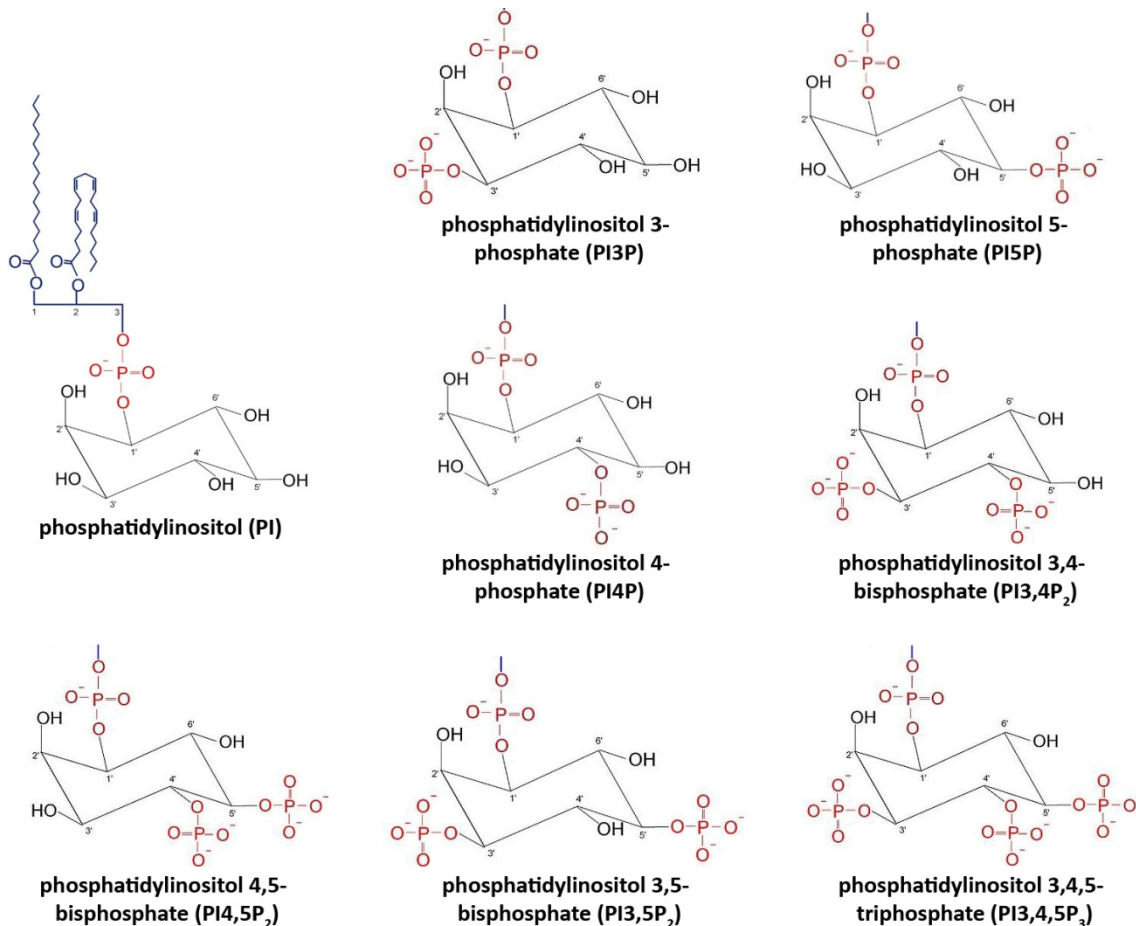


Figure 4 Phosphatidylinositol and its phosphorylated derivatives

Phosphatidylinositol has two non-polar acyl chains and a hydrophilic inositol head group linked via a phosphate group (top left). The inositol ring can be phosphorylated at the 3rd, 4th, and 5th hydroxyl group in seven different combinations. These derivatives are termed phosphatidylinositol phosphates or phosphoinositides.

In the following section, all seven PIPs and associated functions will be briefly discussed with focus on membrane trafficking.

1.3.1 Phosphatidylinositol 4,5-bisphosphate

Until now, the phosphoinositide phosphatidylinositol 4,5-bisphosphate (PI4,5P₂) is the most studied member of this lipid class. It is synthesized by two subsequent phosphorylations of PI by specific kinases (Doughman *et al.*, 2003; section 1.4.1). The vast majority of PI4,5P₂ is found in the cytosolic leaflet of the PM, where it functions as major factor for exo- and endocytosis but also for signal transduction (Martin, 2001; Di Paolo and De Camilli, 2006) and actin regulation (Homma *et al.*, 1998; Desrivières *et al.*, 1998; Raucher *et al.*, 2000). For example, the exocytosis of DCVs is facilitated by PI4,5P₂ (Gong *et al.*, 2005).

Different lines of evidence indicate that PI4,5P₂ is an important regulator of the SV cycle (Di Paolo *et al.*, 2004). SVs proximal to the PM possess the mono-PIP PI4P in their membranes (Guo *et al.*, 2003), a precursor of PI4,5P₂. It is thought that a PI4P 5-kinase transforms the mono-PIP to PI4,5P₂ (Wenk *et al.*, 2001), which mediates the fusion of the SV membrane with the PM together with a machinery of proteins (Bai *et al.*, 2004). PI4,5P₂ is not only involved in SV exocytosis, it is also intricately involved in SV endocytosis and was found to interact with adapter proteins of clathrin. At the synapse, PI4,5P₂ is essential for clathrin-mediated retrieval of membrane and proteins of exocytosed SVs and hence for SV recycling (Cremona and De Camilli, 2001; Zoncu *et al.*, 2007).

In addition, PI4,5P₂ appears to regulate the motor-dependent transport of SV precursors along the axon to the synapse. It is known, that the anterograde motor kinesin-3 prefers SV precursors as its cargo and binds them via a PIP-binding domain. It was shown *in vitro*, that this pleckstrin homology domain binds PI4,5P₂ with highest affinity, pointing towards that SV precursors possess a certain concentration of this phosphoinositide in their membrane (Yonekawa *et al.*, 1998; Klopfenstein *et al.*, 2002; Klopfenstein *et al.*, 2004). Since SV precursors are thought to be generated mainly by the Golgi apparatus, it is not surprising that a low concentration of PI4,5P₂ is detectable in the membranes of this organelle where it is also involved in membrane trafficking (Roth, 2004; De Matteis *et al.*, 2005).

1.3.2 Phosphatidylinositol 4-phosphate

Phosphatidylinositol 4-phosphate (PI4P) is a precursor of PI4,5P₂, but has also many own, specific cellular functions. PI4P is the major phosphoinositide found at the Golgi apparatus and is believed to be essential for Golgi-to-PM membrane transport (Roth, 2004). PI4P in the Golgi membrane can be bound by specifically interacting proteins resulting in a protein coat which drives the budding of a secretory vesicle (Godi *et al.*, 2004). Therefore, the PI4P concentration at the Golgi apparatus is a regulator for the intensity of the biosynthetic-secretory pathway.

1.3.3 Phosphatidylinositol 3-phosphate

Phosphatidylinositol 3-phosphate (PI3P) can be found all along the endosomal/lysosomal membrane trafficking route and is also involved in membrane traffic from the Golgi apparatus to endosomes (Roth, 2004). Since PI3P is highly enriched in the membrane of early endosomes, PI3P-protein binding domains such as the FYVE-domain can be used to label this organelle type in living cells (Stenmark and Aasland, 1999; Stenmark and Gillooly, 2001). Together with PI3P-binding proteins, PI3P regulates the fusion of endosomal compartments, the formation of internal vesicles of multi-vesicular endosomes, and hence the degradation of proteins and membrane material (Seaman, 2008).

1.3.4 Phosphatidylinositol 3,5-bisphosphate

Phosphatidylinositol 3,5-bisphosphate (PI3,5P₂) is synthesized by the phosphorylation of PI3P at the 5-position of the inositol ring (section 1.4.1.3) and acts in the same membrane trafficking pathway as

PI3P (Dove *et al.*, 2009). PI3,5P₂ is enriched at late endosomal compartments and regulates the membrane crosstalk between late endosomes and lysosomes (Michell *et al.*, 2006; Jefferies *et al.*, 2008). Its function was originally characterized in yeast where PI3,5P₂ controls membrane trafficking and size of the vacuole, an organelle which is functionally related to the lysosomes of animal cells (Dove *et al.*, 2009).

1.3.5 Phosphatidylinositol 3,4,5-triphosphate and phosphatidylinositol 3,4-bisphosphate

Phosphatidylinositol 3,4,5-triphosphate (PI3,4,5P₃) is best characterized for its function as a second messenger in signal transduction from the PM to the cell interior, regulating cell survival and proliferation (Myers *et al.*, 1998; Cantley and Neel, 1999). To date, it was not shown to have an important role in membrane trafficking. It is thought to be mainly generated by the phosphorylation of PI4,5P₂ at the D-3 position of the inositol head group by specific kinases (section 1.4.1.1). Its dephosphorylation is believed to be carried out by specific phosphatases (section 1.4.2.1), thereby acting as a switch for downstream signaling pathways (Maehama, 2007). Therefore, it is possible that the balance between PI4,5P₂ and PI3,4,5P₃ has an indirect influence on membrane trafficking events at the PM.

Phosphatidylinositol 3,4-bisphosphate (PI3,4P₂) can be derived from the dephosphorylation of PI3,4,5P₃ or the phosphorylation of PI3P, respectively (sections 1.4.2.1 and 1.4.1.3). Like for PI3,4,5P₃, its major functions appear to be rather linked to cell signaling than to membrane trafficking (Blero *et al.*, 2007). Since the phosphorylation and dephosphorylation of phosphoinositides can be understood as a cell spanning network, PI3,4P₂ synthesis and degradation may have indirect effects on PIP-regulated membrane trafficking.

1.3.6 Phosphatidylinositol 5-phosphate

Phosphatidylinositol 5-phosphate (PI5P) is poorly characterized, hence authors of recent reviews call it the 'orphan PIP' (Lecompte *et al.*, 2008). PI5P may be generated by the phosphorylation of PI but also by the dephosphorylation of PI4,5P₂ and PI3,5P₂ (sections 1.4.1.3, 1.4.2.1 and 1.4.2.2; Shisheva, 2008; Tronchére *et al.*, 2004;). It is also discussed that PI5P may serve as a precursor for PI4,5P₂ generation (Rameh *et al.*, 1997; Coronas *et al.*, 2007). Although putative interacting phosphatases and kinases have been identified, PI5P function and turnover are still elusive. Its synthesis should be directly linked to the generation of PI3P, PI3,5P₂, and PI4,5P₂. Since these PIPs are well characterized regarding functions in endocytosis and membrane trafficking (sections 1.3.1, 1.3.3, and 1.3.4), it is likely that PI5P has a related function. Lecompte and colleagues (2008) speculate that PI5P may be found on endosomal compartments and regulates exocytosis of endosomal derived transport vesicles.

1.4 PIP-metabolizing enzymes

The heterogeneous distribution of PIPs among organelles is maintained by a huge variety of PIP-metabolizing kinases and phosphatases. Since PIPs pilot numerous essential processes in the cell, their misregulation was found to be causal for many diseases, frequently linked to mutations of PIP-metabolizing enzymes (Halstead *et al.*, 2005; Volpicelli and De Camilli, 2007; Vicinanza *et al.*, 2008; Majerus and York, 2009). In the following, the major enzyme classes and prominent members are introduced.

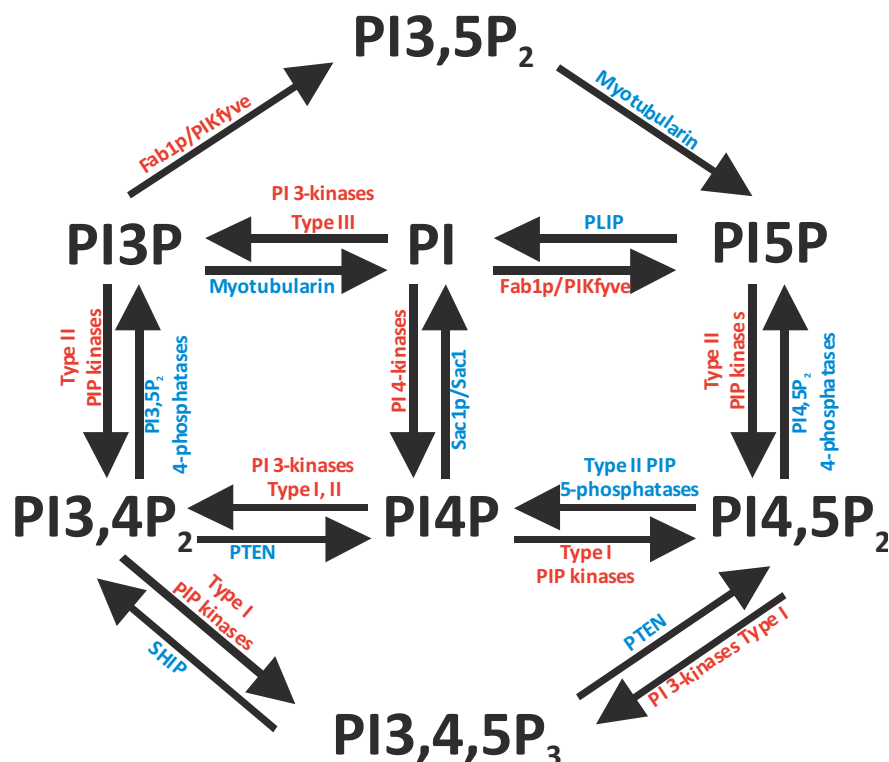


Figure 5 Phosphoinositides are interconvertible

All phosphoinositides can be interconverted by specific kinases (red) and phosphatases (blue) (according to Blero *et al.*, 2007, modified).

1.4.1 PI and PIP kinases

Until today, different classes of PI and PIP kinases have been described which are distinguished by their substrate preference. All these enzymes have a well conserved kinase domain (Fruman *et al.*, 1998; Anderson *et al.*, 1999; Heck *et al.*, 2007). Since they share several key residues in the catalytic domain and also other structure elements with classical protein kinases, it is widely accepted that lipid kinases have evolved from this protein family (Rao *et al.*, 1998; Grishin, 1999). PI and PIP kinases are mainly cytosolic proteins which are recruited to membranes by the binding to their substrates but also by regulating proteins like small guanine nucleotide-binding proteins (Rodriguez-Viciano *et al.*, 1997; Lopez-Illasaca *et al.*, 1997; Santarius *et al.*, 2006).

1.4.1.1 PI and PIP 3-kinases

The multifaceted group of PI and PIP 3-kinases is subdivided into different classes. Subdivision is dependent on protein structure and interaction partners. However, beside the catalytic PIP kinase domain, these enzymes all possess a conserved 3-kinase specific domain (Fruman *et al.*, 1998; Engelman *et al.*, 2006).

So-called Class I enzymes can phosphorylate PI and all other phosphoinositides at the D-3 position *in vitro*. Their main reaction product *in vivo* appears to be PI3,4,5P₃ (section 1.3.5; Vanhaesebroeck *et al.*, 2001). Hence, Class I 3-kinases have an important role in signal transduction from the PM to the cell interior and are known to regulate different pathways associated with cell growth and longevity (Fruman *et al.*, 1998). Beside their lipid kinase activity, they still possess the catalytic activity of their protein kinase ancestors. This protein-targeted catalytic activity is mainly aimed to interacting proteins and the enzyme itself (Vanhaesebroeck *et al.*, 1997; Stoyanova *et al.*, 1997). This autophosphorylation has shown to regulate the intrinsic lipid kinase activity (Wu *et al.*, 2007).

In contrast to Class I or Class III, Class II enzymes do not have regulatory proteins. They can phosphorylate PI and PI4P at the D-3 position of the inositol ring (Falasca and Maffucci, 2007).

Class III enzymes only phosphorylate PI. Therefore, they are designated as PI 3-kinases. The founder of this enzyme family was firstly described in *Saccharomyces cerevisiae* (*S. cerevisiae*) in a screen for mutants defective in vacuolar protein sorting and thus termed Vps34p (Herman *et al.*, 1990). The vacuole of fungi is related to the lysosomes of higher eukaryotes and Vps34p homologs in mammals, drosophila, and *Caenorhabditis elegans* (*C. elegans*) appear to act on the membrane trafficking route between the Golgi apparatus, endosomes, and lysosomes (Volinia *et al.*, 1995; Linassier *et al.*, 1997; Wurmser *et al.*, 1999; Roggo *et al.*, 2002).

1.4.1.2 PI 4-kinases

As indicated in their designation, PI 4-kinases phosphorylate only PI at the D-4 position of the inositol ring. No other phosphoinositides are phosphorylated by these enzymes. The first PI 4-kinases were identified in *S. cerevisiae* and designated Pik1p (Flanagan *et al.*, 1992) and Stt4p (Fruman *et al.*, 1998). Later, mammalian homologs have been identified (Wong *et al.*, 1994; Flanagan *et al.*, 1993). PI 4-kinases are ubiquitously expressed among different tissues and are located at cellular membranes including the Golgi apparatus and various vesicles (Flanagan *et al.*, 1993; Wong *et al.*, 1997; Fruman *et al.*, 1998; Guo *et al.*, 2003).

1.4.1.3 PIP 4-kinases and PIP 5-kinases

PIP 4-kinases and PIP 5-kinases have originally been classified based upon sequence similarities. Later, their substrate preference has been taken as an additional classification criterion (Boronenkov *et al.*, 1995; Ishihara *et al.*, 1996; Loijens *et al.*, 1996). On the basis of both criteria, they are divided into three major groups termed Type I, Type II, and Type III (Fruman *et al.*, 1998).

In mammals, until now three different isoforms of Type I PIP kinases have been described and are well characterized (Rameh *et al.*, 1997; Ishihara *et al.*, 1998). Since their main function in cells appears to be the phosphorylation of PI4P yielding PI4,5P₂ (section 1.3.1), they are designated PI4P 5-kinases (Stephens *et al.*, 1991; Fruman *et al.*, 1998), although they are also able to catalyze other reactions with lower affinity *in vitro* (PI3,4P₂ to PI3,4,5P₃ and PI3P to PI3,5P₂) (Whiteford *et al.*, 1997; Dove *et al.*, 1997; Zhang *et al.*, 1997). Type I PIP kinases localize to the PM, but are also present at the Golgi apparatus and in the nucleus (Boronenkov *et al.*, 1998; Ishihara *et al.*, 1998; Nishikawa *et al.*, 1998). Type I function is required for actin reorganization, secretion, endocytosis, clathrin coat assembly, and regulation of DCV exocytosis (Hay *et al.*, 1995; Ishihara *et al.*, 1998; Arneson *et al.*, 1999; Gong *et al.*, 2005). In *S. cerevisiae*, the sole Type I PIP kinase Mss4p localizes to the PM, and together with the PI 4-kinase Stt4p (section 1.4.1.2), it regulates the organization of the actin cytoskeleton (Homma *et al.*, 1998; Desrivieres *et al.*, 1998; Tolia *et al.*, 1998; Shibasaki *et al.*, 1997). Thus, some functions of Type I PIP kinases may be evolutionarily conserved.

Type II enzymes are also thought to produce mainly PI4,5P₂. But unlike Type I enzymes, they do not use PI4P but PI5P as a substrate and hence are termed PI5P 4-kinases (Rameh *et al.*, 1997; Zhang *et al.*, 1997). Type II enzymes are only found in animals with three occurring isoforms in mammals (Clarke *et al.*, 2007). They can phosphorylate the D-4 position of PI3P *in vitro*, however, PI5P is their preferred substrate (Rameh *et al.*, 1997; Zhang *et al.*, 1997). Although PI5P 4-kinases are thought to generate mainly the same product such as known for PI4P 5-kinases, their functions seem to be unique (Clarke *et al.*, 2007). However, there is some evidence for a probably direct interaction of Type I and Type II enzymes (Hinchliffe *et al.*, 2002). All Type II enzymes are biochemically well characterized, but their physiological roles are still elusive. Different lines of evidence point towards functions ranging from cell signaling to membrane trafficking (Clarke *et al.*, 2007).

Type III PIP kinases catalyze the 5-phosphorylation of PI3P (section 1.3.3) to PI3,5P₂ (section 1.3.4) and are conserved among eukaryotes (Jefferies *et al.*, 2008; Dove *et al.*, 2009). The prototype Fab1p of *S. cerevisiae* comprises a PI3P-binding FYVE domain at its N-terminus, a regulatory domain, and the lipid kinase domain near the C-terminus. Fab1p is found at the yeast vacuole where it is involved in membrane trafficking and vacuolar size regulation by controlling PI3,5P₃ levels (Jefferies *et al.*, 2008). Fab1p and its mammalian homolog PIKfyve are hypothesized to be part of a protein complex build of up- and downstream effectors of Fab1p and PIKfyve, respectively (Gary *et al.*, 2002; Jefferies *et al.*, 2008; Dove *et al.*, 2009). In addition, PIKfyve was observed to phosphorylate PI at the D-5 position *in vitro*, however, this synthesis route for PI5P was not yet shown *in vivo* (Dove *et al.*, 2009).

1.4.2 PIP phosphatases

Up to date, the majority of PIP-metabolizing enzymes identified to play a role in diseases are PIP phosphatases (Volpicelli-Daley and De Camilli, 2007; Majerus and York, 2009; Ooms *et al.*, 2009). Like PI and PIP kinases, they are subdivided by their preferred substrate and are derived from protein-metabolizing enzymes e.g. the family of protein tyrosine phosphatases or the dual-specificity serine/threonine phosphatases (Fauman and Saper, 1996).

1.4.2.1 PIP 3-phosphatases

One of the most extensively studied PIP 3-phosphatases is the human tumor suppressor PTEN (phosphatase and tensin homolog deleted on chromosome 10, also known as MMAC (mutated in multiple advanced cancers); Blero *et al.*, 2007, Maehama *et al.*, 2007). Mutations of the associated gene lead to a variety of human cancers (Li *et al.*, 1997; Maehama and Dixon, 1999; Marsh *et al.*, 1999). Although some protein phosphatase activity is detectable, PTEN seems to prefer PIPs as substrates and is able to dephosphorylate PI3P, PI3,4P₂, and PI3,4,5P₃ *in vitro* at the D-3 position of the inositol ring (Maehama and Dixon, 1998). Its most important substrate *in vivo* is PI3,4,5P₃ (Leslie and Downes, 2004). As described above, PI3,4,5P₃ is an important second messenger in cell signaling (section 1.3.5).

Another important group of PIP 3-phosphatases is the myotubularin family. The founder myotubularin (MTM1) was identified to be mutated in X-linked myotubular myopathy (Laporte *et al.*, 1996). Since then, 14 members of this protein family have been described in humans (Clague and Lorenzo, 2005; Robinson and Dixon, 2006). Some of the family members are involved in myelin neuropathies e.g. Charcot-Marie-Tooth disease (Bolino *et al.*, 2000; Senderek *et al.*, 2006). Interestingly, about half of these proteins are catalytically inactive but possess the ability to form heterodimers with active myotubularin-related (MTMR) proteins (Robinson and Dixon, 2006). MTM1 and active MTMRs can dephosphorylate PI3P and PI3,5P₂ at the D-3 position of the inositol ring (Tronchère *et al.*, 2004; Robinson and Dixon, 2006). PI3P and PI3,5P₂ have shown to be important regulators of endocytosis and membrane trafficking between the Golgi apparatus, endosomes, and lysosomes (sections 1.3.3 and 1.3.4). Studies of the myotubularin homologs of *S. cerevisiae* and *C. elegans* indicate that they could be negative regulators of endocytic trafficking (Xue *et al.*, 2003; Parrish *et al.*, 2004).

1.4.2.2 PIP 4-phosphatases and PIP 5-phosphatases

Dependent on their preferred substrate, phosphoinositide 4-phosphatases fall into two different groups. As denoted in the name, PI3,4P₂ 4-phosphatases hydrolyze the D-4 position of PI3,4P₂ (section 1.3.5). In mammals, two widely expressed isoforms exist, which are still poorly characterized (Norris *et al.*, 1997; Blero *et al.*, 2007). Recent studies revealed that PI3,4P₂ 4-phosphatases are associated with the phenotype of the so-called weeble mutant mice which is mainly characterized by the cellular loss in the cerebellum resulting in uncoordinated movement and neonatal death (Nystuen *et al.*, 2001).

PI4,5P₂ 4-phosphatases were originally described in prokaryotes. Although most bacteria do not possess PIPs or PIP-metabolizing enzymes (Michell, 2008), pathogens like *Shigella flexneri* encode an inositol polyphosphate 4-phosphatase on the invasion plasmid which is injected into the host cell (Cossart *et al.*, 2004). The expression of this 4-phosphatase leads to the conversion of PI4,5P₂ (section 1.3.1) and subsequent increase of PI5P, thus leading to a rearrangement of the actin cytoskeleton and membrane during bacterial entry (Niebuhr *et al.*, 2002). In mammals, two orthologs of this prokaryotic protein have been identified so far (Ungewickell *et al.*, 2005). Both are able to dephosphorylate PI4,5P₂ to PI5P *in vitro*. These proteins are ubiquitously expressed and are

associated with membranes of the endosomal/lysosomal system (Ungewickell *et al.*, 2005; Blero *et al.*, 2007; Coronas *et al.*, 2007).

Enzymes which are able to dephosphorylate the D-5 position of the inositol ring were originally referred to as inositol 5-phosphatases. While Type I 5-phosphatases only use soluble polyphosphate inositols as a substrate, Type II 5-phosphatases hydrolyze primarily the D-5 phosphate group of PI5P, PI4,5P₂, or PI3,4,5P₃ (Blero *et al.*, 2007). Type I and Type II 5-phosphatases share the same catalytic domain but Type II enzymes have extended C-terminal and/or N-terminal regions, containing additional and different domains. Up to date, nine different Type II enzymes have been identified in humans. Studies of their orthologs in yeast implicated essential functions in membrane trafficking (Blero *et al.*, 2007).

An important member of the Type II 5-phosphatase group is OCRL, an enzyme deficient in patients affected by the oculo-cerebro-renal Lowe syndrome. This complex disease has shown to be X-linked recessive, often accompanied by neurological defects (Attree *et al.*, 1992). OCRL seems to prefer PI4,5P₂ as a substrate (Schmid *et al.*, 2004) and localizes to the Golgi apparatus and early endosomes. Phenotypic analysis of Lowe patients' tissues suggests a link to lysosomal trafficking (Lowe, 2005).

Type III enzymes hydrolyze the D-5 position of PIPs and inositol polyphosphate which are also phosphorylated of the 3rd position of the inositol ring (Blero *et al.*, 2007). Amongst others, a SH2 domain can be found at the N-terminus of a subgroup of these proteins, which are in turn named SHIPs (SH2 domain-containing inositol 5-phosphatases). SHIPs are hypothesized to negatively regulate the signaling pathways activated by PI3,4,5P₃ and PIP 3-kinases, respectively, a function suggested also for Type IV phosphatases which were shown to dephosphorylate the D-5 position of PI3,5P₂, PI4,5P₂, and PI3,4,5P₃ (Blero *et al.*, 2007).

A recently discovered PIP 5-phosphatase was identified during the search for PTEN homologs in *Dictyostelium* and named PLIP (PTEN-like phosphatase) (Merlot *et al.*, 2003). The related protein in mammals is named PTPMT1 and was shown to dephosphorylate PI5P *in vitro* (Doughty *et al.*, 2010).

The 5-phosphatase domain is also found in the PIP phosphatase synaptojanin, which is directly implicated in membrane trafficking at the synapse (section 1.2; Figure 3) and is a candidate to be involved in bipolar disorder (McPherson *et al.*, 1996; Guo *et al.*, 1999; Stopkova *et al.*, 2004). Synaptojanin represents the subfamily of 5-phosphatases possessing in total two independent phosphatase domains one of which is named Sac domain (section 1.4.2.3) and located in the proteins' N-terminus (SCIPs, Sac domain-containing inositide 5-phosphatases). Therefore, synaptojanin has a dual phosphatase activity and can remove phosphate from the D-5 as well as from the D-4 position of PI4,5P₂ (Hughes *et al.*, 2000).

1.4.2.3 The Sac domain

The Sac domain is a highly conserved PIP-specific phosphatase domain, found in PIP phosphatases from yeast to mammals (Hughes *et al.*, 2001; Guo *et al.*, 1999). The founder of the Sac domain-containing protein group was identified in *S. cerevisiae*. This protein was termed Sac1p (suppressor of actin) because it has shown to interact with actin-regulating factors (Foti *et al.*, 2001). Sac domain-containing proteins fall into two groups: Synaptojanin-like phosphatases with an additional

5-phosphatase domain (Stefan *et al.*, 2002) and Sac1p-like proteins which possess only the Sac domain (Hughes *et al.*, 2001).

Sac1p in yeast and its mammalian homologs are found at the ER and the Golgi apparatus (Konrad *et al.*, 2002; Nemoto *et al.*, 2000; Rohde *et al.*, 2003). The major part of these transmembrane proteins points to the cytosol (Blagoveshchenskaya and Mayinger, 2009). Their main substrate *in vivo* is supposed to be PI4P, a phosphoinositide described to be essential for membrane trafficking from the Golgi apparatus to the cell periphery (Godi *et al.*, 2004) and for the synthesis of PI4,5P₂ (section 1.3.1). By the shuttling between the ER and the Golgi apparatus, Sac1p and homologs are hypothesized to regulate the concentration of PI4P in response to metabolites, which control cell size and growth (Blagoveshchenskaya and Mayinger, 2009).

S. cerevisiae possess a second Sac1p-like phosphatase named Fig4p which mainly hydrolyzes the D-5 position of PI3,5P₂ in complex with different regulating proteins. Fig4p is supposed to interact with Type III PIP kinase Fab1p (Gary *et al.*, 2002) regulating the PI3,5P₂ concentration at the vacuole in response to osmotic shock (Rudge *et al.*, 2004; Duex *et al.*, 2006a; Duex *et al.*, 2006b). The mammalian homolog Fig4 (for historical reasons also termed Sac3) appears to be a candidate to be mutated in patients with a special subtype of the disease Charcot-Marie-Tooth (Chow *et al.*, 2007). The according knock out mice show massive neuronal degeneration (Chow *et al.*, 2007; Jin *et al.*, 2008). In rats, Fig4 is discussed to be involved in neuronal cell growth (Yuan *et al.*, 2007)

In animals, a third Sac1p-like protein was identified by sequence comparison. Until today, only the human homolog named hSac2 was analyzed regarding its expression in brain, heart, skeletal muscle, and kidney as well as catalytic activity. hSac2 hydrolyzes primarily the D-5 position of PI4,5P₂ and can therefore be expected to be important for the regulation of several cellular functions (Minagawa *et al.*, 2001).

1.5 The soil nematode *C. elegans* as a model system

Since the 1970s, the round worm *C. elegans* (Maupas, 1900; Brenner, 1973) became a more and more popular model organism to address multifaceted questions of basic research, ranging from molecular cell biology to developmental genetics. One of the most cited advantages of this nematode is its small cell number and its conserved cell lineage, meaning that cells and tissues of individual animals divide and develop in a comparable manner (Sulston and Horvitz, 1977). Although adult hermaphrodites have only 959 cells, nearly every cell type identified in higher animals e.g. mammals can be found in *C. elegans*. This 'simplification' is also more or less true for the *C. elegans* genome: In most cases, complex protein families of mammalia which are encoded by many different genes and splicing variants are represented by only one or very few genes of the nematode (The *C. elegans* Sequencing Consortium, 1998). In conclusion, *C. elegans* (mostly termed 'the worm' among the *C. elegans* research community) is a qualified model to answer many essential questions in life sciences.

Since adult hermaphrodites possess only 302 neurons which positions and wiring are completely determined (Figure 6), (Durbin, 1987), the nematode is an appropriate system to analyze the basic principles underlying different neuronal processes. *C. elegans* is transparent from egg to adult and can be easily made transgenic for fusion proteins expressed in the desired subset of cells using well-

characterized specific promoters (Dupuy *et al.*, 2004). Hence, the imaging of living animals under a confocal microscope was often the method of choice during the presented study. In addition, behavioral phenotypes of wild type and mutant nematodes can be conveniently observed and measured by behavior tests or toxin assays (Hope, 1999). Furthermore, the specific knock down of gene expression, mediated by double-stranded ribonucleic acid (dsRNA), should be highlighted. This phenomenon, termed RNA interference (RNAi), was discovered in *C. elegans* (Fire *et al.*, 1998) and turned out to be a conserved pathway among eukaryotes controlling gene expression (Sidahmed and Wilkie, 2010). Up to date, RNAi-mediated knock down by exogenous dsRNA is a widely use application to analyze the function of genes *in vivo*, not only for *C. elegans* but also for other model systems.



Figure 6 *The nervous system of Caenorhabditis elegans*

Nervous system of Caenorhabditis elegans, labeled by the pan-neuronal expressed and green fluorescent protein (GFP)-labeled kinesin-3 (UNC-104). Shortly posterior the head (right), the so-called nerve-ring is visible, an accumulation of neuronal cell bodies and processes (image by Dieter Klopfenstein).

1.6 Aim of this study

Synaptic function relies on tightly regulated membrane trafficking. The different phosphoinositide species regulating these transport processes have been identified and characterized in the last years. However, the protein machinery maintaining the differently phosphorylated PIPs at diverse membrane compartments, thus contributing to neuronal membrane trafficking, is still poorly understood.

This lack of knowledge is basically due to the occurrence of a huge variety of PIP-metabolizing enzymes and isoforms with overlapping functions in mammalia. *C. elegans* possesses homologous PI/PIP kinases and PIP phosphatases, but other than in mammalia, the corresponding genes of *C. elegans* frequently occur as single gene copies (www.wormbase.org, database release WS211). Therefore, the nematode is a promising model organism to shed light on the complex regulation of PIPs in neuronal membrane trafficking. The aim of this study was to identify and further characterize PIP-metabolizing enzymes with a novel function in neuronal membrane trafficking by using the unique properties of *C. elegans*.

2 Material and methods

2.1 Chemicals and reagents

Chemicals and reagents were purchased as listed below (Table 1) from the following companies: SIGMA-ALDRICH CHEMIE GMBH (Steinheim, Germany), CARL ROTH GMBH + CO. KG (Karlsruhe, Germany), FORMEDIUM (Norfolk, United Kingdom), AMERSHAM BIOSCIENCES EUROPE GMBH (Freiburg, Germany), NEW ENGLAND BIOLABS GMBH (Frankfurt am Main, Germany), FLUKA CHEMIKA/BIOCHEMIKA (Buchs, Switzerland), AMBION (EUROPE) LTD (Huntingdon, United Kingdom), WHATMAN GMBH (Dassel, Germany), INVITROGEN (Karlsruhe, Germany), and ROCHE DIAGNOSTICS (Mannheim, Germany).

Table 1 Chemicals and reagents

chemical or reagent	manufacturer
3-(N-morpholino)propanesulfonic acid (MOPS)	SIGMA-ALDRICH
acetic acid	CARL ROTH
acrylamid (Rotiphorese Gel 30)	CARL ROTH
agar agar	CARL ROTH
agarose	CARL ROTH
aldicarb	SIGMA-ALDRICH
ammonium peroxosulfate (APS)	CARL ROTH
ampicillin	CARL ROTH
beta-mercaptoethanol	CARL ROTH
bromphenol blue	SIGMA-ALDRICH
calcium chloride	CARL ROTH
chemiluminescence film	AMERSHAM BIOSCIENCES
chloramphenicol	CARL ROTH
chloroform	FLUKA CHEMIKA
cholesterol	SIGMA-ALDRICH
copper(II) sulfate	SIGMA-ALDRICH
deoxynucleotide solution mix (dNTPs)	NEW ENGLAND BIOLABS
dextrose	CARL ROTH
dimethyl sulfoxide (DMSO)	CARL ROTH
disodium hydrogen phosphate	CARL ROTH
ethanol	CARL ROTH
ethidium bromide	CARL ROTH
ethylenediaminetetraacetic acid (EDTA)	CARL ROTH
G418	SIGMA-ALDRICH
glucose	CARL ROTH
glycerol	CARL ROTH
glycin	CARL ROTH
GlycoBlue	AMBION
hydrochloric acid (HCl)	CARL ROTH
isopropanol	CARL ROTH
isopropyl beta-D-1-thiogalactopyronoside (IPTG)	CARL ROTH
kanamycin sulfate	CARL ROTH
levamisole (tetramisole hydrochloride)	FLUKA CHEMIKA
L-histidine	FLUKA BIOCHEMIKA
lithium acetate	CARL ROTH
L-leucine	FLUKA BIOCHEMIKA
L-methionine	FLUKA BIOCHEMIKA

Table 1 Chemicals and reagents (continued)

magnesium chloride	CARL ROTH
magnesium sulfate	CARL ROTH
manganese(II) chloride	CARL ROTH
methanol	CARL ROTH
nitrocellulose	WHATMAN
nystatin	SIGMA-ALDRICH
pentylenetetrazole	SIGMA-ALDRICH
peptone	CARL ROTH
phenol	CARL ROTH
phosphoric acid	SIGMA-ALDRICH
polyethylene glycol (PEG4000 and PEG8000)	CARL ROTH
potassium chloride	CARL ROTH
potassium dihydrogen phosphate	CARL ROTH
potassium hydroxide	CARL ROTH
protease inhibitor cocktail tablets	ROCHE DIAGNOSTICS
proteinase K	NEW ENGLAND BIOLABS
RNase A	Transcriptome Analysis Laboratory (TAL), University of Göttingen
RNase-free water	CARL ROTH
rubidium chloride	CARL ROTH
salmon sperm DNA	INVITROGEN
sodium acetate	CARL ROTH
sodium chloride	CARL ROTH
sodium dodecyl sulfate (SDS)	CARL ROTH
sodium hydroxide	CARL ROTH
sodium hypochlorite with 12 % chlorine	CARL ROTH
streptomycin	SIGMA-ALDRICH
sucrose	CARL ROTH
tetracycline	SIGMA-ALDRICH
tetramethylethylenediamin (TEMED)	CARL ROTH
tris(hydroxymethyl)aminomethane (Tris)	CARL ROTH
Triton X-100	FLUKA BIOCHEMIKA
TRIzol	INVITROGEN
Tween 20	CARL ROTH
uracil	SIGMA-ALDRICH
yeast extract	CARL ROTH
yeast nitrogen base (with and without inositol)	FORMEDIUM

2.2 Molecular cloning

2.2.1 *E. coli* strains and maintenance

If not stated otherwise, *Escherichia coli* (*E. coli*) strains (Table 2) were grown at 37°C on LB plates (5 g/L yeast extract, 10 g/L peptone, 10 g/L sodium chloride, 15 g/L agar agar; Bertani, 1951) or SOB plates (5 g/L yeast extract, 20 g/L peptone, 0.5 g/L sodium chloride, 0.2 g/L potassium chloride, 15 g/L agar agar; Hanahan, 1983). Liquid bacteria cultures were grown in medium without agar agar at 37°C and 150 rpm. Dependent on *E. coli* strain and transformed vectors, appropriate antibiotics were used (100 mg/L ampicillin, 50 mg/L kanamycin, 25 mg/L streptomycin, or 12.5 mg/L tetracycline (in 50 % (v/v) ethanol), 15 mg/L chloramphenicol (in ethanol)). For long term storage, 400 µL of an overnight culture were mixed with 600 µL of a 1:1 (v/v) solution of LB liquid medium and glycerol and stored at -80°C.

Table 2 *E. coli* strains used for cloning

strain name	genotype	purpose
DB3.1 (INVITROGEN)	F ⁻ <i>gyrA462 endA1 Δ(sr1 -recA) mcrB mrr hsdS20(r_B⁻, m_B⁻) sup E44 ara-14 galK2 lacY1 proA2 rpsL20(Sm^R) xyl-5 lambda-leu mtl1</i>	propagation of Gateway vectors
TOP10 (INVITROGEN)	F ⁻ <i>mcrA Δ(mrr-hsdRMA-mcrBC) phi80lacZΔM15 ΔlacX74 recA1 araD139 Δ(araleu) 7697 galU galK rpsL (StrR) endA1 nupG</i>	general cloning

2.2.2 Polymerase chain reaction

The method of the polymerase chain reaction (PCR; Saiki *et al.*, 1988) was used to amplify different DNA sequences of choice by using specific primers from either *C. elegans* complementary DNA (cDNA), *C. elegans* gDNA, *S. cerevisiae* total DNA, or plasmid DNA for cloning or genotyping. Proof-reading Phusion High Fidelity polymerase or Taq polymerase (both purchased from NEW ENGLAND BIOLABS) were used following the manufacturer's instructions. Oligonucleotides (primers) were purchased from EUROFINs MWG OPERON (Ebersberg, Germany). Sequences can be found in the Appendix.

PCR products were mixed with 6 x loading dye (50 % (v/v) glycerol, 10 mM EDTA (pH = 8.0), 0.25 % (w/v) bromophenol blue) and analyzed by electrophoresis in 1-2 % agarose gels made in TAE buffer (4.84 g/L Tris, 1.4 mL acetic acid, 10 mL 0.5 M EDTA) containing ethidium bromide (10 µg/mL) and visualized by ultraviolet light. DNA band sizes were compared to molecular weight markers obtained from NEW ENGLAND BIOLABS. For gel extraction, DNA bands were cut from the gel and eluted with the MinElute Gel Extraction kit from QIAGEN (Hilden, Germany) according to the manufacturer's instructions.

PCR products were precipitated with PEG8000. The PCR product was mixed with 2 volumes of 30 % PEG8000/30 mM magnesium chloride and 3 volumes of TE buffer (10 mM Tris-HCl, 1 mM EDTA, pH = 7.5) and centrifuged at 16000 x g for 40 minutes at room temperature.

2.2.3 Cloning with Gateway

The Gateway Cloning Technology (INVITROGEN) is based on the attachment (*att*) site-specific recombination mechanism of the bacteriophage lambda (Landy, 1989) and facilitates the transfer of heterologous DNA sequences between vectors (Hartley *et al.*, 2000).

As a first step, the DNA sequence of choice was amplified by PCR from template DNA by specific primers containing *attB* sites. These *attB* sites react specifically with *attP* sites which flank the so-called Gateway cassette in a donor vector. For this study, the donor vector pDONR201 of INVITROGEN was used whose Gateway cassette contains a chloramphenicol resistance gene and the *ccdB* gene (section 2.2.7). The gene product of *ccdB* is lethal to TOP 10 but not DB3.1 *E. coli* (section 2.2.1) which were used to propagate vectors with a Gateway cassette (Bernard and Couturier, 1992; Miki *et al.*, 1992).

The recombination between the *attB* sites of the PCR product and the *attP* sites of the donor vector is catalyzed by a mixture of enzymes binding specifically to these sites. This BP reaction replaces the

Gateway cassette by the sequence of choice and gives rise to *attL*-sites in the newly created Entry vector. Successfully recombined vectors were selected by transformation in TOP10 *E. coli*.

As a second step, the *attL*-flanked sequence of choice was transferred into different destination vectors for RNAi feeding, expression in *C. elegans*, expression in *S. cerevisiae*, or expression in *E. coli* by the so-called LR reaction. The LR reaction facilitates specific recombination of the *attL* sites of the entry clone with *attR* sites which flank a Gateway cassette (comparable to the cassette of pDONR201) of the destination vector and is catalyzed by enzymes binding specifically to these sites.

Cloning with Gateway was performed according to the manufacturer's instructions.

2.2.4 Conventional cloning

For conventional cloning with restriction endonucleases (NEW ENGLAND BIOLABS), the DNA sequence of choice was amplified by PCR from template DNA (section 2.2.2) using specific primers containing appropriate restriction sites. PCR products were then cloned into the pCR Blunt Vector using the Zero Blunt PCR Cloning kit from INVITROGEN.

The chosen target vector was digested with according restriction enzymes and purified by gel elution (section 2.2.2). The DNA sequence of choice was then cut from the pCR Blunt vector using again appropriate restriction endonucleases, gel eluted, and ligated with the target vector. DNA ligation was performed by Ligation Kit 2.1 by TAKARA BIO EUROPE (Saint-Germain-en-Laye, France) following the manufacturer's instructions.

2.2.5 Transformation of *E. coli*

2.2.5.1 Preparation of chemically competent *E. coli*

500 mL *E. coli* culture were grown until an OD₆₀₀ of 0.4 to 0.7 was reached and harvested by centrifugation for 10 minutes at 3345 x g at room temperature. The pellet was resuspended in 150 mL of ice cold buffer 1 (100 mM rubidium chloride, 10 mM calcium chloride, 30 mM potassium chloride, 50 mM manganese(II) chloride, 15 % (v/v) glycerol) and incubated on ice for 15 minutes. After a second centrifugation step, the pellet was resuspended in 20 mL ice cold buffer 2 (10 mM MOPS, 10 mM rubidium chloride, 75 mM calcium chloride, 15 % (v/v) glycerol), aliquoted (200 µL), shock frosted in liquid nitrogen, and stored at -80°C until use.

2.2.5.2 Transformation of chemically competent *E. coli*

100 µL of competent *E. coli* cells were gently mixed with vector DNA and incubated on ice for 40 minutes. After a heat shock at 42°C for 45 seconds, 500 µL of liquid LB or SOB medium were added. Cells were incubated for 1 hour shaking at 37°C, then plated on LB plates with appropriate antibiotics and incubated over night at 37°C.

2.2.6 Plasmid DNA purification and DNA sequencing

Plasmid DNA from *E. coli* liquid culture was purified by using different kits (NucleoSpin Plasmid, Nucleobind AX) from MACHEREY-NAGEL (Dueren, Germany). Plasmid DNA was prepared for sequencing using BigDye Terminator v1.1 Cycle Sequencing Kit of APPLIED BIOSCIENCES (Darmstadt, Germany) following the instructions of the manufacturer. Sequencing was performed by the sequencing facility of the University of Göttingen at the Göttingen Center for Molecular Biosciences.

2.2.7 Vectors used in this study

pDONR201

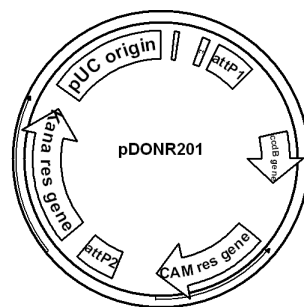


Figure 7 Map of pDONR201 from INVITROGEN

T2, *rrnB* *T2* transcription termination sequence; *T1*, *rrnB* *T1* transcription termination sequence; *attP1*, attachment site; *CAM res gene*, chloramphenicol resistance gene; *attP2*, attachment site; *Kana res gene*, kanamycin resistance gene.

pDONR201 from INVITROGEN was used as a basic cloning vector for cloning with Gateway (section 2.2.3). The Gateway cassette of pDONR201 is flanked by *attP* sites and contains a chloramphenicol resistance gene and the sequence of the *ccdB* gene (Bernard and Couturier, 1992; Miki *et al.*, 1992). In addition, pDONR201 encodes a kanamycin resistance gene (Figure 7).

pCR blunt

pCR Blunt (INVITROGEN) was used together with the Zero Blunt PCR cloning kit from INVITROGEN for sub cloning and used following the manufacturer's instructions.

L4440

The L4440 vector was created in the laboratory of Andrew Fire, Stanford Departments of Pathology and Genetics, U.S.A., for RNAi in *C. elegans* (www.addgene.org, Plasmid 1654: L4440). The multiple cloning site of this vector is flanked by two T7 promoters. Transformed in an appropriate *E. coli* strain, a sequence of choice cloned between these two T7 promoters is transcribed to double-

stranded RNA (section 2.3.8.1). In this study, L4440 without an insert was used as negative control for RNAi feeding (section 2.3.8.3). For Gateway cloning, the modified vector **L4440gtwy** (www.addgene.org, Plasmid 11344: L4440gtwy) was used. In L4440gtwy, a Gateway cassette with *attR* sites (section 2.2.3) was cloned between the T7 promoters using *EcoRV* sites (Figure 8).

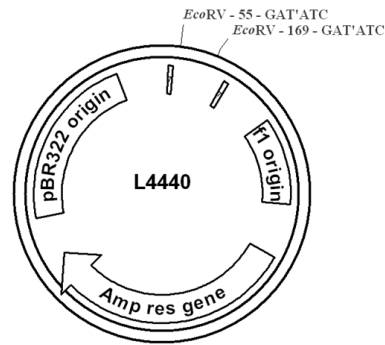


Figure 8 Map of L4440 from the Fire lab

T7, T7 promoter; Amp res gene, ampicillin resistance gene.

Prab-3::GFP::Gateway

This vector is based on the *C. elegans* expression vector pSM *Pmig-13::GFP::Gateway* from the laboratory of Kang Shen, Stanford Institute for Neuro-Innovation & Translational Neurosciences, U.S.A., which was modified for this study by conventional cloning (section 2.2.4). Modification comprised an exchange of the promoter sequence against the promoter sequence of *rab-3*, which was obtained from the plasmid **pUH4 Prab-3::GFP** provided by Stefan Eimer, European Neuroscience Institute, University of Göttingen. The promoter sequence (P) of *mig-13* drives expression only in a specific subset of neurons, whereas the promoter of *rab-3* drives pan-neuronal expression. Thus modified, the newly created vector (Figure 9) enables expression of GFP-tagged fusions in all neurons of *C. elegans*. The sequence of *Prab-3::GFP::Gateway* can be found in the Appendix.

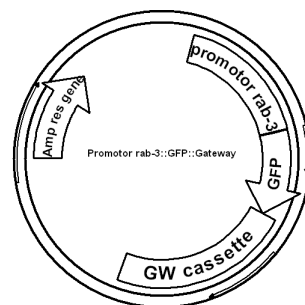


Figure 9 Map of Prab-3::GFP::Gateway

Amp res gene, ampicillin resistance gene; GW cassette, gateway cassette.

Prab-3::mCherry::Gateway

This vector is based on the *C. elegans* expression vector pSM *Pmig-13::mCherry::Gateway* (also from the laboratory of Kang Shen), which was modified essentially as described for *Prab-3::GFP::Gateway* (Figure 9). The sequence of *Prab-3::mCherry::Gateway* (mCherry, red fluorescent protein) can be found in the Appendix.

pGEX-6P-D21

This vector was created by the laboratory of Erich Wanker at the Max Delbrueck Center for Molecular Medicine, Berlin-Buch, Germany. It is based on the pGEX-6P vector series of AMERSHAM BIOSCIENCES for IPTG-induced recombinant protein expression in *E. coli*. pGEX-6P vectors contain a constitutive *tac* promoter and an ampicillin resistance gene. pGEX-6P-D21 encodes a N-terminal GST-tag in frame with a Gateway cassette (section 2.2.3).

pVV215

pVV215 was used for the expression of HA-tagged proteins in *S. cerevisiae* and was purchased from the EUROPEAN *SACCHAROMYCES CEREVISIAE* ARCHIVE FOR FUNCTIONAL ANALYSIS (Frankfurt, Germany). It contains an ampicillin resistance gene and the *URA3* gene as a marker for selecting *S. cerevisiae* transformants. pVV215 encodes the constitutive yeast *PGK* promoter which is located in front of a Gateway cassette in frame with a C-terminal 3xHA-tag (web.uni-frankfurt.de/fb15/mikro/euroscarf/data/pVV215.html).

The following table (Table 3) lists all other vectors used in this study except sub cloning and entry vectors. Sequences cloned for this study were amplified from a *C. elegans* cDNA library from the laboratory of Stefan Eimer or *C. elegans* cDNA library clones from OPEN BIOSYSTEM, part of THERMO FISHER SCIENTIFIC GMBH, Austria.

Table 3 Vectors used in this study

vector	source	description
RNAi feeding		
L4440-C34B7.2	this study	full length cDNA
L4440- <i>daf-18</i>	OPEN BIOSYSTEMS	full length cDNA
L4440-F30A10.6	this study	full length cDNA
L4440-F35H12.4	this study	full length cDNA
L4440- <i>fem-1</i>	laboratory of Stefan Eimer, ENI, Göttingen	truncated cDNA
L4440- <i>mtm-1</i>	this study	full length cDNA
L4440- <i>mtm-3</i>	OPEN BIOSYSTEMS	truncated cDNA
L4440- <i>pos-1</i>	Stefan Eimer	full length cDNA
L4440- <i>ppk-1</i>	this study	full length cDNA
L4440- <i>ppk-2</i>	this study	full length cDNA
L4440- <i>ppk-3</i>	OPEN BIOSYSTEMS	truncated cDNA
L4440- <i>rab-3</i>	OPEN BIOSYSTEMS	truncated cDNA
L4440- <i>snb-1</i>	this study	full length cDNA
L4440- <i>unc-26</i> (5-phosphatase)	this study	truncated cDNA
L4440- <i>unc-26</i> (full length)	this study	full length cDNA
L4440- <i>vps-34</i>	OPEN BIOSYSTEMS	full length cDNA
L4440-W09C5.7	this study	full length cDNA
L4440-Y75B8A.24	this study	full length cDNA
Expression in <i>C. elegans</i>		
Prab-3::CB5::CFP	Eugenia Butkevich, laboratory of Dieter Klopfenstein, Göttingen	Eimer <i>et al.</i> , 2007; CB5 tagged with cyan florescent protein (CFP)
Prab-3::2xFYVE::GFP	Eugenia Butkevich	FYVE-domain of human early endosome antigen 1
Prab-3::GFP::PPK-1	this study	full length cDNA
Prab-3::aman-2::GFP	Eugenia Butkevich	full length cDNA, mannosidase II
Prab-3::mCherry::F30A10.6	this study	full length cDNA
Prab-3::mCherry::ppk-2	this study	full length cDNA
Prab-3::mCherry::ppk-2 (<i>tm3741</i>)	this study	truncated cDNA
Prab-3::mCherry::ppk-2 (<i>ttti8500</i>)	this study	full length cDNA
pFR4 (<i>rol-6</i> (<i>su1006</i>))	Eugenia Butkevich	Cox <i>et al.</i> , 1980
Expression in <i>S. cerevisiae</i>		
pVV215- <i>sac1</i>	this study	full length gDNA
pVV215-F30A10.6	this study	full length cDNA
Expression in <i>E. coli</i>		
pGEX-6P-2	AMERSHAM	GST
pGEX-6P-D21-ppk-2	this study	wild type PPK-2, N-terminal GST

2.3 Working with *C. elegans*

2.3.1 *E. coli* strains for nematode feeding

E. coli strains for nematode feeding (Table 4) were grown in liquid LB medium with appropriated antibiotics (section 2.2.1) and at room temperature prior to plating.

Table 4 *E. coli* strains used for nematode feeding

strain name	genotype
OP50-1	<i>E. coli</i> B, uracil auxotroph, streptomycin resistant (<i>Caenorhabditis</i> Genetics Center, University of Minnesota, U.S.A., (CGC))
Jim Lewis' NA22	<i>E. coli</i> , prototroph, no resistance (CGC)

2.3.2 *C. elegans* maintenance

Nematodes were cultured as described (Brenner, 1973). If not stated otherwise, nematodes were grown on nematode growth medium (NGM) plates (3 g/L sodium chloride, 2.5 g/L peptone, 17 g/L agar agar, added post-autoclaving: 5 mg/L cholesterol (in ethanol), 1 mM calcium chloride, 1 mM magnesium sulfate, 25 mM potassium dihydrogen phosphate pH = 6, 50 mg/L nystatin in DMSO, 25 mg/L streptomycin) seeded with OP50-1 *E. coli* at 20°C. For long time storage, nematodes were grown until the plate was crowded, washed down with M9 buffer (6 g/L disodium hydrogen phosphate, 3 g/L potassium dihydrogen phosphate, 5 g/L sodium chloride, added post-autoclaving: 1 mM magnesium sulfate), mixed 1:1 with freezing medium (100 mM sodium chloride, 50 mM potassium dihydrogen phosphate pH = 6, 33 % (v/v) glycerol, added postautoclaving: 0.3 mM magnesium sulfate) and frozen at -80°C.

2.3.3 Generation of transgenic nematodes by microinjection

To create transgenic nematodes, expression vectors were microinjected in the gonade of young wild type adults as described before (Mello *et al.*, 1991). Foreign DNA is randomly taken up into oocytes and accumulates as a so-called extrachromosomal array in the nucleus. After fertilization, this extrachromosomal array is replicated and can be passed to every cell of the developing animal. Using appropriate promoters, the fusion protein of choice can be specifically expressed in a special tissue or a subset of cells.

The extrachromosomal array can be also transmitted to progeny. However, without an appropriate selection marker its inheritance in the wild type background is not stable what makes it often necessary to use a so-called coinjection marker for easy identification of transgenic animals. For this study, a plasmid encoding *rol-6* (*su1006*) was coinjected at a concentration of 100 ng/μL. The *rol-6* gene encodes a cuticle collagen which is required for normal cuticle morphology. Animals expressing the semidominant allele *rol-6* (*su1006*) (Cox *et al.*, 1980) show a helically twisted cuticle what forces the nematodes to “roll” around their own axis during moving forward. The following table (Table 5) lists all plasmids used for injection.

Table 5 Constructs for microinjection

expression construct	concentration for injection
<i>Prab-3::GFP::ppk-1</i>	10 ng/ μ L
<i>Prab-3::CB5::CFP</i>	10 ng/ μ L
<i>Prab-3::2xFYVE::GFP</i>	5 ng/ μ L
<i>Prab-3::mCherry::ppk-2</i>	20 ng/ μ L
<i>Prab-3::mCherry::ppk-2 (ttTi8500)</i>	20 ng/ μ L
<i>Prab-3::mCherry::ppk-2 (tm3741)</i>	20 ng/ μ L
<i>Prab-3::mCherry::F30A10.6</i>	25 ng/ μ L
<i>Prab-3::aman-2::GFP</i>	5 ng/ μ L
pFR4 (<i>rol-6 (su1006)</i>)	100 ng/ μ L

2.3.4 Isolation of genomic *C. elegans* DNA

30 or more adults were suspended in 100 μ L lysis buffer (200 mM sodium chloride, 100 mM Tris, 5 mM EDTA, 10 % (w/v) SDS, 1 % (v/v) proteinase K (20 mg/mL)), and incubated at 55°C overnight. Debris was pelleted at 16000 x g for 15 minutes at room temperature and the supernatant was transferred into a new reaction tube. For DNA precipitation, 1 volume of isopropanol was added and mixed thoroughly. DNA was pelleted at 16000 x g for 25 minutes at room temperature, washed with 100 μ L ethanol (70 %), air dried, and solved in 50 μ L TE buffer.

2.3.5 RNA isolation and cDNA synthesis

For RNA isolation (performed at Transcriptome Analysis Laboratory, University of Göttingen, Germany), one 6 cm-plate of the nematode strain of choice was grown until the plate was crowded. Nematodes were washed down with M9 buffer and pelleted at 301 x g for 3 minutes. Animals were then transferred to a 1.5 mL reaction tube and spun down at 16000 x g for 2 minutes at room temperature. The supernatant was removed carefully and nematodes were frozen at -80°C overnight. Freezing breaks the cuticle of *C. elegans* and improves lysis. At the next day, 1 mL of TRIzol was added to the pellet and nematodes were homogenized with a small rotor homogenizer. Debris was pelleted by centrifugation at 12000 x g for 10 minutes at 4°C. The supernatant was transferred into a new reaction tube and mixed thoroughly with 200 μ L chloroform. After centrifugation at 12000 x g for 15 minutes at 4°C, the upper aqueous phase was transferred to a fresh reaction tube and mixed with 500 μ L isopropanol and 1 μ L GlycoBlue. RNA and GlycoBlue were precipitated at 12000 x g for 30 minutes at 4°C. The supernatant was removed. The pellet was washed two times with 1 mL ethanol (75 %) and again centrifugated at 12000 x g for 5 minutes at 4°C. The supernatant was removed carefully and the pellet was dried at 37°C before it was dissolved in 100 μ L RNase-free water.

RNA quantity and quality were analyzed using Nano drop and Bioanalyzer 2100 (AGILENT TECHNOLOGIES, Boeblingen, Germany). cDNA was prepared by using the iScript cDNA Synthesis Kit from BIO-RAD LABORATORIES GMBH, Munich, Germany) following the manufacturer's instructions.

2.3.6 Nematode crossing and genotyping

Crossings and classical genetics were used to introduce fluorescent marker proteins in mutant backgrounds. Because males only appear at a very low frequency in wild type and most mutant backgrounds, nematodes were stimulated by heat shock leading to an increased production of male animals. For this, 30 L4 larvae were incubated for 6 hours at 30°C and then grown at 20°C. After 2 days, up to 30 males could be found in the progeny. These males were crossed with hermaphrodites with the same genotype to obtain a F1 generation with 50 % male animals. These crossings were repeated frequently every 7th day so that always enough males were available for crossings.

Hermaphrodites with the mutant background of choice were mated with males expressing an appropriate fusion protein. Later, up to 40 F2 animals were picked to separate plates. For genotyping by PCR (for *ppk-2* (*ttTi8500*) and *ppk-2* (*tm3741*)), the F3 generation were allowed to grow for several days so that enough animals were present for the isolation of genomic DNA (section 2.3.4).

2.3.7 *C. elegans* strains used in this study

Table 6 *C. elegans* strains used in this study

strain	genotype	transgene	source and/or reference
CB1265	<i>unc-104</i> (<i>e1265</i>) II	-	CGC
CB1375	<i>daf-18</i> (<i>e1375</i>) IV	-	CGC; Gil <i>et al.</i> , 1999
EG1285	<i>lin-15B</i> (<i>n765</i>) X	<i>oxIs12</i> [<i>Punc-47::GFP</i> ; <i>lin-15(+)</i>] (integrated on X)	CGC
EG3680	wild type	<i>oxIs206</i> [<i>Paex3::ANF::GFP</i>] (integrated, not mapped)	CGC; Speese <i>et al.</i> , 2007
IE8500	<i>ppk-2</i> (<i>ttTi8500</i>) III	-	NemaGENETAG, University of Lyon, France
KD100	<i>eri-1</i> (<i>mg366</i>) IV; <i>lin-15B</i> (<i>n744</i>) X	<i>Prab-3::GFP::ppk-1</i> , <i>Prab-3::mCherry::ppk-2</i> , pFR4 (<i>rol-6</i> (<i>su1006</i>)) (extrachromosomal)	this study
KD101	<i>ppk-2</i> (<i>ttTi8500</i>) III	<i>oxIs12</i> [<i>Punc-47::GFP</i> ; <i>lin-15(+)</i>] (integrated on X)	this study
KD102	<i>ppk-2</i> (<i>tm3741</i>) III	<i>oxIs12</i> [<i>Punc-47::GFP</i> ; <i>lin-15(+)</i>] (integrated on X)	this study
KD103	<i>ppk-2</i> (<i>tm3741</i>) III	<i>vsIs48</i> [<i>Punc-17::GFP</i>] (integrated, not mapped)	this study
KD104	<i>ppk-2</i> (<i>ttTi8500</i>) III	<i>vsIs48</i> [<i>Punc-17::GFP</i>] (integrated, not mapped)	this study
KD105	wild type	<i>Prab-3::GFP::ppk-1</i> , <i>Prab-3::mCherry::ppk-2</i> , pFR4 (<i>rol-6</i> (<i>su1006</i>)) (extrachromosomal)	this study
KD106	wild type	<i>Prab-3::mCherry::ppk-2</i> , pFR4 (<i>rol-6</i> (<i>su1006</i>)) (extrachromosomal)	this study
KD107	wild type	<i>Prab-3::GFP::ppk-1</i> , pFR4 (<i>rol-6</i> (<i>su1006</i>)) (extrachromosomal)	this study
KD108	wild type	<i>Prab-3::mCherry::ppk-2</i> , <i>Prab-3::amans-2::GFP</i> , pFR4 (<i>rol-6</i> (<i>su1006</i>)) (extrachromosomal)	this study
KD109	wild type	<i>Prab-3::mCherry::ppk-2</i> , <i>Prab-3::2xFYVE::GFP</i> , pFR4 (<i>rol-6</i> (<i>su1006</i>)) (extrachromosomal)	this study

Table 6 *C. elegans* strains used in this study (continued)

KD110	wild type	<i>Prab-3::mCherry::ppk-2 (ttTi8500)</i> , pFR4 (<i>rol-6 (su1006)</i>) (extrachromosomal)	this study
KD111	wild type	<i>Prab-3::mCherry::ppk-2 (tm3741)</i> , pFR4 (<i>rol-6 (su1006)</i>) (extrachromosomal)	this study
KD112	wild type	<i>Prab-3::mCherry::ppk-2 (ttTi8500)</i> , <i>Prab-3::GFP::ppk-1</i> , pFR4 (<i>rol-6 (su1006)</i>) (extrachromosomal)	this study
KD113	wild type	<i>Prab-3::mCherry::ppk-2 (tm3741)</i> , <i>Prab-3::GFP::ppk-1</i> , pFR4 (<i>rol-6 (su1006)</i>) (extrachromosomal)	this study
KD114	<i>unc-104 (e1265)</i> II	<i>Prab-3::mCherry::ppk-2</i> , <i>Prab-3::2xFYVE::GFP</i> , pFR4 (<i>rol-6 (su1006)</i>) (extrachromosomal)	this study
KD115	<i>ppk-2 (tm3741)</i> III	<i>jsls219[pSY3 (sng-1::GFP)</i> ; pFR4 (<i>rol-6 (su1006)</i>)] (integrated on II)	this study
KD116	<i>ppk-2 (ttTi8500)</i> III	<i>jsls219[pSY3 (sng-1::GFP)</i> ; pFR4 (<i>rol-6 (su1006)</i>)] (integrated on II)	this study
KD117	<i>ppk-2 (tm3741)</i> III	<i>oxls206 [Paex3::ANF::GFP]</i> (integrated, not mapped)	this study
KD118	<i>ppk-2 (ttTi8500)</i> III	<i>oxls206 [Paex3::ANF::GFP]</i> (integrated, not mapped)	this study
KD119	wild type	<i>Prab-3::mCherry::ppk-2</i> , <i>Prab-3::CB5::CFP</i> , pFR4 (<i>rol-6 (su1006)</i>) (extrachromosomal)	this study
KD120	wild type	<i>Prab-3::mCherry::F30A10.6</i> , <i>Prab-3::amans-2::GFP</i> , pFR4 (<i>rol-6 (su1006)</i>) (extrachromosomal)	this study
KP3948	<i>eri-1 (mg366)</i> IV; <i>lin-15B(n744)</i> X	-	CGC
LX929	wild type	<i>vsIs48 [Punc-17::GFP]</i> (integrated, not mapped)	CGC
N2 Bristol	wild type	-	CGC
NM1233	wild type	<i>jsls219[pSY3 (sng-1::GFP)</i> ; pFR4 (<i>rol-6 (su1006)</i>) (integrated on II)	Zhao and Nonet, 2001
NM791	<i>rab-3 (js49)</i> II	-	CGC
RB718	<i>daf-18 (ok718)</i> IV	-	CGC
TM3741	<i>ppk-2 (tm3741)</i> III	-	National Bioresource Project of Japan, Tokyo

2.3.8 RNA interference

2.3.8.1 *E. coli* for RNAi feeding (maintenance, transformation, and induction)

For dsRNA production, the RNase III-lacking tetracycline-resistant *E. coli* strain HT115(DE3) (F⁻, *mcrA*, *mcrB*, IN(*rrnD* *rrnE*)1, *mc14*::Tn10(DE3 lysogen: *lavUV5* promoter-T7 polymerase) (IPTG-inducible T7 polymerase) (RNase III minus)) was used (Timmons *et al.*, 2001). Maintenance was performed basically as described in section 2.2.1. Competent HT115(DE3) were obtained by growing a culture in 25 mL liquid SOB medium to an OD₆₀₀ of 0.4. Cells were centrifuged at 3345 x g for 10 minutes at room temperature, the pellet was resuspended in 12.5 mL chilled 50 mM calcium chloride, incubated on ice for 30 minutes and centrifuged again. Cells were then resuspended in 2.5 mL 50 mM calcium chloride and aliquots of 200 µL were used for transformation (section 2.2.5.2) of L4440 vectors (Table 3).

dsRNA production was carried out as described before (Kamath *et al.*, 2001; Kamath and Ahringer, 2003). HT115(DE3) containing the L4440 vector of choice was grown in 25 mL of 2xYT medium (16 g/L peptone, 10 g/L yeast extract, 5 g/L sodium chloride, pH = 7.0) and antibiotics (ampicillin, tetracycline) to an OD₆₀₀ of 0.4, then IPTG (final concentration 0.4 mM) for induction was added and cells were grown for another 4 hours. The culture was spiked with antibiotics and IPTG again and pelleted. Cells were resuspended in 5 mL of the supernatant and distributed on 4 to 6 NGM plates (with 0.4 mM IPTG, ampicillin and tetracycline instead of streptomycin). The bacteria lawn was dried overnight.

2.3.8.2 Preparation of RNAi-hypersensitive nematodes

Since RNAi works only refractory in *C. elegans* neurons, the RNAi-hypersensitive nematode strain KP3948 (Table 6) was used. This strain is deficient in the exonuclease ERI-1, harbors an additional mutation in the locus *lin-15* and has been shown to have an enhance response to dsRNA in neurons (Kennedy *et al.*, 2004; Wang *et al.*, 2005; Sieburth *et al.*, 2005). Worms were grown on 10 cm-plates until the plates were crowded and washed down and cleaned with M9 buffer. To isolate eggs, nematode pellets were shaken thoroughly in a sodium hypochlorite solution (a pellet with the volume of 1 mL was mixed with 8 mL of sterile water, 1 mL 5 N sodium hydroxide, 1 mL sodium hypochlorite with 12 % chlorine) for 5 minutes at room temperature to lyse adult animals and larvae. Due to their chitin shell, eggs are not damaged by sodium hypochlorite treatment. Eggs and debris were pelleted and washed one time with M9 buffer to remove sodium hypochlorite. Pellets were then mixed with 5 mL M9 buffer and 60 % (w/v) sucrose. The resulting solution of 30 % sucrose was covered with a layer of 3 mL 5 % (w/v) sucrose creating a discontinuous gradient and centrifuged at 301 x g for 10 minutes at room temperature. After centrifugation, nematode eggs had accumulated at the boundary surface of the two differently concentrated sucrose layers whereas most of the debris accumulated at the bottom of the tube. Eggs were collected and washed two times with M9 buffer to remove sucrose. Eggs were resuspended in M9 buffer and incubated at room temperature on a rocker over night so that all embryos had enough time to develop and hatch as L1 larvae. If no food is provided, L1 larvae arrest in development and were harvested as a synchronous staged population by pelleting at 301 x g for 3 minutes at room temperature. Larvae concentration was determined by counting in a phase contrast field.

2.3.8.3 Setup of the RNAi screen

A mixed group of target and control constructs (Table 11) was processed blindly (i.e. growing of the bacteria, induction, plating). 100 to 150 L1 larvae (P0) were plated on two RNAi plates per construct and grown at 20°C. After three days, 40 young adults per construct were tested for aldicarb resistance (section 2.3.9.1). For not overcrowding the plate and to provide enough bacteria for all animals, P0 animals were transferred on a second plate with induced bacteria at the 4th day. In order not to confuse P0 with F1, P0 animals were removed after having laid eggs on the second plate. At the 7th day, young F1 adults were tested for aldicarb resistance. Every target construct was at least tested twice.

2.3.8.4 RNAi control constructs

The following plasmids were processed in parallel to target and control constructs (Table 11):

L4440

This vector was created by Andrew Fire (section 2.2.7). Since no or only short dsRNA encoding the multiple cloning site was expected to be produced by this vector when transformed to HT115(DE3) *E. coli*, this vector was used as negative control.

L4440-*fem-1*

This vector was provided by the laboratory of Stefan Eimer. Knock down of the gene product of *fem-1* causes sterility and was used to monitor the efficiency of the RNAi treatment (Timmons and Fire, 1998).

L4440-*pos-1*

This vector was provided by the laboratory of Stefan Eimer. Knock down of the gene product of *pos-1* causes embryonic lethality and was used to monitor the efficiency of the RNAi treatment (Tabara *et al.*, 1998).

2.3.9 Neurotoxin assays

2.3.9.1 Aldicarb

NGM plates with aldicarb were prepared by adding aldicarb solved in 70 % ethanol to the melted medium (temperature between 55°C and 65°C) resulting in a final concentration of 1 mM. Plates were dried over night and have been stored up to 4 weeks at 4°C in a sealed box. 25 to 40 adults were put on each plate and scored for paralysis by prodding animals 3 times on head and tail with a thin platinum wire (Mahoney *et al.*, 2006). Every assay was at least repeated two times.

2.3.9.2 Levamisole

NGM plates without nystatin with a volume of 7.5 mL were poured and dried over night. The next day, different volumes of a 0.5 M levamisole stock solution were added (for example, 15 μ L for a final concentration of 1 mM levamisole) and evenly spread with a glass spatula. The liquid was allowed to dry for one hour at room temperature. 25 adults were put on each plate and scored after 10 minutes for paralysis by prodding with a platinum wire (Lewis *et al.*, 1980). Every assay was at least repeated two times.

2.3.9.3 Pentylentetrazole

NGM plates without nystatin with a volume of 7.5 mL were poured and dried over night. At the next day, a fresh pentylentetrazole (PTZ) stock solution with a concentration of 0.5 g/mL was prepared and 150 μ L were spread with glass spatula on every plate to obtain a final concentration of 10 mg/mL. The liquid was allowed to dry for 40 minutes at room temperature. Then, 40 μ L of an OP50-1 culture (section 2.3.1) were pipetted in the center of every plate and dried to create a food lawn. Since PTZ is less stable than aldicarb or levamisole, PTZ plates were used immediately. 25 adults were put on each plate and scored for paralysis by prodding with a platinum wire after 30, 60, and 90 minutes (Williams *et al.*, 2004; Locke *et al.*, 2008). Every assay was at least repeated two times.

2.3.10 Motility analysis

2.3.10.1 Video tracking

Up to 50 well-fed adult animals were picked to a NGM plate without food and allowed to accommodate for 1 hour at 20°C. Movies were recorded for 5 minutes with 1 frame per second using a digital camera with appending software and at 0.8 x magnification. Nematode velocities per second (single values) were calculated as described (Speese *et al.*, 2007) using the MTrack2 plugin of ImageJ (section 2.6).

2.3.10.2 Trace analysis

Single well-fed adults were picked on an NGM plate with food and allowed to crawl for up to 20 minutes at room temperature. After removing the nematode, the trace on the agar was imaged using a digital camera with appending software at 10 x magnification. Pictures were edited using ImageJ (section 2.6).

2.3.11 Quantification of progeny

10 L4 animals of every genotype were placed separately on agar plates with a food lawn and incubated at 20°C to develop to adults and lay eggs. After 24 and 48 hours, respectively, animals

were transferred to fresh plates. After 72 hours, the nematodes were removed. All plates were incubated at 20°C for 2 days and then scored for progeny and unhatched eggs.

2.3.12 Microscopy

Glass slides for microscopy were covered with a thin agarose pad (3 % agarose). After drying, a 10 µL-drop of 5 mM levamisole was pipetted on the agarose pad and up to 20 nematodes expressing the fluorescent fusion protein of choice were placed in the drop. Drop and paralyzed nematodes were covered with a cover slip. Imaging was performed with a inverted Spinning Disc confocal microscope (ZEISS¹ Axiovert 200M, Nipkow spinning disc unit from VISITRON SYSTEMS, Puchheim, Germany, EM-CCD camera (ANDOR², iXon DV885LC-VP) with appending software using 40 x or 100 x oil immersion objectives. CB5-YFP was imaged with the inverted LEICA³ confocal microscope at the ENI, Göttingen, using a 63 x oil immersion objective.

2.3.13 Analysis of nervous system development

To analyze GABAergic neurons, GABAergic commissures and D-type motor neuron somata were counted in 10 animals per genotype (Table 6) expressing the *transgene oxIs12 [Punc-47::GFP; lin-15(+)]*. To analyze cholinergic neurons, neuron cell bodies were counted in 10 animals per genotype (Table 6) expressing the *transgene vsIs48 [Punc-17::GFP]*. Also the position of commissures and neuron cell bodies was compared between genotypes (Speese *et al.*, 2007).

2.3.14 Analysis of coelomocytes and dorsal cords

Z-stacks with 1 µm-planes were obtained from the posterior coelomocyte of young adults expressing GFP-labeled atrial natriuretic factor (ANF) (Speese *et al.*, 2007; Table 6). Signals were summed up using the Z-project tool of ImageJ (section 2.6). The intensity of four fluorescence patches per coelomocyte was measured and averaged according to Sieburth *et al.*, 2007. Averages of several coelomocytes of different genotypes were normalized to wild type. Z-stacks with 1 µm-planes of the dorsal cord of young adults expressing GFP-labeled synaptogyrin and ANF-GFP (Table 6) were analyzed in a comparable manner.

¹ CARL ZEISS EUROPA, Jena, Germany

² ANDOR Technology, South Windsor, U.S.A.

³ LEICA CAMERA AG, Solms, Germany

2.3.15 Preparation of large synchronous L1 larvae populations and biochemical analysis of phospholipids

2.3.15.1 Preparation of large synchronous L1 larvae populations

Large populations of nematodes were grown on enriched peptone plates (1.2 g/L sodium chloride, 20 g peptone, 25 g agar agar, added post-autoclaving: 5 mg/L cholesterol (in ethanol), 1 mM magnesium sulfate, 25 mM potassium dihydrogen phosphate pH = 6, 50 mg/L nystatin (in DMSO)) seeded with Jim Lewis' NA22 *E. coli* (section 2.3.1). NA22 is a prototroph *E. coli* strain which provides a continuous food source even for crowded plates.

A nematode preculture of 10 plates were grown for 7 days at 20°C until the plates were crowded. Nematodes were then distributed to 40 to 60 plates and grown at 20°C. After 5 days, nematodes were fed with concentrated NA22 suspension to ensure that enough food for the whole population is present. At the 6th day, worm were washed down with M9 buffer and pelleted at 301 x g for 3 minutes at room temperature. Pellets were washed with M9 buffer until the supernatant was clear. Eggs were isolated by sodium hypochlorite treatment and sucrose gradient centrifugation and grown overnight in M9 to L1 larvae (section 2.3.8.2). Larvae were pelleted and brought together, pelleted again, resuspended in 2 mL of M9 buffer and then transferred to a 2 mL-reaction tube. After another pelleting step at 10000 x g for 2 minutes, the supernatant was removed with a pipette, L1 larvae were aliquoted (50 µL to 100 µL), frozen in liquid nitrogen and stored at -80°C until subsequent analysis.

2.3.15.2 Acidic extraction of phospholipids

The frozen worm pellets were extracted as previously described (Cho and Boss, 1995). In brief, pellets were resuspended in 1.5 mL chloroform/methanol [1:2 (v/v)], transferred to a glass tube and mixed with 250 µL 0.5 M EDTA, 500 µL 2.4 N hydrochloric acid, and 500 µL chloroform. The mixture was covered with argon and shaken at 250 rpm for 4 hours at 4°C. Phase separation was achieved by centrifugation at 800 x g for 2 min at room temperature. The organic phase was transferred to a fresh glass tube and covered with argon. The top phase was reextracted with 2 mL chloroform, covered with argon and shaken. After phase separation, the reextracted bottom phase was combined with the organic phase of the previous extraction and mixed with 1.5 mL 0.5 M hydrochloric acid in methanol/water [1:1(v/v)]. The mixture was covered with argon and shaken. After phase separation, the bottom phase was transferred into a fresh glass tube and extraction with 0.5 M hydrochloric acid in methanol/water [v/v (1:1)] was repeated two times. Samples were dried under nitrogen flow, resuspended in 500 µL chloroform and covered with argon for storage at -20 °C.

2.3.15.3 Quantification of phosphoinositides according to gaschromatographic detection of the associated fatty acids

Lipid classes were separated and lipids quantified as previously described (König *et al.*, 2008). In brief, thin-layer-chromatography (TLC) was used to separate lipids on silica gel plates (MERCK KGAA, Darmstadt, Germany) with different developing solvents for phosphoinositides and phosphatidic acid

(chloroform/methanol/ammonium hydroxide/water [57/50/4/11 (v/v/v/v)]) and phosphatidylinositol (chloroform/methyl acetate/isopropanol/methanol/0.25 % aqueous potassium chloride [25:25:25:10:9 [v/v/v/v/v])). 5 µg of lipid standards (phosphatidylinositolbispophosphate, PI4P, phosphatidic acid, PI, phosphatidylcholine (PC), phosphatidylethanolamine) were run in parallel to 25 µL of each sample and lipids were visualized in aqueous 10 % (w/w) copper(II) sulfate containing 8 % phosphoric acid and subsequent heating to 180 °C (unstained lipids were located according to standard migration). Lipids were scraped from the TLC plate, dissolved in 3 mL chloroform/methanol/1 N hydrochloric acid [40:80:1 (v/v/v)], covered with argon, mixed, and shaken 20 minutes at room temperature. Unsolved particles were pelleted and the supernatant was transferred to a new glass tube and dried under nitrogen flow.

Lipids were transmethylated by adding 5 µL tripentadecanoic acid (1 mg/mL) as an internal standard, 333 µL methanol/toluol [2:1 (v/v)], and 167 µL 0.5 M sodium methoxide. Samples were shaken for 20 minutes at room temperature. Then, samples were extracted twice by adding 500 µL 5 M sodium chloride, 50 µL hydrochloric acid (32 %), and 2 mL hexane. Combined hexane phases were cleaned by 2 mL water and then dried under nitrogen flow. Samples were resuspended in up to 200 µL acetonitrile, transferred to vials for gas chromatography (GC), again dried under nitrogen, and then finally resuspended in 10 µL acetonitrile. The fatty acid methyl esters were then quantified using a GC6890 gas chromatograph with flame ionization detection (AGILENT) fitted with a 30 m x 250 µm DB-23 capillary column (AGILENT). Helium flowed as a carrier gas at 1 mL per minute. Samples were injected at 220 °C. After one minute at 150 °C, the oven temperature was raised to 200 °C at the rate of 8 °C per minute and to 250 °C at 25 °C per minute, and then kept at 250 °C for six minutes. Samples (1 µL) were injected using a split of one. Amounts of fatty acids were then quantified in comparison to the internal standard.

2.4 Working with *S. cerevisiae*

2.4.1 *S. cerevisiae* strains and maintenance

Haploid *S. cerevisiae* strains were purchased from the EUROPEAN *SACCHAROMYCES CEREVISIAE* ARCHIVE FOR FUNCTIONAL ANALYSIS and grown on complete YPD (yeast peptone dextrose) medium (10 g/L yeast extract, 20 g/L peptone, 20 g/L dextrose, 20 g/L agar agar) or minimal SD (synthetic minimal glucose) medium (6,7 g/L yeast nitrogen base, 20 g/L dextrose, 25 g/L agar agar) as previously described (Sherman, 2002).

Table 7 *S. cerevisiae* strains used in this study

strain name	genotype
wild type (BY4741)	<i>Mata his3delta1 leu2delta0 met15delta0 ura3delta0</i>
<i>sac1delta</i>	<i>Mata his3delta1 leu2delta0 met15delta0 ura3delta0 sac1::kanMX4</i>
<i>sac1delta (sac1::HA)</i>	<i>Mata his3delta1 leu2delta0 met15delta0 ura3delta0 sac1::kanMX4 (pVV215-sac1)</i>
<i>sac1delta (F30A10.6::HA)</i>	<i>Mata his3delta1 leu2delta0 met15delta0 ura3delta0 sac1::kanMX4 (pVV215-F30A10.6)</i>
<i>sac1delta (empty)</i>	<i>Mata his3delta1 leu2delta0 met15delta0 ura3delta0 sac1::kanMX4 (pVV215)</i>

Yeast strains used in this study are presented in Table 7. The gene locus YKL212w encoding *sac1* was disrupted by the integration of a *kanMX4* cassette encoding a kanamycin resistance gene. Yeast cells expressing this gene are resistant to the kanamycin derivative G418 which is toxic for eukaryotes (Wach *et al.*, 1994). G418 was used at a concentration of 150 mg/L. When needed, supplemental amino acids were added to SD medium (20 mg/L uracil, 20 mg/L L-histidine, 20 mg/L L-methionine, 60 mg/L L-leucin).

2.4.2 Transformation of *S. cerevisiae*

A main culture of the *S. cerevisiae* strain of choice was grown to an OD₆₀₀ of 0.5 to 0.8, the cell number was counted, and cells were spun down at 3345 x g for 10 minutes at room temperature. The pellet was washed two times with sterile water and one time with 0.1 M lithium acetate in TE buffer. After the last centrifugation step, cells were resuspended in 0.1 M lithium acetate in TE buffer to a final concentration of 2 x 10⁹ cells/mL and incubated at 30°C for 15 minutes. 100 µL of the cell suspension (2 x 10⁸ cells) were transferred in a reaction tube and mixed with 10 µL freshly boiled salmon sperm DNA (10 mg/mL). The vector DNA of choice was added, gently mixed with cells and salmon sperm DNA and incubated at 30°C for 30 minutes. Then, 500 µL of 40 % (v/v) PEG4000 and 0.1 M lithium acetate (in TE buffer) were added, carefully mixed, incubated at 30°C for 30 minutes and at 42°C for 15 minutes. Cells were pelleted at 16000 x g for 15 seconds, resuspended in sterile water and plated on appropriate medium.

2.4.3 Isolation of total DNA of *S. cerevisiae*

5 mL of an overnight culture with an OD₆₀₀ not less than 1 were pelleted at 3345 x g for 5 minutes. Cells were resuspended in sterile water, transferred to a 2 mL reaction tube and centrifuged at 16000 x g for 5 minutes. The pellet was dissolved in 100 µL extraction buffer (2 % (v/v) Triton X-100, 1 % (w/v) SDS, 10 mM TRIS-HCl pH = 8, 100 mM sodium chloride, 1 mM EDTA) and mixed with 0.3 g glass beads (0.25 to 0.5 mm in diameter) and 200 µL phenol. To disrupt cells, the suspension was mixed thoroughly for 5 minutes and then centrifugated at 16000 x g for 5 minutes. 360 µL of the supernatant was transferred to a fresh reaction tube and DNA was precipitated by adding of 40 µL 3M sodium acetate and 1 mL ethanol (96 %) and centrifugation at 16000 x g for 10 minutes. The pellet was dissolved in 360 µL TE buffer, mixed with 3 µL RNase A (10 mg/mL) and incubated at 37°C for 30 minutes. Then, the DNA solution was mixed with 400 µL phenol and centrifuged at 16.000 x g for 10 minutes. The aqueous supernatant was transferred into a fresh reaction tube, mixed with 400 µL chloroform and again centrifuged. The supernatant was transferred into a fresh reaction tube and DNA was again precipitated with 40 µL 3M sodium acetate and 1 mL ethanol (96 %) for 1 hour at -20°C, centrifuged at 16000 x g for 25 minutes, washed with ethanol (70 %), air dried and dissolved in 30 µL TE buffer.

2.4.4 Protein extraction of *S. cerevisiae*

10 mL of an overnight culture with an OD₆₀₀ not less than 1 were pelleted at 3345 x g for 5 minutes. The pellet was resuspended in 1 mL of sterile water and transferred to a 2 mL-reaction tube and pelleted again for 2 minutes at 16000 x g. The pellet was mixed thoroughly with 0.3 glass beads and 0.5 mL of lysis buffer (50 mM Tris-HCl pH = 7.5, 150 mM sodium chloride, 5 % glycerol, 5 mM EDTA, protease inhibitor) three times for 30 seconds at 4°C and cooled on ice in between. Glass beads and debris were pelleted for 1 minute at 16000 x g, the supernatant was aliquoted, shock frosted in liquid nitrogen and stored at -80°C until use.

2.4.5 Protein detection by Western Blotting

Separation of proteins in an acrylamid gel by electrophoresis was performed according to Laemmli, 1970. The separating gel was prepared containing 10 % acrylamid and 1.5 M Tris-HCl, pH = 8.8, whereas the stacking gel contained 4 % acrylamid and 125 mM Tris-HCl, pH = 6.8. Electrophoresis buffer consisted of 25 mM Tris, 192 mM glycine and 0.1 % (w/v) SDS. Before gel run, protein samples were mixed 1:1 with sample buffer (100 mM Tris-HCl, 4 % (w/v) SDS, 200 mM beta-mercaptoethanol, 0.2 % (w/v) bromphenol blue, 20 % (v/v) glycerol, pH = 6.8). For protein size determination, protein bands were later compared to prestained molecular weight markers obtained from NEW ENGLAND BIOLABS. After gel run, the gel was blotted on nitrocellulose membrane using a Mini Trans-Blot Electrophoretic Transfer Cell from BIO-RAD following the manufacturer's instructions.

The membrane was then blocked with 10 % (w/v) non-fat milk powder dissolved in TBS (25 mM Tris-HCl, 137 mM sodium chloride, 2.7 mM potassium chloride, pH = 8) for 1 hour on a rocker at room temperature. After a short washing step with TBS, the membrane was incubated with a primary antibody diluted in TBS for 1 hour on a rocker at room temperature.

To detect HA-fusion proteins, a monoclonal antibody from mouse (HA-probe (F-7): sc-7392, SANTA CRUZ BIOTECHNOLOGY, INC., Heidelberg, Germany) was used diluted 1:1000 in TBS and incubated with the membrane for 1 hour at room temperature. The secondary antibody used was an anti-mouse horse radish peroxidase-conjugated IgG produced in goat (A4416, SIGMA-ALDRICH) and was diluted 1:1000 in TBS and incubated with the membrane for 1 hour at room temperature.

After antibody incubation, the membrane was washed twice for 15 minutes plus 5 minutes with 0.05 (v/v) Tween 20 in TBS. Horse radish peroxidase-labeled proteins were then detected using a photo film using the ECL Western Blotting Detection kit from AMERSHAM BIOSCIENCES following the manufacturer's instructions.

2.4.6 Analysis of phenotype characteristics of *sac1delta*

2.4.6.1 Cold sensitivity

The knock out of *sac1* in yeast almost stops to grow at 13°C (Nemoto *et al.*, 1999). To analyze the cold sensitivity of different yeast strains (Table 7), individual clones were streaked out on selective

medium and incubated at 13°C for 2 weeks. Every assay was at least repeated two times for each strain.

2.4.6.2 Slow growth

sac1 knock out yeast grows slightly but significantly slower at normal culture temperature than wild type yeast (Nemoto *et al.*, 1999). To analyze the growth of different yeast strains (Table 7), fresh overnight cultures were diluted with sterile water (1:10, 1:100, 1:1000) and 5 µL of undiluted culture and every dilution were pipetted next to each other as drops on a plate of selective medium, dried, and incubated for 5 days at 30°C. Yeast cultures were imaged with a standard DNA gel documentation set, pixel intensity was analyzed with ImageJ (section 2.6) and normalized to the positive control for every dilution. Every assay was at least repeated two times for each strain.

2.4.6.3 Inositol auxotrophy

sac1 knock out yeast shows reduced growth on medium without inositol (Rivas *et al.*, 1999; Nemoto *et al.*, 2000). To analyze if the growth of different yeast strains is inositol dependent, fresh overnight cultures were diluted with sterile water (1:10, 1:100, 1:1000) and 5 µL of undiluted culture and every dilution were pipetted next to each other as drops on a plate of selective medium, dried, and incubated for 5 days at 30°C. Yeast cultures were imaged with a standard DNA gel documentation set, pixel intensity was analyzed with ImageJ (section 2.6) and normalized to the positive control for every dilution. Every assay was at least repeated two times for each strain.

2.5 Recombinant protein expression in *E. coli* and *in vitro* assays

2.5.1 Recombinant expression of GST-PPK-2

For recombinant protein expression, the cDNA of *ppk-2* (Appendix) was cloned into the vector pGEX-6P-D21 (section 2.2.7) which encodes an N-terminal GST-tag in frame with a Gateway cassette (section 2.2.3) and allows for IPTG-inducible expression in *E. coli*. GST without any fusion protein, encoded by pGEX-6P-2 (Table 3), was expressed in parallel. Expression was tested in different *E. coli* strains (Table 8) and under different conditions (Table 9).

Table 8 *E. coli* strains used for recombinant expression

strain name	genotype
BL21-AI (INVITROGEN)	F- <i>ompT hsdSB</i> (rB-mB-) <i>gal dcm araB::T7RNAP-tetA</i>
BL21 GOLD (DE3) (STRATAGENE ⁴)	<i>E. coli</i> B F- <i>dcm+ Hte ompT hsdS</i> (r _B - m _B -) <i>gal lambda</i> (DE3) <i>endA Tet^r</i>
Rosetta2 (DE3) (NOVAGEN ⁵)	F ⁻ <i>ompT hsdS_B</i> (r _B ⁻ m _B ⁻) <i>gal dcm</i> (DE3) pRARE2 (Cam ^R)

⁴ STRATAGENE PRODUCTS, La Jolla, U.S.A.

⁵ NOVAGEN is a brand of MERCK KGAA, Darmstadt, Germany

In general, bacteria carrying the plasmid encoding GST-PPK-2 were grown as an overnight preculture and added to the main culture (rich medium (10 g/L tryptone, 5 g/L yeast extract, 5 g/L sodium chloride, 100 µg/mL ampicillin) or TPM medium (20 g/L tryptone, 15 g/L yeast extract, 8 g/L sodium chloride, 2 g disodium hydrogen phosphate, 1 g/L potassium dihydrogen phosphate, pH = 7) and grown to an OD₆₀₀ between 0.6 and 0.8. After induction, cultures were grown for several hours and then harvested by centrifugation at 4°C. Cells were resuspended in lysis buffer (buffer 1 (50 mM Tris (pH = 8.0), 300 mM sodium chloride, 1 mM EDTA, 10 % (v/v) glycerol), buffer 2 (30 mM Tris (pH = 7.4), 15 mM magnesium chloride), Tris-HCl buffer (50 mM Tris-HCl (pH = 7.5), 0.1 mM EDTA, 10 mM DTT, 100 mM sodium chloride, 1 mM ATP, 1mM PMSF, 50 µg DNase, 50 µg lysozyme), or PBS buffer (12 mM phosphate, pH 7.4, 10 mM sodium phosphate, 2 mM potassium dihydrogen phosphate, 2.7 mM potassium chloride, 137 mM sodium chloride, 1 mM ATP, 1mM PMSF, 50 µg DNase, 50 µg lysozyme) and lysed by sonication (three times 30 seconds, cooled on ice in between). Debris was pelleted by centrifugation at 4°C and the supernatant was aliquoted, shock frosted in liquid nitrogen, and stored at -80°C. To estimate the amount of expressed GST-PPK-2 and GST, different volumes of the supernatants were run on an acrylamid gel and blotted (section 2.4.5). Proteins were detected using an anti-HA antibody produced in rabbit (H-6908, SIGMA-ALDRICH) as primary and an anti-rabbit-horse radish peroxidase-labeled IgG (A6154, SIGMA-ALDRICH) as secondary antibody (both diluted 1:1000 in TBS).

Table 9 Expression and lysis conditions for recombinant expressed GST-PPK-2

	<i>E. coli</i> strain	lysis buffer	medium	induction by	induction length and temperature
1	BL21-AI	1	rich medium	0.2 % arabinose, 1 mM IPTG	to OD ₆₀₀ = 0.6-0.8 at 37°C, after induction at room temperature for 18 hours
2	BL21-AI	2	rich medium	0.2 % arabinose, 1 mM IPTG	to OD ₆₀₀ = 0.6-0.8 at 37°C, after induction at room temperature for 18 hours
3	BI21 GOLD (DE3)	Tris - HCL	TPM	0.4 mM IPTG	to OD ₆₀₀ = 0.6-0.8 at 37°C, after induction at 20°C for 4 hours
4	Rosetta2 (DE3)	PBS	TPM	0.4 mM IPTG	to OD ₆₀₀ = 0.6-0.8 at 37°C, after induction at 20°C for 4 hours
5	BI21 GOLD (DE3)	Tris - HCL	TPM	0.4 mM IPTG	to OD ₆₀₀ = 0.6-0.8 at 37°C, after induction at 20°C for 4 hours
6	Rosetta2 (DE3)	PBS	TPM	0.4 mM IPTG	to OD ₆₀₀ = 0.6-0.8 at 37°C, after induction at 20°C for 4 hours

2.5.2 Phosphoinositide kinase assay

Recombinant expressed and purified PIP kinase of *Neurospora crassa* (converting PI3P or PI4P to PI3,5P₂ or PI4,5P₂, respectively) and *Homo sapiens* (*H. sapiens*) Type II PIP kinase beta (converting PI5P to PI4,5P₂) as positive controls were provided by Dr. Irene Stenzel, Department of Plant Biochemistry, Albrecht-von-Haller-Institute for Plant Sciences, University of Göttingen, Germany.

Lipid kinase assays were performed as previously described (Stenzel *et al.*, 2008). Per reaction, 6.25 µL of a solution containing 1mg/mL PI3P, PI4P, or PI5P was dried under nitrogen flow and then resuspended in 5 µL 2 % (v/v) Triton X-100. To achieve a homogenous distribution of lipid/detergence liposomes, the mixture was sonicated for 10 minutes on ice in a water bath sonicator. 30 µL of

recombinant expressed PIP kinase were mixed with 20 µL reaction solution (10 µL 75 mM magnesium chloride, 1 µL 50 mM sodium molybdate, 1 µL 50 mM ATP, 1µL gamma-[³²P]ATP (10 µCi /µL), 5 µL liposome substrate in 2 % Triton X-100, 2 µl 30 mM Tris, pH = 7.4) and incubated at room temperature for 1 hour. The reaction was stopped by adding extraction solution (1.5 mL chloroform/methanol [1:2 (v/v)], 0.25 mL 0.5 M EDTA, 0.5 mL 2.4 M hydrochloric acid, 500 µl chloroform). Lipids were extracted by acidic extraction according to the method of Cho and Boss, 1995.

Samples were mixed and after phase separation, the organic bottom phase was transferred into a fresh glass tube and the upper aqueous phase was extracted a second time by 500 µL chloroform. The resulting organic phase was combined with the first organic phase and mixed with 1.5 mL 0.5 M hydrochloric acid in 50 % (v/v) methanol. The organic phase was transferred to a fresh glass tube and dried under nitrogen flow. Samples were resuspended in 30 µL chloroform/methanol [2:1 (v/v)] and pipetted on a TLC plate. The developing solvent was prepared according to Perera *et al.*, 2005 (chloroform/methanol/ammonium hydroxide/water [57:50:4:11 (v/v/v/v)]). Radioactive labeled reaction products were detected using a radiosensitive film (Kodak X-Omat, EASTMAN KODAK, Geneva, Switzerland).

2.6 Bioinformatics and image editing

Beside the Basic Local Alignment Search tools (BLAST) of the *C. elegans* database www.wormbase.org and the homepage of the National Center for Biotechnology Information (NCBI, ncbi.nlm.nih.gov/) following bioinformatics tools and software were used:

Table 10 Bioinformatics tools and software

program name	source and/or reference	purpose
BOXSHADE (mobile portal)	mobyli.pasteur.fr/cgi-bin/portal.py?form=boxshade	creating pretty plots from the multiple alignment output of ClustalW2
ClustalW2	www.ebi.ac.uk/Tools/clustalw2/index.html ; Larkin <i>et al.</i> , 2007	alignments of DNA and primary protein sequences
Deep View	spdbv.vital-it.ch/ ; Guex and Peitsch, 1997	graphical output of crystal structures and superimposing
Esript	esript.ibcp.fr/ESPript/ESPript/ ; Gouet <i>et al.</i> , 1999	creating pretty plots of primary sequence alignments combined with secondary structure
ESyPred3D	www.fundp.ac.be/sciences/biologie/urbm/bioinfo/esypred/ ; Lambert <i>et al.</i> , 2002	tertiary structure modeling
ImageJ	rsbweb.nih.gov/ij/	general image editing, analysis of image stacks, particle calculation, and videotracking
pDraw32	www.acaclone.com	textual output of DNA sequences and ORFs, graphical output of vector maps
Protein Hydrophobicity Plots	www.vivo.colostate.edu/molkit/hydropathy/index.html ; Kyte and Doolittle, 1982	calculation and graphical output of the hydrophobicity of a protein
BOXSHADE 3.21 (EMBNet)	www.ch.embnet.org/software/BOX_form.html	creating pretty plots from the multiple alignment output of ClustalW2

3 Results

3.1 RNAi screen for PIP-metabolizing enzymes in neuronal membrane trafficking

The initial aim of this study was to identify PIP-metabolizing enzymes with novel functions in neuronal membrane trafficking in *C. elegans*. A list of 12 candidates (Table 11) was compiled based upon sequence homologies to PI and PIP kinases as well as phosphatases with already described functions in membrane trafficking and/or neuronal diseases in other organisms. Another selection criterion was the probability of being a major regulator of PIPs at endomembranes and the PM as suggested by the recent literature. In addition, only genes with neuronal expression patterns were chosen (Appendix).

Table 11 Candidates for regulating PIP-dependent neuronal membrane trafficking in *C. elegans*

	gene name or accession no.	description and references
kinases	<i>vps-34</i>	ortholog of PI 3-kinase Vps34p in <i>S. cerevisiae</i> , involved in membrane trafficking between Golgi apparatus, endosomes, and lysosomes (Herman <i>et al.</i> , 1990; Roggo <i>et al.</i> , 2002)
	F35H12.4	homolog to Pik1p in <i>S. cerevisiae</i> , PI 4-kinase, catalyzes first step in biosynthesis of PI ₄ ,5P ₂ (Flanagan <i>et al.</i> , 1992)
	Y75B8A.24	homolog of Stt4p in <i>S. cerevisiae</i> , PI 4-kinase, involved in vacuole morphology and actin cytoskeleton organization (Fruman <i>et al.</i> , 1998)
	<i>ppk-1</i>	Type I PIP kinase ortholog, putative PI4P 5-kinase, regulates neuronal development in <i>C. elegans</i> (Weinkove <i>et al.</i> , 2007)
	<i>ppk-2</i>	Type II PIP kinase ortholog, putative PI5P 4-kinase (Clarke <i>et al.</i> , 2007)
	<i>ppk-3</i>	ortholog of Fab1p in <i>S. cerevisiae</i> /PIKfyve in <i>H. sapiens</i> , PI3P 5-kinase at vacuolar/lysosomal membranes (Nicot <i>et al.</i> , 2006)
phosphatases	<i>mtm-1</i>	ortholog to human MTMR1 and MTMR2, putative PI3P phosphatase, involved in endocytosis (Xue <i>et al.</i> , 2003; Zou <i>et al.</i> , 2009)
	<i>mtm-3</i>	ortholog to human MTMR3 and MTMR4, PI3P phosphatase, C-terminal FYVE domain binds PI3P <i>in vitro</i> (Xue <i>et al.</i> , 2003; Ma <i>et al.</i> , 2008)
	<i>daf-18</i>	homolog of the human tumor suppressor PTEN, PI ₃ ,4,5P ₃ 3-phosphatase, interacts with the phosphoinositide 3-kinase in cell signaling (Solari <i>et al.</i> , 2005)
	C34B7.2	homolog to the PI ₃ ,5P ₂ 5-phosphatase Fig4p in <i>S. cerevisiae</i> , controls PI ₃ ,5P ₂ levels at the vacuole, mammalian homologs are involved in severe neuropathies (Sieburth <i>et al.</i> , 2005; Chow <i>et al.</i> , 2007)
	F30A10.6	homolog to the PI4P phosphatase Sac1p in <i>S. cerevisiae</i> and human Sac1, both essential for Golgi-derived membrane transport (Blagoveshchenskaya and Mayinger, 2009)
	W09C5.7	homolog to the Sac1p-like P ₄ ,5P ₂ 5-phosphatase Sac2 of <i>H. sapiens</i> (Minagawa <i>et al.</i> , 2001)

In order to reveal a possible function for the candidate genes associated with *C. elegans* neuronal membrane trafficking, their expression in living animals was knocked down using RNAi feeding (Kamath *et al.*, 2001). For this, the according cDNA of a candidate gene was cloned into a vector

containing two inverted T7 promoter sites. Every construct was transformed into a suitable *E. coli* strain, thus providing dsRNA with the candidate's cDNA as a template (Figure 10A). These bacteria were then plated on agar plates to create a food lawn for the nematodes. Here, a *C. elegans* strain carrying mutations leading to an enhanced response to RNAi was used in order to maximize efficiency (Sieburth *et al.*, 2005; Chapin *et al.*, 2007).

Misregulation of neuronal membrane trafficking is often reflected in altered neurotransmitter release. The secretion of acetylcholine at NMJs of *C. elegans* can be easily assayed using the neurotoxin aldicarb, which acts as an inhibitor of acetylcholinesterase. Once inhibited, cleaving of acetylcholine and therefore synaptic transmission is blocked. Wild type nematodes treated with aldicarb accumulate acetylcholine at NMJs, leading to acute paralysis and subsequent death (Sieburth *et al.*, 2005; Mahoney *et al.*, 2006a).

Disturbed membrane traffic to/at the synapse in mutants or RNAi-treated animals often results in decreased acetylcholine release what delays the progress of paralysis. This phenotype is termed 'resistant to aldicarb' (*ric*). Hence, assays with this neurotoxin were the method of choice to identify new players in PIP-regulated neuronal membrane trafficking in *C. elegans*.

For RNAi feeding a synchronous population of nematodes in the youngest larva stage (L1) was used. After three days, these animals had developed to young adults (P0 generation) and were tested for aldicarb resistance. For this, nematodes were transferred on agar plates containing 1 mM aldicarb and scored for paralysis after 100 minutes. Adults of the F1 generation were tested four days later (Figure 10B).

As controls, the following genes, described to be essential for synaptic membrane traffic, have been knocked down:

- rab-3*: A small Ras protein involved in fusion of SVs to the synaptic PM (Mahoney *et al.*, 2006b).
- snb-1*: This gene encodes the SV protein synaptobrevin required for synaptic transmission (Nonet *et al.*, 1998).
- unc-26*: This gene encodes the clathrin-interacting PIP phosphatase synaptojanin essential for SV recycling (Harris *et al.*, 2006). For *unc-26*, a construct directed against the full length cDNA and additionally a construct directed against a shortened sequence, encoding solely the 5-phosphatase domain, were used.

Knock down of these control genes mostly induced a *ric* phenotype in not less than 30 % of the tested animals. In order to cover the full scale of the experimental approach with controls, consequently also the empty RNAi feeding vector has been used as negative control. Nematode populations grown on bacteria containing the empty vector showed mostly no or only very low resistance to aldicarb (equal to or less than 10 %). Hence, a candidate result was considered as aldicarb resistant when 30 % or more of the animals were not paralyzed.

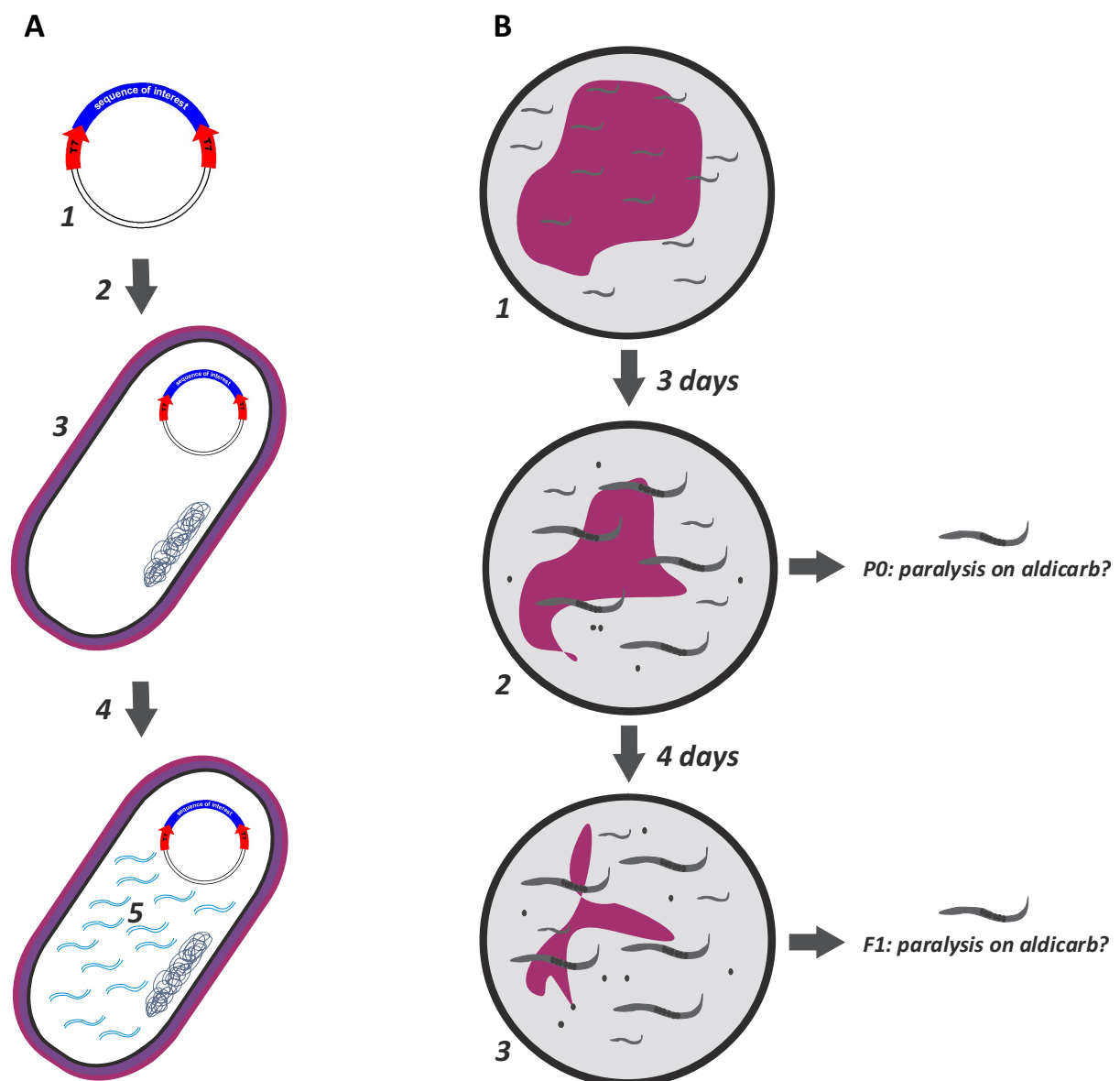


Figure 10 Setup of the RNAi screen

A, preparation of bacteria for RNAi feeding: 1, plasmid for RNAi feeding with sequence of interest flanked by two inverted T7 promoters; 2, transformation of the plasmid in *E. coli* strain HT115(DE3); 3, bacterial cell with RNAi feeding plasmid; 4, induction with IPTG; 5, RNAi feeding plasmid serves as template for dsRNA synthesis. B, *C. elegans* feeding on dsRNA-producing bacteria (simplified): 1, NGM plate with lawn of induced HT115(DE3) *E. coli* containing appropriate plasmid (purple) seeded with L1 larvae (P0 generation); 2, after three days, P0 animals have developed to young adults with eggs of which some are used for aldicarb assay (to prevent overcrowding of the plates, remaining P0 animals are removed later). Eggs and some L1 representing the F1 generation are already present. 3, after four additional days, adult F1 animals are tested for paralysis on aldicarb (eggs and L1 of the F2 generation are indicated).

To minimize the rate of false negatives in the herein presented screen, every target construct was tested for a phenotypic effect in two independently and blindly performed RNAi feeding assays.

Table 12 Results of the RNAi screen

Except *snb-1* and *mtm-3*, all candidates and control constructs were tested in two independent assays comprising two generations each (-, not resistant; *, not tested). The empty vector was always processed in parallel.

	RNAi feeding assay 1		RNAi feeding assay 2		
	P0	F1	P0	F1	
generation					
controls	<i>rab-3</i>	-	<i>ric</i>	<i>ric</i>	-
	<i>snb-1</i>	<i>ric</i>	-	*	*
	<i>unc-26</i> (full length)	<i>ric</i>	-	<i>ric</i>	-
	<i>unc-26</i> (5-phosphatase)	-	<i>ric</i>	-	<i>ric</i>
targets	C34B7.2	-	-	<i>ric</i>	-
	<i>daf-18</i>	-	<i>ric</i>	<i>ric</i>	<i>ric</i>
	F30A10.6	-	<i>ric</i>	<i>ric</i>	-
	F35H12.4	-	-	-	-
	<i>mtm-1</i>	-	-	-	-
	<i>mtm-3</i>	<i>ric</i>	<i>ric</i>	*	*
	<i>ppk-1</i>	-	-	-	-
	<i>ppk-2</i>	<i>ric</i>	-	<i>ric</i>	<i>ric</i>
	<i>ppk-3</i>	-	-	-	-
	<i>vps-34</i>	-	-	-	<i>ric</i>
	W09C5.7	-	-	-	-
	Y75B8A.24	-	-	-	-

As summarized in Table 12, six of 12 target genes turned out to cause a *ric* phenotype when knocked down by RNAi. In detail, four putative PIP phosphatases and two putative PI/PIP kinases have been identified to regulate acetylcholine release at NMJs of *C. elegans* and hence trigger neuronal membrane trafficking:

- C34B7.2 is homologous to the Sac1p-like PI3,5P₂ 5-phosphatase Fig4p in yeast and Fig4 in mammals (Sieburth *et al.*, 2005; Chow *et al.*, 2007)
- F30A10.6 is the homolog to Sac1p in yeast and Sac1 in mammals and supposed to be a PI4P phosphatase (Blagoveshchenskaya and Mayinger, 2009)
- *mtm-3* is related to the myotubularin phosphatase family (Xue *et al.*, 2003)
- *daf-18* encodes a PI3,4,5P₃ 3-phosphatase homologous to the tumor suppressor PTEN (Solari *et al.*, 2005)
- *vps-34* encodes the PI 3-kinase Type III ortholog of *C. elegans* (Roggo *et al.*, 2002)
- *ppk-2* encodes the sole Type II PI5P 4-kinase ortholog of *C. elegans* (Clarke *et al.*, 2007)

For any of the six identified PIP-metabolizing enzymes, a substantial canon of literature is available. This knowledge assigns functions to five of the six enzymes on a well funded basis. The sole exception is *ppk-2*, a putative PI5P 4-kinase ortholog expressed in the nervous system of *C. elegans* (Appendix). Here, no convincing model for its role in the phosphoinositide network is described. In summary, the available literature describing the mammalian orthologs of *ppk-2* appears to be incoherent, thus pointing towards a fundamental lack of knowledge associated with these enzymes. In mammalia, three isoforms of PI5P 4-kinases have been described to localize at different locations within the cell and showing varying expression patterns (Clarke *et al.*, 2007). Hence, the functions of the three Type II PIP kinase isoforms may be overlapping *in vivo*, making a detailed analysis difficult. Thus, a model organism with only one representative of this enzyme family possesses a big potential to discover a physiological function. Therefore, it was decided to dedicate the focus of this study to the yet uncharacterized Type II PIP kinase ortholog *ppk-2* and its putative functions in neuronal membrane trafficking of *C. elegans*.

3.2 Analysis of the putative PI5P 4-kinase PPK-2 in the nervous system of *C. elegans*

Results obtained from the RNAi screen, described in the previous section 3.1, assigned a neuronal function to *ppk-2*, a putative Type II PIP kinase ortholog. *ppk-2* is known to be expressed predominantly in the nervous system of *C. elegans* (Appendix).

The vast majority of knowledge regarding Type II PIP kinases is available for the three Type II PIP kinase isoforms of *H. sapiens* and the two main mammalian model systems *Mus musculus* (*M. musculus*) and *Rattus norvegicus* (*R. norvegicus*) (Clarke *et al.*, 2007; Clarke *et al.*, 2009). The respective isoforms (alpha, beta, gamma) are highly conserved in all three organisms and are supposed to have comparable physiological functions (Clarke *et al.*, 2007). In the following, the term ‘mammalian’ always refers to the Type II PIP kinases of human, mouse, or rat.

3.2.1 PPK-2 is orthologous to mammalian PI5P 4-kinases

The following section will focus on the comparison of *C. elegans* PPK-2 to its mammalian orthologs.

Phylogenetic distances of PPK-2 to its known mammalian orthologs have been determined and are illustrated in Figure 11. Since the mammalian Type II PIP kinases are highly conserved to each other, enzymes of the same isoform of different organisms show similar phylogenetic distances to PPK-2. In summary, all respective Type II PIP kinase isoforms show comparably high homology to *C. elegans* PPK-2, owing between 47 and at most 52 % conserved amino acids (Appendix). For comparison sake, a sequence alignment with PPK-2 orthologs identified in other model organisms such as zebra fish and fruit fly can be found in the Appendix.

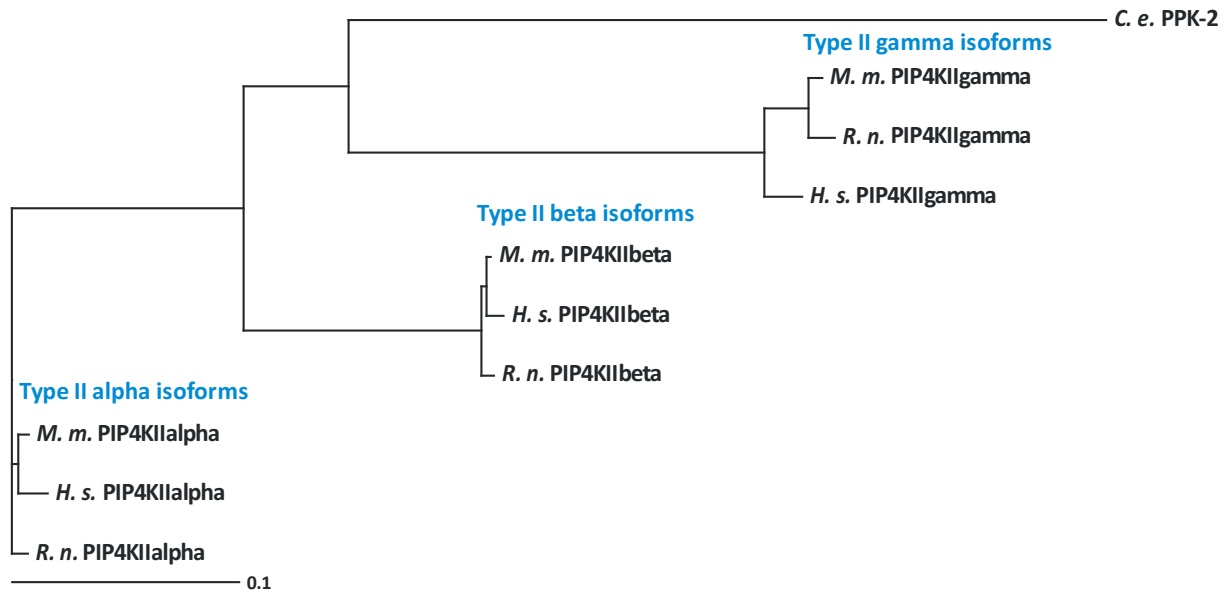


Figure 11 Phylogenetic tree of *C. elegans* PPK-2 and mammalian orthologs

Enzymes of the same isoform of different organisms show similar phylogenetic distances to PPK-2. H. s., *H. sapiens*; M. m., *M. musculus*; R. n., *R. norvegicus*; scale bar, 0.1 substitutions per amino acid site.

The structurally best characterized mammalian Type II PIP kinase is the beta isoform of *H. sapiens* whose structure was solved by crystallization. Beside this structural information also catalytically important amino acids have been identified. Thus, substantiated information linking primary sequence information with tertiary structure-dependent function is available for this protein (Rao *et al.*, 1998; Kunz *et al.*, 2000; Kunz *et al.*, 2002).

In order to assign a putative function to amino acids in the primary sequence of PPK-2, a direct comparison to *H. sapiens* Type II PIP kinase beta has been carried out. To compare the *C. elegans* kinase to all three mammalian Type II PIP kinase isoforms, the two remaining human isoforms alpha and gamma have been considered for the sequence alignment as well.

The multiple sequence alignment shown in Figure 12 demonstrates the high conservation between PPK-2 and any of the human Type II PIP kinase isoforms. Beside the overall sequence similarity also essential amino acids for catalysis and membrane interaction predicted for *H. sapiens* Type II PIP kinase beta are conserved (Rao *et al.*, 1998).

Most importantly, the so-called activation loop of Type II PIP kinases is found to be conserved in the C-terminus of PPK-2. The activation loop was demonstrated to be crucial for subcellular localization (Kunz *et al.*, 2000) and furthermore one of its comprising amino acids determines substrate specificity for PI5P (Kunz *et al.*, 2002). This particular alanine is conserved throughout all Type II PIP kinases, including PPK-2.

Since the primary sequence of PPK-2 is very similar to its human orthologs, it is likely that also the secondary and tertiary structure is conserved. In order to test this, a modeling attempt for PPK-2 has been done. Indeed, it was possible to obtain a tertiary structure model of PPK-2 when using the structure of *H. sapiens* Type II PIP kinase beta as a template. To prelude this, a brief summary

addressing the structure and some characteristics of *H. sapiens* Type II PIP kinase beta is given in the following section, leading to the template based modeling of PPK-2.

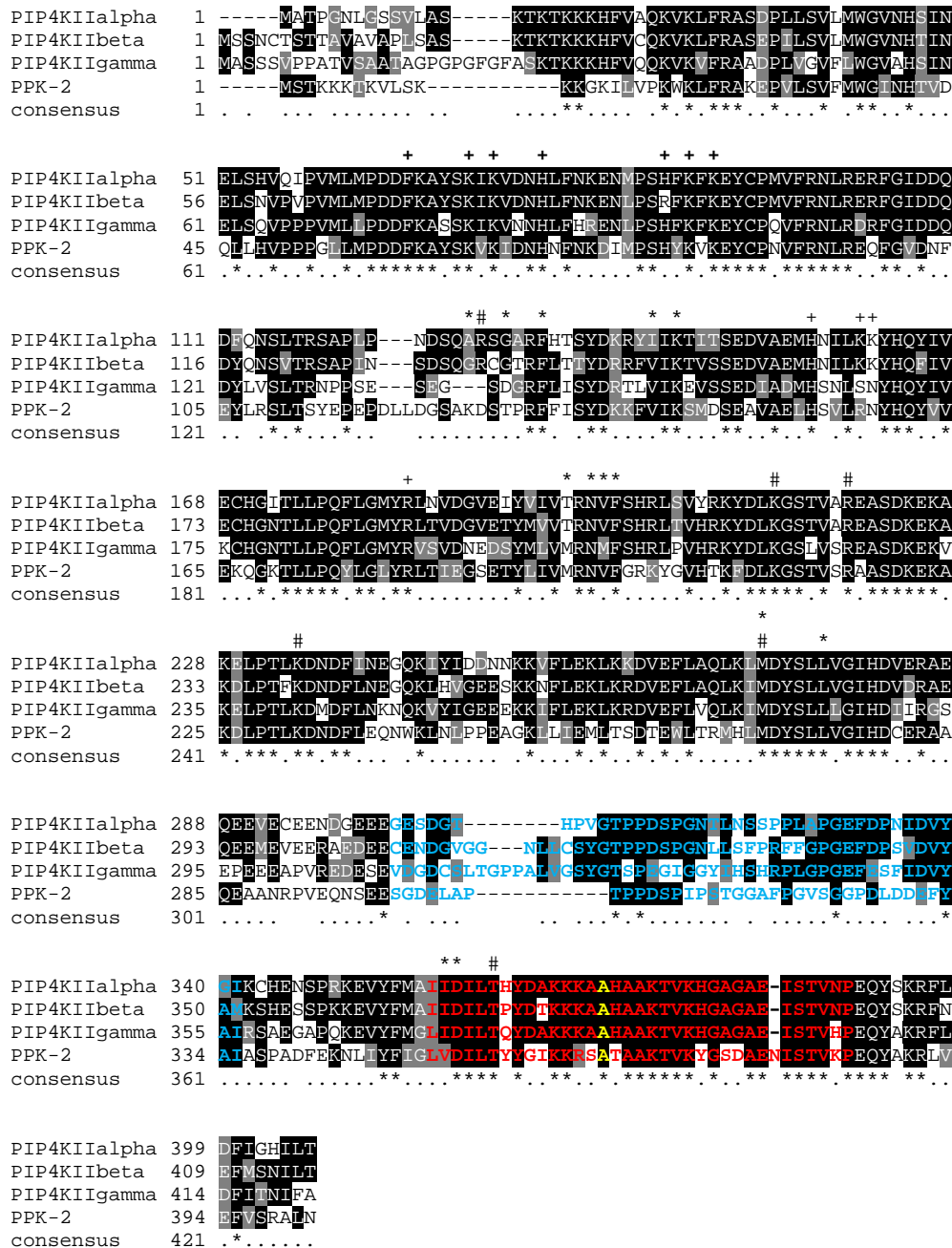


Figure 12 Primary sequence alignment of PPK-2 and human orthologs

The primary sequence of PPK-2 was aligned with all three P15P 4-kinase isoforms of *H. sapiens* (PIP4KIIalpha, PIP4KIIbeta, PIP4KIIgamma). Conserved and similar amino acids are shaded in black and grey, respectively. The variable insert is colored in blue and the activation loop is highlighted in red letters with the conserved alanin essential for substrate specificity (Kunz et al., 2000; Kunz et al., 2002) shown in yellow. Functional amino acids in ATP binding (*), membrane binding (+), and P15P binding (#) are marked according to Rao et al., 1998.

The tertiary structure of *H. sapiens* Type II PIP kinase beta consists of an N-terminal and a C-terminal domain. Both domains in turn are built of an antiparallel beta sheet, whereas according alpha helices form mainly the exterior surface of the protein (Figure 14A). The folding of *H. sapiens* Type II PIP kinase beta is related to the tertiary structure of protein kinases (Rao *et al.*, 1998; Grishin *et al.*, 1999).

The secondary structure of *H. sapiens* Type II PIP kinase beta is comprised of alpha helices as well as beta strands. In Figure 13, the Type II PIP kinase beta topology was projected on its primary sequence aligned with the primary sequence of PPK-2. Amino acids assigned to secondary structure elements of Type II PIP kinase beta were found to be mostly identical to the corresponding amino acids of PPK-2 hence leading to the conclusion that PPK-2 possesses a similar topology.

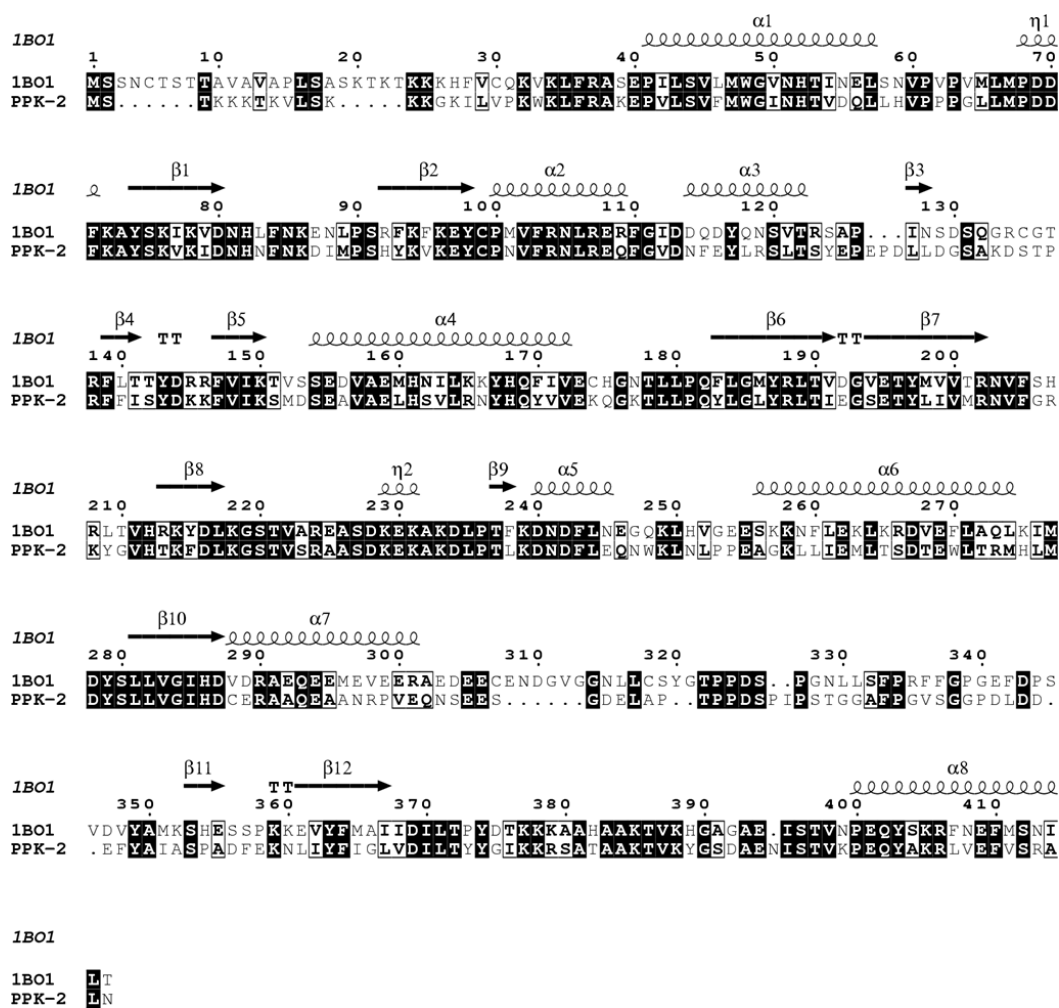


Figure 13 Putative secondary structure of PPK-2

Primary sequence alignment of PPK-2 and human Type II PIP kinase beta (PDB ID 1BO1) combined with the according secondary structure comprised of alpha helices (spirals) and beta strands (arrows) (according to Rao *et al.*, 1998). Identical amino acids are shaded in black, well conserved amino acids are shown in bold and are boxed.

The crystal structure of *H. sapiens* Type II PIP kinase beta possesses two structural disordered regions: the activation loop and the so-called insert (Figures 12 and 14A). As already mentioned, the C-terminal activation loop is essential for cellular localization as well as for substrate recognition and hence catalytic activity (Kunz *et al.*, 2000). The insert is a region located proximally to the activation loop and highly divergent between all Type II PIP kinases (Heck *et al.*, 2007).

The *H. sapiens* Type II PIP kinase beta can form a homodimer (Figure 14B), mediated by the N-termini of both monomers. In addition, the N-terminus contains many basic amino acids and is therefore thought to be important for the interaction with the positively charged head groups of membrane lipids (Rao *et al.*, 1998).

Tertiary structure modeling of PPK-2 was possible using the tertiary structure of *H. sapiens* Type II PIP kinase beta (PDB ID 1BO1) as a template. As illustrated in Figures 14C and D, its putative folding is indeed very similar to the human enzyme.

This tertiary structure information, combined with the primary sequence alignment and derived putative secondary structure elements, allows the conclusion that PPK-2 is a *bona fide* Type II PIP kinase.

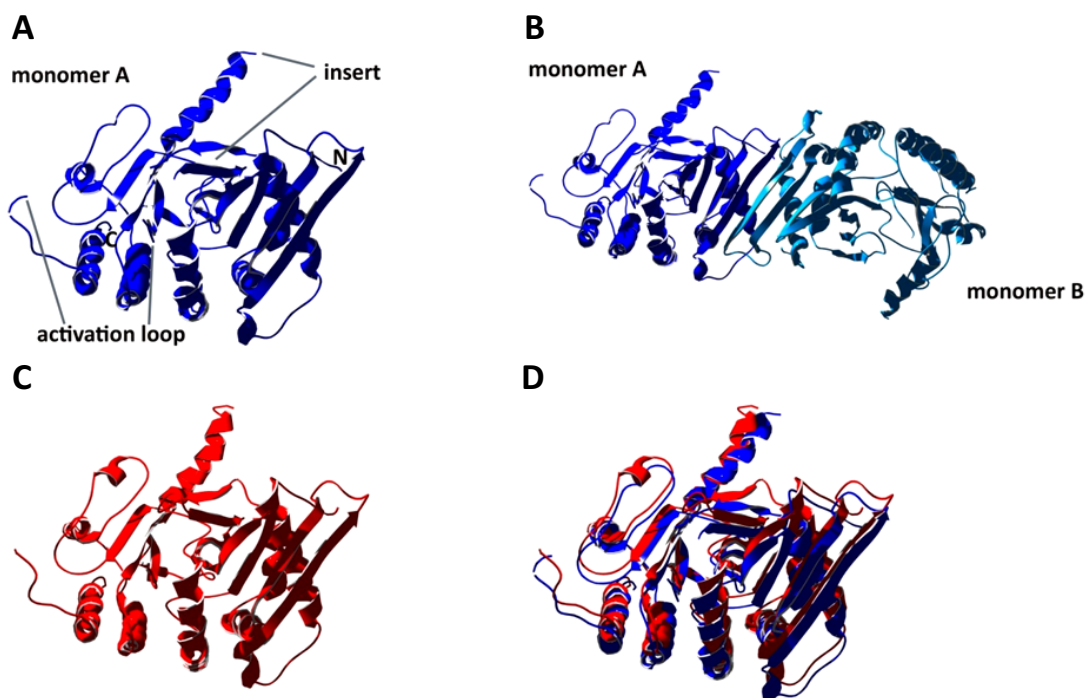


Figure 14 Modeling of the putative tertiary structure of PPK-2

Ribbon drawings. A, tertiary structure of human Type II PIP kinase beta (chain A, PDB ID 1BO1). The highly flexible regions of the insert and the activation loop are sketched. B, postulated homodimer of human Type II PIP kinase beta (Rao *et al.*, 1998). C, tertiary structure of PPK-2 modeled based on the crystal structure of monomer A of human Type II PIP kinase beta. D, superposition of A and C.

3.2.2 RNAi knock down of *ppk-2* is specific

PPK-2 is the sole Type II PIP kinase ortholog of *C. elegans* and as such related to the sole Type I PIP kinase ortholog in the nematode termed PPK-1 (Weinkove *et al.*, 2007; Appendix). Type I PIP kinases are known to regulate the amount of PI4,5P₂ and hence regulate actin reorganization and membrane trafficking at the PM (Heck *et al.*, 2007).

Since a deletion allele of *ppk-1* is not viable, all information about its physiological function was obtained either by its overexpression or RNAi mediated knock down. Overexpressed PPK-1-GFP was described to localize to the PM of neurons, regulate PI4,5P₂ levels, and influence the development of neuronal growth cones (Weinkove *et al.*, 2007). *ppk-1* (RNAi) nematodes showed to be sterile (Xu *et al.*, 2007), however, a physiological function for *ppk-1* in neuronal membrane trafficking was hypothesized based on the knowledge about mammalian Type I PIP kinases, but never shown. Indeed, also in the here presented RNAi screen for decreased acetylcholine release at NMJs, *ppk-1* (RNAi) did not induce any obvious phenotype (section 3.1).

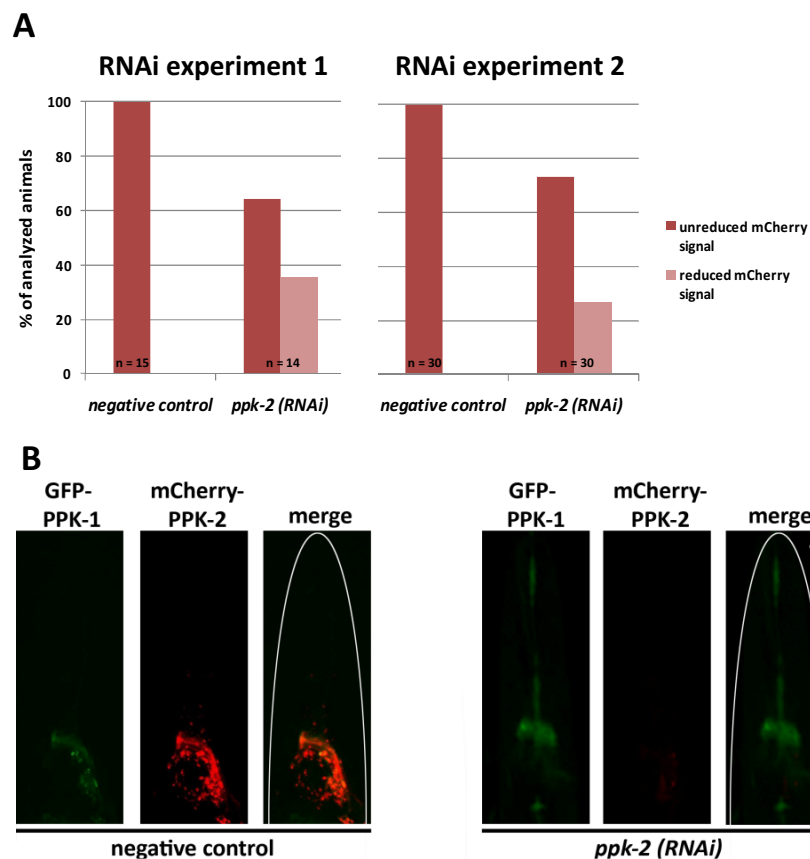


Figure 15 RNAi knock down of *ppk-2* is specific

ppk-2 (RNAi) was performed using a *C. elegans* strain with enhanced RNAi response, expressing mCherry-labeled PPK-2 and GFP-labeled PPK-1 in all neurons. A, statistical results of two independently and blindly conducted RNAi experiments scoring for unreduced or reduced mCherry signals in the head of adult animals. B, mCherry-PPK-2 but not GFP-PPK-1 is depleted in the head neurons of adult animals. The approximate shapes of the nematodes' heads are drawn in the merge pictures. Scale bar, 10 μ m.

Since the transcripts of *ppk-1* and *ppk-2* share some sequence similarities (www.wormbase.org), it is possible that *ppk-2* (RNAi) reduces the expression of both *ppk-1* and *ppk-2*. In order to test for this 'off target' RNAi effect, a *C. elegans* strain with enhanced RNAi response, expressing pan-neuronal mCherry-labeled PPK-2 and GFP-labeled PPK-1, was created and used for RNAi feeding.

Full adult transgenic animals were placed on *ppk-2* dsRNA-expressing bacteria, purposed to lay eggs. After several days, the F1 generation had developed to adults and was analyzed under the microscope for the expression of either GFP-PPK-1 or mCherry-PPK-2. As shown by two independently performed RNAi experiments, the mCherry signal but not the GFP signal was massively depleted in about 30 % of the *ppk-2* (RNAi) animals when compared to the control group (Figure 15A). The reduction of signal could be easily observed in the head of nematodes where many neuronal cell bodies and processes are organized in a dense structure called the nerve ring (Figure 15B).

Taken these results together, it must be concluded that *ppk-2* (RNAi) is specific and does not influence the expression of *ppk-1*.

3.2.3 Analysis of two different *ppk-2* mutants

Two different mutant alleles of *ppk-2* are available. *ppk-2* (*ttTi8500*) was received from the NemaGENETAG mutant bank located at the University of Lyon, France, and possesses a transposon insertion in the third exon (the exon/intron structure of *ppk-2* can be found in the Appendix) what can result in a truncated or misspliced transcript. The second allele *ppk-2* (*tm3741*) was generated by the National Bioresource Project of Japan in Tokyo. In *ppk-2* (*tm3741*), 285 nucleotides are deleted across the first exon/intron border.

3.2.3.1 Transcript analysis

In order to analyze the mutant *ppk-2* transcripts, total RNA was isolated from both mutant strains and used for the synthesis of cDNA. Specific primers were successfully used for the amplification of *ppk-2* transcripts from both alleles, showing that the mutated *ppk2* loci are still transcribed. The obtained PCR amplicates were comparable in size to the transcript of *ppk-2* wild type (1201 nucleotides, Appendix).

Subsequent sequencing revealed the deletion and exchanges of several nucleotides in the transcript of *ppk-2* (*ttTi8500*) from position 487 to 532 (Figure 16A). The transcript of *ppk-2* (*tm3741*) showed multiple mutations from position 1 to 181, resulting in a striking alteration of the sequence (Figure 16B), thus destroying the original start codon.

Both transcripts still comprised open reading frames for mutated PPK-2 proteins. In PPK-2 (*ttTi8500*), a stretch of 14 amino acids from position 165 to 178 is deleted. The neighboring valine at position 163 is changed to glutamine and arginine 180 to lysine, respectively (Figure 16C). *Inter alia* due to the missing start codon of *ppk-2* (*tm3741*), the N-terminus of the protein cannot be translated. However, an alternative start codon has been identified at position 250 (Figure 16B), resulting in a truncated protein here named PPK-2 (*tm3741*) (Figure 16C).

3.2.3.2 Putative structural changes of PPK-2 mutants

As described under 3.2.3.1, in PPK-2 (*ttTi8500*) several amino acids are deleted or exchanged (Figure 16C). Assuming a topology of PPK-2 comparable to human Type II PIP kinase beta, this alteration affects the amino acid stretch between alpha helix 4 and beta strand 6 (Figure 17A).

The N-terminal half of alpha helix 4 and the beta strands 1, 2, 6, and 7 are supposed to form the surface of the kinase, hypothesized to be essential for membrane attachment (Rao *et al.*, 1998). Assuming that PPK-2 (*ttTi8500*) folds comparable to PPK-2 wild type, the deletion of the amino acid stretch most likely results in an alteration of the protein region putative responsible for membrane attachment (Figures 17B to G).

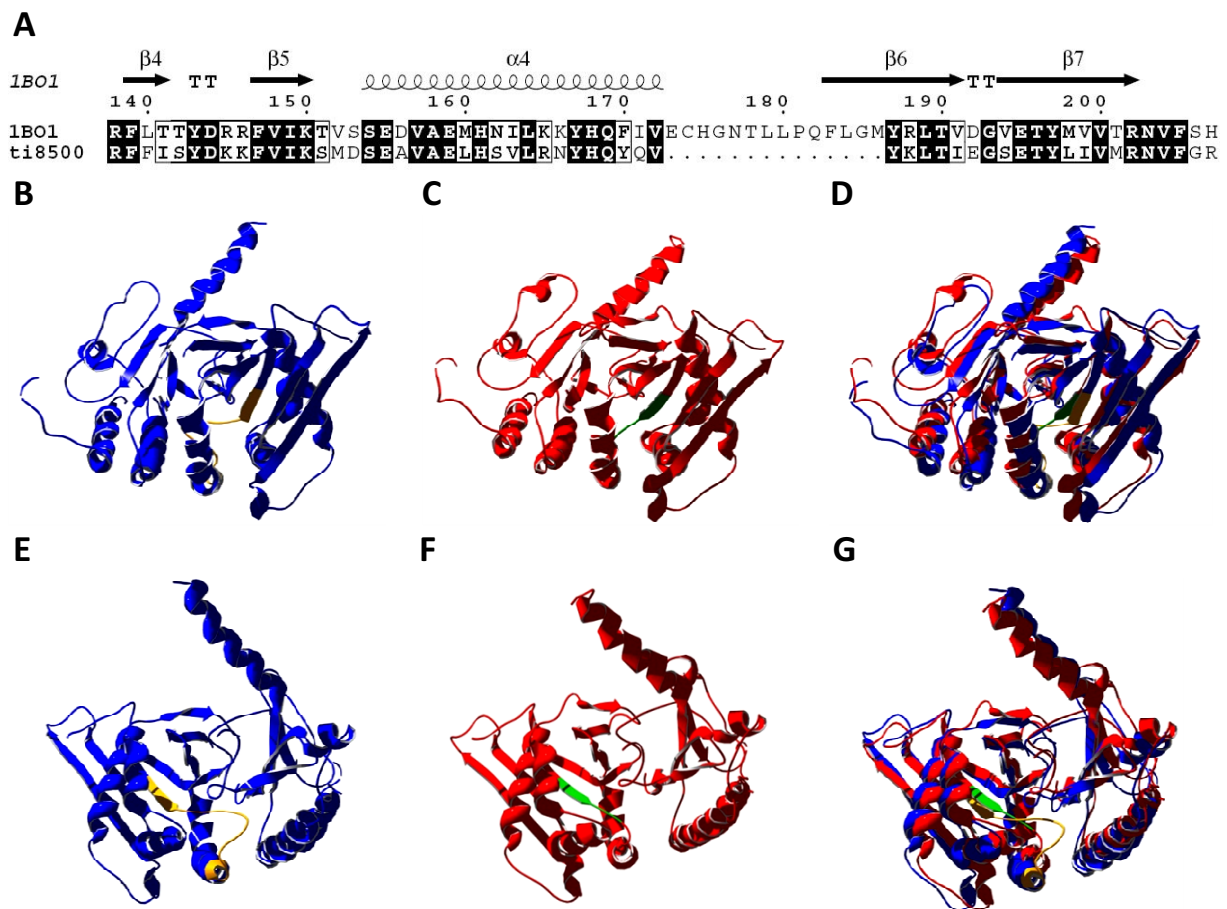


Figure 17 Putative secondary and tertiary structure of PPK-2 (*ttTi8500*)

A, primary sequence alignment of PPK-2 (*ttTi8500*) and human Type II PIP kinase beta (PDB ID 1BO1). The secondary structure of human Type II PIP kinase beta is depicted above the alignment (spirals, alpha helices; arrows, beta strands). Identical amino acids are shaded in black, well conserved amino acids are shown in bold and are boxed. B and E, crystal structure of monomer A of human Type II PIP kinase beta from two different angles (PDB ID 1BO1). The peptide stretch homologous to the mutated region in PPK-2 (*ttTi8500*) is colored in yellow. C and F, putative structure of PPK-2 (*ttTi8500*) derived from the modeled structure of PPK-2 in Figure 11C from two different angles. The mutated region is highlighted in green. D and G, superposition of B and C, and E and F, respectively.

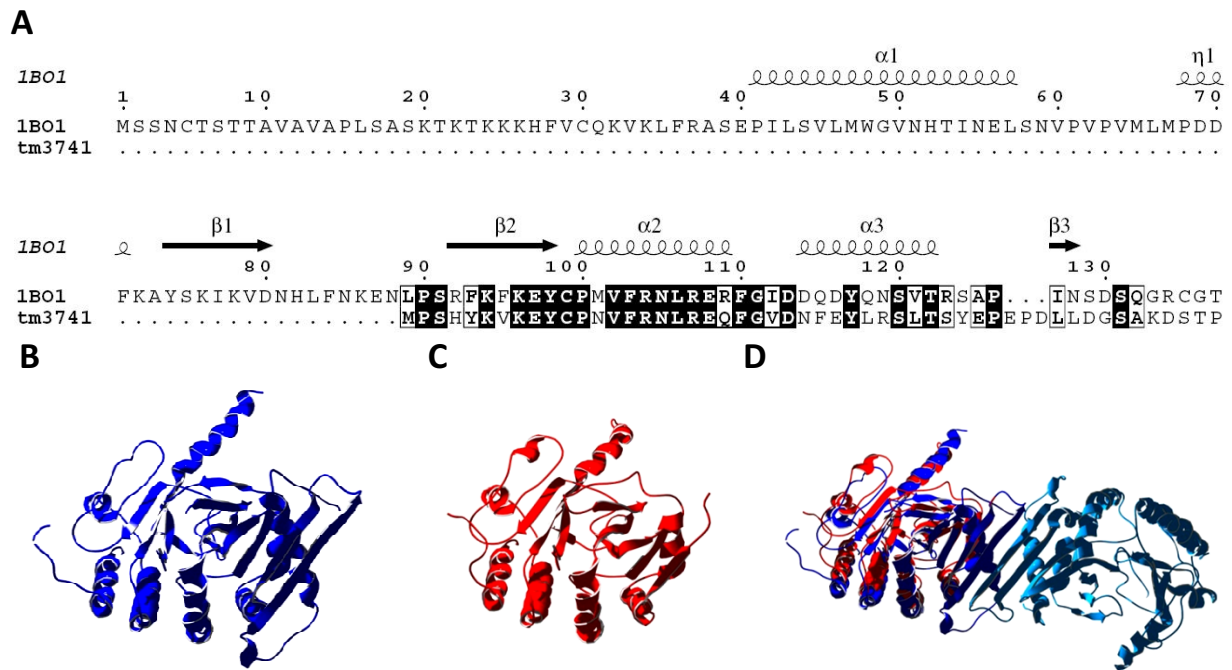


Figure 18 Putative secondary and tertiary structure of PPK-2 (tm3741)

A, primary sequence alignment of PPK-2 (tm3741) and human Type II PIP kinase beta (PDB ID 1BO1), combined with the according secondary structure comprised of alpha helices (spirals) and beta strands (arrows). Identical amino acids are shaded in black, well conserved amino acids are shown in bold and are boxed. B, crystal structure of monomer A of human Type II PIP kinase beta (PDB ID 1BO1). C, putative structure of PPK-2 (tm3741) derived from the modeled structure of PPK-2 in Figure 11C. D, superposition of PPK-2 (tm3741) with monomer A of the Type II PIP kinase beta homodimer (PDB ID 1BO1).

The altered transcript of *ppk-2* (*tm3741*) results in an N-terminally truncated translation product, whereby most of the membrane interacting amino acids are deleted (Figure 18A). Since the N-terminus is thought to be responsible for dimerization, this may be affected as well (Figure 18B to D).

Taken together, the mutations of both *ppk-2* alleles most likely result in significantly changed N-terminus of the according protein.

3.2.3.3 Neurotoxin assays

The RNAi-mediated knock down of *ppk-2* expression results in the decrease of acetylcholine release at NMJs, as revealed by aldicarb assays (section 3.1). Consequently, the aldicarb resistance of both *ppk-2* mutant strains was compared to wild type and a *rab-3* mutant in a blinded assay (Figure 19A). Adults of each strain were placed on agar plates containing 1 mM aldicarb and the progress of paralysis was observed after one and two hours, respectively.

ppk-2 (*ttTi8500*) shows not a *ric* but a so-called *hic* phenotype, meaning that animals react hypersensitive to aldicarb and are earlier paralyzed than wild type nematodes (Mahoney *et al.*, 2006a). Indeed, more than 80 % of *ppk-2* (*ttTi8500*) animals are already paralyzed after one hour, but

less than 20 % of wild type animals. In contrast, *ppk-2 (tm3741)* shows no significant resistance or hypersensitivity to aldicarb. Indeed, its response to the neurotoxin is very comparable to the wild type with about 80 % of paralyzed nematodes after two hours. The *rab-3* mutant, used as a positive control, does not react significantly to aldicarb.

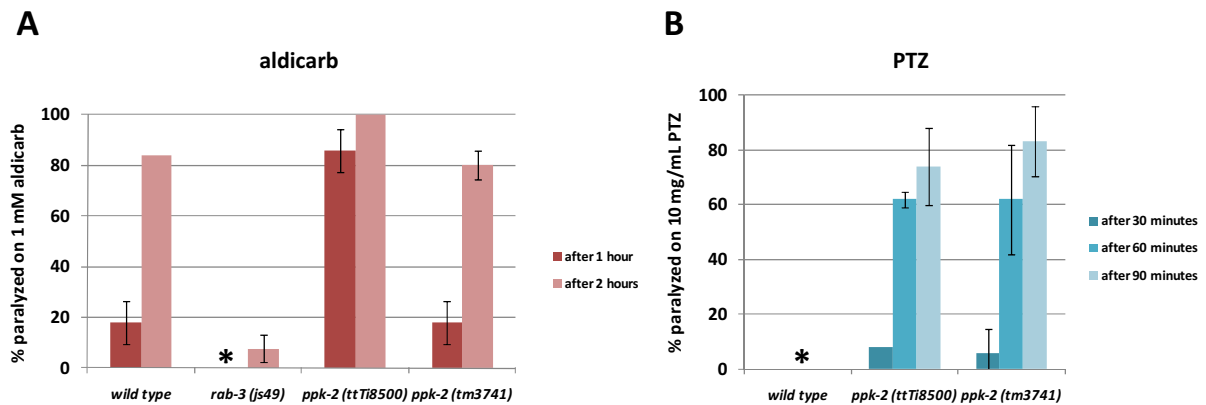


Figure 19 Aldicarb and PTZ assays of *ppk-2* mutants

A, aldicarb assay of both *ppk-2* mutants compared to wild type nematodes and a *rab-3* mutant as positive control. B, PTZ assay of both *ppk-2* mutants in comparison to wild type. *, no paralyzed nematodes observed, error bars, standard deviation. Every assay was at least repeated two times.

An alternative method to analyze the neurotransmitter release of *C. elegans* is an assay with the GABA antagonist PTZ, blocking the function of inhibitory synapses. Mutants lacking negative regulation of neurotransmitter release, thereby exocytosing excessive acetylcholine, become paralyzed on PTZ (Locke *et al.*, 2008).

As illustrated in Figure 19B, both *ppk-2* mutants show comparable reactions when placed on agar plates containing 10 mg/mL PTZ. The mutants displayed sensitive behavior to PTZ, as documented by paralysis of approximately 60 and 80 % of the analyzed nematodes after 60 and 90 minutes, respectively. Wild type nematodes did not show any paralysis in this blinded assay. Taken together, these two different neurotoxin assays reveal that *ppk-2 (ttTi8500)* as well as *ppk-2 (tm3741)* secretes more acetylcholine at NMJs than wild type animals.

To exclude the possibility of a postsynaptic defect in *ppk-2* mutants, both alleles were additionally tested for the reaction to the acetylcholine antagonist levamisole. Levamisole blocks synaptic transmission at excitatory synapses leading in turn to paralysis of wild type animals. Alteration of the postsynapse in mutants often results in levamisole resistance (Lewis *et al.*, 1980).

The response to levamisole was tested for both *ppk-2* mutants in comparison to wild type and in a blinded assay. As shown in Figure 20, all three strains showed 100 % paralysis after 10 minutes on agar plates containing 1 mM and 2 mM levamisole, respectively, indicating that the postsynapses of *ppk-2* mutants function comparable to wild type.

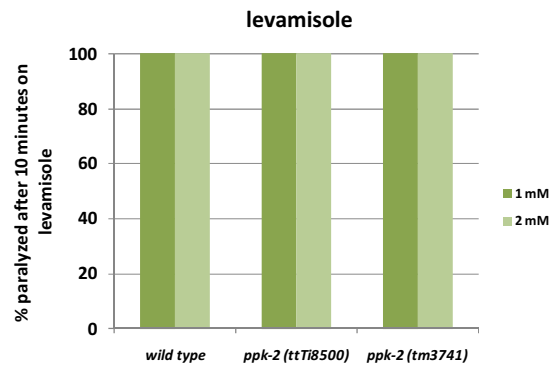


Figure 20 Levamisole assay of ppk-2 mutants

Response to levamisole of ppk-2 mutants compared to wild type, quantified after 10 minutes on agar plates containing 1 mM and 2 mM levamisole. Respective standard deviations = 0. The assay was repeated three times.

3.2.3.4 Motility analysis

A defect in synaptic transmission is often reflected in the motility of nematodes. Therefore, the appearance of the ppk-2 mutants' traces on agar was analyzed. Adults of wild type, ppk-2 (ttTi8500), and ppk-2 (tm3741) were placed on agar plates with a bacterial food lawn and allowed to crawl, leaving a track on the agar (Figure 21). Wild type animals make sinusoidal traces when moving forward. The traces of ppk-2 (ttTi8500) and ppk-2 (tm3741) are less regular varying from flattened tracks to irregular curvature.

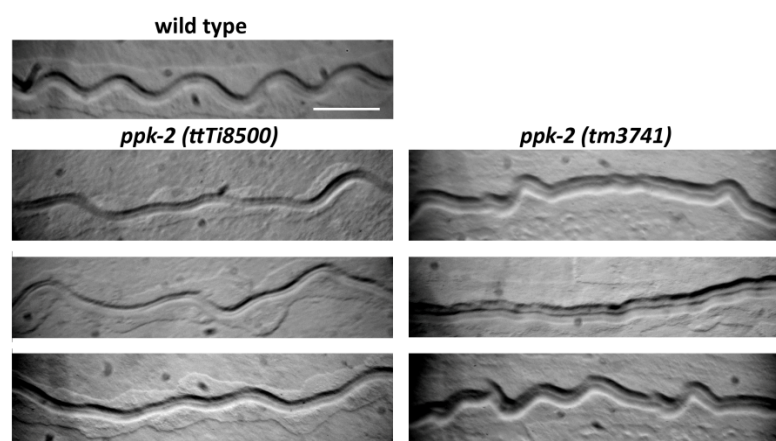


Figure 21 ppk-2 mutants display uncoordinated movements on agar

Representative traces of adult animals of wild type, ppk-2 (ttTi8500), and ppk-2 (tm3741) on agar.

To determine the velocity of ppk-2 mutants, small populations of every genotype have been analyzed by video tracking. Hereby, the distance every single nematode of a population moves per second has

been recorded. The frequency of any measured distance traveled within one second by the individual animals of a population was averaged and graphed as a cumulative plot (Figure 22).

Basically, this graph illustrates the different frequencies of traveled distances per second within a population. Dependent on the frequency with which the different velocities occur, graphs representing different nematode strains either possess a steep ascent or a flat ascent. A flat ascent is caused by the accumulated occurrence of animals moving relatively fast, while a steep ascent is caused by the accumulated occurrence of animals in the population moving relatively slow.

The cumulative graph representing the wild type population ascends continually from 0 to almost 100 %, thereby covering a velocity range from 0 to 0.25 mm/sec. The *ppk2 (ttTi8500)* mutant differs: The distribution of the counted traveled distances is slightly broader. Single animals of the mutant population move with up to 0.3 mm/sec resulting in a mildly flattened ascent of the cumulative graph. However, this difference is marginal, thus maybe not significant.

The *ppk2 (tm3741)* mutant differs considerably from wild type: A significantly higher percentage of this mutant population moves relative slow reflected in a steeper ascent of the cumulative graph in the lower velocity range.

Taken together with the results obtained from the trace analysis, it can be concluded that both *ppk2* mutants show a mild uncoordinated phenotype.

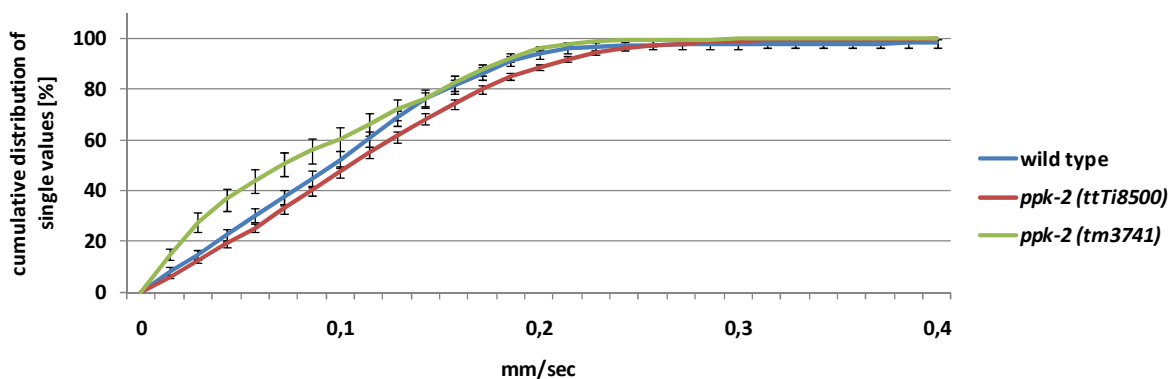


Figure 22 Cumulative distribution of velocities displayed by *ppk-2* mutants and wild type

Averaged frequencies of any measured distance traveled within one second by the individual animals (single values) of populations of wild type ($n = 82$), *ppk-2 (ttTi8500)* ($n = 52$), and *ppk-2 (tm3741)* ($n = 49$). Error bars, standard error of the mean.

3.2.3.5 Development of cholinergic and GABAergic neurons

Altered neurotransmission release in *C. elegans* can be caused by misdevelopment of the nervous system. To analyze this issue, cytosolic GFP driven by different promoters specific for either cholinergic or GABAergic neurons was used as marker for according neuron types. The position and number of somata of representative cell populations along the ventral cord were determined in young adult animals for both *ppk-2* mutant backgrounds and compared to wild type.

As shown in Figure 23A, the number of cholinergic neurons in *ppk-2* mutants was found to be normal. Also the position of somata was not significantly changed compared to wild type (Appendix).

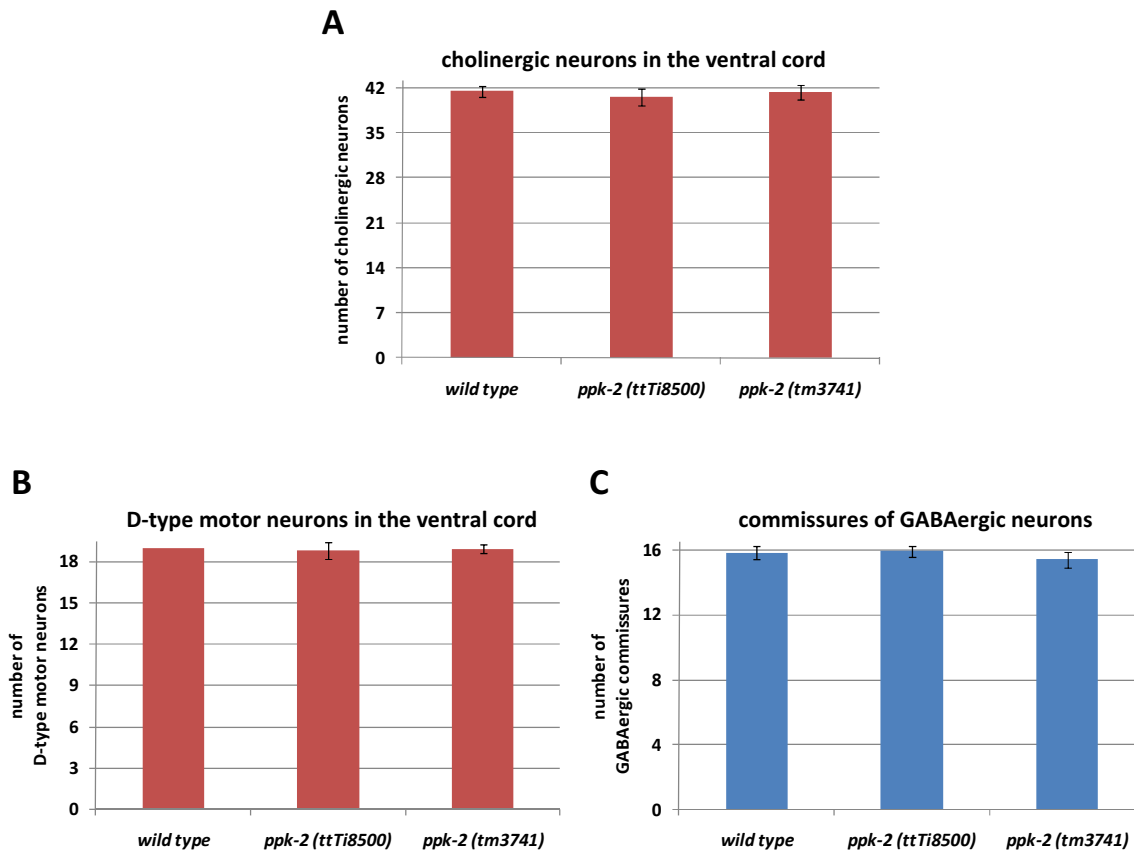


Figure 23 Quantification of cholinergic and GABAergic somata and commissures

Statistical analysis of the number of cell bodies of the respective neuron types in different genotypes (ten adults each). A, cholinergic somata along the ventral cord. B, GABAergic D-type motor neurons along the ventral cord. C, GABAergic commissures. Error bars, standard deviation.

The number and positions of a GABAergic neuron subtype, D-type motor neurons, along the ventral cord were analyzed for each genotype and found to be normal in *ppk-2* mutants as compared to control animals (Figure 23B). The strong expression of the GABAergic GFP in addition allowed the analysis of according commissures pointing towards the dorsal cord (Figure 23C). Positions and number of the neuronal processes match with those of wild type nematodes (Appendix).

Taken together, these representative subpopulations of neurons showed no abnormalities, indicating that the overall development of the nervous system is not affected in *ppk-2* mutants.

2.2.3.6 Quantification of progeny

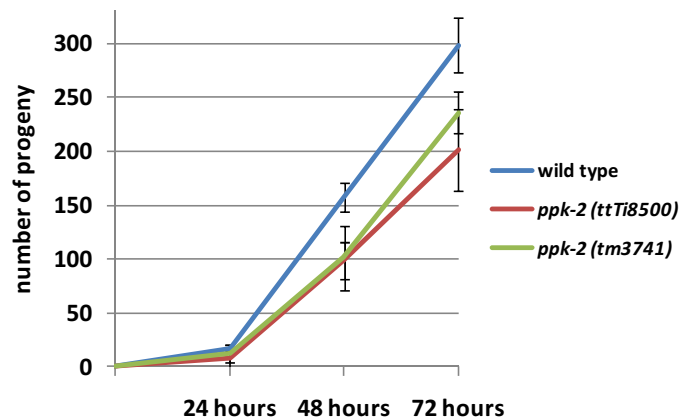


Figure 24 Quantification of progeny

The progeny of both *ppk-2* mutants and wild type animals was quantified over three days (ten adults each). No unhatched eggs have been observed. Error bar, standard deviation.

To analyze whether or not *ppk-2* mutations affect reproduction, the progeny of both *ppk-2* mutant alleles was counted and compared with the number of offspring derived from wild type nematodes (Figure 24). This comparison revealed a decreased number of progeny, derived from both mutant *ppk-2* alleles. Noteworthy, no unhatched eggs have been observed when screening the plates with the *ppk-2* mutant nematodes for progeny. Thus, the decreased number of offspring must be caused by an intrinsic defect in the reproduction system of the mother animals.

Taken together, both *ppk-2* mutant alleles are causal for a decreased number of progeny.

3.2.3.7 Analysis of SV and DCV markers

Acetylcholine release at NMJs is dependent on the correct exo- and endocytosis and therefore localization of SVs. To analyze this localization in neurons of *ppk-2* mutants, the protein synaptogyrin was used as marker for SVs (Zhao and Nonet, 2001).

A *C. elegans* synaptogyrin (SNG-1) GFP-fusion was expressed driven by its own promoter in wild type and both *ppk-2* mutant backgrounds, thus allowing the visualization of SVs at the synapse (Zhao and Nonet, 2001). A high density of synapses in *C. elegans* is found in the so-called dorsal cord, where mostly the axons of motor neurons are bundled. Hence, a strong SNG-1-GFP signal was detected along the whole length of the dorsal cord of wild type animals and has shown to be the same in both *ppk-2* mutants (Figure 25A).

The majority of processes forming the dorsal cord are derived from somata located in the ventral cord. The ventral cord bundles axons as well as dendrites and according neuronal cell bodies. Since

synaptogyrin is synthesized in cell bodies, also here a fluorescence signal is detectable in wild type nematodes. The same is true for both *ppk-2* mutant strains (Figure 25A).

The fluorescence signals obtained from dorsal cords from wild type, *ppk-2* (*ttTi8500*), and *ppk-2* (*tm3741*) animals have been quantified, averaged and normalized to wild type (Figure 25B). An increase or decrease of SNG-1-GFP fluorescence would indicate a significant change in SV localization pattern. However, no differences to wild type nematodes have been observed.

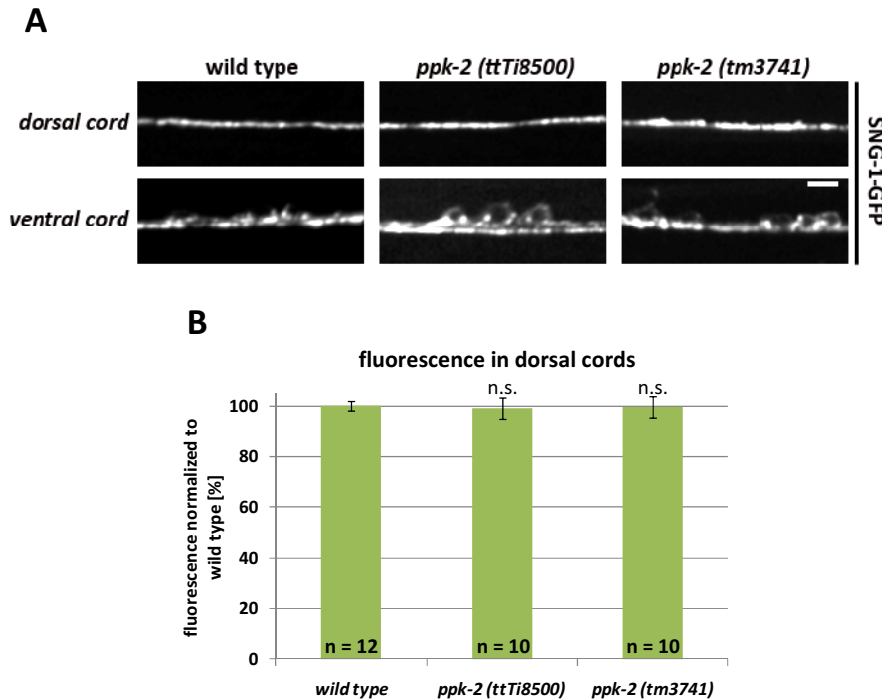


Figure 25 Synaptogyrin localization in *ppk-2* mutants

A, the localization of GFP-labeled synaptogyrin (SNG-1) was analyzed in dorsal as well as ventral cords of young adults. Scale bar, 5 μ m. B, SNG-1-GFP fluorescence was quantified in the dorsal cords (n) of both *ppk-2* mutants and normalized to the wild type average. Error bar, standard error of the mean, n.s., not significant, Student's t-test.

SNG-1-GFP was also detected in the long sublateral axons of young adults. Since SNG-1 is known to localize primarily to synapses (Zhao and Nonet, 2001), this allowed the imaging of synaptic clusters along these neuronal processes (Figure 26A). For analysis, images of axon tracts have been straightened and colors were inverted (Figure 26B). The statistical evaluation revealed a significant increase of the number of SNG-1-GFP puncta in the axon tracts of *ppk-2* (*ttTi8500*) animals compared to wild type. For *ppk-2* (*tm3741*), a slight increase was observed, however, this was not statistically significant (Figure 26C).

Another important class of secretory vesicles in neurons are DCVs. DCVs are not loaded with neurotransmitters e.g. acetylcholine or GABA but with signaling peptides. These neuropeptides, not

exclusively exocytosed at the same site as SVs, regulate synaptic transmission and hence the release of neurotransmitters (Sieburth *et al.*, 2006).

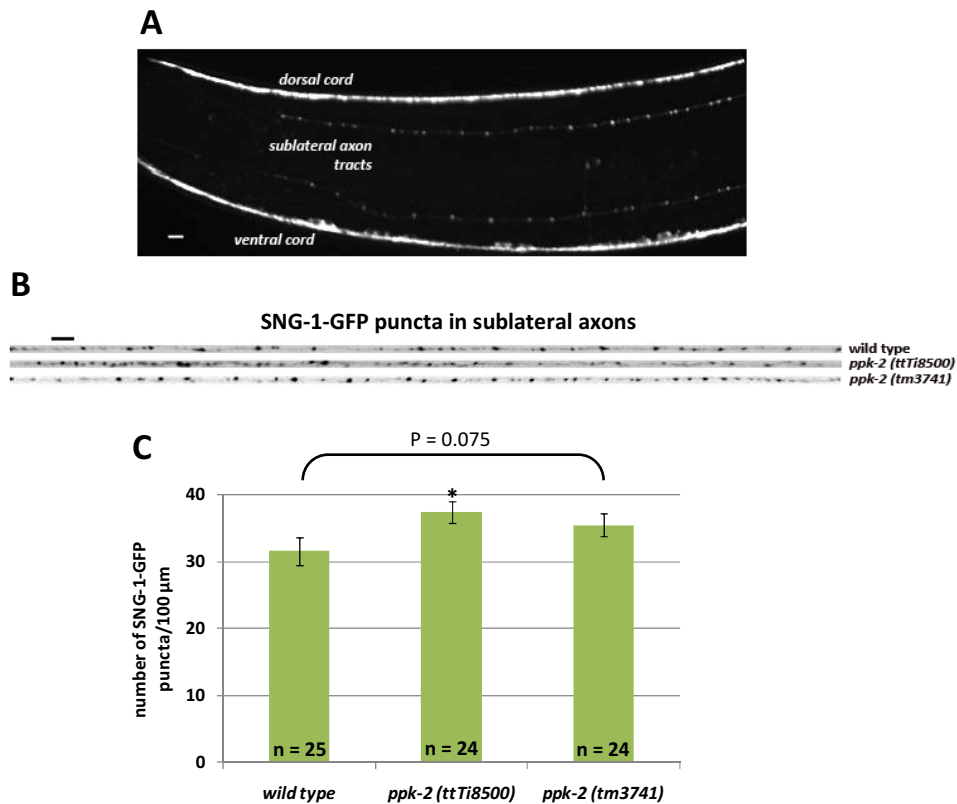


Figure 26 Quantification of SNG-1-GFP clusters along axons

A, posterior of a young adult expressing SNG-1-GFP in neurons e.g. sublateral axon tracts. Scale bar, 5 μm. B, representative straightened and inverted images of sublateral axons from wild type, *ppk-2 (ttTi8500)*, and *ppk-2 (tm3741)* animals. Scale bar, 5 μm. C, quantification of SNG-1-GFP puncta along 100 μm of sublateral axons (n). *, $P < 0.05$, Student's t-test.

The neuropeptide ANF was used as a DCV marker (Speese *et al.*, 2007) and expressed as a GFP-fusion driven by a pan-neuronal promoter. Fluorescence was detected in the dorsal cord as well as the ventral cord of wild type animals. This localization pattern was essentially the same in *ppk-2 (ttTi8500)* as well as *ppk-2 (tm3741)* backgrounds (Figure 27A).

As for SNG-1-GFP, the ANF-GFP signals recorded from dorsal cords from wild type and both *ppk-2* mutants were quantified and normalized to the average of the wild type signal. As illustrated in Figure 27B, the level of fluorescence in *ppk-2 (tm3741)* animals differs not significantly from wild type animals, but a slight decrease is observable in *ppk-2 (ttTi8500)* animals. However, this alteration is not statistically significant.

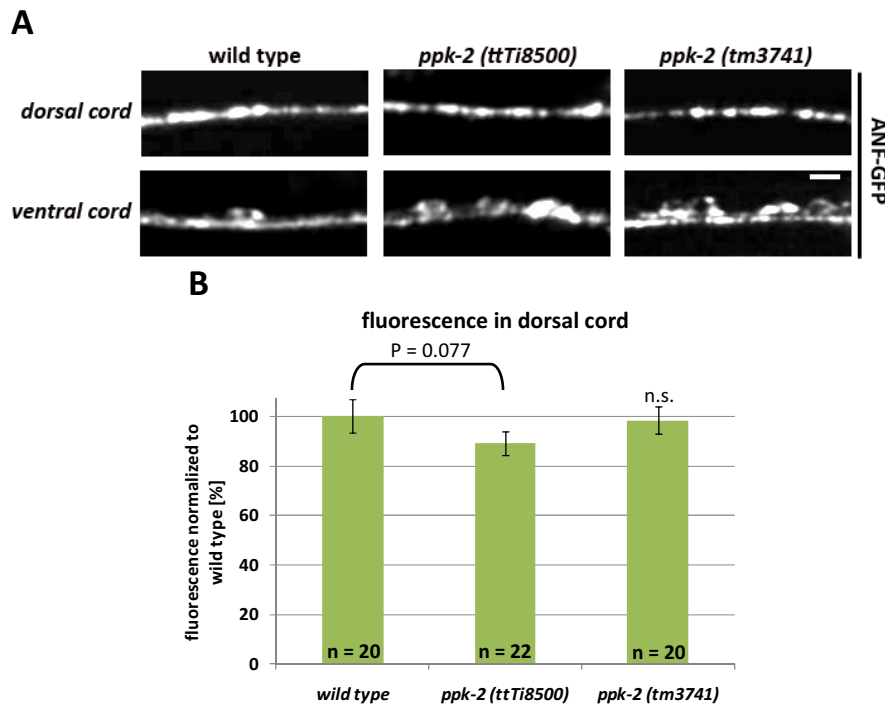


Figure 27 ANF-GFP localization in *ppk-2* mutants

A, the localization of GFP-labeled neuropeptide ANF was analyzed in dorsal as well as ventral cords of young adults. Scale bar, 5 μ m. B, ANF-GFP fluorescence was quantified in the dorsal cords (*n*) of both *ppk-2* mutants and normalized to the wild type average. Error bars, standard error of the mean, n.s., not significant, Student's *t*-test.

ANF-GFP is exocytosed by neuronal DCVs and therefore found in the body cavity of nematodes (Speese *et al.*, 2007). The abundance of secreted GFP-fusion protein and hence the intensity of exocytosis can be indirectly measured. Therefore, a special type of non-neuronal cells, the so-called coelomocytes, was imaged. Coelomocytes are scavenger cells, endocytosing continuously and fluid and macromolecules from the body cavity. A morphological feature of these cells is a big number of large vesicles from which endocytosed material is degraded (Fares and Greenwald, 2001).

Neuronal secreted ANF-GFP was observed in the posterior coelomocyte of young wild type adults and also in *ppk-2 (ttTi8500)* and *ppk-2 (tm3741)* (Figures 28A and B). The ANF-GFP fluorescence detected in coelomocytes of wild type and both *ppk-2* mutants was quantified and normalized to the wild type average. As illustrated in Figure 28C, *ppk-2 (ttTi8500)* as well as *ppk-2 (tm3741)* animals show a highly significant increase of fluorescence of more than 30 % compared to control animals. Consequently, it must be concluded that the DCV-mediated exocytosis of ANF-GFP is increased in both *ppk-2* mutants.

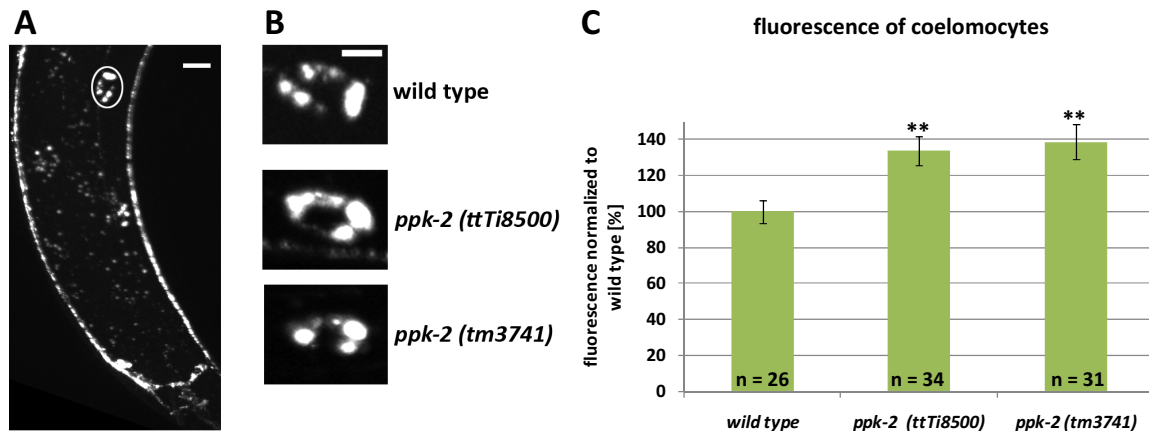


Figure 28 Increased ANF-GFP fluorescence in coelomocytes of *ppk-2* mutants

A, posterior of a young wild type adult expressing ANF-GFP in neurons. The posterior coelomocyte (encircled) is stained by ANF-GFP as well. Scale bar, 10 μ m. B, representative detail images of ANF-GFP stained coelomocytes of wild type, *ppk-2 (ttTi8500)*, and *ppk-2 (tm3741)*. Scale bar, 5 μ m. C, ANF-GFP fluorescence detected in coelomocytes (n) was quantified and normalized to the wild type average. Error bars, standard error of the mean, **, $P < 0.01$, Student's t-test.

Taken together, mutations in *ppk-2* influence the number of SNG-1-GFP stained clusters along the sublateral axons. Furthermore, both *ppk-2 (ttTi8500)* and *ppk-2 (tm3741)* show enhanced secretion of neuropeptides.

3.2.3.8 Biochemical analysis of phospholipids

As described in section 3.2.1, PPK-2 is assumed to be a Type II PIP kinase orthologs of *C. elegans*. Furthermore, the mutant alleles *ppk-2 (ttTi8500)* and *ppk-2 (tm3741)* have been found to comprise significantly altered open reading frames likely yielding in mutated proteins (section 3.2.3.1).

Type II PIP kinases of mammalia were described to phosphorylate the D-4 position either of PI5P or PI3P (Clarke *et al.*, 2007) resulting in double-phosphorylated phosphoinositides (PIP₂). In order to determine, if the mutation of the putative Type II PIP kinase PPK-2 of *C. elegans* influences PIP₂ levels *in vivo*, a biochemical analysis of phospholipids was carried out.

A large synchronous population of L1 larvae of both wild type and *ppk-2 (ttTi8500)* was prepared and used for the acidic extraction of phospholipids. Lipids were separated via TLC, identified by comparison to a standard, scraped from the TLC plate, and quantified by GC. The biochemical analysis was performed by Dr. Irene Stenzel and Alina Mosblech, Department of Plant Biochemistry, Albrecht-von-Haller-Institute for Plant Sciences, Göttingen.

PIP₂ amounts were normalized to the amounts of the non-phosphoinositide PC derived from the same sample. The according ratios are shown in Figure 29: The PIP₂/PC ratio of L1 wild type larvae is 0.51 whereas the ratio of *ppk-2 (ttTi8500)* animals is threefold higher (1.56). Hence, it must be concluded that the overall PIP₂ level in this *ppk-2* mutant is significantly higher than in wild type.

Due to technical difficulties, the phospholipid analysis of *ppk-2* (*tm3741*) was not completed up to the submission date of the here presented study.

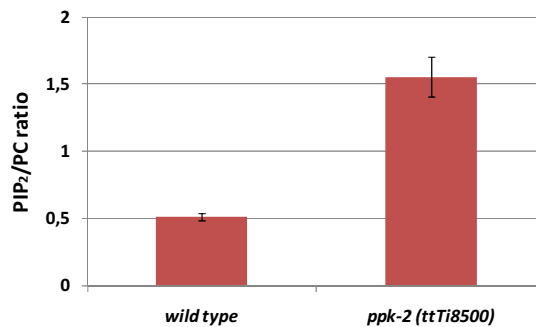


Figure 29 The PIP₂ level of *ppk-2* (*ttTi8500*) and wild type nematodes

PIP₂/PC ratio of synchronous L1 populations of wild type compared to *ppk-2* (*ttTi8500*). Averages of two independent GC runs. Error bars, standard deviation.

3.2.4 Subcellular localizations of PPK-2

3.2.4.1 Localization of PPK-2 in neurons

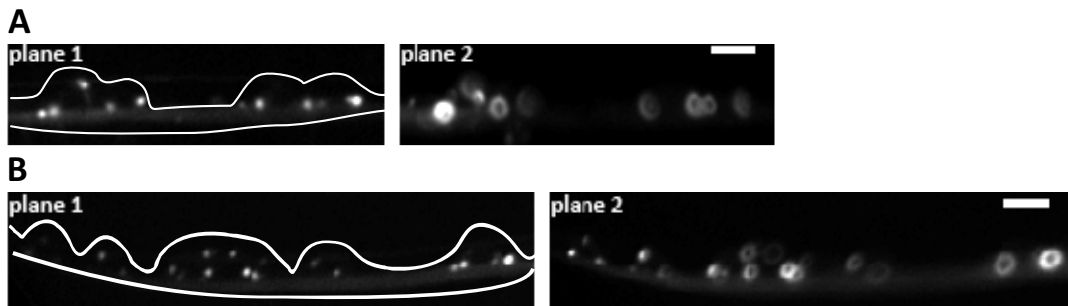


Figure 30 Subcellular localization of mCherry-PPK-2 in neuronal cell bodies

A and B, mCherry-PPK-2 localizes as distinct puncta in somata of the ventral cord (plane 1), a marginal change of the focus plane reveals a ring-like localization pattern (plane 2). The approximate shapes of the cell bodies are indicated. Scale bars, 5 μ m.

In order to determine the subcellular localization in neurons, mCherry has been fused N-terminally to the PPK-2 protein. mCherry-PPK-2 was expressed in wild type background driven by a pan-neuronal promoter. Figures 30A and B show two sections of ventral cords of transgenic adults. mCherry-PPK-2 was observed to localize as distinct puncta in the neuronal cell bodies with a slight staining of the cytosol. Upon a marginal change of the focus plane, the signals of the puncta changed to ring-like structures which are typical for endomembrane-associated proteins.

To analyze a possible colocalization of mCherry-PPK-2 with components of the endomembrane system, mCherry-PPK-2 was initially coexpressed with the GFP-labeled Golgi marker mannosidase II (MANS II-GFP) (Paschinger *et al.*, 2006) in neurons of wild type animals. As illustrated in Figure 31, partial but no total overlapping of these two fusion proteins was observed in the ventral cord of young adults.

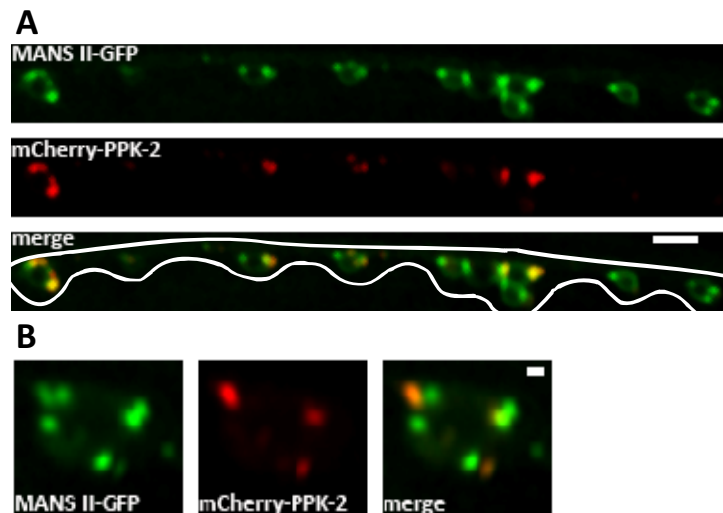


Figure 31 Localization of mCherry-PPK-2 and MANS II-GFP in neurons

A, mCherry-PPK-2 signals in somata of the ventral cord (wild type background) overlap incomplete with the GFP-labeled Golgi marker mannosidase II (MANS II-GFP). The approximate shapes of the cell bodies are indicated. Scale bar, 5 μm . B, detail image of a single soma of the ventral cord. Scale bar, 1 μm .

Next, the localization of mCherry-PPK-2 compared to the ER was analyzed. For this, the ER-resident protein cytochrome b5 (Mitoma and Ito, 1992) was coexpressed in wild type neurons, C-terminally fused with CFP. Imaging of the ventral cord of young adults revealed that both fusion proteins do not show any significant overlap (Figure 32).

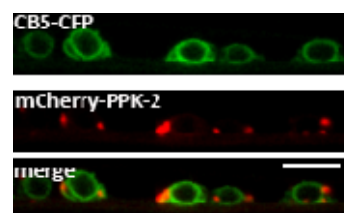


Figure 32 Localization of mCherry-PPK-2 and CB5-CFP in neurons

mCherry-PPK-2 signals in somata of the ventral cord (wild type background) do not overlap with the CFP-labeled marker cytochrome b5 (CB5-CFP). Scale bar, 5 μm .

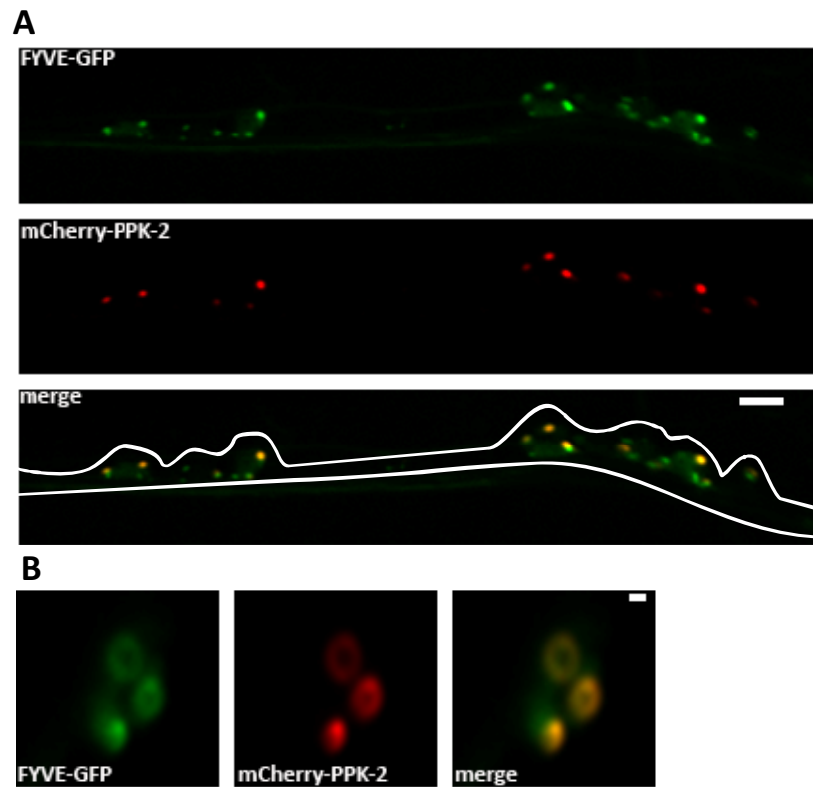


Figure 33 Localization of *mCherry-PPK-2* and *FYVE-GFP* in neurons

A, *mCherry-PPK-2* signals in somata of the ventral cord (wild type background) colocalize with the GFP-labeled PI3P-binding FYVE domain (*FYVE-GFP*). The approximate shapes of the cell bodies are indicated. Scale bar, 5 μm .
B, detail image of a single soma of the ventral cord. Scale bar, 1 μm .

In contrast, *mCherry-PPK-2* shows a colocalization with neuronally expressed *FYVE-GFP*. FYVE is a phosphoinositide binding domain with specificity for PI3P and thus stains mainly the cytosolic membrane face of early endosomes (Stenmark and Aasland, 1999; Stenmark and Gillooly, 2001). As illustrated in Figure 33A, *mCherry-PPK-2* puncta are observed to overlap almost perfectly with *FYVE-GFP* signals. Further, *FYVE-GFP* localizes in the same ring-like structures as observed for *mCherry-PPK-2* (Figure 33B). However, not for every *FYVE-GFP* signal an according *mCherry-PPK-2* signal was observed.

Taken together, neuronally expressed *mCherry-PPK-2* appears to be predominantly associated with membranes of early endosomes in wild type background.

3.2.4.2 Localization of PPK-2 mutants in neurons

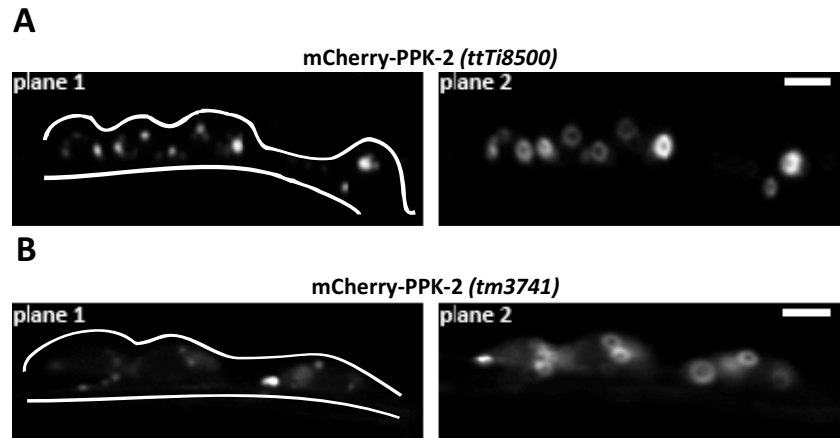


Figure 34 Subcellular localizations of mCherry::PPK-2 (ttTi8500) and mCherry::PPK-2 (tm3741)

A and B, wild type background, mCherry-PPK-2 (ttTi8500) and mCherry-PPK-2 (tm3741) localize as distinct puncta in somata of the ventral cord (plane 1), marginal change of the focus plane reveals ring-like structures (plane 2). mCherry-PPK-2 (tm3741) stains the cytosol as well. The approximate shapes of the cell bodies are indicated. Scale bars, 5 μ m.

As described in section 3.2.3.1, *ppk-2* mutant alleles comprise altered but still intact open reading frames. In order to test whether they lead to according translation products, respective coding sequences were used to create N-terminally labeled mCherry-fusion proteins. As described for mCherry-PPK-2 wild type, these fusions were expressed in wild type background driven by a pan-neuronal promoter.

As illustrated in Figure 34A, mCherry-PPK-2 (ttTi8500) localizes very similar to mCherry-PPK-2 wild type. The fusion protein was observed as distinct puncta in the cell bodies of young adults' ventral cords. mCherry-PPK-2 (tm3741) was observed to localize in a comparable pattern, however, an additional blurry staining of the cytosol was detected (Figure 34B). Both mutant protein fusions localize in ring-like structures (Figures 34A and B).

Although derived from severely altered transcripts, both PPK-2 mutants were expressible as mCherry-fusion proteins in wild type neurons. Most interestingly, their localizations are highly comparable to the wild type protein (Figure 30).

3.2.4.3 Coexpression of PPK-2 and PPK-1 in neurons

Nothing is known about putative interaction partners of PPK-2 yet. However, in mammalian recent publications report a possible interaction between Type I and Type II PIP kinases *in vivo* (Hinchliffe *et al.*, 2002).

Beside *ppk-2*, the *C. elegans* genome harbors also a single Type I PIP kinase ortholog. Consequently, both proteins have been coexpressed as differently labeled fusion proteins in wild type neurons.

Initially, the expression pattern of GFP-labeled PPK-1 has been determined. Therefore, GFP-PPK-1 was expressed driven by a pan-neuronal promoter.



Figure 35 Localization of GFP-PPK-1 neurons

A, GFP-PPK-1 stains the PM of neurons (wild type background) of the ventral cord. Scale bar, 5 μm . B, GFP-PPK-1 stains the PM of neurons in the head. Scale bar, 10 μm . The detail shows two neuronal cell bodies of the nerve ring. Scale bar, 5 μm .

Localization studies in this study have been carried out using an N-terminally labeled PPK-1 which clearly stains the neuronal PM (Figure 35). This is congruent with the already known localization pattern for C-terminally labeled PPK-1 (Weinkove *et al.*, 2007).

Next, GFP-PPK-1 and mCherry-PPK-2 have been coexpressed in neurons and their localizations were imaged in young wild type adults. As shown by several representative images in Figure 36, the coexpression of both fusion proteins influences their both localizations patterns.

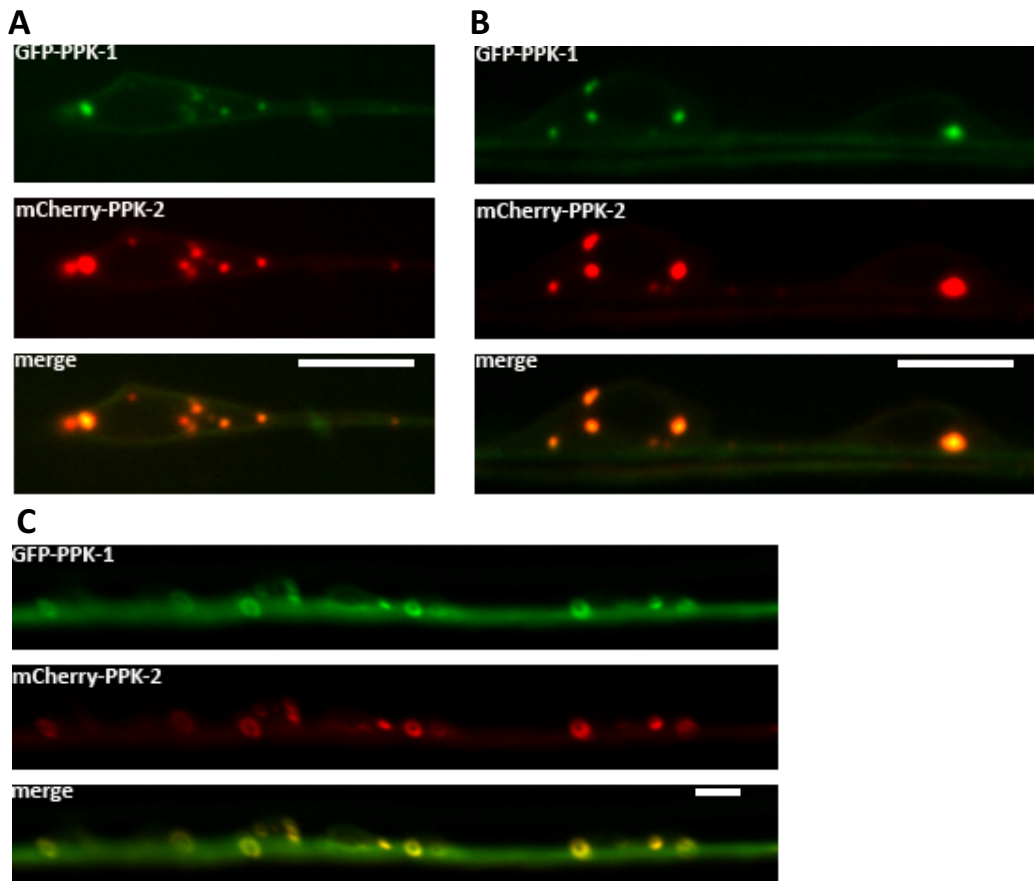


Figure 36 Localization of coexpressed mCherry-PPK-2 and GFP-PPK-1 in neurons

A, colocalization of mCherry-PPK-2 and GFP-PPK-1 at the PM and in the cell interior of a channel associated neuron (axon to the right). Scale bar, 5 μ m. B, and C, colocalization of mCherry-PPK-2 and GFP-PPK-2 at the PM and in the cell interior of the ventral cord. Wild type background. Scale bars, 5 μ m.

mCherry-PPK-2 was still forming distinct puncta in cell bodies, but additionally it was found to localize the neuronal PM. GFP-PPK-1 was detected at the PM where it colocalizes with mCherry-PPK-2. However, GFP-PPK-1 was also observed as distinct puncta in the cell interior, overlapping perfectly with the mCherry-PPK-2 signals. Furthermore, these puncta turned out be the already described ring-like structures (Figure 30) but now stained by both mCherry-PPK-2 and GFP-PPK-1 (Figure 36C).

In summary, the coexpression of mCherry-PPK-2 and GFP-PPK-1 influences the localization patterns of both fusion proteins, resulting in their almost complete colocalization in neurons.

3.2.4.4 Coexpression of PPK-2 mutants and PPK-1 in neurons

In order to determine if localizations of the mutant proteins PPK-2 (*ttTi8500*) and PPK-2 (*tm3741*) can be also influenced by the coexpression of GFP-PPK-1, respective fusion proteins were simultaneously expressed in wild type neurons.

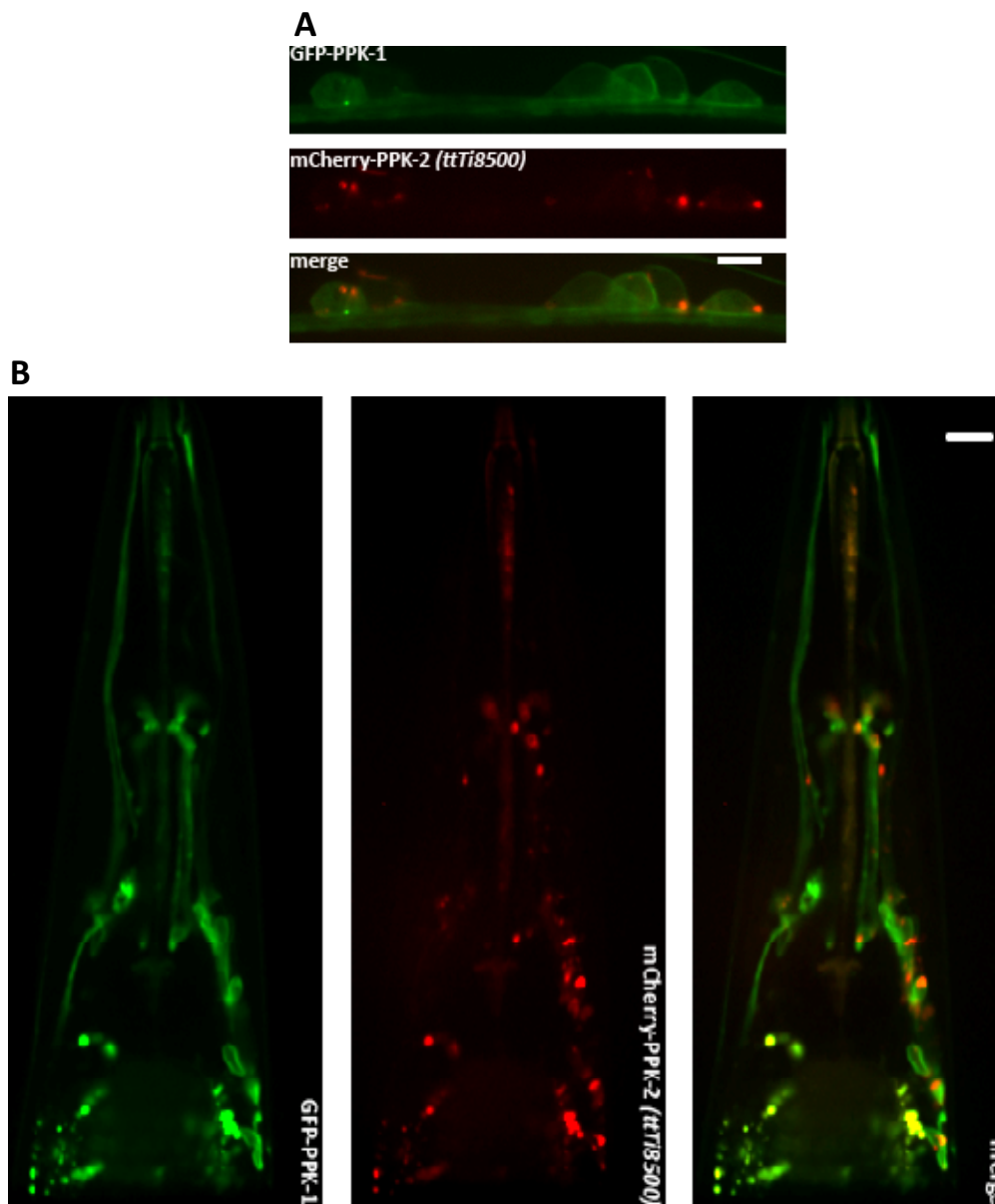


Figure 37 *mCherry::PPK-2 (ttTi8500) coexpressed with GFP::PPK-1 in neurons*

A, colocalization of mCherry-PPK-2 (ttTi8500) and GFP-PPK-1 at the PM and as distinct puncta in the cell interior of the ventral cord. Scale bar, 5 μ m. B, localization patterns of mCherry-PPK-2 (ttTi8500) and GFP-PPK-1 in the neurons of the head. Wild type background. Scale bar, 10 μ m.

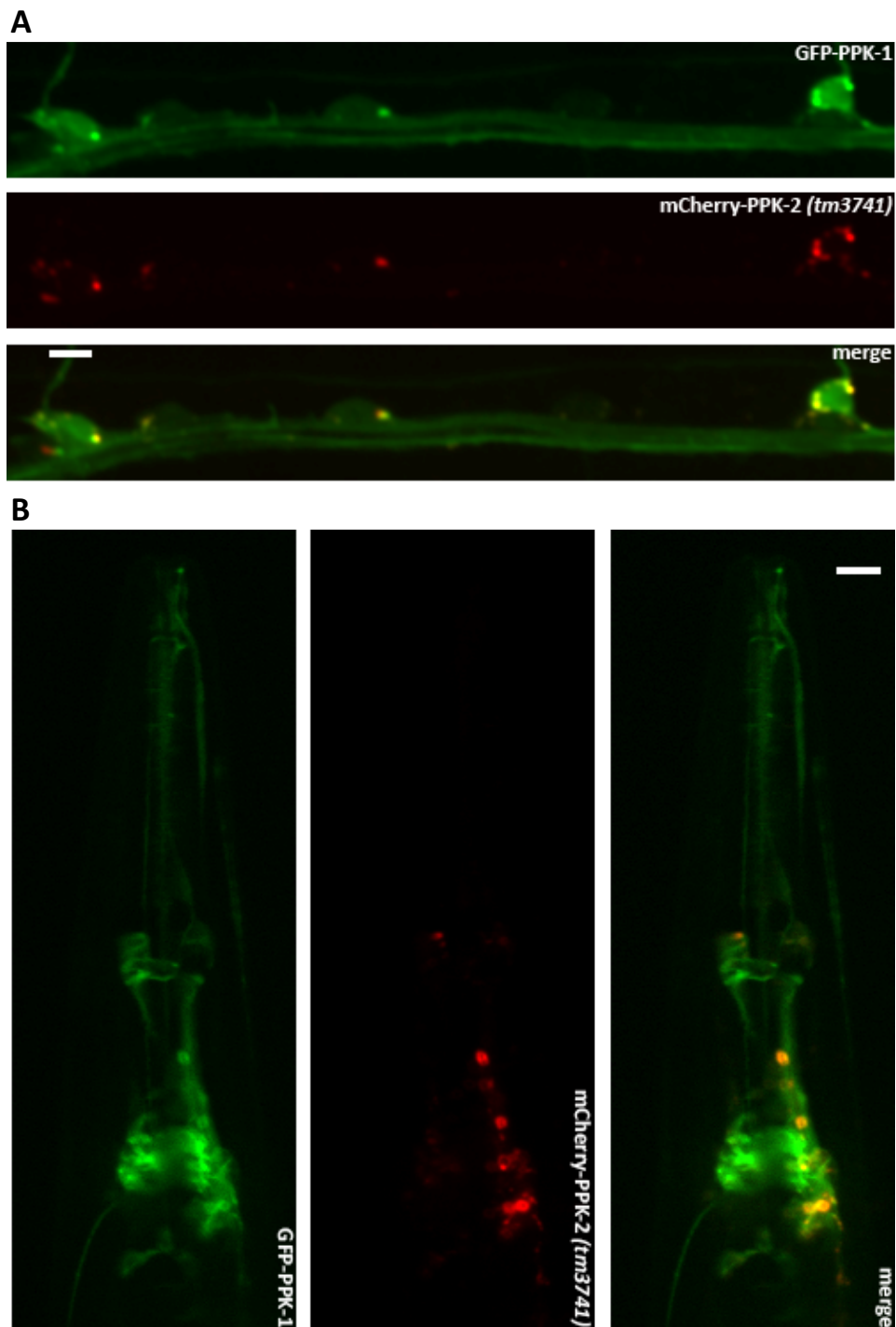


Figure 38 *mCherry::PPK-2 (tm3741) coexpressed with GFP::PPK-1 in neurons*

A, colocalization of mCherry-PPK-2 (tm3741) and GFP-PPK-1 at the PM and as distinct puncta in the cell interior of the ventral cord. Scale bar, 5 μ m. B, localization patterns of mCherry-PPK-2 (tm3741) and GFP-PPK-1 in the neurons of the head Wild type background. Scale bar, 10 μ m.

Figure 37 shows representative images for the coexpression of GFP-PPK-1 and mCherry-PPK-2 (*ttTi8500*) in young wild type adults. GFP-PPK-1 was observed to localize to the PM as well as distinct puncta and ring-like structures in the cell interior. These puncta and rings are also stained by mCherry-PPK-2 (*ttTi8500*). However, no PM localization but only a slight staining of the cytosol was detected for this fusion protein.

mCherry-PPK-2 (*tm3741*) does not localize to the neuronal PM when coexpressed with GFP-PPK-1. Noteworthy, both GFP-PPK-1 and mCherry-PPK-2 (*tm3741*) colocalize to distinct puncta in the somata (Figure 38).

Taken together, it was observed that coexpression of mCherry-labeled PPK-2 mutant proteins with GFP-PPK-1 alters the localization of GFP-PPK-1 but not *vice versa*.

3.2.4.5 PPK-2 particles move along neuronal processes

A PPK-2 fusion protein was observed to localize in distinct puncta in neuronal cell bodies when expressed in wild type (Figure 30). This localization pattern has found to overlap almost complete with a marker for early endosomes indicating that PPK-2 is associated to endosomal membranes (Figure 33).

To analyze the localization of mCherry-labeled PPK-2 in neuronal processes such as axons and dendrites, nervous cells outlying the dense structure of the ventral cord have been imaged in young adults.

The channel associated (CAN) neuron is found relatively isolated in the center of the nematodes' bodies. It projects a long straight axon in the anterior and a dendrite in the posterior direction. As illustrated in Figure 39A, mCherry-PPK-2 was found to localize as distinct puncta in the CAN somata. Most interestingly, similar mCherry signals were observed to be distributed along both the CAN axon and dendrite.

Further imaging of additional neurons revealed, that the mCherry-PPK-2 stained puncta move dynamically and travel anterograde and retrograde along processes. To image these movements, time series of the mCherry-PPK-2 stained puncta moving in axons and dendrites were recorded.

Figure 39B shows a representative dendrite of a tail neuron at three different points of a time series. The anterograde and retrograde movements of mCherry-PPK-2 particles along this process were analyzed by plotting particle dynamics as a kymograph. A kymograph is a graphical representation of the spatial position of a particle subjected to time. Hereby, the ordinate represents time e.g. single frames of the time series. This results in a graph-like depiction of particle movement, which can be used to calculate the velocity: A steep ascending graph represents a slow moving particle whereas a flat ascending graph represents a fast moving particle.

As illustrated in the corresponding kymograph in Figure 39B, the mCherry-PPK-2 particles in the imaged dendrite move very dynamic and with different velocities. Noteworthy, a particle not only moves unidirectional but can shift its moving direction from anterograde to retrograde and back.

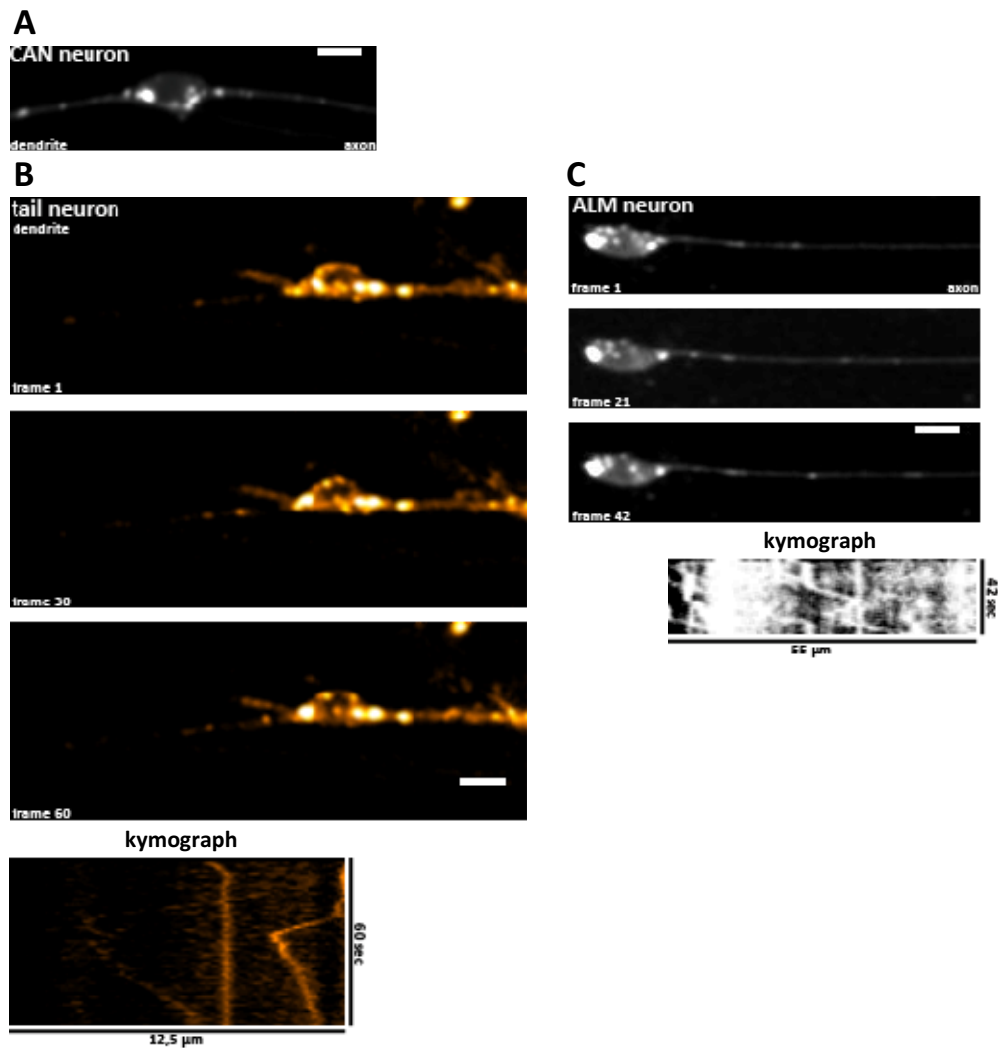


Figure 39 *mCherry-PPK-2 movement along processes*

A, localization of mCherry-PPK-2 particles in a CAN neuron. Scale bar, 5 μm . B, movement of mCherry-PPK-2 particles along the dendrite of a tail neuron. Scale bar, 5 μm . Movement of particles from a time series of 60 seconds with one frame per second have been plotted as a kymograph. False colors have been employed for better contrast of signals and background. C, mCherry-PPK-2 particles movements along an ALM axon. Scale bar, 5 μm . The kymograph plots particle movements from a time series of 42 seconds with one frame per second.

The particle movements in axons were analyzed by imaging a representative ALM neuron (anterior lateral microtubule cell). This neuron type is found in the anterior body half projecting a long straight axon to the head. In turn, the dendrite is very short and hardly detectable. Figure 39C shows an ALM neuron at three different points of a time series. As observable in the corresponding kymograph, mCherry-PPK-2 particles move anterograde and retrograde and with different velocities along the axon.

mCherry-PPK-2 was observed to colocalize with the early endosome marker FYVE-GFP in cell bodies (Figure 33). In order to determine, if the mCherry-PPK-2 particles moving along neuronal processes

are stainable by FYVE-GFP, both fusion proteins were coexpressed in the neurons of wild type animals.

Figure 40 shows a representative CAN neuron. As can be seen in the merge picture (Figure 40A), the signals of FYVE-GFP and mCherry-PPK-2 mostly overlap in the cell body. However, no significant localization of FYVE-GFP to the processes was observed, although many mCherry-PPK-2 particles were detected along both the axon and the dendrite. According kymographs (Figure 40C) show highly dynamic movements of mCherry-PPK-2 along both processes. The kymograph depicting dendritic movement in the green channel shows no significant signal. However, the according plot for the axon revealed one hardly detectable track maybe resulting from a marginal stained FYVE-GFP particle (Figure 40B).

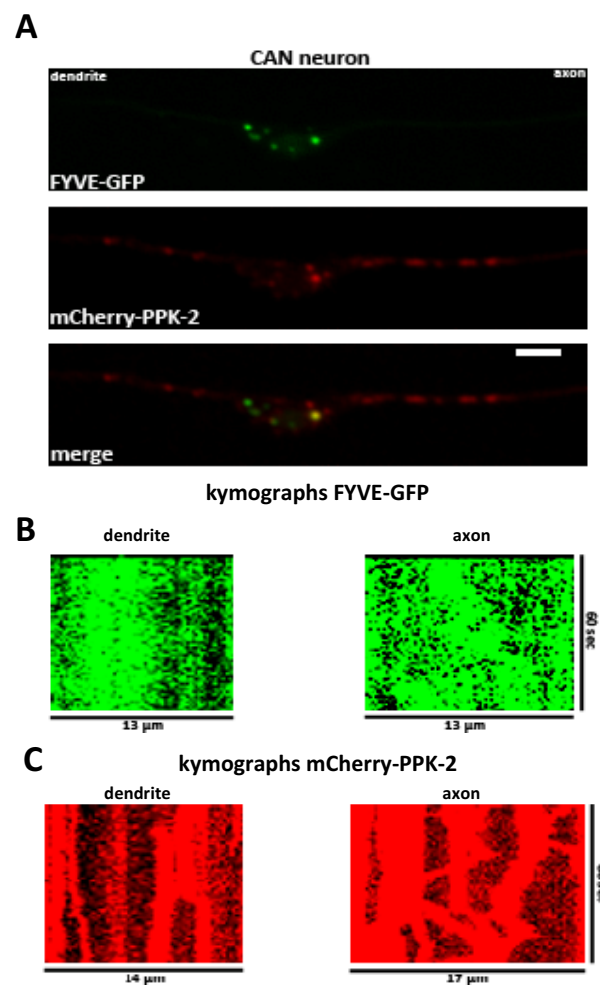


Figure 40 Movements of mCherry-PPK-2 and FYVE::GFP particles in a CAN neuron

A, mCherry-PPK-2 and GFP-FYVE were imaged in the CAN neuron of a young adult nematode. Scale bar, 5 μm. According time series were recorded for 60 seconds with one frame per second and plotted as kymographs for FYVE-GFP (B) and mCherry-PPK-2 (C).

Taken together, mCherry-PPK-2 stained particles move highly dynamic anterograde and retrograde along axons and dendrites of neurons in nematodes. Furthermore, mCherry signals located in processes are not costained by the early endosome marker FYVE-GFP indicating a different identity for these particles.

3.2.4.6 Particles of PPK mutant fusions move along neuronal processes

As described under 3.2.3.1, the altered open reading frames identified for both *ppk-2* mutant alleles are expressible as mCherry fusion proteins under a pan-neuronal promoter in wild type background. Noteworthy, the localization of these mutant fusions in somata of the ventral cord (Figure 34) is highly comparable to the mCherry-labeled wild type protein (Figure 30).

In the previous section, it was shown that mCherry-PPK-2 (wild type) localizes to the processes of neurons and moves along them anterograde and retrograde in a highly dynamic manner. In order to determine, if this localization pattern is also observable for the mutant proteins, the localization of according mCherry-fusions was analyzed in wild type CAN neurons.

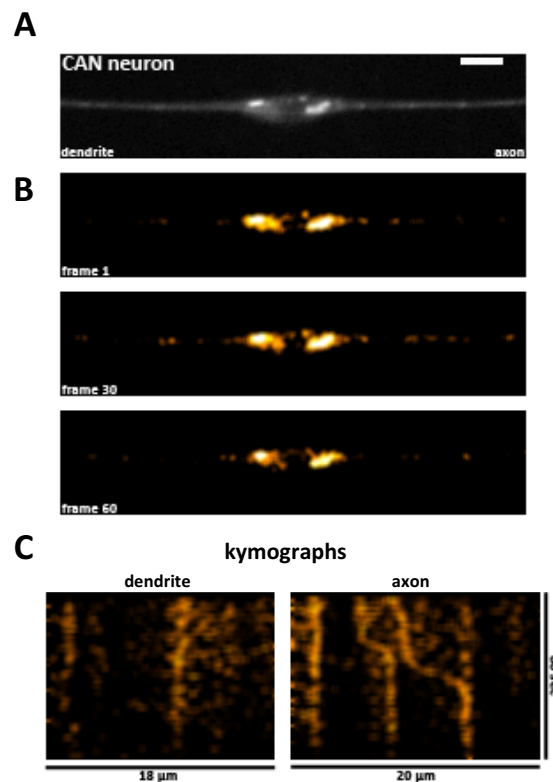


Figure 41 *mCherry-PPK-2 (ttTi8500) localization in a CAN neuron*

A, unedited picture of the CAN neuron. Scale bar, 5 μm . *B*, according images of the time series are shown in false colors in order to increase contrast of the particles in the processes to their background. Kymographs (*C*) were plotted from time series (60 seconds) with one frame per second.

Figure 41B shows the localization of mCherry-PPK-2 (*ttTi8500*) in a representative CAN neuron at different points of a time series. mCherry particles are detectable in the cell body as well as in both axon and dendrite. Noteworthy, these particles move dynamically anterograde and retrograde along both processes as illustrated by corresponding kymographs (Figure 41C).

The localization of mCherry-PPK-2 (*tm3741*) in a young adults' CAN neuron is shown in Figure 42. The fusion protein was observed to localize as distinct particles in the cell body and to the axon as well to the dendrite of the nervous cell. As illustrated by the three images representing three points of a time series also mCherry-PPK-2 (*tm3741*) particles move anterograde and retrograde along both processes (Figure 42A). The according kymographs revealed these particles to be highly dynamic as well (Figure 42B).

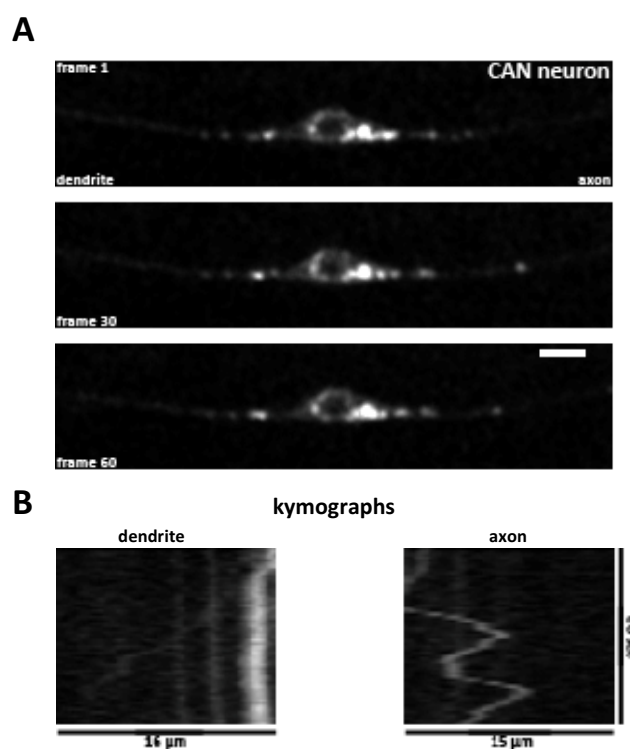


Figure 42 *mCherry-PPK-2 (tm3741) localization in a CAN neuron*

A, three images of a time series of a CAN neuron expression mCherry-PPK-2 (*tm3741*) recorded for 60 seconds with one frame per second. Scale bar, 5 μm . B, corresponding kymograph plots.

In summary, both PPK-2 mutant fusion proteins localize similar to wild type PPK-2 as distinct particles along both axons and dendrites of neurons. Furthermore, these particles display dynamic bidirectional movement along processes for both mCherry-PPK-2 (*ttTi8500*) and mCherry-PPK-2 (*tm3741*).

3.2.4.7 Velocities of PPK-2 particles in neuronal processes

In order to determine the average velocities of the particles stained by mCherry-PPK-2 and both mutant fusion proteins, anterograde and retrograde movements were quantified in axons and dendrites, respectively.

Table 13 Velocities of particles of PPK-2 and mutants in neurons

Averaged velocities of particles (n) travelling along neuronal processes in wild type animals stained by mCherry-PPK-2, mCherry-PPK-2 (ttTi8500), and mCherry-PPK-2 (tm3741), respectively. In Figure 43, the same data is shown as a bar plot.

	axon		dendrite	
	anterograde	retrograde	anterograde	retrograde
PPK-2				
average	0.265 $\mu\text{m}/\text{sec}$	0.311 $\mu\text{m}/\text{sec}$	0.272 $\mu\text{m}/\text{sec}$	0.227 $\mu\text{m}/\text{sec}$
maximum	0.348 $\mu\text{m}/\text{sec}$	0.487 $\mu\text{m}/\text{sec}$	0.608 $\mu\text{m}/\text{sec}$	0.495 $\mu\text{m}/\text{sec}$
minimum	0.154 $\mu\text{m}/\text{sec}$	0.013 $\mu\text{m}/\text{sec}$	0.034 $\mu\text{m}/\text{sec}$	0.08 $\mu\text{m}/\text{sec}$
n	16	16	16	16
PPK-2 (ttTi8500)				
average	0.338 $\mu\text{m}/\text{sec}$	0.355 $\mu\text{m}/\text{sec}$	0.282 $\mu\text{m}/\text{sec}$	0.33 $\mu\text{m}/\text{sec}$
maximum	1.073 $\mu\text{m}/\text{sec}$	1.049 $\mu\text{m}/\text{sec}$	0.599 $\mu\text{m}/\text{sec}$	0.994 $\mu\text{m}/\text{sec}$
minimum	0.087 $\mu\text{m}/\text{sec}$	0.104 $\mu\text{m}/\text{sec}$	0.111 $\mu\text{m}/\text{sec}$	0.073 $\mu\text{m}/\text{sec}$
n	10	10	16	16
PPK-2 (tm3741)				
average	0.246 $\mu\text{m}/\text{sec}$	0.226 $\mu\text{m}/\text{sec}$	0.318 $\mu\text{m}/\text{sec}$	0.316 $\mu\text{m}/\text{sec}$
maximum	0.469 $\mu\text{m}/\text{sec}$	0.492 $\mu\text{m}/\text{sec}$	1.053 $\mu\text{m}/\text{sec}$	0.753 $\mu\text{m}/\text{sec}$
minimum	0.03 $\mu\text{m}/\text{sec}$	0.035 $\mu\text{m}/\text{sec}$	0.03 $\mu\text{m}/\text{sec}$	0.018 $\mu\text{m}/\text{sec}$
n	17	17	16	16

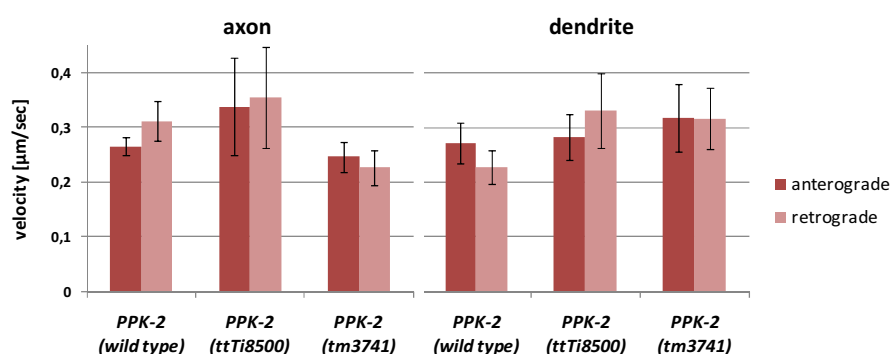


Figure 43 Velocities of PPK-2 and mutants in neurons

Averaged velocities of particles travelling along neuronal processes in living animals stained by mCherry-PPK-2, mCherry-PPK-2 (ttTi8500), and mCherry-PPK-2 (tm3741), respectively. Data presented corresponds to Table 13. Error bars, standard error of the mean.

As summarized in Table 13 and Figure 43, particles stained by mCherry-PPK-2 wild type travel bidirectional with average velocities ranging from 0.23 to 0.31 μm per second along both axons and dendrites. Both PPK-2 mutants were observed to move anterograde and retrograde in both processes with comparable velocities. Thus, particles stained by mCherry-PPK-2, mCherry-PPK-2 (*ttTi8500*), and mCherry-PPK-2 (*tm3741*) move relatively fast. These high velocities indicate that the movement is not random but actively regulated. Hence, it must be concluded that the particles stained by mCherry-PPK-2 and mutant fusions are a putative cargo for axonal motor proteins.

3.2.4.8 The localization of PPK-2 depends on kinesin-3

mCherry-PPK-2 was shown to localize as distinct puncta or particles in the cell bodies as well processes of neurons in wild type background (Figure 30). The particles in the processes move anterograde and retrograde along axons and dendrites with relative high velocities (Table 13).

This indicates an active transport mechanism, mediated by motor proteins. Furthermore, mCherry-PPK-2 signals in the cell bodies but not in the processes overlap with the early endosome marker FYVE-GFP (Figure 33).

A motor protein described to be essential for neuronal function is kinesin-3 (Yonekawa *et al.*, 1998). In *C. elegans*, the kinesin-3 homolog is termed UNC-104 (Hall and Hedgecock, 1991). Kinesin-3/UNC-104 is known to transport *inter alia* SV precursors along the microtubules of the axon from the soma to the nerve terminal. Thus kinesin-3/UNC104 is crucial for the assembling of SV at the synapse and therewith synaptic transmission.

In order to determine, if mCherry-PPK-2 dynamics are regulated by kinesin-3/UNC-104, the fusion protein was expressed, driven by a pan-neuronal promoter, in the background of an *unc-104* mutant. For comparison sake, pan-neuronal FYVE-GFP was coexpressed. The kinesin-3 mutant allele *unc-104* (*e1265*) possesses a point mutation in its open reading frame, resulting in a motor protein with an altered cargo binding domain (Klopfenstein *et al.*, 2004).

When imaging the head of wild type animals coexpressing mCherry-PPK-2 and FYVE-GFP, both fusion proteins were detected predominantly in the nerve ring, where their signals mostly overlap (Figure 44A). A small portion of both fusion proteins was observed to localize to dendritic processes, projecting from the nerve ring to the tip of the head. However, these localizations were found to be proximal to the nerve ring and did not range to the terminals of processes.

When expressed in *unc-104* (*e1265*), the localization of mCherry-PPK-2 as well as FYVE-GFP is strikingly different (Figure 44B). Distinct mCherry-PPK-2 puncta were found to accumulate at the endings of dendritic processes projecting to the head's tips of *unc-104* (*e1265*) animals. In the nerve ring, mCherry-PPK-2 was observed to localize in a defragmented pattern compared to wild type. Most interestingly, the same altered localization was observed for FYVE-GFP. GFP signals from this fusion protein overlap partially with mCherry-PPK-2. This has been observed in the nerve ring as well as in dendritic endings in the head's tip (Figure 44B).

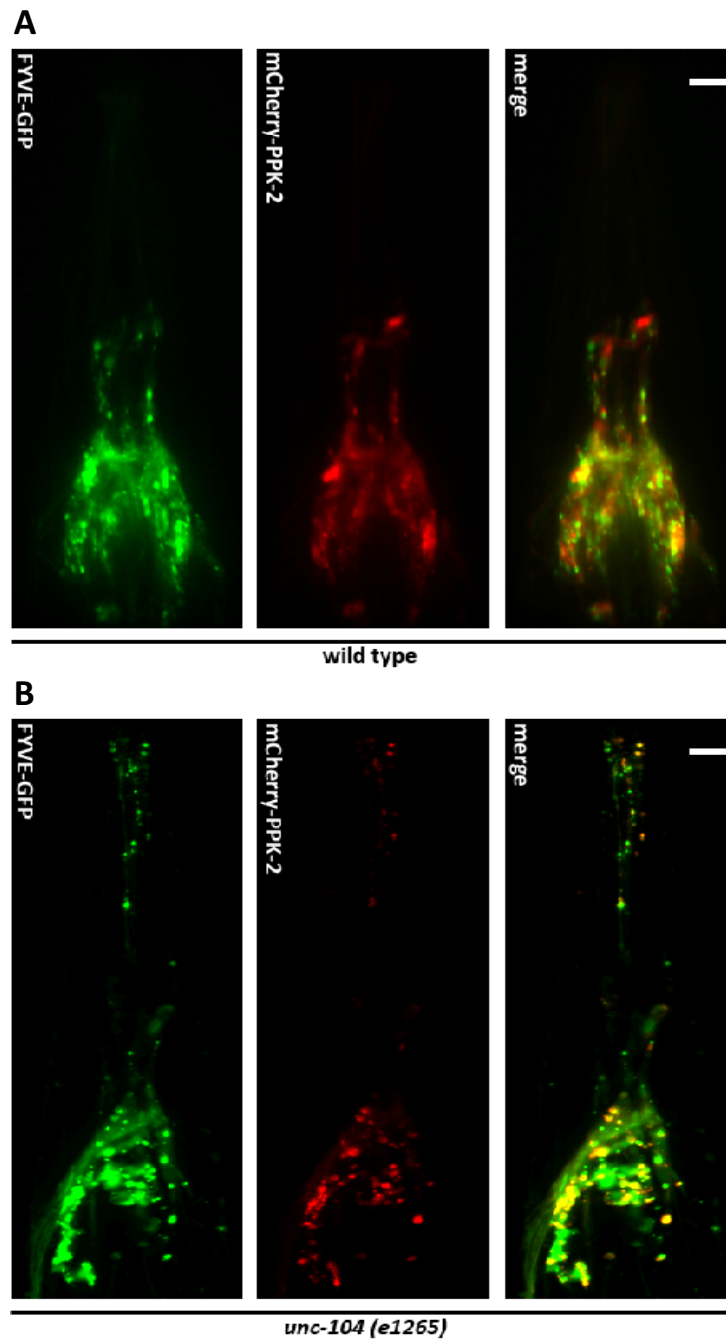


Figure 44 Localization of mCherry-PPK-2 and FYVE-GFP in wild type and *unc-104 (e1265)*

A, localization of mCherry-PPK-2 and FYVE-GFP in the head of a young wild type adult. Scale bar, 10 μm . B, mCherry-PPK-2 and FYVE-GFP in the head of an *unc-104 (e1265)* mutant. Scale bar, 10 μm .

The altered localization of mCherry-PPK-2 and FYVE-GFP in *unc-104 (e1265)* was analyzed more detailed by imaging additional neurons. Figure 45A shows the cell body and axon of an ALM neuron. Both mCherry-PPK-2 and FYVE-GFP were found as partial overlapping punctuated signals in the soma. However, no significant portion of mCherry-PPK-2 or FYVE-GFP was observed to localize in the axon.

In the somata of the ventral cord, mCherry-PPK-2 was observed to localize as distinct puncta (Figure 45B) comparable to the localization in wild type background (Figure 30). These particles show partial overlapping with FYVE-GFP puncta, however, here FYVE-GFP stains also diffusely the whole cell body (Figure 45B).

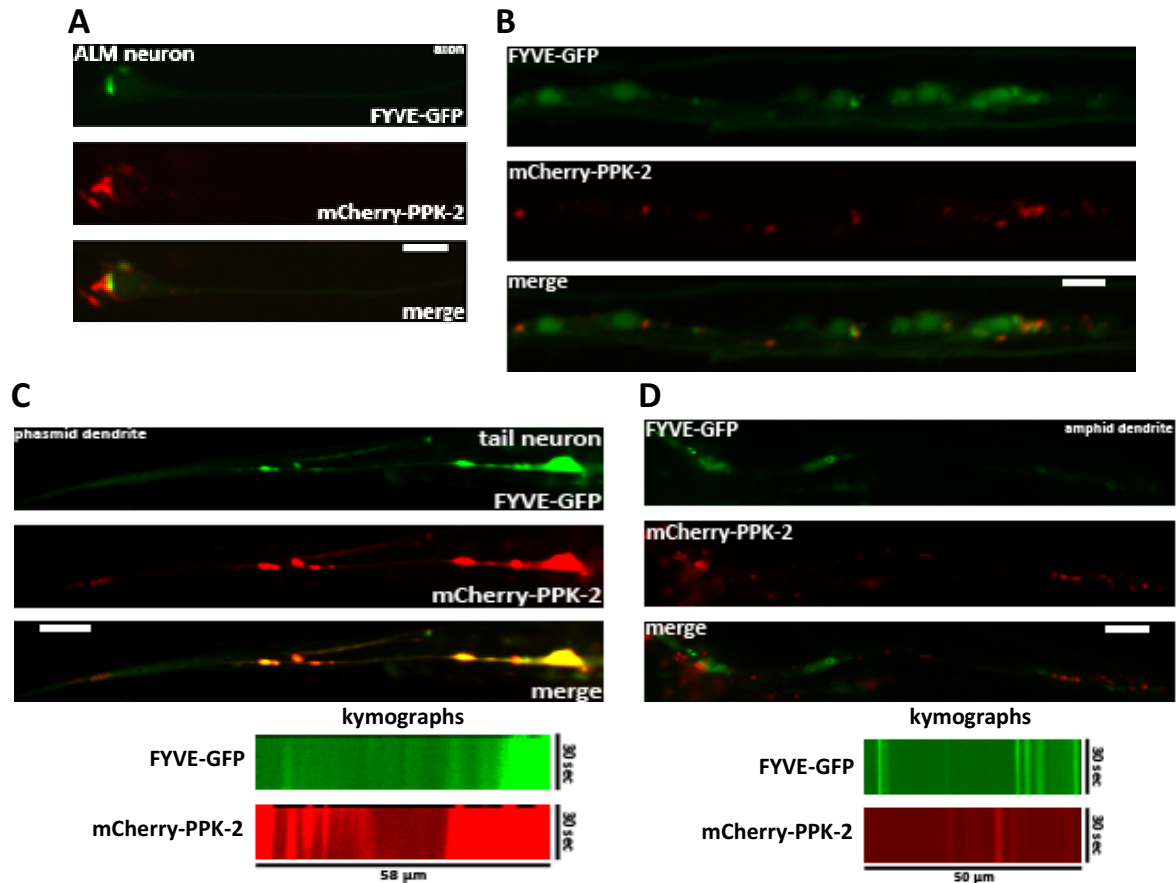


Figure 45 Localization of mCherry-PPK-2 and FYVE-GFP in *unc-104* (e1265)

A, mCherry-PPK-2 and FYVE-GFP in the cell body of an ALM neuron. Scale bar, 5 μ m. B, mCherry-PPK-2 and FYVE-GFP in the somata of the ventral cord. Scale bar, 5 μ m. C, mCherry-PPK-2 and FYVE-GFP in a dendritic process of the phasmid. Corresponding kymographs were plotted from a 30 sec time series with one frame per second. Scale bar, 10 μ m. D, mCherry-PPK-2 and FYVE-GFP in the process of an amphid dendrite in the head (comparable to Figure 44). Corresponding kymographs are shown. Scale bar, 10 μ m.

Localization and dynamics of mCherry-PPK-2 and FYVE-GFP particles were analyzed in the dendrites of tail neurons of *unc-104* (e1265) animals. Processes in the tail of nematodes are summarized under the term phasmid. As shown in Figure 45C, both fusion proteins were found to localize along the process as well as to its tip. However, the according kymograph does not indicate dynamic movements. The same analysis was done for the dendritic processes in the head (called amphid; Figure 45D). Beside their punctate localization along the process, mCherry-PPK-2 and FYVE-GFP accumulate as partial overlapping puncta at the tip of the head. However, the corresponding kymograph shows that these particles are stationary and do not move.

Taken together, the localization of mCherry-PPK-2 as well as FYVE-GFP particles is dependent on kinesin-3/UNC-104. Significant portions of both fusion proteins mislocalize to the tip of dendritic processes whereas no signals were detected in axons. However, the punctate localization patterns of both fusion proteins are not changed.

3.2.5 *In vitro* assay of PPK-2 kinase activity

Extensive sequence and structure comparisons revealed that *C. elegans* PPK-2 is a *bona fide* ortholog of mammalia Type II PI5P 4-kinases (section 3.2.1). In order to analyze the specificity of PPK-2 towards PI5P and other mono-phosphorylated PIPs, it was recombinantly expressed as an N-terminal GST fusion protein in *E. coli*. For comparison sake, GST was solely expressed. Both translation products correlated very well with corresponding molecular masses (GST, 26 kDa, GST-PPK-2, 26 + 45.5 kDa, Figure 46A).

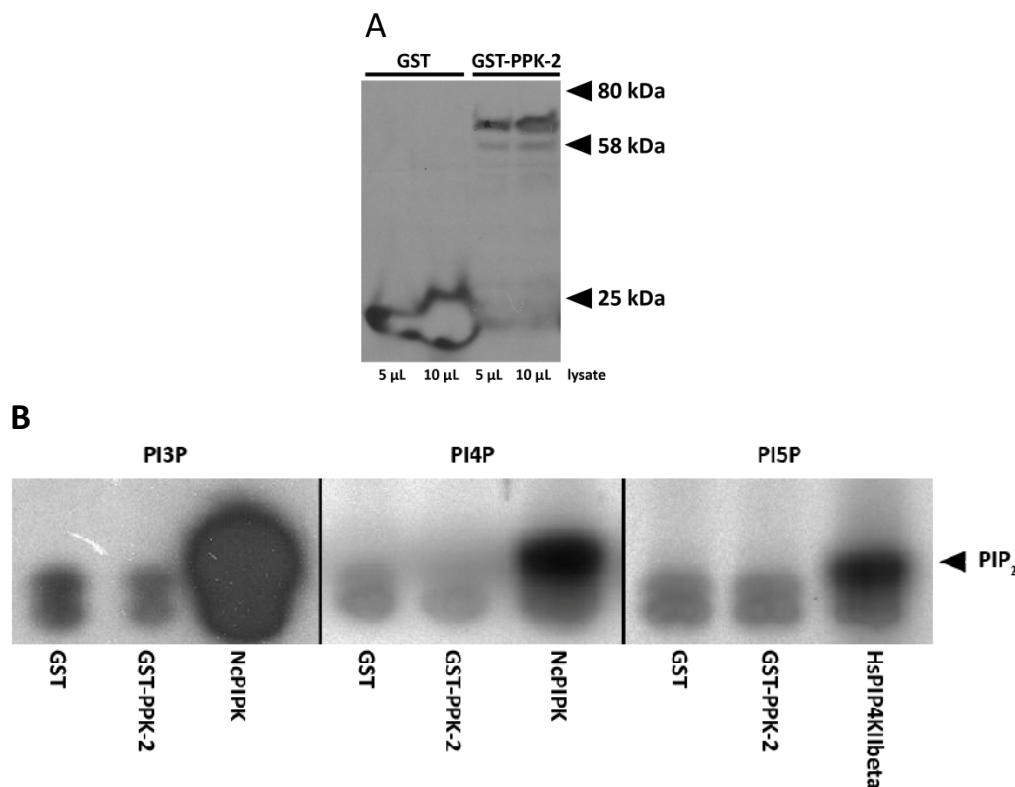


Figure 46 *In vitro* kinase assay of GST-PPK-2

A, immunoblot of different amounts of *E. coli* lysates harboring GST and GST-PPK-2, respectively. B, autoradiograms resulting from *in vitro* kinase assays with PI3P, PI4P, or PI5P as substrates. NcPIPK, PIP kinase of *Neurospora crassa*, HsPI4KIIbeta, *H. sapiens* Type II PIP kinase beta.

E. coli lysates harboring GST or GST-PPK-2 were used for *in vitro* kinase assays. Since *E. coli* does not possess any PIP-metabolizing activity (Michell, 2008), it is a suitable system for recombinant overexpression of eukaryotic PIP kinases. Lysates and putative substrates (PI3P, PI4P, PI5P) were coincubated in the presence of gamma-[³²P]ATP. Then, phosphoinositides were separated by TLC. Figure 46B shows autoradiograms of representative TLC plates.

Different expression conditions and varying lysis conditions have been tested for GST-PPK-2 (section 2.5.1). The biochemical analysis was performed by Dr. Irene Stenzel and Alina Mosblech, Department of Plant Biochemistry, Albrecht-von-Haller-Institute for Plant Sciences, Göttingen. However, using different mono phosphorylated PIPs as substrates, no significant catalytic activity of GST-PPK-2 was detected (Figure 46B). Since the parallel processed positive controls have found to phosphorylate mono-phosphoinositides, it was assumed that GST-PPK-2 indeed showed no detectable kinase activity to any of the three offered substrates.

3.3 Initial characterizations of two PIP phosphatases

The RNAi screen described in section 3.1 revealed in total four PIP phosphatases and two PI/PIP kinases being involved in regulation of acetylcholine release at NMJs of *C. elegans* and thus synaptic transmission. This study focused on the characterization of the putative Type II PIP kinase ortholog PPK-2 since this was expected to have the biggest potential to obtain new substantial knowledge regarding the PIP metabolism and PIP-regulated membrane trafficking in neurons (section 3.2). However, an extensive analysis of all identified enzymes would be beyond the scope of this study. None the less, the following section documents the basic characterization of two of the four identified PIP phosphatases.

3.3.1 Initial characterization of the *C. elegans* Sac1p homolog

The *C. elegans* genome harbors one homolog to the yeast PIP phosphatase Sac1p and the human Sac1 (www.wormbase.org). Sac1p and Sac1 were described to regulate PI4P-dependent membrane trafficking from the Golgi apparatus to the cell periphery and are functionally conserved (Konrad *et al.*, 2002; Nemoto *et al.*, 2000; Rohde *et al.*, 2003). A recent model describes the shuttling of Sac1p and Sac1, respectively, between the ER and the Golgi apparatus mediated by the COPI transport complex and stimulated by growth factors. Sac1p and Sac1 regulate PI4P levels and hence membrane trafficking from the Golgi apparatus during cellular growth. Human Sac1 was found to be expressed in nervous tissue (Blagoveshchenskaya and Mayinger, 2009). However, the majority of knowledge addressing its function has been obtained from studies in fibroblasts and HeLa cells. Nothing is known about its possible assignment(s) in neurons yet.

The RNAi knock down of the Sac1p/Sac1 homolog of *C. elegans* results in a decrease of acetylcholine release and is a first hint linking this protein with a function in neuronal membrane trafficking. In the following, the nematode homolog was analyzed, including an *in silico* sequence analysis and subcellular localization in neurons.

3.3.1.1 *C. elegans* F30A10.6 is homolog to yeast Sac1p and human Sac1

The locus encoding the *C. elegans* homolog to *S. cerevisiae* Sac1p and *H. sapiens* Sac1 is designated F30A10.6. For comparison sake, the according primary sequence of the putative translation product was aligned with the sequences of yeast and human. As illustrated by the alignment in Figure 48, all

three proteins share a high degree of identical as well as similar amino acids. Furthermore, residues important for catalytic activity are conserved in F30A10.6:

- the catalytic motif
- amino acids assembling a leucine zipper motif
- C-terminal COPI binding domain

Sac1p-homologs are thought to have two C-terminal transmembrane domains which are embedded in the cytosolic leaflet of the membrane of the ER and the Golgi apparatus, respectively, whereas the main portion of the protein is projected to the cytosol. These transmembrane domains were experimentally characterized for the human Sac1 protein. In order to determine whether or not these domains are conserved in *C. elegans* F30A10.6, its putative hydrophobicity was analyzed by plotting the primary sequence as a Kyte-Doolittle-plot. For comparison sake, *H. sapiens* Sac1 and *S. cerevisiae* Sac1p were plotted as well (Figure 47).

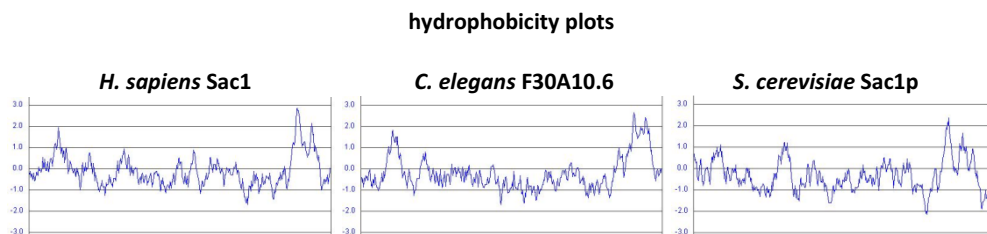


Figure 47 Hydrophobicity plots of *C. elegans* F30A10.6 and homologs

Kyte Doolittle hydrophobicity plots derived from the complete primary sequence of *H. sapiens* Sac1, *C. elegans* F30A10.6, and *S. cerevisiae* Sac1p. The two outstanding peaks proximal to the C-terminus (to the right) of the human protein represent two experimental verified transmembrane domains (Blagoveshchenskaya and Mayinger, 2009). Comparable peaks were observed for F30A10.6 and Sac1p.

The two transmembrane domains of *H. sapiens* Sac1 are represented by two extraordinary high peaks proximal to the protein's C-terminus. Similar peaks were observed proximal to the C-terminus of *C. elegans* F30A10.6 as well as *S. cerevisiae* Sac1p.

In summary, the primary sequence and amino acids assembling important structural elements are well conserved in *C. elegans* F30A10.6, revealing its high homology to human Sac1 and yeast Sac1p.

3.3.1.2 *C. elegans* F30A10.6 can replace Sac1p in yeast

In order to study the functional conservation of the putative Sac1p/Sac1 homologs of *C. elegans* *in vivo*, it was analyzed whether or not the *C. elegans* PIP phosphatase F30A10.6 can replace the function of Sac1p in *S. cerevisiae*.

The coding sequence of F30A10.6 was fused C-terminally with a HA-tag. F30A10.6-HA was expressed driven by a constitutive yeast promoter in a *S. cerevisiae* strain harboring a *sac1* knock out allele

human protein are underlined in red. Conserved amino acids comprising a leucin zipper motif are highlighted in red, whereas a COPI-binding motif at the very C-terminus is highlighted in yellow (Blagoveshchenskaya and Mayinger, 2009).

The deletion of *sac1* in *S. cerevisiae* is causal for several severe phenotypes as such as cold sensitivity and reduced growth (Nemoto *et al.*, 2000). The ability of F30A10.6-HA to compensate those phenotypes was tested with three different assays.

sac1 knock out yeast show almost no growth when cultured at 13°C. Deletion strains carrying the plasmids encoding Sac1p-HA and F30A10.6-HA, respectively, were incubated for several days at 13°C. As a control, the empty vector was used. In the following, these strains were examined for growth. As shown in Figure 49B, both deletion strains expressing Sac1p-HA and F30A10.6-HA, respectively, were observed to grow to dense cell lawns, whereas the negative control failed to do so.

Deletion strains of *sac1* are known to show slightly reduced growth on complete medium at standard incubation temperatures, but severely reduced growth on medium without inositol. In order to determine, whether or not F30A10.6-HA is able to compensate these phenotypes, dilution series of liquid cultures of every strain were plated on according medium and incubated for several days at 30°C. The growth of yeast colonies was analyzed by quantifying the mean intensity of according images (Figure 49C). Results were normalized to the positive control *sac1*delta Sac1p-HA.

As illustrated in Figure 49D, indeed a slight decrease of growth was observed for the negative control on complete medium, what was partially compensated in *sac1*delta F30A10.6-HA. On medium without inositol, the growth reduction of the negative control is even more severe. However, *sac1*delta F30A10.6-HA shows growth intensity comparable to the positive control.

Taken together, these three different assays revealed that *C. elegans* F30A10.6 can indeed replace Sac1p in yeast. Thus, its physiological and catalytic function appears to be highly conserved.

3.3.1.3 Subcellular localization of F30A10.6 in neurons

The RNAi-mediated knock down of F30A10.6 in *C. elegans* showed to cause a reduction of acetylcholine release at NMJs (section 3.1). Therefore, it is likely that this putative PIP phosphatase has a function in neurons, although its expression patterns in the nematode are not yet determined (Appendix).

In order to analyze the subcellular localization of F30A10.6 in wild type neurons, the coding sequence was N-terminally fused with mCherry and expressed driven by a pan-neuronal promoter. Since the homologous proteins in yeast and human were reported to localize at the Golgi apparatus (Konrad *et al.*, 2002; Nemoto *et al.*, 2000; Rohde *et al.*, 2003), the Golgi marker mannosidase II was coexpressed as a GFP fusion (MANS II-GFP).

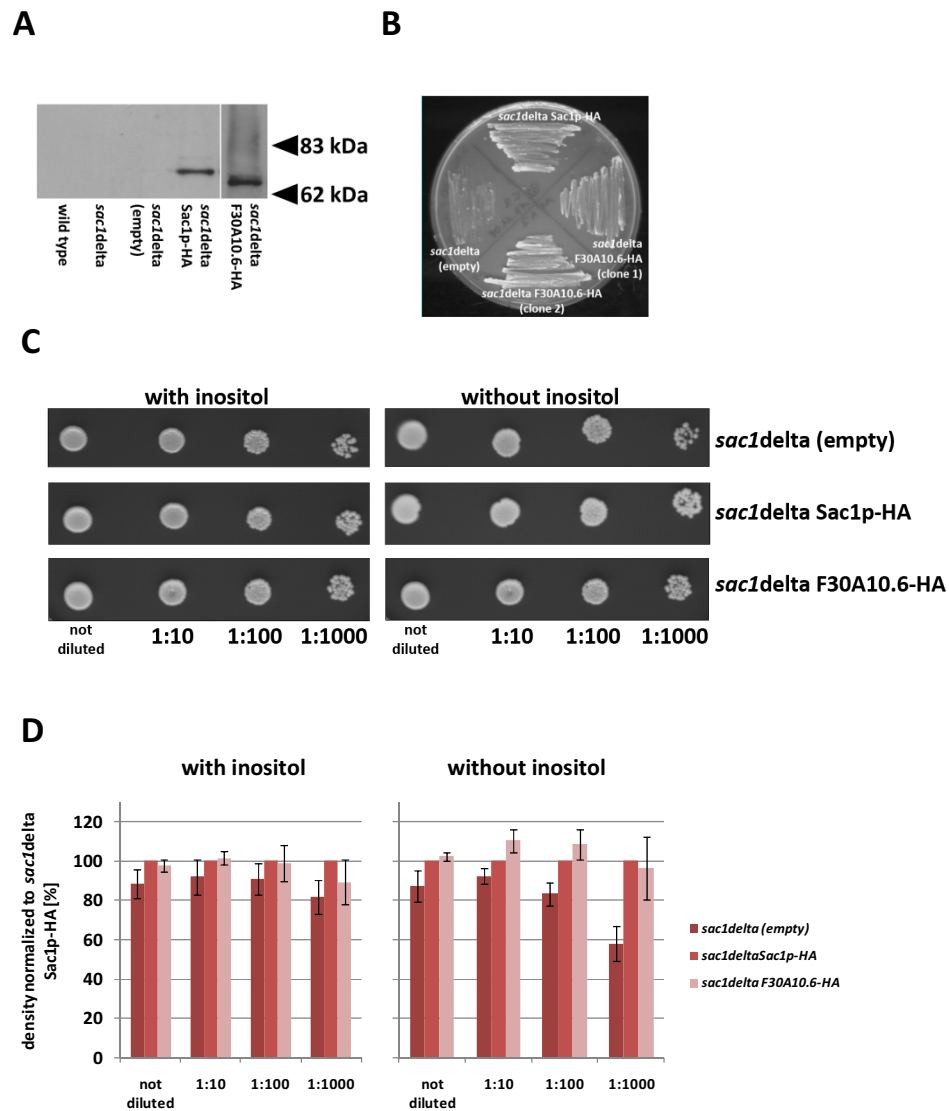


Figure 49 *F30A10.6 can substitute for Sac1p in yeast*

A, *Sac1p*-HA and *F30A10.6*-HA are detectable in *sac1delta* by immunoblotting. Wild type, *sac1delta*, and *sac1delta* transformed with the empty vector were tested for comparison sake. B, *F30A10.6*-HA is able to compensate the cold sensitivity of *sac1* knock out yeast. The assay was repeated two times. C, dilution series of liquid cultures plated on complete medium (with inositol) and medium without inositol. D, growth intensity of yeast colonies shown in C were quantified and normalized to the positive control. The assay was repeated two times.

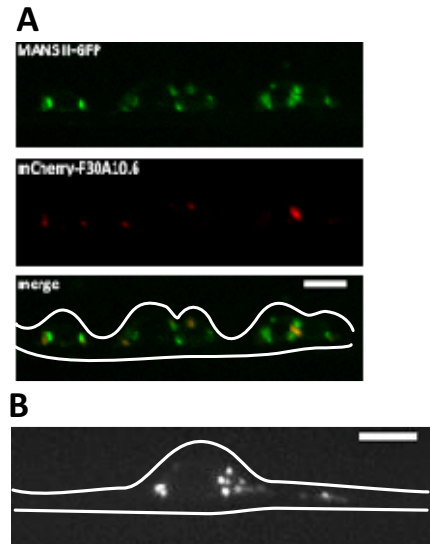


Figure 50 Subcellular localization of F30A10.6 in neurons

A, colocalization of mCherry-F30A10.6 with the GFP-labeled Golgi marker mannosidase II (MANS II-GFP) in neurons of the ventral cord. The approximate cell shapes are indicated in the bottom image. Scale bar, 5 μ m. B, localization of mCherry-F30A10.6 in a CAN neuron (axon to the right). The approximate cell shape is indicated. Scale bar, 5 μ m.

As shown in Figure 50A, mCherry-F30A10.6 localizes as distinct puncta in the neuronal cell body of the ventral cord of young adults. Overall, these signals overlap almost completely with puncta of MANS II-GFP. However, some GFP-signals do not overlap with the mCherry-signals. Figure 50B shows the localization of mCherry-F30A10.6 in the CAN neuron of a young adult animal. Distinct puncta were detected in the cell body but also in the axon.

Taken together, the F30A10.6 fusion protein localizes in a distinct Golgi-associated pattern in the cell body as well as in the axon of neurons in *C. elegans*.

3.3.2 Initial characterization of the *C. elegans* PTEN homolog

PTEN is a PI3,4,5P₃ 3-phosphatase known to regulate the level of the second messenger PI3,4,5P₃ at the PM. Thus, it is essential for cellular signaling. PTEN was found to be a tumor suppressor and mutations of the according gene are causal for many different types of cancer (Maehama, 2007).

The PTEN homolog of *C. elegans* is named DAF-18 and was described to regulate cell signaling and thereby longevity and nematode dauer formation (Solari *et al.*, 2005). It is expressed in almost all

tissues (Appendix), however, a specific function in neuronal signaling was not yet reported. Hence, the according result of the herein presented RNAi screen (section 3.1) is the first evidence of a role for DAF-18 in synaptic transmission.

In the following, two different *daf-18* mutant alleles were analyzed regarding acetylcholine release, velocity, and *in vivo* PIP₂ levels.

3.3.2.1 *daf-18* mutants show resistance to aldicarb

Two different *daf-18* mutant alleles are available and were both received from CGC. *daf-18* (*e1375*) harbors an insertion of 30 nucleotides in exon 4 and is supposed to result in a C-terminally truncated protein which consists only of the phosphatase domain (Gil *et al.*, 1999). *daf-18* (*ok480*) possesses a deletion comprising exons 4 and 5 as well as intron 4.

The RNAi knock down of *daf-18* results in a decrease of acetylcholine release at NMJs, as revealed by aldicarb assays (section 3.1). Consequently, the response of both *daf-18* mutants to this neurotoxin was analyzed.

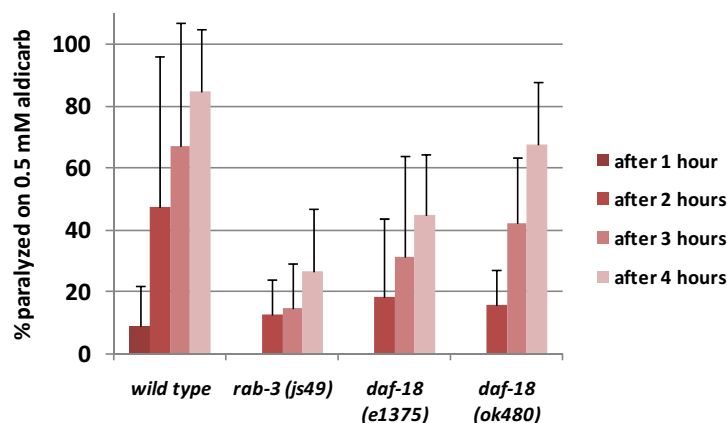


Figure 51 Aldicarb assay of *daf-18* mutants

Aldicarb assay of both *daf-18* mutants compared to wild type nematodes and a *rab-3* mutant as positive control. The assay was repeated three times.

Young adults of wild type, *daf-18* (*e1375*), *daf-18* (*ok480*), and a *rab-3* mutant as positive control were placed on agar plates containing 0.5 mM aldicarb and observed for paralysis for several hours. As illustrated in Figure 51, *daf-18* (*e1375*) shows a significant resistance to aldicarb with less than 10 % of the animals paralyzed after three hours. Even after four hours, less than 20 % of the nematodes are paralyzed. In contrast, about 40 and 70 % of wild type nematodes are paralyzed after three and four hours, respectively. *daf-18* (*ok480*) shows a milder *ric* phenotype than *daf-18* (*e1375*). However, the paralysis quotes are still significant lower as compared to the wild type. The aldicarb resistant control *rab-3* (*js49*) shows only a paralysis of 20 % after four hours.

Taken together, this neurotoxin assay revealed that both *daf-18* mutants possess decreased acetylcholine release at NMJs.

3.3.2.2 Velocity of *daf-18* mutants

In order to determine, if the changed neurotransmitter release influences the motility, i.e. velocity of *daf-18* mutants, their movement was analyzed by video tracking as already described in section 3.2.3.4.

In brief, the movements of a small population of adult animals were recorded and the different distances every single nematode of this population moves per second have been determined. The frequency of any measured distance traveled within one second by the individual animals of the population was averaged and graphed as a cumulative plot. The ascent of this graph illustrates the relative velocity of the animals of a population: A flat ascent is caused by the accumulated occurrence of animals moving relatively fast. A steep ascent is caused by the accumulated occurrence of animals in the population moving relatively slow.

The graph representing the wild type population ascends continually from 0 to almost 100%. The covered velocities range from 0 to approximately 0.3 mm/sec. The graphs of both *daf-18* mutants cover the same velocity range, however, their ascents differ strikingly from wild type (Figure 52). Both graphs are much more flat as compared to the wild type graph. This documents, that animals of both mutant populations move comparably fast.

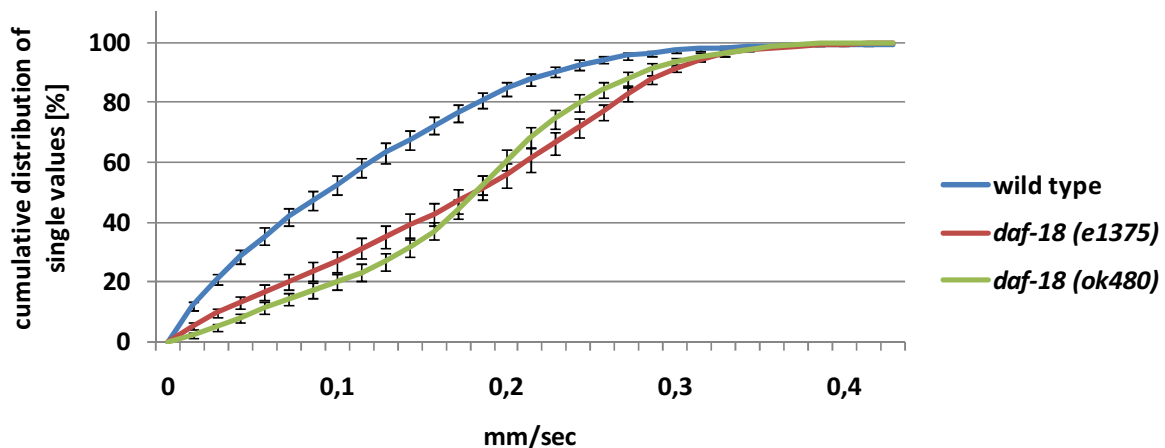


Figure 52 Cumulative distribution of velocities displayed by *daf-18* mutants

Averaged frequencies of any measured distance traveled within one second by the individual animals (single values) of populations of wild type ($n = 129$), *daf-18 (e1375)* ($n = 99$), and *daf-18 (ok480)* ($n = 97$). Error bars, standard error of the mean.

In summary, *daf-18 (e1375)* as well as *daf-18 (ok480)* animals were observed to move with a higher velocity than wild type nematodes.

3.2.2.3 Biochemical analysis of phospholipids

DAF-18 is postulated to regulate PI3,4,5P₃ levels at the PM by dephosphorylating the D-3 position of this phosphoinositide, resulting in PI4,5P₂ (Solari *et al.*, 2005). Therefore, a mutation of the according gene is likely to influence the level of double phosphorylated PIPs *in vivo*. In order to test this possibility, the PIP₂ levels of both *daf-18* mutants have been analyzed.

As already described under 3.2.3.8, large synchronous populations of L1 larvae were used for acidic extraction. Extracted phospholipids were separated and identified by TLC, and further quantified by GC. PIP₂ amounts were normalized to the amounts of the non-phosphoinositide PC derived from the same sample.

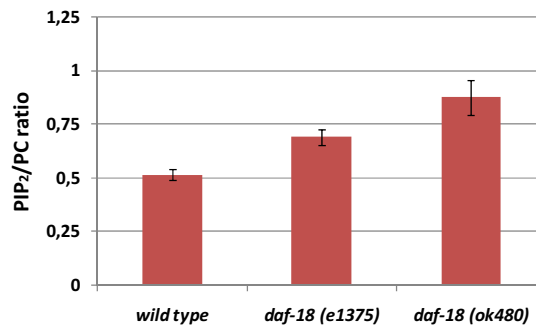


Figure 53 The PIP₂ levels of *daf-18* mutants are increased compared to wild type

PIP₂/PC ratio of synchronous L1 populations of wild type compared to *daf-18 (e1375)* and *daf-18 (ok480)*. Averages of two independent GC runs. Error bars, standard deviation.

As illustrated in Figure 53, the PIP₂/PC ratio of wild type is 0.51. In contrast, both *daf-18* mutants possess increased ratios of 0.69 for *daf-18 (e1375)* and 0.87 for *daf-18 (ok480)*, respectively. Therefore, it must be concluded that the PIP₂ levels in both *daf-18* mutants is significantly higher compared to wild type animals.

4 Discussion

Synaptic transmission relies on the highly organized membrane transport in neurons. In turn, membrane trafficking must be tightly regulated. The targeted transport of membrane-enclosed vesicles and other membranous organelles is dependent on distinct membrane identities so that different types of vesicles and organelles can be distinguished by the different intracellular transport machineries (Munro, 2004; Itoh and De Camilli, 2004). Essential players building this identity in concert with specific proteins are the phosphorylated derivatives of the phospholipid PI termed PIPs or phosphoinositides (Roth, 2004; Di Paolo and De Camilli, 2006).

PIPs comprise only minor components of the cytosolic leaflet of eukaryotic endomembranes and the PM, but they have many crucial cellular functions including membrane trafficking in neurons as well as in all other cell types (Wenk and De Camilli, 2001; Cremona and De Camilli, 2001). Thus, their misregulation is causal for many different diseases ranging from cancer to neuropathies (Halstead *et al.*, 2005; Volpicelli-Daley and De Camilli, 2007; Vicinanza *et al.*, 2008; Majerus and York, 2009). However, the role of PIPs and their metabolizing enzymes in neuronal membrane transport is still elusive. The aim of this study was to identify enzymes with novel functions in the neuronal phosphoinositide network regarding synaptic transmission and neuronal membrane trafficking.

4.1 New players in neuronal membrane traffic in *C. elegans*

A selected group of putative PIP-metabolizing enzymes was screened for a function in neuronal membrane trafficking in the nematode *C. elegans*. All candidates are homologous to proteins in yeast and/or mammalia which are already known or hypothesized to act in membrane trafficking.

In order to study gene functions, the expression of the candidate genes was knocked down using RNAi. This method has several advantages, especially if no appropriate mutant strains are available or according alleles are lethal. RNAi can induce a phenotype which is less severe, thus allowing it to study the respective gene function.

As readout, the acetylcholine release at NMJs was measured by analyzing RNAi-treated nematodes for their response to the acetylcholinesterase inhibitor aldicarb (Mahoney *et al.*, 2001). Altered exocytosis of this neurotransmitter at the presynapse can indicate a defect in the SV cycle or may display a general defect in neuronal membrane trafficking (Sieburth *et al.*, 2005). Thus, in total six new players in *C. elegans* neuronal membrane trafficking have been revealed (section 3.1):

daf-18 is the homolog of the tumor suppressor PTEN which is mutated in many different cancer types in humans (Blero *et al.*, 2007 Solari *et al.*, 2005). PTEN antagonizes PIP 3-kinases at the PM by dephosphorylating the D-3 position of PI3,4,5P₃ and therefore negatively regulates PI3,4,5P₃-dependent cellular signaling to the cell interior (Maehama *et al.*, 2007). A lack of DAF-18 was initially described to influence dauer larva formation (Ogg and Ruvkun, 1998; Gil *et al.*, 1999).

F30A10.6 is homologous to yeast Sac1p and mammalian Sac1 (Foti *et al.*, 2001; Rohde *et al.*, 2003). Sac1p/Sac1 is a PIP phosphatase which regulates the PI4P pool at the Golgi apparatus and hence PI4P-dependent coat formation and vesicle budding.

Sac1p/Sac1 shuttles between the ER and the Golgi apparatus stimulated by nutrients, thereby regulating cell growth and proliferation (Blagoveshchenskaya and Mayinger, 2009).

- mtm-3** is a member of the myotubularin phosphatase family (Xue *et al.*, 2003). MTM-3 was described to dephosphorylate PI3P *in vivo* and *in vitro* and possesses a FYVE domain (Ma *et al.*, 2008). Despite this PI3P-specific binding domain, the human homolog MTMR3 has not been reported to localize to the membrane of early endosomes (Lorenzo *et al.*, 2005). Indeed, MTMR3 is hypothesized to regulate a PI3P pool at the ER or the Golgi apparatus (Robinson and Dixon, 2006).
- vps-34** is related to a PI 3-kinase named Vps34p which was originally described in yeast (Herman *et al.*, 1990). In current models, Vps34p homologs are discussed to be essential for endosomal sorting (Wurmser *et al.*, 1999; Seaman, 2008). In *C. elegans*, VPS-34 is hypothesized to be involved in membrane trafficking from the cell interior to the periphery and its product PI3P is located at many different endomembranes including vesicles. Nematodes deficient in this PI 3-kinase possess significantly reduced PI3P levels (Roggo *et al.*, 2002).
- C34B7.2** is a homolog of the PIP phosphatase Fig4p of yeast and Fig4 of mammals, respectively (Duex *et al.*, 2006a; Chow *et al.*, 2007). In yeast, Fig4p dephosphorylates PI3,5P₂ to PI3P and regulates PI3,5P₂ levels in response to osmotic shock by a close interaction with the PI3P 5-kinase Fab1p (Duex *et al.*, 2006a; Duex *et al.*, 2006b). Both Fig4p and Fab1p are located to the vacuolar membrane of yeast (Duex *et al.*, 2006a). A homologous complex is hypothesized to regulate PI3,5P₂ levels at the lysosome of mammals (Jin *et al.*, 2008; Sbrissa *et al.*, 2008) and may also exist in *C. elegans* (Nicot *et al.*, 2006). However, Fig4p homologs in animals seem to have important neuronal functions. Fig4 knock out mice have severe neuronal disorders and human Fig4 was found to be mutated in Charcot-Marie-Tooth patients (Chow *et al.*, 2007).
- ppk-2** is the sole Type II PIP kinase homolog of *C. elegans* and supposed to be a PI5P 4-kinase. Type II PIP kinases of mammals are known to phosphorylate PI5P to PI4,5P₂ *in vitro* (Rameh *et al.*, 1997). Which phosphoinositides are phosphorylated by Type II PIP kinases *in vivo* and which physiological function these enzymes play in membrane trafficking is still elusive and currently under discussion (Clarke *et al.*, 2007).

For all these six proteins a substantial background of literature is available what allows assigning well-founded functions to five of them. The sole exception is *ppk-2*. *ppk-2* is homologous to the PI5P 4-kinases or Type II PIP kinases, which are exclusively found in animals but not in fungi or plants (Clarke *et al.*, 2007).

In mammals, three isoforms of Type II PIP kinases have been described so far (Clarke *et al.*, 2007). However, the available information about this enzyme family is incoherent, thus the physiological function(s) is still elusive. The *in vivo* analysis of PI5P 4-kinases in higher animals may be also limited by possible functional overlapping of the different isoforms. Consequently, the model organism *C. elegans*, which possesses only a sole PI5P 4-kinase homolog, provides a big potential to identify a physiological role for Type II PIP kinases.

4.2 Characterization of the Type II PIP kinase PPK-2

A detailed analysis of the primary sequence of PPK-2 revealed its close homology to the three isoforms of Type II PIP kinases of mammalia (section 3.2.1). These enzymes are hypothesized to constitute an alternative pathway for the synthesis of the multifunctional phosphoinositide PI4,5P₂. The isoforms alpha, beta, and gamma show differing expression patterns as well as subcellular localizations. However, the physiological function of this enzyme family is poorly characterized.

In *C. elegans*, *ppk-2* is predominantly expressed in the nervous system (Appendix) and indeed it has a function at synapses: Reduced expression of the putative Type II PIP kinase results in a decreased acetylcholine release at NMJs (section 3.1).

RNAi mediated knock down in *C. elegans* is a suitable tool for initial characterization of gene functions. However, RNAi effects are only transient and can vary in their intensities. Nematode strains harboring mutations in the *ppk-2* locus may have phenotypic defects which are invariable and stable inherited. Therefore, the physiological function of *ppk-2* in neurons was analyzed using two different *ppk-2* mutant strains.

4.2.1 *ppk-2* regulates neurotransmitter and neuropeptides release

Two different mutant alleles of *ppk-2* were analyzed in this study. *ppk-2* (*ttTi8500*) harbors a transposon insertion in exon 3, whereas in *ppk-2* (*tm3741*) a long stretch of nucleotides across the border of exon 1 and intron 1 is deleted. Analysis of the respective mRNAs revealed that given that both alleles are still expressed yielding PPK-2 proteins with altered N-termini (sections 3.2.3.2 and 3.2.4.2).

To analyze the synaptic transmission at NMJs, both *ppk-2* mutant strains were tested for their release of acetylcholine by an aldicarb assay. Surprisingly, *ppk-2* (*ttTi8500*) animals turned out to be hypersensitive to this neurotoxin, reflecting an increased release of acetylcholine. Thus, this mutant shows an opposite phenotype as described for *ppk-2* (RNAi). *ppk-2* (*tm3741*) animals did not show any hypersensitivity or resistance to aldicarb (section 3.2.3.3).

In order to verify *ppk-2* mutant phenotypes, both strains were tested for their response to the GABA-antagonist PTZ. This complementally assay revealed that both *ppk-2* mutants display elevated acetylcholine release at NMJs compared to wild type animals (sections 3.2.3.3) whereby this phenotype appear to be more pronounced in *ppk-2* (*ttTi8500*) animals. Consequently, it must be concluded that both mutant alleles of *ppk-2* result in a gain of function characterized by increased acetylcholine release and therefore exocytosis of SVs at NMJs.

Acetylcholine release at NMJs predominantly regulates the motility of nematodes and its misregulation mostly results in uncoordinated movement. Such a phenotype was observed for both *ppk-2* mutants: Compared to wild type animals, their movements were flattened and irregular. However, the velocity of both *ppk-2* (*ttTi8500*) and *ppk-2* (*tm3741*) was not severely affected (section 3.2.3.4). Since the nervous system was observed to develop normal (section 3.2.3.5) and the postsynapses appear to be unaffected (section 3.2.3.3), the cause for this uncoordinated phenotype

must be the significant elevated presynaptically acetylcholine release by SVs at motor neurons of *ppk-2* mutants. Consequently, the subcellular localization of SVs was analyzed.

The *C. elegans* synaptogyrin ortholog SNG-1 was used as SV marker protein (Zhao and Nonet, 2001) and expressed as a GFP-fusion in the nervous system of both *ppk-2* mutants. The localization of SNG-1-GFP was not changed compared to wild type. In order to determine the amount of SNG-1-GFP at synapses, the fluorescence was quantified in the synapse-dense region of the dorsal cord and was not found to differ between *ppk-2* mutants and wild type (section 3.2.3.7). The unchanged amount of SNG-1-GFP at *ppk-2* presynapses indicates that the transport of SV precursors and the generation of SVs are not impaired.

SNG-1-GFP is known to localize specifically at synapses and therefore can be used as marker for synaptic clusters along axons (Zhao and Nonet, 2001). The quantification of individual synaptic clusters along the sublateral axon tracts of young adult animals revealed a minor increase of those SNG-1-GFP stained clusters in both *ppk-2* mutant backgrounds (section 3.2.3.7). However, it appears unlikely that the significantly enhanced release of acetylcholine arises only from few additional synapses.

Altered exocytosis of neurotransmitters is known to be mostly caused by defects in the exocytosis machinery (Sieburth *et al.*, 2005; Sieburth *et al.*, 2007; Speese *et al.*, 2007) which is essentially triggered by PI4,5P₂. However, the major PI4,5P₂-producing enzyme at the PM of *C. elegans* neurons was demonstrated to be the Type I PIP kinase PPK-1 and not PPK-2 (Weinkove *et al.*, 2007). Consistent with this, *in vitro* assays with recombinant expressed PPK-2 did not demonstrate any measurable catalytic activity towards PI3P, PI4P, or PI5P, suggesting that PPK-2 does not significantly contribute to the levels of double-phosphorylated phosphoinositides in *C. elegans* (section 3.2.5). But most interestingly, the biochemical analysis of phospholipids revealed a significant increase of PIP₂ in *ppk-2* (*ttTi8500*) animals (section 3.2.3.8). This points towards a crucial function of PPK-2 in the phosphoinositide network even if the enzyme itself has no or only very poor activity. However, what PIP species is represented by the elevated PIP₂ level was not determinable with the applied method. But since PI4,5P₂ is a major trigger for synaptic transmission, an increase of this phosphoinositide is an explanation for the increased acetylcholine release of *ppk-2* mutants.

PI4,5P₂ does not only regulate the exocytosis of SVs, but also the exocytosis of DCVs. DCVs differ from SVs in their biogenesis, trafficking, and content. Instead of neurotransmitters such as acetylcholine and GABA, they transport neuropeptides which regulate synaptic transmission and neurotransmitter release by binding to guanine nucleotide-binding protein-coupled receptors (Sieburth *et al.*, 2007; Speese *et al.*, 2007). Exocytosis of these signaling peptides does not essentially occur at the active site of the presynapse but also elsewhere at the PM. However, DCVs are in part dependent on the exocytosis machinery of SVs regulated by PI4,5P₂ (Sieburth *et al.*, 2007; Speese *et al.*, 2007).

In order to analyze whether the subcellular localization of DCVs is influenced by *ppk-2*, their subcellular localization has been analyzed in both *ppk-2* mutants. For localization studies, a well described neuropeptide, ANF (Speese *et al.*, 2007), was expressed as a GFP-fusion in neurons of both *ppk-2* mutants and wild type. ANF-GFP localization in *ppk-2* (*ttTi8500*) and *ppk-2* (*tm3741*) was essentially the same as observed in wild type nematodes (section 3.2.3.7). Hence, the subcellular distribution of DCVs in *C. elegans* neurons is not affected by both *ppk-2* mutant alleles.

However, the quantification of fluorescence in the dorsal cord revealed a slight decrease of ANF-GFP in *ppk-2 (ttTi8500)* but not in *ppk-2 (tm3741)* mutants (section 3.2.3.7). A reduction of fluorescence can be interpreted as a decreased transport of ANF-GFP to the presynapse or as increased exocytosis of neuropeptides to the cell environment. In order to test the last notion, ANF-GFP signals detected in coelomocytes were quantified. Coelomocytes are scavenger cells, which continuously endocytose and degrade fluid and macromolecules from the nematodes' body cavity (Fares and Greenwald, 2001). Indeed, the ANF-GFP fluorescence in coelomocytes of young adults of both *ppk-2 (ttTi8500)* and *ppk-2 (tm3741)* was significantly increased by more than 30 % compared to wild type (section 3.2.3.7). This indicates an increased release of ANF-GFP to the body cavity at synaptic terminals, pointing towards a dramatic increase of DCV exocytosis in *ppk-2* mutants. This phenotype appears to be more pronounced in *ppk-2 (ttTi8500)* animals as compared to *ppk-2 (tm3741)*.

Analysis of the physiological effect of both *ppk-2* alleles has shown the elevated release of acetylcholine and neuropeptides at NMJs affecting the motility of nematodes. Thus, an increased exocytosis of SVs but also DCVs must be assumed. Therefore, it is very likely that *ppk-2* is involved in synaptic exocytosis either directly or indirectly.

4.2.2 PPK-2 interacts with PPK-1

The phenotypes regarding acetylcholine exocytosis of *ppk-2 (RNAi)* and *ppk-2* mutant animals are contradictory. A comparable observation was reported for a synaptic protein which is directly implicated in the exocytosis of DCVs in *C. elegans*.

Nematodes lacking protein kinase C-1 (PKC-1) are resistant to aldicarb, but animals expressing a constitutive active mutant of PKC-1 response in a hypersensitive manner to aldicarb. PKC-1 was shown to be essential for neuropeptide exocytosis. When PKC-1 is missing, neuropeptide release at NMJs is significantly reduced, thereby neurotransmitter signaling is downregulated. The phenotype of the constitutive active mutant is thought to be caused by significantly increased neuropeptide release (Sieburth *et al.*, 2007).

PKC-1-mediated DCV exocytosis is triggered by diacylglycerol (DAG). DAG in turn derives from the cleaving of PI4,5P₂ by phospholipase C at the synapse (Lackner *et al.*, 1999). Artificial overactivation of PKC-1 leads to aldicarb hypersensitivity caused by elevated DCV exocytosis (Sieburth *et al.*, 2007). Significantly increased neuropeptide release accompanied by aldicarb hypersensitivity was observed for *ppk-2* mutants as well. This allows the conclusion that the PI4,5P₂-dependent pathway regulating DCV exocytosis via PKC-1 is affected.

ppk-2 (ttTi8500) animals have an elevated PIP₂ level. Most interestingly, elevated PI4,5P₂ was shown for nematodes overexpressing the *C. elegans* Type I PIP kinase PPK-1 in the nervous system (Weinkove *et al.*, 2007). Despite its apparent function in the neuronal PIP metabolism, *ppk-1* was not identified in the here presented RNAi screen. However, when working with RNAi it should be always considered that the effectiveness of a knock down is dependent on many variables and that RNAi is known for its relatively high rate of false negatives (Kamath *et al.*, 2003).

Proteins interacting with PPK-1 and thereby regulating its activity are not known. However, Type I PIIP kinases of *H. sapiens* have been recently described to interact with Type II PIP kinase alpha. In

HeLa cells, Type II PIP kinase alpha localizes mainly to the cytoplasm. Most interestingly, coexpression with any of the three isoforms of human Type I PIP kinases causes Type II PIP kinase alpha to change its localization and to colocalize with the Type I enzymes at the PM. Furthermore, Type II PIP kinase alpha coimmunoprecipitates with any of the three Type I PIP kinase isoforms (Hinchliffe *et al.*, 2002).

The localizations of mCherry-PPK-2 and GFP-PPK-1 were analyzed in the neurons of wild type nematodes. GFP-PPK-1 localized to PM (section 3.2.4.3) as already described (Weinkove *et al.*, 2007), whereas mCherry-PPK-2 predominantly localized to endosomal membranes but also partially to the Golgi apparatus (section 3.2.4.1). However, when coexpressed, mCherry-PPK-2 was also detectable at the PM and GFP-PPK-1 at endomembranes. Both differently labeled proteins showed an almost perfect overlap of their localization patterns (section 3.2.4.3). This leads to the conclusion, that the interaction of Type I and Type II PIP kinases observed in human cells is also conserved in *C. elegans*.

Analysis of the subcellular localization of mCherry-fusion proteins encoded by the transcripts of *ppk-2* (*ttTi8500*) and *ppk-2* (*tm3741*) revealed that they localize to endomembranes, as also observed for the PPK-2 wild type protein (section 3.2.4.2). In order to test, how mCherry-PPK-2 (*ttTi8500*) and mCherry-PPK-2 (*tm3741*) localize in the presence of GFP-PPK-1, according fusion proteins were coexpressed in wild type neurons. It was found that both PPK-2 mutant proteins do not colocalize with GFP-PPK-1 at the PM. In contrast, GFP-PPK-1 was still observed to localize at the same endomembranes as the mutant mCherry-fusions (section 3.2.4.4). The function of PPK-1 at endomembranes is not known, but recent publications describe mammalian Type I PIP kinase isoforms to regulate PI4,5P₂ at lysosomal membranes and therefore clathrin-mediated vesicle budding (Arneson *et al.*, 1999).

The localization studies of PPK-1, PPK-2, and PPK-2 mutant proteins point towards an interaction of Type I PIP kinases and Type II PIP kinases at the PM. Since both PPK-2 mutant proteins possess an altered N-terminus, the mechanism regulating this interaction is supposed to be dependent on this protein region.

4.2.3 PPK-2 localizes to endomembranes

The analysis of both *ppk-2* mutant strains suggests that PPK-2 regulates the release of neuropeptides and hence neurotransmitters in a negative manner, as documented by their aldicarb hypersensitivity. Potentially this occurs by interacting with PPK-1 at the PM (sections 4.2.1 and 4.2.2). However, the RNAi-mediated knock down of *ppk-2* resulted in resistance to aldicarb (section 3.1) what in contrast indicates that PPK-2 regulates this process positively. This contradictory observation needs to be discussed.

In general, RNAi effects are equivalent or very similar to a complete gene knock out (Kamath *et al.*, 2001; Kamath *et al.*, 2003) at last due to the reduced transcription of the respective protein. Hence, *ppk-2* (RNAi) results in the depletion of PPK-2 at the neuronal PM as well as at the endomembrane system. According to the model discussed above, a lack of PPK-2 at PM would cause an overactivation of DAG signaling. However, PPK-2 localizes also to endomembranes. Therefore, despite of its obvious function in exocytosis, PPK-2 may have an additional function in endomembrane trafficking.

Most components of SVs and DCVs are primarily synthesized by the ER. During their maturation they travel through the Golgi apparatus where they are packed into different transport vesicles (Hannah *et al.*, 1999). Some of these membranous containers can travel directly to the PM, but many of them undergo a passage through the endosomal sorting machine Richmond and Broadie, 2002; Edwards *et al.*, 2009). This sorting process is well described for DCVs in *C. elegans*: An 'immature' DCV which buds from the Golgi apparatus is hypothesized to pass through the sorting endosome and emerges as a 'mature' DCV which subsequently travels to the synaptic PM.

Recently, it was shown that missorting of DCV constituents by endosomes results in significantly decreased acetylcholine release at NMJs and hence aldicarb resistance of nematodes (Sumakovic *et al.*, 2009). Thus, a defect at endomembranes can lead to the same synaptic phenotype as observed in *ppk-2* (RNAi) animals. The knock down of *ppk-2* may result in a dysfunction of membrane trafficking from the endomembrane system to the cell periphery. Supportive evidence for this hypothesis comes from the subcellular localization of PPK-2 mutant proteins which exclusively localize to endomembranes even when coexpressed with PPK-1 (section 3.2.4.3). This indicates that these altered PPK-2 proteins still function at membranes in the cell interior but not at the PM, resulting in aldicarb hypersensitivity. As a consequence of this hypothesis two sites of actions must be assigned to PPK-2, namely the PM and the endomembrane system.

Colocalization studies with several organelle marker proteins revealed that mCherry-PPK-2 colocalizes in part with the Golgi apparatus. An almost complete signal overlap was observed by using a GFP-labeled FYVE-domain (section 3.2.4.1). FYVE-GFP is known to bind to PI3P in a highly specific manner (Stenmark and Aasland, 1999; Stenmark and Gillooly, 2001), which is enriched in the membrane of early and sorting endosomes (Roth, 2004; Seaman, 2008). Interestingly, a comparable localization pattern was recently described for the neuronal expressed gamma isoform of Type II PIP kinases in mice. This kinase was characterized to localize to vesicular structures of the endomembrane system and shows partial colocalization with Golgi and endosome markers (Clarke *et al.*, 2009).

In their previous publication the same authors demonstrate that recombinant expressed Type II PIP kinase gamma does not show any measurable PIP kinase activity *in vitro* (Clarke *et al.*, 2008). However, modifications of the assay and the substantial increase of the recombinant expressed kinase revealed that Type II PIP kinase gamma indeed shows catalytic activity towards PI5P although this activity is very low. The authors therefore hypothesize that Type II PIP kinase gamma is implicated in the transport of vesicles, shuttling between different compartments by regulating local PI5P pools (Jon Clarke and Robin Irvine, University of Cambridge, personal communication). A phylogenetic analysis revealed that PPK-2 rather corresponds to Type II PIP kinase gamma than to the other two mammalian isoforms (section 3.2.1), thus supporting the postulated function of PPK-2 at endomembranes.

Consistent with the endomembrane localization of PPK-2 and Type II PIP kinase gamma, a significant pool of PI5P is hypothesized to be located at the membrane of endosomal compartments (Lecompte *et al.*, 2008) and at membranes of the Golgi apparatus (Merlot *et al.*, 2003). Based on different lines of evidence, Lecompte and colleagues (2002) furthermore suggest that PI5P is implicated in the regulation of membrane trafficking from endosomal compartments to the plasma membrane (Sbrissa *et al.*, 2004). Yet, no PIP kinase activity was shown for PPK-2 although crucial structure elements and important functional amino acids, conserved in every Type II PIP kinase, are present

(section 3.2.1). However, its activity is maybe below the detection limit of the applied assay. By phosphorylating PI5P to PI4,5P₂ – even with a low activity –, PPK-2 may significantly contribute to the differently PIP-regulated membrane trafficking routes between endosomes to the PM.

How the membranous localization of PPK-2 is achieved is not known. The structure derived by the comparison to the Type II PIP kinase beta of *H. sapiens* did not reveal a membrane-spanning domain (section 3.2.1). However, it was hypothesized that the flat and negatively charged face of a kinase dimer is implicated in membrane attachment. This protein area is formed by the N-termini of both monomers which are also supposed to mediate dimerization (Rao *et al.*, 1998).

Both PPK-2 mutant proteins analyzed in this study were shown to possess significantly altered N-termini. PPK-2 (*ttTi8500*) lacks a short stretch of amino acids linking an alpha helix to a beta sheet whereas in PPK-2 (*tm3741*) a big portion of the N-terminus is deleted (section 3.2.1). However, both proteins were expressible as mCherry-fusion proteins in *C. elegans* neurons and were observed to localize at endomembranes as shown for the wild type protein (section 3.2.3.2). Therefore, it must be concluded that an intact N-terminus is not essential for the endomembrane association of PPK-2, but for the colocalization with PPK-1 at the PM.

Based on the structure of *H. sapiens* Type II PIP kinase beta (Rao *et al.*, 1998), PPK-2 is supposed to fold in an N-terminal and a C-terminal domain both comprised of one beta sheet and additional alpha helices (section 3.2.1). The C-terminal domain harbors the complete catalytic core which is composed of the insert and the activation loop. The activation loop was shown to determine substrate specificity, but also essentially regulates the subcellular localization of Type II PIP kinases (Kunz *et al.*, 2000; Kunz *et al.*, 2002; Rao *et al.*, 1998). In case that both PPK-2 mutant proteins fold correctly, the C-terminal domain is still intact and may mediate the association to endosomal membranes.

However, PPK-2 localization at the PM as well as at endomembranes is assumed to be reliant on additional factors. Most PIP kinases are known to be activated and recruited to membranes by small G-proteins such as Rab, Rho, Rac, or Arf (Donaldson, 2005; Santarius *et al.*, 2006; Di Paolo and De Camilli, 2006). Therefore, it is likely that the related Type II PIP kinases including PPK-2 are recruited by similar proteins.

4.2.4 PPK-2 is actively transported into neuronal processes

Beside the localization at endomembranes in neuronal cell bodies, vesicle-like particles stained by mCherry-PPK-2 were observed to travel anterograde and retrograde along both dendrites and axons (section 3.2.4.5). Similar particles are stained by mCherry-fusions of both PPK-2 mutants (section 3.2.4.6). This supports the hypothesized role for PPK-2 in membrane trafficking from endosomes to the cell periphery. However, these particles were not stained by FYVE-GFP indicating that these organelles are neither early nor sorting endosomes and possess a different identity.

Both wild type and mutant mCherry-PPK-2 particles move bidirectional with an approximate velocity of 0.3 $\mu\text{m}/\text{sec}$ (section 3.2.4.7). This relatively fast speed indicates that these unidentified vesicles are actively transported by motor proteins. Indeed, the localization of PPK-2 particles was significantly affected in mutants of the *C. elegans* kinesin-3 ortholog UNC-104 (Hall and Hedgecock, 1991).

mCherry-PPK particles as well as particles costained with FYVE-GFP are no longer found in the axon, but accumulate at dendritic tips and appear to be stationary (section 3.2.4.8).

UNC-104 is known to transport SV precursors as well as DCVs (Hall and Hedgecock, 1991; Zahn *et al.*, 2004). However, these transport processes were described to occur at much higher speed than the velocities which were measured for the PPK-2 particles (Zhou *et al.*, 2001; Zahn *et al.*, 2004). Furthermore, DCV and SV marker proteins remain in the neuronal cell bodies of *unc-104* mutant animals but do not accumulate in dendrites. This indicates that additional motors may be involved in the transport of PPK-2 as for example kinesin-1 or dynein (Dinu *et al.*, 2007; Zheng *et al.*, 2008; Kardon and Vale, 2009). None the less, an interrelation of UNC-104 with PPK-2 supports the idea that this kinase is a regulator of membrane trafficking.

The identity of mCherry-PPK-2 particles along dendrites and neurons was not further determined. But since they are distributed to both dendrites and axons and appear to be transported by different motor proteins, it is likely that these particles comprise different vesicle types. Whether or not some of them are DCVs which matured by the passage through the sorting endosome or SV precursors is speculative. However, mCherry-PPK-2 has never been observed at synapses. Thus, if some of these vesicles travel to the nerve terminal, PPK-2 dissociates completely from its cargo during traveling along the process.

4.2.5 Two sites of action for PPK-2

The conclusions drawn from the obtained results of this study revealed two different sites of action for the Type II PIP kinase ortholog PPK-2 in neurons of *C. elegans*, namely the PM and the endomembrane system.

The localization at endomembranes and active transport of PPK-2 to neuronal processes point towards an important function in membrane trafficking from the cell body to nerve terminals, maybe by regulating small pools of PI5P by the conversion to PI4,5P₂ (Figure 54A).

However, PPK-2 appears to have a second function directly at PM (Figure 54B). By its coexpression with the Type I PIP kinase PPK-1, PPK-2 is recruited to the PM of neurons. Mutations of *ppk-2* which do not affect the ability of the protein to localize to endomembranes but to the PM resulting a massive increase of neuropeptide release. This allows the conclusion of increased PKC-1 signaling at the synapse, probably induced by increased PI4,5P₂-levels. Moreover, the interrelation of PPK-2 and PPK-1 supports the hypothesis that PPK-2 act in PI4,5P₂-signaling at the synapse.

To fortify the postulated roles of PPK-2 at the PM as well as at endomembranes further research with a special focus on biochemistry is necessary. An important first aim would be the determination of the catalytic activity of PPK-2 *in vitro*, using a new assay designed by Clarke and Irvine (personal communication). Secondly, the levels of different PIPs in both *ppk-2* mutants need to be analyzed by more dissective methods to identify distinct PIP species. In addition, the interaction of PPK-2 and PPK-1 has to be further examined e.g. by coimmunoprecipitation. The position of *ppk-2* in the pathways of endosomal membrane trafficking and DCV exocytosis at the synapse needs to be analyzed, for example by genetic interaction studies.

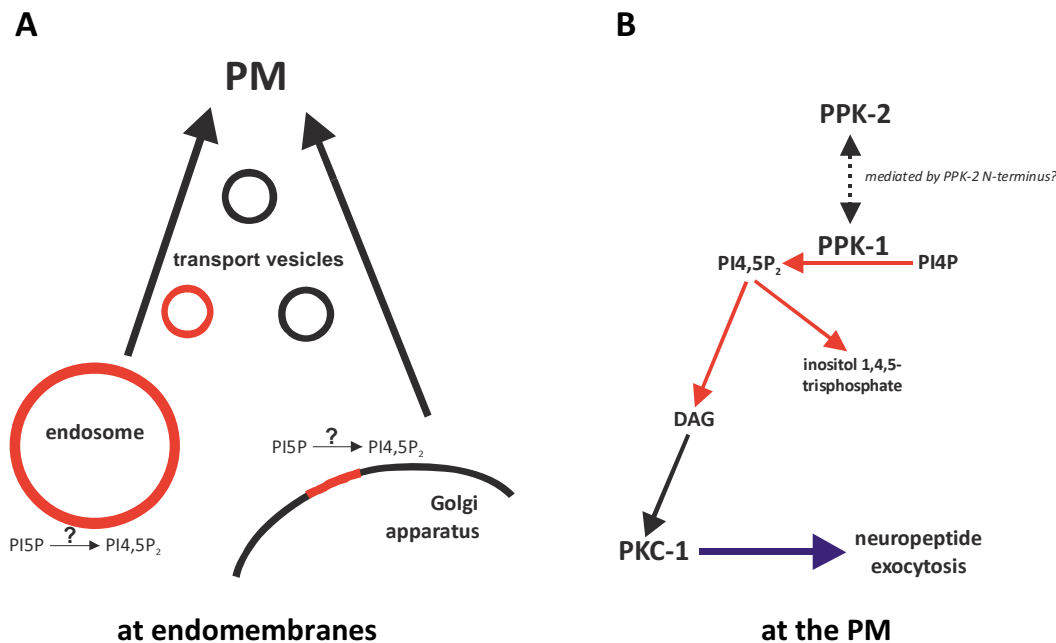


Figure 54 Two sites of action for PPK-2

A, PPK-2 (red) localizes to endosomes, vesicles, and to the Golgi apparatus where it may convert PI5P to PI4,5P₂. Arrows indicate membrane trafficking routes from endosomes and the Golgi to the PM. B, interrelation of PPK-2 with PPK-1 links PPK-2 to the PI4,5P₂-dependent pathway regulating neuropeptide release at the PM.

Two observations of this study leave some room to speculate about additional functions of PPK-2. The small increase of synaptic clusters in *ppk-2* (*ttTi8500*) as well as *ppk-2* (*tm3741*) (section 3.2.3.7) might be due to altered PI4,5P₂ levels at the neuronal PM. Interestingly, PI4,5P₂ is supposed to regulate synapse formation in *C. elegans* (Tanizawa *et al.*, 2006). Furthermore, PI4,5P₂ signaling in the gonade was also described to regulate the brood size of nematodes (Xu *et al.*, 2007) consistent with the observation that *ppk-2* mutants are less fertile compared to wild type (section 3.2.3.6). However, this points towards additional and even more complex functions of PPK-2 which need to be addressed by further research work.

4.3 Novel functions in neuronal membrane trafficking for six PIP-metabolizing enzymes in *C. elegans*

This study focused on the analysis of the Type II PIP kinase ortholog **PPK-2** of *C. elegans* and unveiled its function at the PM and endomembranes of neurons. However, beside PPK-2, **five** additional PIP-metabolizing enzymes have been discovered to act in neuronal membrane trafficking and synaptic function (section 3.1). In the following, two of these five proteins will be briefly discussed.

DAF-18, homologous to the human tumor suppressor PTEN, is supposed to regulate PI4,5P₂ pools at the PM (Maehama, 2007). The knock down of *daf-18* by RNAi resulted in decreased acetylcholine

release at NMJs, what is the first observation linking *daf-18* to synaptic transmission. An initial characterization of *daf-18* mutants revealed some substantial results.

Two different *daf-18* mutant alleles were found to cause decreased acetylcholine release (section 3.3.2.1). Surprisingly, this decreased neurotransmitter release did not restrict the mutants' motility. Quite contrary, *daf-18* mutant animals move significantly faster than wild type animals (section 3.3.2.2). And, although DAF-18 is supposed to produce PI₄,5P₂ by dephosphorylating PI₃,4,5P₃, (Solari *et al.*, 2005) both mutants showed increased instead of decreased PIP₂ levels (section 3.3.2.3).

Since DAF-18 is hypothesized to function at the PM (Solari *et al.*, 2005), it may influence exo- or endocytosis. However, *daf-18* is ubiquitously expressed (Appendix) and is known to indirectly regulate a transcription factor which drives a multitude of different genes (Weinkove *et al.*, 2006). Hence, mutations in *daf-18* are thought to cause a complex and pleiotropic phenotype (Suzuki and Han, 2006) making it difficult to draw conclusions about its function in synaptic transmission.

The second basically characterized protein is the homolog to yeast Sac1p (Foti *et al.*, 2001) annotated as **F30A10.6** in the *C. elegans* genome database. An elaborated comparison of F30A10.6 to its putative homologs in yeast and human revealed that its overall sequence and amino acids contributing to important structural features are highly conserved (section 3.3.1.1). Consequently, the ectopic expression of F30A10.6 in a yeast deletion strain demonstrated that the *C. elegans* phosphatase can substitute Sac1p (section 3.3.1.2). Based on this data, it was concluded that F30A10.6 is a *bona fide* Sac1p. Accordingly, the gene was named *sac-1* (www.wormbase.org, database release WS211).

Sac1p in yeast and Sac1 in mammals, respectively, were described to regulate PI₄P at the membrane of the Golgi apparatus by dephosphorylating its D-4 position (Blagoveshchenskaya and Mayinger, 2009). PI₄P acts as a ligand for coat proteins for vesicle budding and is therefore essential for membrane trafficking from the Golgi to the cell periphery (Godi *et al.*, 2004; D'Angelo *et al.*, 2008). Consistent with this, a F30A10.6/SAC-1 fusion protein localizes to Golgi apparatus in *C. elegans* neurons and to likely Golgi-derived transport vesicles in the axon (section 3.3.1.3). Hence, decreased acetylcholine release resulting from RNAi-mediated knock down may be caused by a misregulation of PI₄P at the Golgi apparatus

A function for a Sac1p homolog in neuronal membrane trafficking was not yet reported. Therefore, the presented results are the first link of the according enzyme function to synaptic function. How F30A10.6/SAC-1 functions in Golgi-derived neuronal membrane trafficking and neurotransmitter release has to be addressed by further studies.

Moreover, two additional PIP phosphatases and one PI 3-kinase have been identified in the here presented RNAi screen. Since they have been not further studied, their functions in neuronal membrane trafficking remain speculative. However, for all three a function in endomembrane transport was suggested.

MTM-3 is hypothesized to localize to the Golgi apparatus and dephosphorylates PI₃P (Robinson and Dixon, 2006; Ma *et al.*, 2008). This phosphoinositide eventually derives from membrane material retrieved from early and sorting endosomes which are enriched PI₃P (Roth, 2004). At endosomal membranes, PI₃P is thought to be generated by **VPS-34**, a PI 3-kinase (Herman *et al.*, 1990; Roggo *et al.*, 2002). For both proteins, this study is the first report linking them to synaptic transmission.

PI3P is the precursor of PI3,5P₂ which accompanies the maturation from early to late endosomes and lysosomes (Dove, 2009). In yeast and mice, the balance between PI3P and PI3,5P₂ is regulated by a PI3,5P₂ 5-phosphatase named Fig4p or Fig4 (Duex *et al.*, 2006a; Chow *et al.*, 2007). The homolog in *C. elegans*, **C34B7.2**, was identified as a regulator of acetylcholine regulator at NMJs. This observation verifies the result of Sieburth *et al.*, 2005, who showed exactly the same phenotype. Taken together, this data provides a direct link of endosomal membrane trafficking and membrane transport to the synapse.

4.4 Concluding remarks

In summary, four PIP phosphatases and two kinases were identified to have a novel function in neuronal membrane trafficking in *C. elegans*. Most of these PIP-metabolizing enzymes are supposed to act rather at the Golgi apparatus or endosomal/lysosomal compartments than at the PM. This highlights the importance of endomembrane trafficking as prerequisite for the correct function of synaptic transmission.

The Type II PIP kinase PPK-2 was shown to act at both the endomembrane system as well as the PM of neurons thereby, demonstrating the complexity of PIP-regulated membrane transport. The here presented study provides essential knowledge for the understanding of this complex network by assigning novel functions to PPK-2 and five additional PIP-metabolizing enzymes in neuronal membrane traffic.

5 Summary

Synaptic transmission relies on the tightly regulated membrane transport between the neuronal cell body and the nerve terminal. Important regulators of membrane trafficking in neurons as well as in other cell types are the phosphorylated derivatives of the phospholipid phosphatidylinositol (PI), phosphatidylinositolphosphates (PIPs). Distinct cellular PIP pools, located at the membranes of different organelles and at the plasma membrane (PM), are maintained by a network of PI/PIP kinases and PIP phosphatases.

An RNAi screen revealed six PIP-metabolizing enzymes to be involved in synaptic transmission of the nematode *Caenorhabditis elegans* (*C. elegans*). Functions in membrane trafficking have been assigned to five of these enzymes. The sole exception was the neuronally expressed *C. elegans* ortholog to mammalian PI5P 4-kinases, PPK-2. Knock down of *ppk-2* by RNAi resulted in the decrease of acetylcholine release at neuromuscular junctions (NMJs). In contrast, two *ppk-2* gain-of-function-alleles showed increased acetylcholine as well as neuropeptide release at NMJs.

The PPK-2 wild type protein localized to endosomal and Golgi membranes in *C. elegans* neurons. When coexpressed with the PM-associated PI4P 5-kinase PPK-1, PPK-2 was not observed to localize exclusively to endomembranes but also to the PM.

Each *ppk-2* gain-of-function-allele was found to encode a mutated PPK-2 protein. The respective coding sequences of these alleles were expressible in neurons and both mutant proteins localized to endomembranes as observed for PPK-2 wild type. When coexpressed with PPK-1, PPK-2 mutant proteins were detected solely at endomembranes but not at the PM. Each of the mutant proteins lacks a substantial part of the aminoterminal, pointing towards that this area of the protein is implicated in its association to the PM.

Beside its localization to endomembrane structures in neuronal cell bodies, particles of PPK-2 wild type protein were observed to localize along dendrites and axons. These particles moved anterograde and retrograde with approximately 0.3 μm per second, pointing towards actively mediated transport. Consistent with this, the localization and motility of PPK-2 particles was dependent on the motor protein kinesin-3. Therefore, a function of PPK-2 in endomembrane trafficking was assumed.

The decreased acetylcholine release of *ppk-2* (RNAi) animals was traced back to the lack of PPK-2 at endomembranes and hence a disfunction in membrane trafficking to the cell periphery. The opposing phenotypes of both *ppk-2* mutants were concluded to result from an additional function of PPK-2.

An important regulator for exocytosis at the synapse is PI4,5P₂. In *C. elegans*, PPK-1 is the major producer of PI4,5P₂ at the PM. The colocalization of PPK-2 with PPK-1 at the PM was assumed to have a regulatory function in neuropeptide release what is consistent with the increased neuropeptide release observed for *ppk-2* mutants. The function of PPK-2 at endomembranes may be still intact in those mutants.

As a conclusion, two sites of actions have been assigned to PPK-2, namely the PM and the endomembrane system.

6 References

- Alberts, B, A. Johnson, J Lewis, M Raff, and P Walter. "Molecular Biology of the Cell (Fifth Edition)." (2008) *Garland Science*, New York, U.S.A.
- Anderson, R A, I V Boronenkov, S D Doughman, J Kunz, and J C Loijens. "Phosphatidylinositol phosphate kinases, a multifaceted family of signaling enzymes." *The Journal of Biological Chemistry* 274, no. 15 (April 9, 1999): 9907-9910.
- Andrews, N W. "Regulated secretion of conventional lysosomes." *Trends in Cell Biology* 10, no. 8 (August 2000): 316-321.
- Arneson, L S, J Kunz, R A Anderson, and L M Traub. "Coupled inositide phosphorylation and phospholipase D activation initiates clathrin-coat assembly on lysosomes." *The Journal of Biological Chemistry* 274, no. 25 (June 18, 1999): 17794-17805.
- Attree, O, I M Olivos, I Okabe, L C Bailey, D L Nelson, R A Lewis, R R McInnes, and R L Nussbaum. "The Lowe's oculocerebrorenal syndrome gene encodes a protein highly homologous to inositol polyphosphate-5-phosphatase." *Nature* 358, no. 6383 (July 16, 1992): 239-242.
- Bai, J, W C Tucker, and E R Chapman. "PIP₂ increases the speed of response of synaptotagmin and steers its membrane-penetration activity toward the plasma membrane." *Nature Structural & Molecular Biology* 11, no. 1 (January 2004): 36-44.
- Bernard, P, and M Couturier. "Cell killing by the F plasmid *CcdB* protein involves poisoning of DNA-topoisomerase II complexes." *Journal of Molecular Biology* 226, no. 3 (August 5, 1992): 735-745.
- Bertani, G. "Studies on lysogenesis. I. The mode of phage liberation by lysogenic *Escherichia coli*." *Journal of Bacteriology* 62, no. 3 (September 1951): 293-300.
- Blagoveshchenskaya, A, and P Mayinger. "SAC1 lipid phosphatase and growth control of the secretory pathway." *Molecular bioSystems* 5, no. 1 (January 2009): 36-42.
- Blankenship, R E. "Photosynthesis: The Light Reactions. Plant Physiology, fourth Edition." (2006): *Sinauer Publishing*, Sunderland, MA, U.S.A.
- Blero, D, B Payrastra, S Schurmans, and C Erneux. "Phosphoinositide phosphatases in a network of signalling reactions." *Pflügers Archiv: European Journal of Physiology* 455, no. 1 (October 2007): 31-44.
- Bolino, A, M Muglia, F L Conforti, E LeGuern, M A Salih, D M Georgiou, K Christodoulou, *et al.* "Charcot-Marie-Tooth type 4B is caused by mutations in the gene encoding myotubularin-related protein-2." *Nature Genetics* 25, no. 1 (May 2000): 17-19.
- Bonanomi, D, F Benfenati, and F Valtorta. "Protein sorting in the synaptic vesicle life cycle." *Progress in Neurobiology* 80, no. 4 (November 2006): 177-217.
- Bonifacino, J S, and L M Traub. "Signals for sorting of transmembrane proteins to endosomes and lysosomes." *Annual Review of Biochemistry* 72 (2003): 395-447.
- Boronenkov, I V, and R A Anderson. "The sequence of phosphatidylinositol-4-phosphate 5-kinase defines a novel family of lipid kinases." *The Journal of Biological Chemistry* 270, no. 7 (February 17, 1995): 2881-2884.

- Boronenkov, I V, J C Loijens, M Umeda, and R A Anderson. "Phosphoinositide signaling pathways in nuclei are associated with nuclear speckles containing pre-mRNA processing factors." *Molecular Biology of the Cell* 9, no. 12 (December 1998): 3547-3560.
- Brenner, S. "The genetics of *Caenorhabditis elegans*." *Genetics* 77, no. 1 (May 1974): 71-94.
- C. elegans* Sequencing Consortium. "Genome sequence of the nematode *C. elegans*: a platform for investigating biology." *Science (New York, N.Y.)* 282, no. 5396 (December 11, 1998): 2012-2018.
- Cantley, L C, and B G Neel. "New insights into tumor suppression: PTEN suppresses tumor formation by restraining the phosphoinositide 3-kinase/AKT pathway." *Proceedings of the National Academy of Sciences of the United States of America* 96, no. 8 (April 13, 1999): 4240-4245.
- Chapin, A, P Correa, M Maguire, and R Kohn. "Synaptic neurotransmission protein UNC-13 affects RNA interference in neurons." *Biochemical and Biophysical Research Communications* 354, no. 4 (March 23, 2007): 1040-1044.
- Cho, M H, and W F Boss. "Transmembrane signaling and phosphoinositides." *Methods in Cell Biology* 49 (1995): 543-554.
- Chow, C Y, Y Zhang, J J Dowling, N Jin, M Adamska, K Shiga, K Szigeti, M E Shy, J Li, X Zhang, J R Lupski, L S Weisman and M H Meisler. "Mutation of FIG4 causes neurodegeneration in the pale tremor mouse and patients with CMT4J." *Nature* 448, no. 7149 (July 5, 2007): 68-72.
- Clague, M J, and O Lorenzo. "The myotubularin family of lipid phosphatases." *Traffic (Copenhagen, Denmark)* 6, no. 12 (December 2005): 1063-1069.
- Clarke, J H, P C Emson, and R F Irvine. "Distribution and neuronal expression of phosphatidylinositol phosphate kinase IIgamma in the mouse brain." *The Journal of Comparative Neurology* 517, no. 3 (November 20, 2009): 296-312.
- Clarke, J, P Emson and R Irvine "Localization of phosphatidylinositol phosphate kinase IIgamma in kidney to a membrane trafficking compartment within specialized cells of the nephron." *American Journal of Physiology. Renal Physiology* 295, no. 5 (November 2008): F1422-1430.
- Clarke, J H, J P Richardson, K A Hinchliffe, and R F Irvine. "Type II PtdInsP kinases: location, regulation and function." *Biochemical Society Symposium*, no. 74 (2007): 149-159.
- Coronas, S, D Ramel, C Pendaries, F Gaits-Iacovoni, H Tronchère, and B Payrastra. "PtdIns5P: a little phosphoinositide with big functions?." *Biochemical Society Symposium*, no. 74 (2007): 117-128.
- Cossart, P, and P J Sansonetti. "Bacterial invasion: the paradigms of enteroinvasive pathogens." *Science (New York, N.Y.)* 304, no. 5668 (April 9, 2004): 242-248.
- Cox, G N, J S Laufer, M Kusch, and R S Edgar. Genetic and phenotypic characterization of roller mutants of *C. elegans*. (February 8, 1980): *Genetics* 95:317-339.
- Cremona, O, and P De Camilli. "Phosphoinositides in membrane traffic at the synapse." *Journal of Cell Science* 114, no. Pt 6 (March 2001): 1041-1052.
- D'Angelo, G, M Vicinanza, A Di Campli, and M A De Matteis. "The multiple roles of PtdIns(4)P - not just the precursor of PtdIns(4,5)P₂." *Journal of Cell Science* 121, no. Pt 12 (June 15, 2008): 1955-1963.

- De Matteis, M A, A Di Campli, and A Godi. "The role of the phosphoinositides at the Golgi complex." *Biochimica Et Biophysica Acta* 1744, no. 3 (July 10, 2005): 396-405.
- Desrivieres, S, F T Cooke, P J Parker, and M N Hall. "MSS4, a phosphatidylinositol-4-phosphate 5-kinase required for organization of the actin cytoskeleton in *Saccharomyces cerevisiae*." *The Journal of Biological Chemistry* 273, no. 25 (June 19, 1998): 15787-15793.
- Di Paolo, G, and P De Camilli. "Phosphoinositides in cell regulation and membrane dynamics." *Nature* 443, no. 7112 (October 12, 2006): 651-657.
- Di Paolo, G, H S Moskowitz, K Gipson, M R Wenk, S Voronov, M Obayashi, R Flavell, R M Fitzsimonds, T A Ryan, and P De Camilli. "Impaired PtdIns(4,5)P₂ synthesis in nerve terminals produces defects in synaptic vesicle trafficking." *Nature* 431, no. 7007 (September 23, 2004): 415-422.
- Dinu, C Z, D B Chrisey, S Diez, and J Howard. "Cellular motors for molecular manufacturing." *Anatomical Record (Hoboken, N.J.: 2007)* 290, no. 10 (October 2007): 1203-1212.
- Donaldson, J G. "Arfs, phosphoinositides and membrane traffic." *Biochemical Society Transactions* 33, no. Pt 6 (December 2005): 1276-1278.
- Doughman, R L, A J Firestone, and R A Anderson. "Phosphatidylinositol phosphate kinases put PI4,5P₂ in its place." *The Journal of Membrane Biology* 194, no. 2 (July 15, 2003): 77-89.
- Doughty, S D, J D Joseph, J Zhang, D J Pagliarini, Y Kim, D Lu, J E Dixon, and P J Casey. "Pharmacological Targeting of the Mitochondrial Phosphatase PTPMT1." *The Journal of Pharmacology and Experimental Therapeutics* (February 18, 2010).
- Dove, S K, K Dong, T Kobayashi, F K Williams, and R H Michell. "Phosphatidylinositol 3,5-bisphosphate and Fab1p/PIKfyve under PIP₂ endo-lysosome function." *The Biochemical Journal* 419, no. 1 (April 1, 2009): 1-13.
- Duex, J E, F Tang, and L S Weisman. "The Vac14p-Fig4p complex acts independently of Vac7p and couples PI3,5P₂ synthesis and turnover." *The Journal of Cell Biology* 172, no. 5 (February 27, 2006a): 693-704.
- Duex, J E, J J Nau, E J Kauffman, and L S Weisman. "Phosphoinositide 5-phosphatase Fig 4p is required for both acute rise and subsequent fall in stress-induced phosphatidylinositol 3,5-bisphosphate levels." *Eukaryotic Cell* 5, no. 4 (April 2006b): 723-731.
- Dupuy, D, Q Li, B Deplancke, M Boxem, T Hao, P Lamesch, R Sequerra, S Bosak, Doucette-Stamm, I A Hope, D E Hill, A Walhout and M Vidal. "A first version of the *Caenorhabditis elegans* Promoterome." *Genome Research* 14, no. 10B (October 2004): 2169-2175.
- Durbin, R. "Studies on the Development and Organisation of the Nervous System of *C.elegans*" (April 1987): PhD thesis, King's College, Cambridge, United Kingdom.
- de Duve, C. "The lysosome turns fifty." *Nature Cell Biology* 7, no. 9 (September 2005): 847-849.
- Dyall, S D, M T Brown, and P J Johnson. "Ancient invasions: from endosymbionts to organelles." *Science (New York, N.Y.)* 304, no. 5668 (April 9, 2004): 253-257.
- Edidin, M. "Lipids on the frontier: a century of cell-membrane bilayers." *Nature Reviews. Molecular Cell Biology* 4, no. 5 (May 2003): 414-418.

- Edwards, S L, N K Charlie, J E Richmond, J Hegermann, S Eimer, and K G Miller. "Impaired dense core vesicle maturation in *Caenorhabditis elegans* mutants lacking Rab2." *The Journal of Cell Biology* 186, no. 6 (September 21, 2009): 881-895.
- Eimer, S, A Gottschalk, M Hengartner, H R Horvitz, J Richmond, W R Schafer, and J-L Bessereau. "Regulation of nicotinic receptor trafficking by the transmembrane Golgi protein UNC-50." *The EMBO Journal* 26, no. 20 (October 17, 2007): 4313-4323.
- Ellgaard, L, and A Helenius. "Quality control in the endoplasmic reticulum." *Nature Reviews. Molecular Cell Biology* 4, no. 3 (March 2003): 181-191.
- Engelman, J A, J Luo, and L C Cantley. "The evolution of phosphatidylinositol 3-kinases as regulators of growth and metabolism." *Nature Reviews. Genetics* 7, no. 8 (August 2006): 606-619.
- Falasca, M, and T Maffucci. "Role of class II phosphoinositide 3-kinase in cell signalling." *Biochemical Society Transactions* 35, no. Pt 2 (April 2007): 211-214.
- Fares, H, and I Greenwald. "Genetic analysis of endocytosis in *Caenorhabditis elegans*: coelomocyte uptake defective mutants." *Genetics* 159, no. 1 (September 2001): 133-145.
- Farsad, K, and P De Camilli. "Neurotransmission and the synaptic vesicle cycle." *The Yale Journal of Biology and Medicine* 75, no. 5-6 (December 2002): 261-284.
- Fauman, E B, and M A Saper. "Structure and function of the protein tyrosine phosphatases." *Trends in Biochemical Sciences* 21, no. 11 (November 1996): 413-417.
- Fire, A, S Xu, M K Montgomery, S A Kostas, S E Driver, and C C Mello. "Potent and specific genetic interference by double-stranded RNA in *Caenorhabditis elegans*." *Nature* 391, no. 6669 (February 19, 1998): 806-811.
- Flanagan, C A, E A Schnieders, A W Emerick, R Kunisawa, A Admon, and J Thorner. "Phosphatidylinositol 4-kinase: gene structure and requirement for yeast cell viability." *Science (New York, N.Y.)* 262, no. 5138 (November 26, 1993): 1444-1448.
- Flanagan, C A, and J Thorner. "Purification and characterization of a soluble phosphatidylinositol 4-kinase from the yeast *Saccharomyces cerevisiae*." *The Journal of Biological Chemistry* 267, no. 33 (November 25, 1992): 24117-24125.
- Foti, M, A Audhya, and S D Emr. "Sac1 lipid phosphatase and Stt4 phosphatidylinositol 4-kinase regulate a pool of phosphatidylinositol 4-phosphate that functions in the control of the actin cytoskeleton and vacuole morphology." *Molecular Biology of the Cell* 12, no. 8 (August 2001): 2396-2411.
- Fruman, D A, R E Meyers, and L C Cantley. "Phosphoinositide kinases." *Annual Review of Biochemistry* 67 (1998): 481-507.
- Gary, J D, T K Sato, C J Stefan, C J Bonangelino, L S Weisman, and S D Emr. "Regulation of Fab1 phosphatidylinositol 3-phosphate 5-kinase pathway by Vac7 protein and Fig4, a polyphosphoinositide phosphatase family member." *Molecular Biology of the Cell* 13, no. 4 (April 2002): 1238-1251.
- Gil, E B, E Malone Link, L X Liu, C D Johnson, and J A Lees. "Regulation of the insulin-like developmental pathway of *Caenorhabditis elegans* by a homolog of the PTEN tumor suppressor gene." *Proceedings of the National Academy of Sciences of the United States of America* 96, no. 6 (March 16, 1999): 2925-2930.

- Glick, B S. "Organization of the Golgi apparatus." *Current Opinion in Cell Biology* 12, no. 4 (August 2000): 450-456.
- Godi, A, A Di Campi, A Konstantakopoulos, G Di Tullio, D R Alessi, G S Kular, T Daniele, P Marra, J M Lucocq, and M A De Matteis. "FAPPs control Golgi-to-cell-surface membrane traffic by binding to ARF and PtdIns(4)P." *Nature Cell Biology* 6, no. 5 (May 2004): 393-404.
- Goldstein, A Y N, X Wang, and T L Schwarz. "Axonal transport and the delivery of pre-synaptic components." *Current Opinion in Neurobiology* 18, no. 5 (October 2008): 495-503.
- Gong, L-W, G Di Paolo, E Diaz, G Cestra, M-E Diaz, M Lindau, P De Camilli, and D Toomre. "Phosphatidylinositol phosphate kinase type I gamma regulates dynamics of large dense-core vesicle fusion." *Proceedings of the National Academy of Sciences of the United States of America* 102, no. 14 (April 5, 2005): 5204-5209.
- Gouaux, E, and R Mackinnon. "Principles of selective ion transport in channels and pumps." *Science (New York, N.Y.)* 310, no. 5753 (December 2, 2005): 1461-1465.
- Gouet, P, X Robert, and E Courcelle. "ESPrpt/ENDscript: Extracting and rendering sequence and 3D information from atomic structures of proteins." *Nucleic Acids Research* 31, no. 13 (July 1, 2003): 3320-3323.
- Grishin, N V. "Phosphatidylinositol phosphate kinase: a link between protein kinase and glutathione synthase folds." *Journal of Molecular Biology* 291, no. 2 (August 13, 1999): 239-247.
- Gruenberg, J, and H Stenmark. "The biogenesis of multivesicular endosomes." *Nature Reviews. Molecular Cell Biology* 5, no. 4 (April 2004): 317-323.
- Guex, N, and M C Peitsch. "SWISS-MODEL and the Swiss-PdbViewer: an environment for comparative protein modeling." *Electrophoresis* 18, no. 15 (December 1997): 2714-2723.
- Guo, J, M R Wenk, L Pellegrini, F Onofri, F Benfenati, and P De Camilli. "Phosphatidylinositol 4-kinase type IIalpha is responsible for the phosphatidylinositol 4-kinase activity associated with synaptic vesicles." *Proceedings of the National Academy of Sciences of the United States of America* 100, no. 7 (April 1, 2003): 3995-4000.
- Guo, S, L E Stolz, S M Lemrow, and J D York. "SAC1-like domains of yeast SAC1, INP52, and INP53 and of human synaptojanin encode polyphosphoinositide phosphatases." *The Journal of Biological Chemistry* 274, no. 19 (May 7, 1999): 12990-12995.
- Hall, D H, and E M Hedgecock. "Kinesin-related gene *unc-104* is required for axonal transport of synaptic vesicles in *C. elegans*." *Cell* 65, no. 5 (May 31, 1991): 837-847.
- Halstead, J R, K Jalink, and N Divecha. "An emerging role for PtdIns(4,5)P₂-mediated signalling in human disease." *Trends in Pharmacological Sciences* 26, no. 12 (December 2005): 654-660.
- Hanahan, D. "Studies on transformation of *Escherichia coli* with plasmids." *Journal of Molecular Biology* 166, no. 4 (June 5, 1983): 557-580.
- Hannah, M J, A A Schmidt, and W B Huttner. "Synaptic vesicle biogenesis." *Annual Review of Cell and Developmental Biology* 15 (1999): 733-798.
- Harris, T W, E Hartweg, H R Horvitz, und E M Jorgensen. "Mutations in synaptojanin disrupt synaptic vesicle recycling." *The Journal of Cell Biology* 150, no. 3 (August 7, 2000): 589-600.

- Hartley, J L, G F Temple, and M A Brasch. "DNA cloning using in vitro site-specific recombination." *Genome Research* 10, no. 11 (November 2000): 1788-1795.
- Hay, J C, P L Fiset, G H Jenkins, K Fukami, T Takenawa, R A Anderson, and T F Martin. "ATP-dependent inositol phosphorylation required for Ca^{2+} -activated secretion." *Nature* 374, no. 6518 (March 9, 1995): 173-177.
- Heck, J N, D L Mellman, K Ling, Y Sun, M P Wagoner, N J Schill, and R A Anderson. "A conspicuous connection: structure defines function for the phosphatidylinositol-phosphate kinase family." *Critical Reviews in Biochemistry and Molecular Biology* 42, no. 1 (February 2007): 15-39.
- Herman, P K, and S D Emr. "Characterization of VPS34, a gene required for vacuolar protein sorting and vacuole segregation in *Saccharomyces cerevisiae*." *Molecular and Cellular Biology* 10, no. 12 (December 1990): 6742-6754.
- Hetzler, M W, T C Walther, and I W Mattaj. "Pushing the envelope: structure, function, and dynamics of the nuclear periphery." *Annual Review of Cell and Developmental Biology* 21 (2005): 347-380.
- Hinchliffe, K A, M L Giudici, A J Letcher, and R F Irvine. "Type I α phosphatidylinositol phosphate kinase associates with the plasma membrane via interaction with type I isoforms." *The Biochemical Journal* 363, no. Pt 3 (May 1, 2002): 563-570.
- Hirokawa, N. "Kinesin and dynein superfamily proteins and the mechanism of organelle transport." *Science (New York, N.Y.)* 279, no. 5350 (January 23, 1998): 519-526.
- Homma, K, S Terui, M Minemura, H Qadota, Y Anraku, Y Kanaho, and Y Ohya. "Phosphatidylinositol-4-phosphate 5-kinase localized on the plasma membrane is essential for yeast cell morphogenesis." *The Journal of Biological Chemistry* 273, no. 25 (June 19, 1998): 15779-15786.
- Hope, I (editor). "*C. elegans*; a practical approach." (2002), Oxford University Press
- Hughes, W E, F T Cooke, and P J Parker. "Sac phosphatase domain proteins." *The Biochemical Journal* 350 Pt 2 (September 1, 2000): 337-352.
- Ishihara, H, Y Shibasaki, N Kizuki, T Wada, Y Yazaki, T Asano, and Y Oka. "Type I phosphatidylinositol-4-phosphate 5-kinases. Cloning of the third isoform and deletion/substitution analysis of members of this novel lipid kinase family." *The Journal of Biological Chemistry* 273, no. 15 (April 10, 1998): 8741-8748.
- Itoh, T, and P De Camilli. "Membrane trafficking: dual-key strategy." *Nature* 429, no. 6988 (May 13, 2004): 141-143.
- Jefferies, H B J, F T Cooke, P Jat, C Boucheron, T Koizumi, M Hayakawa, H Kaizawa, T Ohishi, P Workman, M Waterfield and P Parker. "A selective PIKfyve inhibitor blocks PtdIns(3,5)P₂ production and disrupts endomembrane transport and retroviral budding." *EMBO Reports* 9, no. 2 (February 2008): 164-170.
- Jin, N, C Y Chow, L Liu, S N Zolov, R Bronson, M Davisson, J L Petersen, Y Zhang, S Park, J Duex, D Goldowitz, M Meisler and L Weisman. "VAC14 nucleates a protein complex essential for the acute interconversion of PI3P and PI(3,5)P₂ in yeast and mouse." *The EMBO Journal* 27, no. 24 (December 17, 2008): 3221-3234.
- Kamath, R S, M Martinez-Campos, P Zipperlen, A G Fraser, and J Ahringer. "Effectiveness of specific RNA-mediated interference through ingested double-stranded RNA in *Caenorhabditis elegans*." *Genome Biology* 2, no. 1 (2001): RESEARCH0002.

- Kamath, R S, and J Ahringer. "Genome-wide RNAi screening in *Caenorhabditis elegans*." *Methods (San Diego, Calif.)* 30, no. 4 (August 2003): 313-321.
- Kardon, J R, and R D Vale. "Regulators of the cytoplasmic dynein motor." *Nature Reviews. Molecular Cell Biology* 10, no. 12 (December 2009): 854-865.
- Kennedy, S, D Wang, and G Ruvkun. "A conserved siRNA-degrading RNase negatively regulates RNA interference in *C. elegans*." *Nature* 427, no. 6975 (February 12, 2004): 645-649.
- Klopfenstein, D R, M Tomishige, N Stuurman, and R D Vale. "Role of phosphatidylinositol(4,5)bisphosphate organization in membrane transport by the Unc104 kinesin motor." *Cell* 109, no. 3 (May 3, 2002): 347-358.
- Klopfenstein, D R, and R D Vale. "The lipid binding pleckstrin homology domain in UNC-104 kinesin is necessary for synaptic vesicle transport in *Caenorhabditis elegans*." *Molecular Biology of the Cell* 15, no. 8 (August 2004): 3729-3739.
- König, S, M Hoffmann, A Mosblech, and I Heilmann. "Determination of content and fatty acid composition of unlabeled phosphoinositide species by thin-layer chromatography and gas chromatography." *Analytical Biochemistry* 378, no. 2 (July 15, 2008): 197-201.
- Konrad, G, T Schlecker, F Faulhammer, and P Mayinger. "Retention of the yeast Sac1p phosphatase in the endoplasmic reticulum causes distinct changes in cellular phosphoinositide levels and stimulates microsomal ATP transport." *The Journal of Biological Chemistry* 277, no. 12 (March 22, 2002): 10547-10554.
- Kunz, J, M P Wilson, M Kisseleva, J H Hurley, P W Majerus, and R A Anderson. "The activation loop of phosphatidylinositol phosphate kinases determines signaling specificity." *Molecular Cell* 5, no. 1 (January 2000): 1-11.
- Kunz, J, A Fuelling, L Kolbe, and R A Anderson. "Stereo-specific substrate recognition by phosphatidylinositol phosphate kinases is swapped by changing a single amino acid residue." *The Journal of Biological Chemistry* 277, no. 7 (February 15, 2002): 5611-5619.
- Kyte, J, and R F Doolittle. "A simple method for displaying the hydropathic character of a protein." *Journal of Molecular Biology* 157, no. 1 (May 5, 1982): 105-132.
- Lackner, M R, S J Nurrish, and J M Kaplan. "Facilitation of synaptic transmission by EGL-30 Gqalpha and EGL-8 PLCbeta: DAG binding to UNC-13 is required to stimulate acetylcholine release." *Neuron* 24, no. 2 (October 1999): 335-346.
- Laemmli, U K. "Cleavage of structural proteins during the assembly of the head of bacteriophage T4." *Nature* 227, no. 5259 (August 15, 1970): 680-685.
- Lambert, C, N Léonard, X De Bolle, and E Depiereux. "ESyPred3D: Prediction of proteins 3D structures." *Bioinformatics (Oxford, England)* 18, no. 9 (September 2002): 1250-1256.
- Landy, A. "Dynamic, structural, and regulatory aspects of lambda site-specific recombination." *Annual Review of Biochemistry* 58 (1989): 913-949.
- Laporte, J, L J Hu, C Kretz, J L Mandel, P Kioschis, J F Coy, S M Klauck, A Poustka, and N Dahl. "A gene mutated in X-linked myotubular myopathy defines a new putative tyrosine phosphatase family conserved in yeast." *Nature Genetics* 13, no. 2 (June 1996): 175-182.

- Larkin, M A, G Blackshields, N P Brown, R Chenna, P A McGettigan, H McWilliam, F Valentin, *et al.* "Clustal W and Clustal X version 2.0." *Bioinformatics (Oxford, England)* 23, no. 21 (November 1, 2007): 2947-2948.
- Lecompte, O, O Poch, and J Laporte. "PtdIns5P regulation through evolution: roles in membrane trafficking?." *Trends in Biochemical Sciences* 33, no. 10 (October 2008): 453-460.
- Lee, M C S, E A Miller, J Goldberg, L Orci, and R Schekman. "Bi-directional protein transport between the ER and Golgi." *Annual Review of Cell and Developmental Biology* 20 (2004): 87-123.
- Lemmon, M A, K M Ferguson, and C S Abrams. "Pleckstrin homology domains and the cytoskeleton." *FEBS Letters* 513, no. 1 (February 20, 2002): 71-76.
- Leslie, N R, and C P Downes. "PTEN function: how normal cells control it and tumour cells lose it." *The Biochemical Journal* 382, no. Pt 1 (August 15, 2004): 1-11.
- Lewis, J A, C H Wu, H Berg, and J H Levine. "The genetics of levamisole resistance in the nematode *Caenorhabditis elegans*." *Genetics* 95, no. 4 (August 1980): 905-928.
- Li, J, C Yen, D Liaw, K Podsypanina, S Bose, S I Wang, J Puc, *et al.* "PTEN, a putative protein tyrosine phosphatase gene mutated in human brain, breast, and prostate cancer." *Science (New York, N.Y.)* 275, no. 5308 (March 28, 1997): 1943-1947.
- Linassier, C, L K MacDougall, J Domin, and M D Waterfield. "Molecular cloning and biochemical characterization of a *Drosophila* phosphatidylinositol-specific phosphoinositide 3-kinase." *The Biochemical Journal* 321 (Pt 3) (February 1, 1997): 849-856.
- Locke, C, K Berry, B Kautu, K Lee, K Caldwell, and G Caldwell. "Paradigms for pharmacological characterization of *C. elegans* synaptic transmission mutants." *Journal of Visualized Experiments: JoVE*, no. 18 (2008).
- Loijens, J C, and R A Anderson. "Type I phosphatidylinositol-4-phosphate 5-kinases are distinct members of this novel lipid kinase family." *The Journal of Biological Chemistry* 271, no. 51 (December 20, 1996): 32937-32943.
- Lopez-Illasaca, M, P Crespo, P G Pellici, J S Gutkind, and R Wetzker. "Linkage of G protein-coupled receptors to the MAPK signaling pathway through PI 3-kinase gamma." *Science (New York, N.Y.)* 275, no. 5298 (January 17, 1997): 394-397.
- Lorenzo, O, S Urbé, and M J Clague. "Analysis of phosphoinositide binding domain properties within the myotubularin-related protein MTMR3." *Journal of Cell Science* 118, no. Pt 9 (May 1, 2005): 2005-2012.
- L, Martin. "Structure and function of the Lowe syndrome protein OCRL1." *Traffic (Copenhagen, Denmark)* 6, no. 9 (September 2005): 711-719.
- Ma, J, F Zeng, W T Ho, L Teng, Q Li, X Fu, and Z J Zhao. "Characterization and functional studies of a FYVE domain-containing phosphatase in *C. elegans*." *Journal of Cellular Biochemistry* 104, no. 5 (August 1, 2008): 1843-1852.
- Maehama, T, and J E Dixon. "PTEN: a tumour suppressor that functions as a phospholipid phosphatase." *Trends in Cell Biology* 9, no. 4 (April 1999): 125-128.
- Maehama, T, and J E Dixon. "The tumor suppressor, PTEN/MMAC1, dephosphorylates the lipid second messenger, phosphatidylinositol 3,4,5-trisphosphate." *The Journal of Biological Chemistry* 273, no. 22 (May 29, 1998): 13375-13378.

- Maehama, Tomohiko. "PTEN: its deregulation and tumorigenesis." *Biological & Pharmaceutical Bulletin* 30, no. 9 (September 2007): 1624-1627.
- Mahoney, T R, S Luo, and M L Nonet. "Analysis of synaptic transmission in *Caenorhabditis elegans* using an aldicarb-sensitivity assay." *Nature Protocols* 1, no. 4 (2006): 1772-1777.
- Majerus, P W, and J D York. "Phosphoinositide phosphatases and disease." *Journal of Lipid Research* 50 Suppl (April 2009): S249-254.
- Marsh, D J, V Coulon, K L Lunetta, P Rocca-Serra, P L Dahia, Z Zheng, D Liaw, *et al.* "Mutation spectrum and genotype-phenotype analyses in Cowden disease and Bannayan-Zonana syndrome, two hamartoma syndromes with germline PTEN mutation." *Human Molecular Genetics* 7, no. 3 (March 1998): 507-515.
- Martin, T F. "PI(4,5)P₂ regulation of surface membrane traffic." *Current Opinion in Cell Biology* 13, no. 4 (August 2001): 493-499.
- Maupas. "Modes et formes de reproduction des nematodes." (1900): *Archives de Zoologie Experimentale et Generale* 8: 463-624.
- Maxfield, F R, and T E McGraw. "Endocytic recycling." *Nature Reviews. Molecular Cell Biology* 5, no. 2 (February 2004): 121-132.
- McPherson, P S, E P Garcia, V I Slepnev, C David, X Zhang, D Grabs, W S Sossin, R Bauerfeind, Y Nemoto, and P De Camilli. "A presynaptic inositol-5-phosphatase." *Nature* 379, no. 6563 (January 25, 1996): 353-357.
- Mellman, I. "Endocytosis and molecular sorting." *Annual Review of Cell and Developmental Biology* 12 (1996): 575-625.
- Mellman, I, and G Warren. "The road taken: past and future foundations of membrane traffic." *Cell* 100, no. 1 (January 7, 2000): 99-112.
- Mello, C C, J M Kramer, D Stinchcomb, and V Ambros. "Efficient gene transfer in *C.elegans*: extrachromosomal maintenance and integration of transforming sequences." *The EMBO Journal* 10, no. 12 (December 1991): 3959-3970.
- Merlot, S, R Meili, D J Pagliarini, T Maehama, J E Dixon, and R A Firtel. "A PTEN-related 5-phosphatidylinositol phosphatase localized in the Golgi." *The Journal of Biological Chemistry* 278, no. 41 (October 10, 2003): 39866-39873.
- Michell, Robert H. "Inositol derivatives: evolution and functions." *Nature Reviews. Molecular Cell Biology* 9, no. 2 (February 2008): 151-161.
- Michell, R H, V L Heath, M A Lemmon, and S K Dove. "Phosphatidylinositol 3,5-bisphosphate: metabolism and cellular functions." *Trends in Biochemical Sciences* 31, no. 1 (January 2006): 52-63.
- Miki, T, J A Park, K Nagao, N Murayama, and T Horiuchi. "Control of segregation of chromosomal DNA by sex factor F in *Escherichia coli*. Mutants of DNA gyrase subunit A suppress letD (*ccdB*) product growth inhibition." *Journal of Molecular Biology* 225, no. 1 (May 5, 1992): 39-52.
- Mitoma, J, and A Ito. "The carboxy-terminal 10 amino acid residues of cytochrome b5 are necessary for its targeting to the endoplasmic reticulum." *The EMBO Journal* 11, no. 11 (November 1992): 4197-4203.

- Munro, S. "Organelle identity and the organization of membrane traffic." *Nature Cell Biology* 6, no. 6 (June 2004): 469-472.
- Myers, M P, I Pass, I H Batty, J Van der Kaay, J P Stolarov, B A Hemmings, M H Wigler, C P Downes, and N K Tonks. "The lipid phosphatase activity of PTEN is critical for its tumor suppressor function." *Proceedings of the National Academy of Sciences of the United States of America* 95, no. 23 (November 10, 1998): 13513-13518.
- Nemoto, Y, B G Kearns, M R Wenk, H Chen, K Mori, J G Alb, P De Camilli, and V A Bankaitis. "Functional characterization of a mammalian Sac1 and mutants exhibiting substrate-specific defects in phosphoinositide phosphatase activity." *The Journal of Biological Chemistry* 275, no. 44 (November 3, 2000): 34293-34305.
- Nicot, A-S, H Fares, B Payraastre, A D Chisholm, M Labouesse, and J Laporte. "The phosphoinositide kinase PIKfyve/Fab1p regulates terminal lysosome maturation in *Caenorhabditis elegans*." *Molecular Biology of the Cell* 17, no. 7 (July 2006): 3062-3074.
- Niebuhr, K, S Giuriato, T Pedron, D J Philpott, F Gaits, J Sable, M P Sheetz, C Parsot, P J Sansonetti, and B Payraastre. "Conversion of PtdIns(4,5)P₂ into PtdIns(5)P by the *S.flexneri* effector IpgD reorganizes host cell morphology." *The EMBO Journal* 21, no. 19 (October 1, 2002): 5069-5078.
- Nishikawa, K, A Toker, K Wong, P A Marignani, F J Johannes, and L C Cantley. "Association of protein kinase Cmu with type II phosphatidylinositol 4-kinase and type I phosphatidylinositol-4-phosphate 5-kinase." *The Journal of Biological Chemistry* 273, no. 36 (September 4, 1998): 23126-23133.
- Norris, F A, R C Atkins, and P W Majerus. "The cDNA cloning and characterization of inositol polyphosphate 4-phosphatase type II. Evidence for conserved alternative splicing in the 4-phosphatase family." *The Journal of Biological Chemistry* 272, no. 38 (September 19, 1997): 23859-23864.
- Nystuen, A, M E Legare, L D Shultz, and W N Frankel. "A null mutation in inositol polyphosphate 4-phosphatase type I causes selective neuronal loss in weebie mutant mice." *Neuron* 32, no. 2 (October 25, 2001): 203-212.
- Ogg, S, and G Ruvkun. "The *C. elegans* PTEN homolog, DAF-18, acts in the insulin receptor-like metabolic signaling pathway." *Molecular Cell* 2, no. 6 (December 1998): 887-893.
- Ooms, L M, K A Horan, P Rahman, G Seaton, R Gurung, D S Kethesparan, and C A Mitchell. "The role of the inositol polyphosphate 5-phosphatases in cellular function and human disease." *The Biochemical Journal* 419, no. 1 (April 1, 2009): 29-49.
- Parker, P J. "The ubiquitous phosphoinositides." *Biochemical Society Transactions* 32, no. Pt 6 (December 2004): 893-898.
- Parrish, W R, C J Stefan, and S D Emr. "Essential role for the myotubularin-related phosphatase Ymr1p and the synaptojanin-like phosphatases Sjl2p and Sjl3p in regulation of phosphatidylinositol 3-phosphate in yeast." *Molecular Biology of the Cell* 15, no. 8 (August 2004): 3567-3579.
- Paschinger, K, M Hackl, Mn Gutternigg, D Kretschmer-Lubich, U Stemmer, V Jantsch, G Lochnit, and I B H Wilson. "A deletion in the golgi alpha-mannosidase II gene of *Caenorhabditis elegans* results in unexpected non-wild-type N-glycan structures." *The Journal of Biological Chemistry* 281, no. 38 (September 22, 2006): 28265-28277.
- Perera, I Y, A J Davis, D Galanopoulou, Y J Im, and W F Boss. "Characterization and comparative analysis of Arabidopsis phosphatidylinositol phosphate 5-kinase 10 reveals differences in Arabidopsis and human phosphatidylinositol phosphate kinases." *FEBS Letters* 579, no. 16 (June 20, 2005): 3427-3432.

- Rameh, L E, K F Tolias, B C Duckworth, and L C Cantley. "A new pathway for synthesis of phosphatidylinositol-4,5-bisphosphate." *Nature* 390, no. 6656 (November 13, 1997): 192-196.
- Rao, V D, S Misra, I V Boronenkov, R A Anderson, and J H Hurley. "Structure of type IIbeta phosphatidylinositol phosphate kinase: a protein kinase fold flattened for interfacial phosphorylation." *Cell* 94, no. 6 (September 18, 1998): 829-839.
- Raucher, D, T Stauffer, W Chen, K Shen, S Guo, J D York, M P Sheetz, and T Meyer. "Phosphatidylinositol 4,5-bisphosphate functions as a second messenger that regulates cytoskeleton-plasma membrane adhesion." *Cell* 100, no. 2 (January 21, 2000): 221-228.
- Richmond, J E, and K S Broadie. "The synaptic vesicle cycle: exocytosis and endocytosis in *Drosophila* and *C. elegans*." *Current Opinion in Neurobiology* 12, no. 5 (October 2002): 499-507.
- Rivas, M P, B G Kearns, Z Xie, S Guo, M C Sekar, K Hosaka, S Kagiwada, J D York, and V A Bankaitis. "Pleiotropic alterations in lipid metabolism in yeast *sac1* mutants: relationship to "bypass Sec14p" and inositol auxotrophy." *Molecular Biology of the Cell* 10, no. 7 (July 1999): 2235-2250.
- Robinson, F L, and J E Dixon. "Myotubularin phosphatases: policing 3-phosphoinositides." *Trends in Cell Biology* 16, no. 8 (August 2006): 403-412.
- Rodriguez-Viciano, P, P H Warne, A Khwaja, B M Marte, D Pappin, P Das, M D Waterfield, A Ridley, and J Downward. "Role of phosphoinositide 3-OH kinase in cell transformation and control of the actin cytoskeleton by Ras." *Cell* 89, no. 3 (May 2, 1997): 457-467.
- Roggo, L, V Bernard, A L Kovacs, A M Rose, F Savoy, M Zetka, M P Wymann, and F Müller. "Membrane transport in *Caenorhabditis elegans*: an essential role for VPS34 at the nuclear membrane." *The EMBO Journal* 21, no. 7 (April 2, 2002): 1673-1683.
- Rohde, H M, F Y Cheong, G Konrad, K Paiha, P Mayinger, and G Boehmelt. "The human phosphatidylinositol phosphatase SAC1 interacts with the coatamer I complex." *The Journal of Biological Chemistry* 278, no. 52 (December 26, 2003): 52689-52699.
- Rohrbough, J, and K Broadie. "Lipid regulation of the synaptic vesicle cycle." *Nature Reviews. Neuroscience* 6, no. 2 (February 2005): 139-150.
- Roth, Michael G. "Phosphoinositides in constitutive membrane traffic." *Physiological Reviews* 84, no. 3 (July 2004): 699-730.
- Rouillé, Y, W Rohn, and B Hoflack. "Targeting of lysosomal proteins." *Seminars in Cell & Developmental Biology* 11, no. 3 (June 2000): 165-171.
- Saiki, R K, D H Gelfand, S Stoffel, S J Scharf, R Higuchi, G T Horn, K B Mullis, and H A Erlich. "Primer-directed enzymatic amplification of DNA with a thermostable DNA polymerase." *Science (New York, N.Y.)* 239, no. 4839 (January 29, 1988): 487-491.
- Santarius, M, C H Lee, and R A Anderson. "Supervised membrane swimming: small G-protein lifeguards regulate PIPK signalling and monitor intracellular PtdIns(4,5)P₂ pools." *The Biochemical Journal* 398, no. 1 (August 15, 2006): 1-13.
- Saraste, M. "Oxidative phosphorylation at the fin de siècle." *Science (New York, N.Y.)* 283, no. 5407 (March 5, 1999): 1488-1493.

- Sbrissa, D, O C Ikonov, H Fenner, and A Shisheva. "ArPIKfyve homomeric and heteromeric interactions scaffold PIKfyve and Sac3 in a complex to promote PIKfyve activity and functionality." *Journal of Molecular Biology* 384, no. 4 (December 26, 2008): 766-779.
- Schmid, A C, H M Wise, C A Mitchell, R Nussbaum, and R Woscholski. "Type II phosphoinositide 5-phosphatases have unique sensitivities towards fatty acid composition and head group phosphorylation." *FEBS Letters* 576, no. 1-2 (October 8, 2004): 9-13.
- Seaman, M N J. "Endosome protein sorting: motifs and machinery." *Cellular and Molecular Life Sciences: CMLS* 65, no. 18 (September 2008): 2842-2858.
- Senderek, J, C Bergmann, V T Ramaekers, E Nelis, G Bernert, A Makowski, S Züchner, P De Jonghe, K Zerres and J M Schröder. "Mutations in the ganglioside-induced differentiation-associated protein-1 (GDAP1) gene in intermediate type autosomal recessive Charcot-Marie-Tooth neuropathy." *Brain: A Journal of Neurology* 126, no. Pt 3 (March 2003): 642-649.
- Sherman, Fred. "Getting started with yeast." *Methods in Enzymology* 350 (2002): 3-41.
- Shibasaki, Y, H Ishihara, N Kizuki, T Asano, Y Oka, and Y Yazaki. "Massive actin polymerization induced by phosphatidylinositol-4-phosphate 5-kinase in vivo." *The Journal of Biological Chemistry* 272, no. 12 (March 21, 1997): 7578-7581.
- Shisheva, A. "PIKfyve: Partners, significance, debates and paradoxes." *Cell Biology International* 32, no. 6 (June 2008): 591-604.
- Sidahmed, A M E, and B Wilkie. "Endogenous antiviral mechanisms of RNA interference: a comparative biology perspective." *Methods in Molecular Biology (Clifton, N.J.)* 623 (2010): 3-19.
- Sieburth, D, Q Ch'ng, M Dybbs, M Tavazoie, S Kennedy, D Wang, D Dupuy, J Rual, D Hill, M Vidal, G Ruvkun and J Kaplan. "Systematic analysis of genes required for synapse structure and function." *Nature* 436, no. 7050 (July 28, 2005): 510-517.
- Sieburth, D, J M Madison, and J M Kaplan. "PKC-1 regulates secretion of neuropeptides." *Nature Neuroscience* 10, no. 1 (January 2007): 49-57.
- Solari, F, A Bourbon-Piffaut, I Mase, B Payrastra, A M-L Chan, and M Billaud. "The human tumour suppressor PTEN regulates longevity and dauer formation in *Caenorhabditis elegans*." *Oncogene* 24, no. 1 (January 6, 2005): 20-27.
- Spang, A. "The life cycle of a transport vesicle." *Cellular and Molecular Life Sciences: CMLS* 65, no. 18 (September 2008): 2781-2789.
- Speese, S, M Petrie, K Schuske, M Ailion, K Ann, K Iwasaki, E M Jorgensen, and T F J Martin. "UNC-31 (CAPS) is required for dense-core vesicle but not synaptic vesicle exocytosis in *Caenorhabditis elegans*." *The Journal of Neuroscience: The Official Journal of the Society for Neuroscience* 27, no. 23 (June 6, 2007): 6150-6162.
- Stahelin, R V. "Lipid binding domains: more than simple lipid effectors." *Journal of Lipid Research* 50 Suppl (April 2009): S299-304.
- Stenmark, H, and R Aasland. "FYVE-finger proteins--effectors of an inositol lipid." *Journal of Cell Science* 112 (Pt 23) (December 1999): 4175-4183.

- Stenmark, H, and D J Gilooley. "Intracellular trafficking and turnover of phosphatidylinositol 3-phosphate." *Seminars in Cell & Developmental Biology* 12, no. 2 (April 2001): 193-199.
- Stenzel, I, T Ischebeck, S König, A Hołubowska, M Sporysz, B Hause, und I Heilmann. "The type B phosphatidylinositol-4-phosphate 5-kinase 3 is essential for root hair formation in *Arabidopsis thaliana*." *The Plant Cell* 20, no. 1 (Januar 2008): 124-141.
- Stopkova, P, J Vevera, I Paclt, I Zukov, and H M Lachman. "Analysis of SYNJ1, a candidate gene for 21q22 linked bipolar disorder: a replication study." *Psychiatry Research* 127, no. 1-2 (June 30, 2004): 157-161.
- Stoyanova, S, G Bulgarelli-Leva, C Kirsch, T Hanck, R Klinger, R Wetzker, and M P Wymann. "Lipid kinase and protein kinase activities of G-protein-coupled phosphoinositide 3-kinase gamma: structure-activity analysis and interactions with wortmannin." *The Biochemical Journal* 324 (Pt 2) (June 1, 1997): 489-495.
- Sudhof, T C. "The synaptic vesicle cycle." *Annual Review of Neuroscience* 27 (2004): 509-547.
- Sulston, J E, and H R Horvitz. "Post-embryonic cell lineages of the nematode, *Caenorhabditis elegans*." *Developmental Biology* 56, no. 1 (March 1977): 110-156.
- Sumakovic, M, J Hegemann, L Luo, S J Husson, K Schwarze, C Olendrowitz, L Schoofs, J Richmond, and S Eimer. "UNC-108/RAB-2 and its effector RIC-19 are involved in dense core vesicle maturation in *Caenorhabditis elegans*." *The Journal of Cell Biology* 186, no. 6 (September 21, 2009): 897-914.
- Suzuki, Y, and M Han. "Genetic redundancy masks diverse functions of the tumor suppressor gene PTEN during *C. elegans* development." *Genes & Development* 20, no. 4 (February 15, 2006): 423-428.
- Tabara, H, A Grishok, and C C Mello. "RNAi in *C. elegans*: soaking in the genome sequence." *Science (New York, N.Y.)* 282, no. 5388 (October 16, 1998): 430-431.
- Tanizawa, Y, A Kuhara, H Inada, E Kodama, T Mizuno, and I Mori. "Inositol monophosphatase regulates localization of synaptic components and behavior in the mature nervous system of *C. elegans*." *Genes & Development* 20, no. 23 (December 1, 2006): 3296-3310.
- Timmons, L, and A Fire. "Specific interference by ingested dsRNA." *Nature* 395, no. 6705 (October 29, 1998): 854.
- Tolias, K F, L E Rameh, H Ishihara, Y Shibasaki, J Chen, G D Prestwich, L C Cantley, and C L Carpenter. "Type I phosphatidylinositol-4-phosphate 5-kinases synthesize the novel lipids phosphatidylinositol 3,5-bisphosphate and phosphatidylinositol 5-phosphate." *The Journal of Biological Chemistry* 273, no. 29 (July 17, 1998): 18040-18046.
- Traub, L M, and S Kornfeld. "The trans-Golgi network: a late secretory sorting station." *Current Opinion in Cell Biology* 9, no. 4 (August 1997): 527-533.
- Tronchère, H, J Laporte, C Pendaries, C Chaussade, L Liaubet, L Pirola, J-Ls Mandel, and B Payrastre. "Production of phosphatidylinositol 5-phosphate by the phosphoinositide 3-phosphatase myotubularin in mammalian cells." *The Journal of Biological Chemistry* 279, no. 8 (February 20, 2004): 7304-7312.
- Ungewickell, A, C Hugge, M Kisseleva, S-C Chang, J Zou, Y Feng, E E Galyov, M Wilson, and P W Majerus. "The identification and characterization of two phosphatidylinositol-4,5-bisphosphate 4-phosphatases." *Proceedings of the National Academy of Sciences of the United States of America* 102, no. 52 (December 27, 2005): 18854-18859.

- Vanhaesebroeck, B, S J Leever, K Ahmadi, J Timms, R Katso, P C Driscoll, R Woscholski, P J Parker, and M D Waterfield. "Synthesis and function of 3-phosphorylated inositol lipids." *Annual Review of Biochemistry* 70 (2001): 535-602.
- Vanhaesebroeck, B, M J Welham, K Kotani, R Stein, P H Warne, M J Zvelebil, K Higashi, S Volinia, J Downward, and M D Waterfield. "P110delta, a novel phosphoinositide 3-kinase in leukocytes." *Proceedings of the National Academy of Sciences of the United States of America* 94, no. 9 (April 29, 1997): 4330-4335.
- Vicinanza, M, G D'Angelo, A Di Campli, and M A De Matteis. "Phosphoinositides as regulators of membrane trafficking in health and disease." *Cellular and Molecular Life Sciences: CMLS* 65, no. 18 (September 2008): 2833-2841.
- Vicinanza, M, G D'Angelo, A Di Campli, and M A De Matteis. "Function and dysfunction of the PI system in membrane trafficking." *The EMBO Journal* 27, no. 19 (October 8, 2008): 2457-2470.
- Voeltz, G K, M M Rolls, and T A Rapoport. "Structural organization of the endoplasmic reticulum." *EMBO Reports* 3, no. 10 (October 2002): 944-950.
- Volinia, S, R Dhand, B Vanhaesebroeck, L K MacDougall, R Stein, M J Zvelebil, J Domin, C Panaretou, and M D Waterfield. "A human phosphatidylinositol 3-kinase complex related to the yeast Vps34p-Vps15p protein sorting system." *The EMBO Journal* 14, no. 14 (July 17, 1995): 3339-3348.
- Volpicelli-Daley, L, and P De Camilli. "Phosphoinositides' link to neurodegeneration." *Nature Medicine* 13, no. 7 (July 2007): 784-786.
- Wach, A, A Brachat, R Pöhlmann, and P Philippsen. "New heterologous modules for classical or PCR-based gene disruptions in *Saccharomyces cerevisiae*." *Yeast (Chichester, England)* 10, no. 13 (December 1994): 1793-1808.
- Wang, D, S Kennedy, D Conte, J K Kim, H W Gabel, R S Kamath, C C Mello, and G Ruvkun. "Somatic misexpression of germline P granules and enhanced RNA interference in retinoblastoma pathway mutants." *Nature* 436, no. 7050 (July 28, 2005): 593-597.
- Weinkove, D, M Bastiani, T A M Chessa, D Joshi, L Hauth, F T Cooke, N Divecha, and K Schuske. "Overexpression of PPK-1, the *Caenorhabditis elegans* Type I PIP kinase, inhibits growth cone collapse in the developing nervous system and causes axonal degeneration in adults." *Developmental Biology* 313, no. 1 (January 1, 2008): 384-397.
- Weinkove, D, J R Halstead, D Gems, and N Divecha. "Long-term starvation and ageing induce AGE-1/PI 3-kinase-dependent translocation of DAF-16/FOXO to the cytoplasm." *BMC Biology* 4 (2006): 1.
- Wenk, M R, L Pellegrini, V A Klenchin, G Di Paolo, S Chang, L Daniell, M Arioka, T F Martin, and P De Camilli. "PIP kinase Igamma is the major PI(4,5)P(2) synthesizing enzyme at the synapse." *Neuron* 32, no. 1 (October 11, 2001): 79-88.
- Wenk, M R, and P De Camilli. "Protein-lipid interactions and phosphoinositide metabolism in membrane traffic: insights from vesicle recycling in nerve terminals." *Proceedings of the National Academy of Sciences of the United States of America* 101, no. 22 (June 1, 2004): 8262-8269.
- Whiteford, C C, C A Brearley, and E T Ulug. "Phosphatidylinositol 3,5-bisphosphate defines a novel PI 3-kinase pathway in resting mouse fibroblasts." *The Biochemical Journal* 323 (Pt 3) (May 1, 1997): 597-601.

- Williams, S N, C J Locke, A L Braden, K A Caldwell, and G A Caldwell. "Epileptic-like convulsions associated with LIS-1 in the cytoskeletal control of neurotransmitter signaling in *Caenorhabditis elegans*." *Human Molecular Genetics* 13, no. 18 (September 15, 2004): 2043-2059.
- Wong, K, and L C Cantley. "Cloning and characterization of a human phosphatidylinositol 4-kinase." *The Journal of Biological Chemistry* 269, no. 46 (November 18, 1994): 28878-28884.
- Wong, K, Meyers ddR, and L C Cantley. "Subcellular locations of phosphatidylinositol 4-kinase isoforms." *The Journal of Biological Chemistry* 272, no. 20 (May 16, 1997): 13236-13241.
- Wu, H, Y Yan, and J M Backer. "Regulation of class IA PI3Ks." *Biochemical Society Transactions* 35, no. Pt 2 (April 2007): 242-244.
- Wurmser, A E, J D Gary, and S D Emr. "Phosphoinositide 3-kinases and their FYVE domain-containing effectors as regulators of vacuolar/lysosomal membrane trafficking pathways." *The Journal of Biological Chemistry* 274, no. 14 (April 2, 1999): 9129-9132.
- Xu, X, H Guo, D L Wycuff, and M Lee. "Role of phosphatidylinositol-4-phosphate 5' kinase (ppk-1) in ovulation of *Caenorhabditis elegans*." *Experimental Cell Research* 313, no. 11 (July 1, 2007): 2465-2475.
- Xue, Y, H Fares, B Grant, Z Li, A M Rose, S G Clark, and E Y Skolnik. "Genetic analysis of the myotubularin family of phosphatases in *Caenorhabditis elegans*." *The Journal of Biological Chemistry* 278, no. 36 (September 5, 2003): 34380-34386.
- Yonekawa, Y, A Harada, Y Okada, T Funakoshi, Y Kanai, Y Takei, S Terada, T Noda, and N Hirokawa. "Defect in synaptic vesicle precursor transport and neuronal cell death in KIF1A motor protein-deficient mice." *The Journal of Cell Biology* 141, no. 2 (April 20, 1998): 431-441.
- Yuan, Y, X Gao, N Guo, H Zhang, Z Xie, M Jin, B Li, L Yu, and N Jing. "rSac3, a novel Sac domain phosphoinositide phosphatase, promotes neurite outgrowth in PC12 cells." *Cell Research* 17, no. 11 (November 2007): 919-932.
- Zahn, T R, J K Angleson, M A MacMorris, E Domke, J F Hutton, C Schwartz, and J C Hutton. "Dense core vesicle dynamics in *Caenorhabditis elegans* neurons and the role of kinesin UNC-104." *Traffic (Copenhagen, Denmark)* 5, no. 7 (July 2004): 544-559.
- Zhang, X, J C Loijens, I V Boronenkov, G J Parker, F A Norris, J Chen, O Thum, G D Prestwich, P W Majerus, and R A Anderson. "Phosphatidylinositol-4-phosphate 5-kinase isozymes catalyze the synthesis of 3-phosphate-containing phosphatidylinositol signaling molecules." *The Journal of Biological Chemistry* 272, no. 28 (July 11, 1997): 17756-17761.
- Zhao, H, and M L Nonet. "A conserved mechanism of synaptogyrin localization." *Molecular Biology of the Cell* 12, no. 8 (August 2001): 2275-2289.
- Zheng, Y, J Wildonger, B Ye, Y Zhang, A Kita, S H Younger, S Zimmerman, L Y Jan, and Y N Jan. "Dynein is required for polarized dendritic transport and uniform microtubule orientation in axons." *Nature Cell Biology* 10, no. 10 (October 2008): 1172-1180.
- Zhou, H M, I Brust-Mascher, and J M Scholey. "Direct visualization of the movement of the monomeric axonal transport motor UNC-104 along neuronal processes in living *Caenorhabditis elegans*." *The Journal of Neuroscience: The Official Journal of the Society for Neuroscience* 21, no. 11 (June 1, 2001): 3749-3755.

Zoncu, R, R M Perera, R Sebastian, F Nakatsu, H Chen, T Balla, G Ayala, D Toomre, and P V De Camilli. "Loss of endocytic clathrin-coated pits upon acute depletion of phosphatidylinositol 4,5-bisphosphate." *Proceedings of the National Academy of Sciences of the United States of America* 104, no. 10 (March 6, 2007): 3793-3798.

7 Figures and tables

List of figures

	<i>page</i>
Figure 1	12
Figure 2	14
Figure 3	15
Figure 4	17
Figure 5	20
Figure 6	26
Figure 7	31
Figure 8	32
Figure 9	32
Figure 10	52
Figure 11	55
Figure 12	56
Figure 13	57
Figure 14	58
Figure 15	59
Figure 16	61
Figure 17	62
Figure 18	63
Figure 19	64
Figure 20	65
Figure 21	65
Figure 22	66
Figure 23	67
Figure 24	68
Figure 25	69
Figure 26	70
Figure 27	71
Figure 28	72
Figure 29	73
Figure 30	73
Figure 31	74
Figure 32	74
Figure 33	75
Figure 34	76
Figure 35	77
Figure 36	78
Figure 37	79
Figure 38	80
Figure 39	82
Figure 40	83
Figure 41	84
Figure 42	85
Figure 43	86
Figure 44	88

Figure 45	Localization of mCherry-PPK-2 and FYVE-GFP in <i>unc-104</i> (<i>e1265</i>)	89
Figure 46	<i>In vitro</i> kinase assay of GST-PPK-2	90
Figure 47	Hydrophobicity plots of <i>C. elegans</i> F30A10.6 and homologs	91
Figure 48	<i>C. elegans</i> F30A10.6 is homologous to PIP phosphatases of <i>H. sapiens</i> and yeast	93
Figure 49	F30A10.6 can substitute for Sac1p in yeast	95
Figure 50	Subcellular localization of F30A10.6 in neurons	96
Figure 51	Aldicarb assay of <i>daf-18</i> mutants	97
Figure 52	Cumulative distribution of velocities displayed by <i>daf-18</i> mutants	98
Figure 53	The PIP ₂ levels of <i>daf-18</i> mutants are increased compared to wild type	99
Figure 54	Two sites of action for PPK-2	109

List of tables

		<i>page</i>
Table 1	Chemicals and reagents	27
Table 2	<i>E. coli</i> strains used for cloning	29
Table 3	Vectors used in this study	34
Table 4	<i>E. coli</i> strains used for nematode feeding	35
Table 5	Constructs for microinjection	36
Table 6	<i>C. elegans</i> strains used in this study	37
Table 7	<i>S. cerevisiae</i> strains used in this study	44
Table 8	<i>E. coli</i> strains used for recombinant expression	47
Table 9	Expression and lysis conditions for recombinant expressed GST-PPK-2	48
Table 10	Bioinformatics tools and software	49
Table 11	Candidates for regulating PIP-dependent neuronal membrane trafficking in <i>C. elegans</i>	50
Table 12	Results of the RNAi screen	53
Table 13	Velocities of particles of PPK-2 and mutants in neurons	86

8 At the very end... acknowledgements!

At the very end, I would like to mention all the people who joined and supported my life and work in the last few years.

I would like to thank **Dr. Dieter Klopfenstein** for the big opportunity to develop this project on my own and thereby growing as a scientist and a person. I also want to thank him for his support and his trust in my ideas and abilities.

I would like to thank **Prof. Dr. Ivo Feußner** and **Prof. Dr. Nils Brose** to take part in my thesis committee and for their constructive criticism and ideas regarding my project.

Without **Dr. Eugenia Butkevich**, this dissertation would not have so many beautiful microscopy pictures! She is a magician at the microinjection, but I also want to thank her for many long discussions and advice.

I would like to thank **Dr. Ingo Heilmann** for many discussions and suggestions. I want to thank as well his group members **Dr. Irene Stenzel** and **Alina Mosblech** who did all phosphoinositide analyses shown in this work.

What would a doctoral student be without helping hands? A big thank to my students: **Anna Bobrowska** (best master student ever!), **Judith Wälde** (best Hiwi ever!), and **Christian Thiele** (best diploma student ever!).

I also want to express my gratitude to all the others for numerous advice, help, and reagents: **Gabriela Salinas-Riesters and group, Oliver Wagner, Kerstin von Roden, Barbara Köhler, Volker Henschel, Sailaja Mandalapu, Ulrike Schulz, Charlotte Wilms, Martina Wirth, Stefan Eimer, Kang Shen, John Chua, Erich Wanker, Robin Irvine and Jon Clarke, Sandhya Koushika, Matt Petrie and Thomas Martin, and Derek Sieburth.** (I hope I did not forget anybody!)

I would like to thank the **GGNB office** for help and advice and the **committee** of the GGNB doctoral program 'Cells' for financial support.

At last, but absolutely not at least, I would like to thank (and wave a big **HELLO!** to): **My family** and new and old **friends**.

This dissertation would not be what it is without the help, support, and patience of **Dr. Tobias Kruse** (love, it's done!).

9 Appendix

- 9.1 Expression patterns of candidates genes**
- 9.2 Alignment of PPK-2 with Type I and Type II PIP kinases of other organisms**
- 9.3 BLAST search for mammalian *ppk-2* orthologs**
- 9.4 Genomic sequence of *ppk-2***
- 9.5 cDNA sequence of *ppk-2***
- 9.6 Cholinergic and GABAergic neurons in wild type nematodes**
- 9.7 Vector sequences**
- 9.8 Primer sequences**

9.1 Expression patterns of candidate genes

Table 9-1 Expression patterns of putative PI/PIP kinases and PIP phosphatases of *C. elegans* (according to www.wormbase.org, database release WS211).

	gene name/ accession no.	expression patterns
kinases	<i>vps-34</i>	not determined
	F35H12.4	nervous system (head neurons, tail neurons), pharynx, intestine, reproductive system (vulva), seam cells, unidentified cells in head, unidentified cells in tail
	Y75B8A.24	not determined
	<i>ppk-1</i>	nervous system (ventral nerve cord, neuronal cell bodies near the nerve ring, tail neurons, nerve ring, dorsal nerve cord, lateral nerve cords, head neurons, mechanosensory neurons, pharyngeal neurons, neurons along body), reproductive system (vulva, developing vulva, gonad, distal tip cell of the gonad), uterine and vulva muscles, intestine, head mesodermal cell, hypodermal seam cells, body wall muscle, broadly expressed in early embryos
	<i>ppk-2</i>	nervous system (nerve ring, ventral nerve cord, dorsal nerve cord, lateral nerve cords, head neurons, neurons along body, tail neurons), pharynx, intestine, rectal gland cells, stomato-intestinal muscle, anal depressor muscle, rectal epithelium, reproductive system (distal tip cell, developing vulva, developing uterus), vulval muscle, body wall muscle, excretory cell
	<i>ppk-3</i>	nervous system (pan-neuronal), pharyngeal muscle, vulval muscle, anal depressor, hypodermis
phosphatases	<i>mtm-1</i>	nervous system (neurons in head and tail), hypodermal cells, body wall muscle cells, pharyngeal muscle cells and sheath cells, vulva cells, distal tip cells, coelomocytes
	<i>mtm-3</i>	predominantly in neurons in the head, expression also detected in posterior intestinal cells, body wall muscle, eggs
	<i>daf-18</i>	during larval development (from the bean stage onwards), in many if not all tissues, with elevated expression levels in a few head neurons and in the intestine from L1 to adult stage. A wide up-regulation of expression levels in many if not all tissues was observed during the transition between L1 and pre-dauer L2D stage. Once dauer tissues were fully remodeled, high GFP levels were then limited to head neurons and ventral and dorsal nerve cords.
	C34B7.2	neuronal system (GABAergic motor neurons, head, tail), intestine, body wall muscle
	F30A10.6	not determined
	W09C5.7	not determined

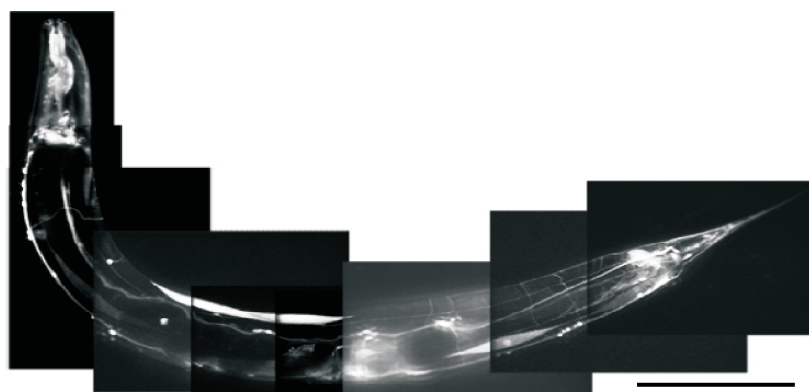


Figure 9-1 Expression pattern of *ppk-2*

ppk-2 expression has been reexamined for this study by analyzing the expression pattern of cytosolic GFP driven by the promoter of *ppk-2* (strain BC15528 from CGC). Scale bar, 0.1 mm.

9.2 Alignment of PPK-2 with Type I and Type II PIP kinases of other organisms

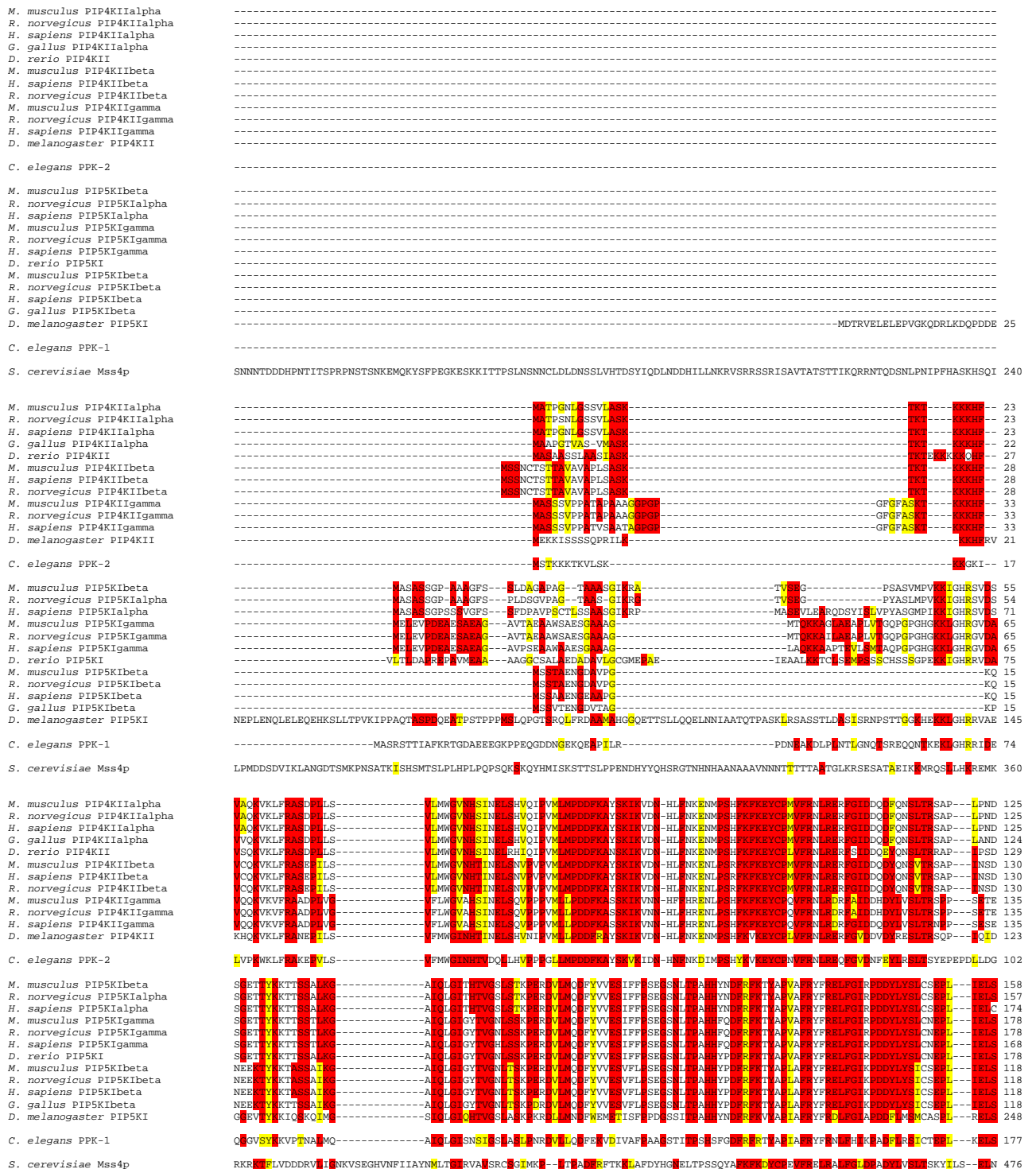


Figure 9-2 Multiple sequence alignment with *C. elegans* PPK-2 and PPK-1

Multiple sequence alignment of *C. elegans* PPK-2 and PPK-1 with selected Type II and Type I PIP kinases of other organisms. Identical amino acids are shaded in red and similar amino acids, respectively (identity threshold 0.1).

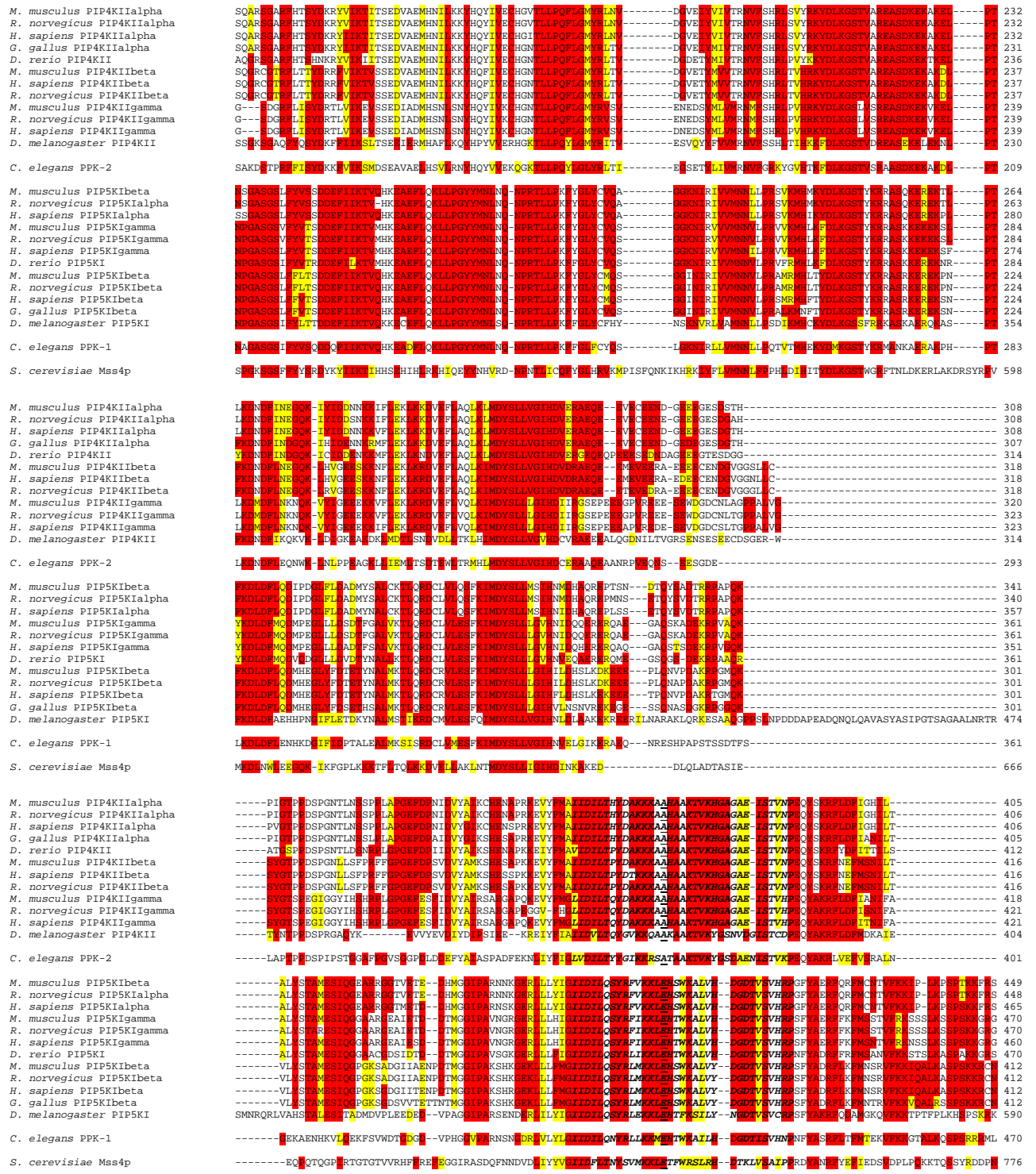


Figure 9-2 Multiple sequence alignment with C. elegans PPK-2 and PPK-1 (continued)

Multiple sequence alignment of C. elegans PPK-2 and PPK-1 with selected Type II and Type I PIP kinases of other organisms. Identical amino acids are shaded in red and similar amino acids in yellow, respectively (identity threshold 0.1).

9.3 BLAST search for mammalian *ppk-2* orthologs

Table 9-2 BLAST search for PPK-2 orthologs in human, mouse, and rat

Results of BLAST searches using the primary sequence of *C. elegans* PPK-2 (length = 401 aa) as query for sequence data deposited at NCBI. Hits are ordered by bit score, a statistical value calculated from the number of gaps and substitutions associated with each aligned sequence.

organism	protein	score	identities	positives	gaps
<i>M. musculus</i>	phosphatidylinositol 5-phosphate 4-kinase, type II, alpha (405 aa)	382 bits	208/403 (51 %)	280/403 (69 %)	12/403 (2 %)
<i>R. norvegicus</i>	phosphatidylinositol 5-phosphate 4-kinase, type II, alpha (406 aa)	382 bits	208/403 (51 %)	279/403 (69 %)	12/403 (2 %)
<i>H. sapiens</i>	phosphatidylinositol 5-phosphate 4-kinase, type II, beta (416 aa)	382 bits	206/394 (52 %)	272/394 (69 %)	16/394 (4 %)
<i>H. sapiens</i>	phosphatidylinositol 5-phosphate 4-kinase, type II, alpha (406 aa)	379 bits	206/403 (51 %)	278/403 (68 %)	12/403 (2 %)
<i>R. norvegicus</i>	phosphatidylinositol 5-phosphate 4-kinase, type II, beta (416 aa)	378 bits	206/394 (52 %)	269/394 (68 %)	16/394 (4 %)
<i>M. musculus</i>	phosphatidylinositol 5-phosphate 4-kinase, type II, beta (416 aa)	374 bits	206/394 (52 %)	271/394 (68 %)	16/394 (4 %)
<i>H. sapiens</i>	phosphatidylinositol 5-phosphate 4-kinase, type II, gamma (421 aa)	359 bits	189/396 (47 %)	271/396 (68 %)	18/396 (4 %)
<i>R. norvegicus</i>	phosphatidylinositol 5-phosphate 4-kinase, type II, gamma (421 aa)	341 bits	189/396 (47 %)	265/396 (66 %)	19/396 (4 %)
<i>M. musculus</i>	phosphatidylinositol 5-phosphate 4-kinase, type II, gamma (421 aa)	347 bits	188/396 (47 %)	266/396 (67 %)	18/396 (4 %)

9.4 Genomic sequence of *ppk-2*

```

1 TTTTCCGCCA ACAAACCTCG GCATGTGCGAC AAAAAAGAAG ACAAAGGTCC
51 TATCGAAGAA AAAAGGCAAG ATTTTGGTGC CAAAATGGAA GCTTTTCCGC
101 GCCAAAGAGC CTGTCTTGTC GGTTTTCATG TGGGGAATCA ATCATAACGGT
151 GGATCAGCTG CTTTCATGTCC CTCCGCCAGG GCTTCTAATG CCAGATGACT
201 TCAAGGCAGG TGGAAATTTG AAAAAATCAC AAAAAATTGG CCTAGACGAG
251 TGAAAATTTG AGAAAAATCG GAAGAAAAAC GACGAAAAAA CCAAAAATTG
301 TAGGACACAG CTGAAATCAG TGCTACCGTA GTCAAAAATT TCGAAAAAAT
351 GCGAAAATAG GTCAATTTTG CGCGGAAAT TCAAATTTTC CACTGATTTT
401 TCATAAAAAA TCCGATTTTT CAGGCATATT CGAAAGTAAA AATCGATAAT
451 CACAATTTCA ACAAAGATAT TATGCCGTCA CACTACAAAG TCAAAGAATA
501 CTGTCCAAAT GTGTTCCGTA ACCTTCGTGA GCAATTTGGT GTCGACAATT
551 TCGAATATCT ACGCTCGCTG ACGTCATACG AGCCGGAGCC CGACTTGTTC
601 GATGGCTCGG CAAAGGATTC CACGCCGAGA TTCTTTATAT CGTATGATAA
651 GAAGTTTGTG ATCAAGGTTT GTGTGTGGAG AAATCGAGAA AATCGTAGGA
701 TTTTGACCGA AAAAAATGCGA AAATTCGGCT TCAAAGTGTG AATTTTGCCC
751 TAAAACGCAA ATTTTGGCCT AAAAACTGAA AATTTAGCCC TAAAACGTG
801 AATTTTAGTC CTAAAAATGT AAATTTTAGG CATAAAAACG TAAATTTTAG
851 GCATAAAAAC GTAAATTTTA AGCTTAAAAA CGTGAATTTT AAGCCTAAAA
901 CCGTGAATTT TAAGCCTAAA ACCGTGAATT TTAAGCCTAA AAACGTGAAT
951 TTTAGGCCTA AAAACGTAAA ATTTAGCCCT AAAAACTGAA ATTTTAGGCC
1001 TAAAACGTA AATTTTAGGC CTAAAAACTT AAATTTTAAG TGTGAAACCG
1051 TGAATTTTAA GCCTAAAAAC TTAAATTTTA AGCCTAAAAA CCTAAATTTT
1101 AGGCCTGAAA ACGTAAATTT TAAGCCTAAA AACGTAAATT TTAAGCCTAA
1151 AAATGTAAAT TTTAGGCCTA AAACCGTGAA TTTTAGGCCCT AAAAATGTAA
1201 CTTTTAGGCC TAAAAACATA CATTTTGGGT CTAAAAACGT AAATTGTAGT
1251 GCTAAAAACG CAAATTAAG CCTAAAACCT TGATTTTAA GCCTAGAAAC
1301 TFGGATTTTA GCCCTAAAAA CGTGAATTTT AGGTCGTAAA AACGTGAAAA
1351 TTAGGCCTAA AAACGCAGAT TTCAGTGTGC TGAATTCCTA TATCATCAGA
1401 AAATGTGAAA AAATTGGGTC TCGAAGCGAA AAATGCGAAA AATTACGTTT
1451 TTCAACTAAA AATTTCAAAT TTTCAACCAA AACTACCCGA AATTTCAAAA
1501 AAAAAAAAAA TTTTCAAAT TTCAGTCAAT GGACTCCGAA GCGGTCGCCG
1551 AGCTCCACTC AGTACTCCGG AATTATCATC AATATGTCGT CGAAAAGCAA
1601 GGAAAACCC TTTTGCCGCA ATATTTGGGA CTTTATAGGT AAAAAGTCGA
1651 ATTCAAGCTCG CCGTGGGCTT CAATTTGACA CCAAAAATTC AGGAAAAATC
1701 GATAAATTTT GAAAAAAAAA ATTTTTTTAA GAAACAATTT TGAAACTTTG
1751 AAATTTTTTC TGCAAAATTC TAAGTTTTCA CTAAAATGTT TATATTTTTG
1801 AACTCAGCTC ACCGAGAGCT TTAAAATGAC CCCCATATCG GCTAGGTTCC
1851 GCCAATTTTG GGTCCCGCCG CGAAAACCTAC AGTACCCTTC TTGTCGGGAC
1901 CCAGTTTTTCG CGGCGGGACC CAGAATTGCC GGAACCTAGT CGATATGGGA
1951 GTCATTTGAA AGCTCTCGGT GAGCTGAATA CGAATTTGAC GCGGAAAAAT
2001 TAAACAACCT GAAAATTTTT TTTTTTAAGA AAATGAATTT TTGAAAAAAA
2051 ATTTTTTTTT TTTGGAATTT TTTAAATTTT TATTGAAATTT TTCATACTTT
2101 CGAACTCAGC TCACCGAGAG CTTCAAATG GCCCCATAT CGGCTAGGCT
2151 CCGTCAATTT TGGGTCTCGC CGCGAAAAC ACAGTACCCT TCGTGTCCGG
2201 ACCCAGTTTT CGCGCGGGGA CCAAAAATCG GCGAACCTAG CGGATATGGG
2251 AGTCATTGTG AAGGTCTGAG CGAGCGGAAT ACAAATTTTA CGAAAAAAA
2301 TTCATAAATT TTCGAAAAAA AAATTATTTT TAGAAATTGA ATTCAAAAAA
2351 AAAATTTTTT TTTGGAATTT AGATTTTTTC TACCTAAATT TTATTCAATC
2401 TCTTTTTGCA ATGTTTTGCA ATATTTTCAG ACTAACAATC GAGGGCTCAG
2451 AGACATACCT GATCGTAATG CGCAACGTGT TCGGCCGAAA GTACGGTGTG
2501 CATACAAAAT TCGACCTTAA AGGATCTACA GTATCCCGTG CGGCGTCCGA
2551 TAAGGAAAAA GCCAAAGATC TCCCAACACT GAAAGATAAC GATTTCTGCG
2601 AACAAAACCTG GAAGCTTAAC CTGCCGCCAG AGGCCGAAA ACTGCTCAT
2651 GAGATGCTCA CTAGTGATAC GGAATGGCTC ACGAGAATGC ATTTGATGGA
2701 TTATTGCTG CTAGTTGTA CCGTACAAAA TACCGGAAAA ATGCAAAATT

```

Figure 9-3 Gene structure of *ppk-2* and mutations

Genomic sequence of *ppk-2*. Exons are alternating highlighted in red and yellow. The transposon insertion site of allele ttTi8500 in exon 3 is marked by red letters. The nucleotides deleted in tm3741 are underlined (according to www.wormbase.org, database release WS211).

```

2751 TCGGAAAAAT CAATAATTCT TAAAATTTTCG AGAAAATGTT TTTTTTGGAA
2801 ATTTTCTAGA TTATTTTTTC AAAGTTCCAT ATTTCAGAAT AATTTCCAAA
2851 AATCTGAATT CAGCTCACCA GGACCTTCAA AATGACCCCC TTCATGCCTA
2901 GGTTCCGCCA ATTTTGAGTT TTTGGGTCTC GCCACGCGGG GTACTGTAGC
2951 TATGGTTTCA GCTGTGTCTGA AACTCGAAAT TGACGGAGCC AAGGCGTGGT
3001 GGGGGTCATT TGAAAGATCT TGATGAGCTG AATTCGATTA ATTTAAATAT
3051 ACTTTGAGAA TGAAATTTTG AGTTAAAAAA ATTTTGTTGA AAATTTCCAA
3101 AAAAAAAGA ATTTTTTTTCG AATTTCACTT TTCTTAActA ATTTCAAAAA
3151 ATTTTAATTC AGCTCACCAA TACCGTTAAA ATGACCCCCA TCATGCCTAG
3201 GTTCCGACGA ATTTGAGAA TTTGGGTCTC GCCACGCGGG GTACTGTAGC
3251 TATGGCTTCA GCTGTGTCTGA AACTCGAAAT TGACGCAGCC TAGGCGTGGT
3301 GGGGGTCATT TGAAAGATCT TGATGAGCTG AATTCGATTT TAATGTCAA
3351 ATATTTAGAA ATCTTTTGAA AAAATTAAT TTTGAGAGAA AATTTTTC
3401 TGAAAATTTT CAAAAAAGAA GAATTTTTTT CGAATTTTCA ATTTTCCACG
3451 CTAATTTTAA AAAATTTGAA TTCAGCTCGC CAGTACCTTC AAAATGACCC
3501 CCATCATGCC CAGGTTCCGC CAATTTGAG TTTTGGGTCTC TCGCCACGCT
3551 GGGTACTGTA GCTATGGTTT CAGCTGTGTC GAAACTCAAA ATTGACGCAA
3601 CCTAGGCATG TTGGGGTCA TTTGAAAGGT CTTGGTGAGC TGAATTCAAA
3651 TATTACAGTA GTTGTTTTCA AGAATTTTCA TTTTTCAGAA TTTTAAACT
3701 GTTCCAAAAA TTAAAAAATA ATTATTCCAG GTATCCACGA CTGCGAACGT
3751 GCCGCCCAAG AAGCCGCCAA TCGTCCCCTA GAACAAAACA GTGAAGAATC
3801 GGGCGACGAG CTCGCCCCGA CGCCCCAGA CTCGCCGATC CCGTCAACGG
3851 GCGGCGCATT TCCCGGAGTT TCGGGCGGTC CCGACCTCGA TGATGAATTT
3901 TACGCCATCG CAAGTCCCCT GGATTTTGTG AAAAATTTGA TCTATTTTAT
3951 TGGGCTCGTC GATATTCTCA CCTACTACGG CATCAAGAAA CGCAGTCCGA
4001 CGGCCGCGAA AACTGTGAAA TATGGCTCAG ATGCCGAGAA TATTAGCACT
4051 GTAAACCGG AACAGGTGCG GATTTGCGGA ATTGCAAAAA AAAATGGAAA
4101 AAATCCCGAA ATTTTGAGGA TTTTTGGAGA AAAATTGAGA TTTTTTTGGAA
4151 AATTTCTTAA TTTTTTTGAT TTGTAGTGTG ATTTTCTTTT CCAGCACACT
4201 GAGAGCTTCA ATGTAACCCC AATATCGGCT TTTTTCCGCC ATTTTTGACA
4251 CATTTTGGGT CCTGCCACGA AAACTACAGT ACCCCTTTTC TGGTGGGACC
4301 CGAAATCTC AAAGTCGGCG GAATATAGGC ATGTTGGAGG TCATTTGAAT
4351 GGGTTCCGTG AGCTGAATTC AAATTTAATG CCGACTTTAA AAAATTTACA
4401 AAAAATTGAA AAAAAATCC CGAAAATTGA CGATTTTCGG AAAAATTTGA
4451 AATTTCTCAG TTTTTTTCGA AAATTCACCT GAATTTTCAA TTTTTCAGTCC
4501 AATTTTTTCA CTCAACACAC TGAGAGGTTT AATTTGACCC CATTTTGACG
4551 ATTTTCCGTC AATTTCTACA CTTTTTGGGT CTCGCCACGA AAACTACAGT
4601 AACCCTTTTC TGGTGGGACC CAAAAATCTC AAAGTCGGCG GAATATAGGC
4651 ATGTTGGGG TCATTTGAAA CGTCTCGGTG AGCTGAATTC AATTTTAAA
4701 ATGAGAATCT ACAGAAATGG GTCTCGACGC GAAAAATGGT TTTTTTTTTCG
4751 AAAATACAAA ATTTTCAAAA AAAAACTTTT TTTTTTCTGA AAAATTAATA
4801 AACTTCTAA TCTCAATTTT TTTCAGTATG CCAAACGACT CGTCAATTC
4851 STAAGCCGGG CTCTCAACTG ACCCCGCCCA CCATCTACAG TAACCCCGCC
4901 CTGCCCGGCC CCCCTTTTGC ACCTTTAATT TCGCACATTG ATCTCAATTT
4951 TCAATTTTTT TGTAATAATA AGCTGAAAAG AAAAAATAT ACCAAAAATT
5001 ATAATTTATT TCCGATATTT TCCTGCTTTG CTCTCCCGCC CCCGTCGCCC
5051 TAAGCTCCGC CCATTTCTGA CCCGCTAAAA TTCCCGATTT ATAATTTTTT
5101 TTTGATTTTC TCCTGAAAAT TTGTCTGTAA TTTATCCCCC GCTATTACCT
5151 TTATATTTTT GTGTAAAAAT AAACAG

```

Figure 9-3 Gene structure of *ppk-2* and mutations (continued)

Genomic sequence of *ppk-2*. Exons are alternating highlighted in red and yellow. The transposon insertion site of allele *ttTi8500* in exon 3 is marked by red letters. The nucleotides deleted in *tm3741* are underlined (according to www.wormbase.org, database release WS211).

9.5 cDNA sequence of *ppk-2*

```

1 ATGTCGACAA AAAAGAAGAC AAAGGTCCTA TCGAAGAAAA AAGGCAAGAT
M S T K K K T K V L S K K K G K I
51 TTTGGTGCCA AAATGGAAGC TTTTCCGCGC CAAAGAGCCT GTCTTGTCGG
L V P K W K L F R A K E P V L S V
101 TTTTCATGTG GGAATCAAT CATACGGTGG ATCAGCTGCT TCATGTCCCT
F M W G I N H T V D Q L L H V P
151 CCGCCAGGGC TTCTAATGCC AGATGACTTC AAGGCATATT CGAAAAGTAAA
P P G L L M P D D F K A Y S K V K
201 AATCGATAAT CACAATTTCA ACAAAGATAT TATGCCGTCA CACTACAAAG
I D N H N F N K D I M P S H Y K V
251 TCAAAGAATA CTGTCCAAAT GTGTTCCGTA ACCTTCGTGA GCAATTTGGT
K E Y C P N V F R N L R E Q F G
301 GTCGACAATT TCGAATATCT ACGTCGCTG ACGTCATACG AGCCGGAGCC
V D N F E Y L R S L T S Y E P E P
351 CGACTTGTTG GATGGCTCGG CAAAGGATTC CACGCCGAGA TTCTTTATAT
D L L D G S A K D S T P R F F I S
401 CGTATGATAA GAAGTTTGTG ATCAAGTCAA TGGACTCCGA AGCGGTGCGC
Y D K K F V I K S M D S E A V A
451 GAGTCCACT CAGTACTCCG GAATTATCAT CAATATGTCG TCGAAAAGCA
E L H S V L R N Y H Q Y V V E K Q
501 AGGAAAAACC CTTTTGCCGC AATATTTGGG ACTTTATAGA CTAACAATCG
G K T L L P Q Y L G L Y R L T I E
551 AGGGCTCAGA GACATACCTG ATCGTAATGC GCAACGTGTT CGGCCGAAAG
G S E T Y L I V M R N V F G R K
601 TACGGTGTCC ATACAAAATT CGACCTTAAA GGATCTACAG TATCCCCTGC
Y G V H T K F Y D L K G S T V S R A
651 GGCGTCCGAT AAGGAAAAAG CCAAAGATCT CCCAACACTG AAAGAATACC
A S D K E K A K D L P T L K D N D
701 ATTTTCTGGA ACAAACCTGG AAGCTTAACC TGCCGCCAGA GGCCGGAAAA
F L E Q N W K L N L P P E A G K
751 CTGCTCATTG AGATGCTCAC TAGTGATACG GAATGGCTCA CGAGAATGCA
L L I E M L T S D T E W L T R M H
801 TTTGATGGAT TATTCGCTGC TAGTTGGTAT CCACGACTGC GAACGTGCCG
L M D Y S L L V G I H D C E R A A
851 CCCAAGAAGC CGCCAATCGT CCCGTAGAAC AAAACAGTGA AGAATCGGGC
Q E A A N R P V E Q N S E E S G
901 GACGAGCTCG CCCCGACGCC CCCAGACTCG CCGATCCCGT CAACGGGCGG
D E L A P T P P D S P I P S T G G
951 CGCATTTCCT GGAGTTTCGG GCGGTCCCGA CCTCGATGAT GAATTTTACG
A F P G V S G G P D L D D E F Y A
1001 CCATCGCAAG TCCCGCGGAT TTTGAGAAAA ATTTGATCTA TTTTATTGGG
I A S P A D F E K N L I Y F I G
1051 CTCGTCGATA TTCTCACCTA CTACGGCATC AAGAAACGCA GTGCGACGGC
L V D I L T Y Y G I K K R S A T A
1101 CGCGAAAAC TGTAAATATG GCTCAGATGC CGAGAATATT AGCACTGTTA
A K T V K Y G S D A E N I S T V K
1151 AACC GGAACA GTATG CCAA CGACTCGTCG AATTCGTAAG CCGGGCTCTC
P E Q Y A K R L V E F V S R A L
1201 AACTGA
N *

```

Figure 9-4 cDNA and translation product of *ppk-2*

Exons are alternating highlighted in red and yellow (according to www.wormbase.org, database release WS211).

9.6 Cholinergic and GABAergic neurons in wild type nematodes

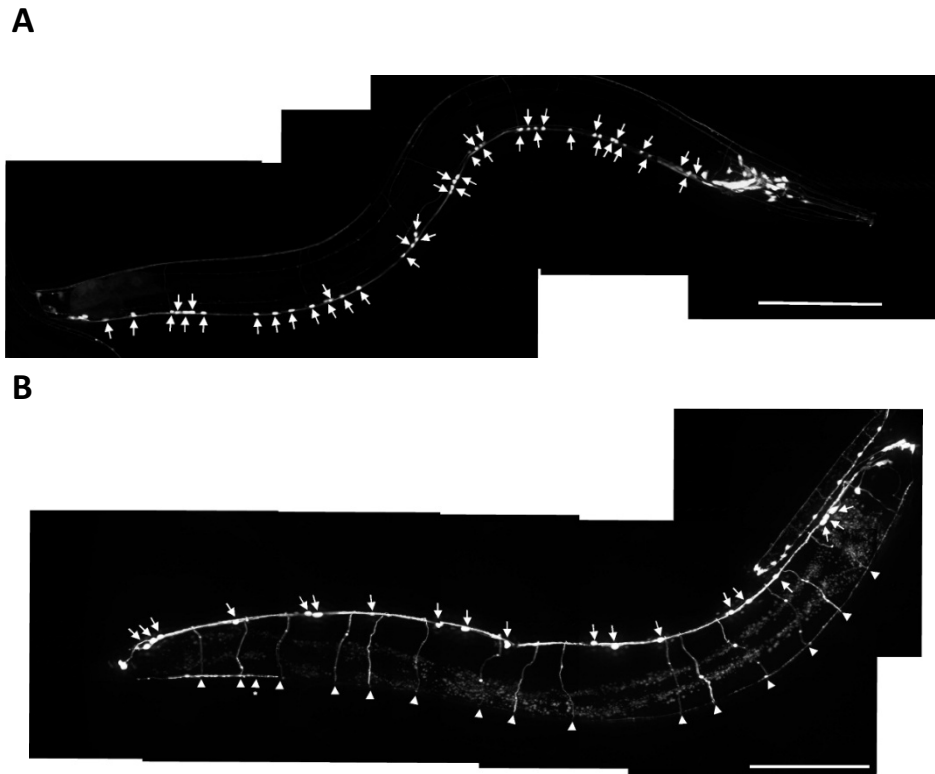


Figure 9-5 Cholinergic and GABAergic neurons in wild type background

Position of somata (arrows) and commissures (arrow heads) of cholinergic (A) and GABAergic (B) neurons in wild type adults. Scale bars, 0.1 mm.

9.7 Vector sequences

The vector *Prab-3::GFP::Gateway* was used for the expression of fusion proteins in *C. elegans* neurons. The sequence of the pan-neuronal promoter of *rab-3* is shaded in grey, GFP in black, and the Gateway cassette again in grey. Flanking restriction sites are highlighted in red (Figure 9-6). The sequence of *Prab-3::mCherry::Gateway* is essentially the same, but with a mCherry sequence instead of a GFP sequence (Figure 9-7).

Prab-3::GFP::Gateway

```

1 ATGACCATGA TTACGCCAAG CTTGCATGGC ATGCCTGCAG GATCTTCAGA
51 TGGGAGCAGT GGA CTGTCTA TTTGATATC TTAAAATGTA CTCTATAAAA
101 GATGAAACTG TAATGACCAA TTCCTACAT AAATATTTT AACTAATTGG
151 TCGGATATTT GGGGATCAGA GAAGTACTTG TTTTTCGAT ATTAATAATG
201 ATATATTTT CTAGTAAAAA AATGTTAAGC GATTTGTGAA TAATTAAGTT
251 GGCTTGAAAA AGATTTTGTG ATAGCTATGT ATTTTGTAA TTTAAATCAG
301 ATTTTAAAAA TTTATTATG ACTATTTATA TATATTATAT ATTATATAT
351 TTCATGGTTT AATCAAAATC TATTAAATTA TTTCTAAAAT CTCTAAATAT
401 CGAATTCTCT AAAAAGCTTC ATCAACAAAA GCATTTCAAT TATCTAACAC
451 AATGAGAATA ATTCAAGAAC TGAAATAGAA AGAAATCTAG AAAAAAAGA
501 GAGTGAGGTG CCCTATTAAA TCGGTGCTCT CCTCTCTAAC AGAAGCGCT
551 ACACGCACCC AAGAGAGCTC TTTTCTTTC TTTTTCGGA GCACACATAC
601 ACGCATACAC TCCTCAGAAG TGTATAGAGA AAATGGGAGA AGAAGCGAAA
651 GAAGACGAAG AAGCGGTGTG GATGTATGCA TCGGGCGTTT CTATCTCTCT
701 CCGTGAGCAA CGAGCTAGTC AACCATCGA TCCATTTTGG TGAGCACACA
751 CAGAGAGAGA CTCAAACACA CTCACAGCTT CACACTGAGC TCCAAGAGCT
801 CTGTAGAGAG AAGCCAGAGT ATGCTTTCCT CGATTTTCCT AACGTCTTCT
851 TCTTCTGCTT TTTTCTTTT CCCAACGAGT TGTAGTCCAC TAACTTCAAT
901 TTTTCTCCA GAGAAAGAGT TTTAGAGAGA CAGCTGATAA ATACACTAGA
951 GAAATAAAAA GAATGATAAA AATTTGCTAT TTTAATCAGT TCCCTCTCGT
1001 TTCTCTAAGT TTTGTTGTTG GGTGGGAAA TTAAAATTGG AAAAAAGAAA
1051 TAACGTTTTT TTCTGTCTAA TCTTGAATTC TCCAGACATT TCTTATTTCC
1101 TTTTTTGTG CAAGTTTTTC TTCCTTCTCT AATTTTTAAT CAAAGATATC
1151 TCGCTATGAA CTTTGAATTT TTGATATTTT GATTCTATAA ATACATAAAG
1201 TAATCTAAAT GCTCTTTTAA AATAAATCTA CAGTAGCCCT ATTTTCAGGG

1251 ATCCTATCGA TTCGCGGCCG CTGTACACCC GGGTGCCGGC GCGCC TGACA

1301 CTAAGTTTCT CTGCACGCGC CTCTAGAGGA TC C C C C G G AT GAGTAAAGGA
1351 GAAGA ACTTT TCACTGGAGT TGTCCCAATT CTTGTTGAAT TAGATGGTGA
1401 TGTTAATGGG CACAAATTTT CTGTCAGTGG AGAGGGTGAA GGTGATGCAA
1451 CATACGAAA ACTTACCCTT AAATTTATTT GCACTACTGG AAAACTACCT
1501 GTTCCATGGG TAAGTTTAAA CATATATATA CTAACTAACC CTGATTATTT
1551 AAATTTT CAG CCAACACTTG TCACTACTTT CTGTTATGGT GTTCAATGCT
1601 TCTCGAGATA CCCAGATCAT ATGAAACGCG ATGACTTTTT CAAGAGTGCC
1651 ATGCCCGAAG GTTATGTACA GGAAAGA ACT ATATTTTTCA AAGATGACGG
1701 GAACTACAAG ACACGTAAGT TTAAACAGTT CGGTACTAAC TAACCATACA
1751 TATTTAAAT TFCAGGTGCT GAAGTCAAGT TTGAAGGTGA TACCCTTGT
1801 AATAGAATCG AGTTAAAAGG TATTGATTTT AAAGAAGATG GAAACATTCT
1851 TGGACACAAA TTGGAATACA ACTATAACTC ACACAATGTA TACATCATGG
1901 CAGACAAACA AAAGAATGGA ATCAAAGTTG TAAGTTTAAA CTGGACTTA
1951 CTAACTAACG GATTATATTT AAATTTTCAG AACTTCAAAA TTAGACACAA
2001 CATTGAAGAT GGAAGCGTTC AACTAGCAGA CCATTATCAA CAAAATACTC
2051 CAATTGGCGA TGGCCCTGTC CTTTACCAG ACAACCATTA CCTGTCCACA
2101 CAATCTGCC TTTTCGAAAGA TCCAACGAA AAGAGAGACC ACATGGTCTC
2151 TCTTGAGTT GTAACAGCTG CTGGGATTAC ACATGGCATG GATGAACTAT

2201 ACAAATAG GC TAGCACAAGT TTGTACAAAA AAGCTGAACG AGAAACGTAA
2251 AATGATATAA ATATCAATAT ATTAAATTAG ATTTTGCATA AAAAAACAGAC

```

Figure 9-6 Vector sequence of *Prab-3::GFP::Gateway*

```

2301 TACATAATAC TGTA AACAC AACATATCCA GTCATATTGG CGGCCGCATT
2351 AGGCACCCCA GGCTTTACAC TTTATGCTTC CGGCTCGTAT AATGTGTGGA
2401 TTTTGAGTTA GGATCCGTCG AGATTTTCAG GAGCTAAGGA AGCTAAAATG
2451 GAGAAAAAAA TCACTGGATA TACCACCGTT GATATATCCC AATGGCATCG
2501 TAAAGAACAT TTTGAGGCAT TTCAGTCAGT TGCTCAATGT ACCTATAACC
2551 AGACCGTTCA GCTGGATATT ACGGCCTTTT TAAAGACCGT AAAGAAAAAT
2601 AAGCACAAGT TTTATCCGGC CTTTATTAC ATTCTTGCCC GCCTGATGAA
2651 TGCTCATCCG GAATTCGGTA TGGCAATGAA AGACGGTGAG CTGGTGATAT
2701 GGGATAGTGT TCACCCTTGT TACACCCTTT TCCATGAGCA AACTGAAACG
2751 TTTTCATCGC TCTGGAGTGA ATACCACGAC GATTTCCGGC AGTTTCTACA
2801 CATATATTCG CAAGATGTGG CGTGTTACGG TGAAAACCTG CCTATTTC
2851 CTAAAGGGTT TATTGAGAAT ATGTTTTTCG TCTCAGCCAA TCCCTGGGTG
2901 AGTTTCACCA GTTTTGATTT AAACGTGGCC AATATGGACA ACTTCTTCGC
2951 CCCCCTTTTC ACCATGGGCA AATATTATAC GCAAGGCGAC AAGGTGCTGA
3001 TGCCGCTGGC GATTCAGGTT CATCATGCCG TTTGTGATGG CTTCCATGTC
3051 GGCAGAATGC TTAATGAATT ACAACAGTAC TGCGATGAGT GGCAGGGCGG
3101 GGCGTAAACG CGTGGATCCG GCTTACTAAA AGCCAGATAA CAGTATCCGT
3151 ATTTGCGCGC TGATTTTTGC GGTATAAGAA TATATACTGA TATGTATACC
3201 CGAAGTATGT CAAAAAGAGG TATGCTATGA AGCAGCGTAT TACAGTGACA
3251 GTTGACAGCG ACAGCTATCA GTTGCTCAAG GCATATATGA TGTCAATATC
3301 TCCGGTCTGG TAAGCACAAC CATGCAGAAAT GAAGCCCGTC GTCTGCGTGC
3351 CGAACGCTGG AAAGCGGAAA ATCAGGAAGG GATGGCTGAG GTCGCCCCGT
3401 TTATTGAAAT GAACGGCTCT TTTGCTGACG AGAACAGGGG CTGGTGAAT
3451 GCAGTTTAAAG GTTTACACCT ATAAAAGAGA GAGCCGTTAT CGTGTGTTG
3501 TGGATGTACA GAGTGATATT ATTGACACGC CCGGGCGACG GATGGTGATC
3551 CCCCTGGCCA GTGCACGTCT GCTGTCAGAT AAAGTCTCCC GTGAACTTTA
3601 CCCGGTGGTG CATATCGGGG ATGAAAGCTG GCGCATGATG ACCACCGATA
3651 TGGCCAGTGT GCCGGTCTCC GTTATCGGGG AAGAAGTGGC TGATCTCAGC
3701 CACCGCGAAA ATGACATCAA AAACGCCATT AACCTGATGT TCTGGGGAAT
3751 ATAAATGTCA GGCTCCCCTA TACACAGCCA GTCTGCAGGT CGACCATAGT
3801 GACTGGATAT GTTGTGTTTT ACAGCATTAT GTAGTCTGTT TTTTATGCAA
3851 AATCTAATTT AATATATTGA TATTTATATC ATTTTACGTT TCTCGTTTCC

                                KpnI
3901 CTTTCTTGTA CAAAGTGGTG ATGGTACCAT GGTATTGATA TCTGAGCTCC
3951 GCATCGGCCG CTGTCATCAG ATCGCCATCT CGCGCCCGTG CCTCTGACTT
4001 CTAAGTCCAA TTACTCTTCA ACATCCCCTAC ATGCTCTTTC TCCCTGTGCT
4051 CCCACCCCTT ATTTTTGTTA TTATCAAAAA AACTTCTTCT TAATTTCTTT
4101 GTTTTTTAGC TTCTTTTAAG TCACCTCTAA CAATGAAATT GTGTAGATT
4151 AAAAATAGAA TTAATTCGTA ATAAAAAGTC GAAAAAATT GTGCTCCCTC
4201 CCCCATTAA TAATAATTCT ATCCCAAAAT CTACACAATG TTCTGTGTAC
4251 ACTTCTTATG TTTTTTTTAC TTCTGATAAA TTTTTTTTGA AACATCATAG
4301 AAAAAACCGC ACACAAAATA CCTTATCATA TGTTACGTTT CAGTTTATGA
4351 CCGCAATTTT TATTTCTTCG CACGCTGGG CCTCTCATGA CGTCAAATCA
4401 TGCTCATCGT GAAAAAGTTT TGGAGTATTT TTGGAATTTT TCAATCAAGT
4451 GAAAGTTTAT GAAATTAATT TTCCTGCTTT TGCTTTTTGG GGGTTTCCCC
4501 TATTGTTTGT CAAGAGTTTC GAGGACGGCG TTTTCTTGC TAAAATCACA
4551 AGTATTGATG AGCACGATGC AAGAAAGATC GGAAGAAGGT TTGGGTTTGA
4601 GGCTCAGTGG AAGGTGAGTA GAAGTTGATA ATTTGAAAGT GGAGTAGTGT
4651 CTATGGGGTT TTTGCCTTAA ATGACAGAAT ACATTCCCAA TATACCAAAC
4701 ATAACTGTTT CCTACTAGTC GGCCGTACGG GCCCTTTCGT CTCGCGCGTT
4751 TCGGTGATGA CGGTGAAAAC CTCTGACACA TGCAGCTCCC GGAGACGGTC
4801 ACAGCTTGTC TGTAAGCGGA TGCCGGGAGC AGACAAGCCC GTCAGGGCGC
4851 GTCAGCGGGT GTTGGCGGGT GTCGGGGCTG GCTTAACTAT GCGGCATCAG
4901 AGCAGATTGT ACTGAGAGTG CACCATATGC GGTGTGAAAT ACCGCACAGA
4951 TGCGTAAGGA GAAAATACCG CATCAGGCGG CCTTAATTAA GGGCCTCGTG
5001 ATACGCCAT TTTTATAGGT TAATGTCATG ATAATAATGG TTTCTTAGAC
5051 GTCAGGTGGC ACTTTTCGGG GAAATGTGCG CGGAACCCCT ATTTGTTTAT
5101 TTTTCTAAAT ACATTCAAAT ATGTATCCGC TCATGAGACA ATAACCCTGA
5151 TAAATGCTTC AATAATATTG AAAAAGGAAG AGTATGAGTA TTCAACATTT
5201 CCGTGTGCGC CTTATTCCCT TTTTTCGGC ATTTTGCCTT CCTGTTTTTG
5251 CTCACCCAGA AACGCTGGTG AAAGTAAAAG ATGCTGAAGA TCAGTTGGGT
5301 GCACGAGTGG GTTACATCGA ACTGGATCTC AACAGCGGTA AGATCCTTGA
5351 GAGTTTTTCG CCCGAAGAAC GTTTTCCAAT GATGAGCACT TTTAAAGTTC
5401 TGCTATGTGG CCGGTATTA TCCCGTATTG ACGCCGGGCA AGAGCAACTC
5451 GGTGCGCGCA TACACTATTC TCAGAATGAC TTGGTTGAGT ACTCACCAGT

```

Figure 9-6

Vector sequence of Prab-3::GFP::Gateway (continued)

```

5501 CACAGAAAAG CATCTTACGG ATGGCATGAC AGTAAGAGAA TTATGCAGTG
5551 CTGCCATAAC CATGAGTGAT AACACTGCGG CCAACTTACT TCTGACAACG
5601 ATCGGAGGAC CGAAGGAGCT AACCGCTTTT TTGCACAACA TGGGGGATCA
5651 TGTAACTCGC CTTGATCGTT GGAACCGGA GCTGAATGAA GCCATACCAA
5701 ACGACGAGCG TGACACCACG ATGCCTGTAG CAATGGCAAC AACGTTGCGC
5751 AAAPTATTA CTGGCGAACT ACTTACTCTA GCTTCCCGGC AACAAATTAAT
5801 AGACTGGATG GAGGCGGATA AAGTTGCAGG ACCACTTCTG CGCTCGGCC
5851 TTCCGGCTGG CTGGTTTAT TCTGATAAAT CTGGAGCCGG TGAGCGTGGG
5901 TCTCGCGGTA TCATTGCAGC ACTGGGGCCA GATGGTAAGC CCTCCCCTAT
5951 CGTAGTTATC TACACGACGG GGAGTCAGC AACTATGGAT GAACGAAATA
6001 GACAGATCGC TGAGATAGGT GCCTCACTGA TTAAGCATTG GTAACGTCA
6051 GACCAAGTTT ACTCATATAT ACTTTAGATT GATTTAAAAC TTCATTTTTA
6101 ATTTAAAAGG ATCTAGGTGA AGATCCTTTT TGATAATCTC ATGACCAAAA
6151 TCCCTTAACG TGAGTTTTTCG TTCCACTGAG CGTCAGACCC CGTAGAAAAG
6201 ATCAAAGGAT CTTCTTGAGA TCCTTTTTTTT CTGCGCGTAA TCTGCTGCTT
6251 GCAAACAAA AAACCACCGC TACCAGCGGT GGTGTGTTG CCGGATCAAG
6301 AGCTACCAAC TCTTTTTCCG AAGGTAACGT GCTTCAGCAG ACTGAGCTTA
6351 CCAAATACTG TCCTTCTAGT GTAGCCGTAG TTAGGCCACC ACTTCAAGAA
6401 CTCTGTAGCA CCGCCTACAT ACCTCGCTCT GCTAATCCTG TTACCAGTGG
6451 CTGCTGCCAG TGGCGATAAG TCGTGTCTTA CCGGGTTGGA CTCAAGACGA
6501 TAGTTACCGG ATAAGGCGCA GCGGTGCGGC TGAACGGGGG GTTCGTGCAC
6551 ACAGCCCAGC TTGGAGCGAA CGACCTACAC CGAACTGAGA TACCTACAGC
6601 GTGAGCATTG AGAAAGCGCC ACGCTTCCCG AAGGGAGAAA GGGGACAGG
6651 TATCCGGTAA GCGGCAGGTT CGGAACAGGA GAGCGCACGA GGGAGCTTCC
6701 AGGGGAAAC GCCTGGTATC TTTATAGTCC TGTCGGGTTT CGCCACCTCT
6751 GACTTGAGCG TCGATTTTTG TGATGCTCGT CAGGGGGGCG GAGCCTATGG
6801 AAAAACGCCA GCAACGCGGC CTTTTTACGG TTCCTGGCCT TTTGCTGGCC
6851 TTTTGCTCAC ATGTTCTTTC CTGCGTTATC CCCTGATTCT GTGGATAACC
6901 GTATTACCGC CTTTGTAGTA GCTGATACCG CTCGCCGAG CCAACGACC
6951 GAGCGCAGCG AGTCAGTGAG CGAGGAAGCG GAAGAGCGCC CAATACGCA
7001 ACCGCCCTCT CCGCGCGGTT GGCCGATTCA TTAATGCAGC TGGCAGCACA
7051 GGTTCGCCGA CTGGAAAGCG GGCAGTGAGC GCAACGCAAT TAATGTGAGT
7101 TAGCTCACTC ATTAGGCACC CCAGGCTTTA CACTTTATGC TTCGGGCTCG
7151 TATGTTGTGT GGAATTGTGA GCGGATAACA ATTTACACA GAAACAGCT
7201 GGGGGTGGGG GGGGGTGGG GGGTGGGGT TTGTTGGGGT GTGTTTTGTG
7251 T

```

Figure 9-6 Vector sequence of Prab-3::GFP::Gateway (continued)

sequence of mCherry

*Sma*I

```

CCCGGATGG TCTCAAAGGG TGAAGAAGAT AACATGGCAA TTATTAAGA
GTTTATGCGT TTCAAGGTGC ATATGGAGGG ATCTGTCAAT GGGCATGAGT
TTGAAATGA AGGTGAAGGA GAAGGCCGAC CATATGAGGG AACACAAACC
GCAAACTAA AGGTAAGTTT AAACATATAT ATACTAACTA ACCCTGATTA
TTTAAATTT CAGGTAACTA AAGGCGGACC ATTACCATTG GCCTGGGACA
TCCTCTCTCC ACAGTTCATG TATGGAAGTA AAGCTTATGT TAAACATCCG
GCAGATATAC CAGATTATTT GAAACTTTCA TTCCCGGAGG GTTTTAAGTG
GGAACGCGTA ATGAATTTG AAGACGAGG AGTTGTTACA GTGACGCAAG
ACTCAAGGTA AGTTTAAACA GTTCGGTACT AACTAACCAT ACATATTTAA
ATTTTCAGCC TCCAAGATGG AGAATTTATT TATAAAGTCA AACTTCGAGG
AACGAATTT CCCTCGGATG GACCTGTTAT GCAGAAGAAG ACTATGGGAT
GGGAAGCTTC AAGTGAAGA ATGTACCCTG AAGACGGTGC TCTTAAGGGA
GAGATTAAC AACGCTTAA ATTGAAAGAT GGAGGACATT ACGATGCTGA
GGTAAGTTA AACATGATTT TACTAACTAA CTAATCTGAT TTAAATTTTC
AGGTGAAGAC AACTTACAAA GCCAAAAAAC CAGTTCAGCT GCCAGGAGCG
TACAATGTTA ATATTAACCT GGATATCACC TCCCACAACG AGGATTACAC
TATCGTTGAG CAATATGAAA GAGCTGAAGG GCGGCACTCG ACAGTGGCA

```

*Nhe*I

```

TGGATGAATT GTATAAGACT AGTGGATCCG CTAGC

```

Figure 9-7 Sequence of mCherry in Prab-3::mCherry::Gateway

9.8 Primer sequences

Table 9-3 Primers used for molecular cloning

Primers are shown without attB-sequences which are necessary for Gateway cloning (INVITROGEN). Optional start and stop codons are put in parentheses. Restriction sites used for the cloning of promoter rab-3 are highlighted in red. FL, full length.

sequence name	primer pair	
	forward	reverse
cDNA C34B7.2	CCATGTCGGCTGCGAAAATC	TGTTGCTTGCATATACTTTG
cDNA F30A10.6	(ATG) GACATCTACGAGAGTTT CAACTTG	(TTA) GTCCAGTTTGAGCTTCGGAGC
cDNA F35A10.4	AAATCCGAAAGCGATGTGG	ATGGATTCCATTTGTGTAATATTG
cDNA <i>mtm-1</i>	AAAGACTATAAATTTAGCGAAAC	CAACGTGACCCTTAGTCGCGCCG
cDNA <i>ppk-1</i>	GCTTCTCGGTCCACAACAATCG	AGCGACAGGTGTGTCACCACTC
cDNA <i>ppk-2</i> (<i>tm3741</i>)	ATGCCGTCACTACAAAGTC	TCAGTTGAGAGCCCGGCTTAC
cDNA <i>ppk-2</i> *	TCGACAAAAAGAAGACAAAGGTCC	(TCA) GTTGAGAGCCCGGCTTAC
cDNA <i>snb-1</i>	ATGGACGCTCAAGGAGATGCCGG	TTTTCTCCAGCCCATAAAACG
cDNA <i>unc-26</i> 5-phosphatase	CAATCCATTAATAATTCGTTGG	GCCAACTTTAAAAGTTTCCACTTTG
cDNA <i>unc-26</i> FL	ATGTCAGTTCGAGGGATTCGG	CTACATATTTTTTGGTCTAGG
cDNA W09C5.7	TCAATAATTTACACAACACCAACAGC	CAAAAGTGAAATTTTAGTTTGACA
cDNA Y75B8A.24	CACGAGATATCGAGGATTTTG	ATATGGAATTTTATTCTGG
gDNA <i>sac1</i>	ATGACAGGTCCAATAGTGTACGTTT	ATCTCTTTTTAAAGGATCCGGCTTG
promoter <i>rab-3</i>	<i>Sph</i> GCATGC CTGCAGGATCTTCAG	<i>Asc</i> GGCGGCC AATACGACTCACTATAGG

*the same primer pair was used for the cloning of the cDNA of *ppk-2* (*ttTi8500*)

Teaching and supervision

during the study period	<u>2004 - 2005</u> Student assistant in the School lab at the Helmholtz Center for Infection Research, Braunschweig, supervision of grammar school students <u>2005 - 2006</u> Method course "Bacteria and phage genetics" Method course "Yeast genetics" (two week-practicals for students in biology and biotechnology, Institute of Genetics, University of Braunschweig) Lab rotation of Jessica Prilop (student in biology), Institute of Genetics, University of Braunschweig)
during the doctoral thesis	<u>2007 - 2008</u> Method course "Synaptic transmission of <i>C. elegans</i> " Master's thesis of Anna Bobrowska (Molecular biology graduate program) Lab rotation of Christian Thiele (student in biology), followed by employment as a student assistant <u>2007 - 2009</u> Judith Wälde (student in business) as a student assistant <u>2009 - 2010</u> Lab rotation of Alice Hansch (student in biology) Diploma thesis of Christian Thiele

Conferences and publications

SFB523 Symposium 'Intracellular Transport and Trafficking'. April 3 - 4, 2008, Max-Planck-Institute for Biophysical Chemistry, Göttingen, Germany

Poster: Sassen, W A, A Bobrowska and D Klopfenstein. "Novel neuronal function of PIP kinases and phosphatases in *Caenorhabditis elegans* revealed by RNAi."

17th International *C. elegans* Meeting, Genetics Society of America. June 24 - 28, 2009, University of California, Los Angeles, U.S.A.

Poster: Sassen, W A, E Butkevich, and D Klopfenstein. „Sac1p- and Fig4p-like lipid phosphatases act in the nervous system of *Caenorhabditis elegans*.”
(supported by a GGNB travel grant)

6th International PhD Student Symposium 'Horizons in Molecular Biology'. September 9 - 12, 2009, Göttingen, Germany

Poster: Sassen, W A, E Butkevich, A Mosblech, I Heilmann, and D Klopfenstein. "The Phosphatidylinositol-5-phosphate 4-kinase of *Caenorhabditis elegans* acts in the nervous system."

Publication Sassen, W A, E Butkevich, C Thiele, A Mosblech, I Heilmann, and D Klopfenstein. "The PI5P 4-kinase ortholog of *Caenorhabditis elegans* regulates neuropeptide release." *(in preparation)*

